CHEMOGENETIC ABLATION OF DOPAMINERGIC NEURONS IN THE BRAIN OF LARVAL AND ADULT ZEBRAFISH (*DANIO RERIO*): PHENOTYPES AND REGENERATIVE ABILITY

RAFAEL SOARES GODOY

Thesis submitted to the
Faculty of Graduate and Postdoctoral Studies
in partial fulfillment of the requirements for the
Doctorate in Philosophy degree in Biology

Department of Biology
Faculty of Science
University of Ottawa

PREFACE

This thesis was written in partial fulfillment of the Ph.D. requirement for the Biology Department at the University of Ottawa and followed a thesis as a series of articles format. Chapter 2 entitled, “Chemogenetic ablation of dopaminergic neurons leads to transient locomotor inpairments in zebrafish larvae” by Rafael Godoy, Sandra Noble, Kevin Yoon, Hymie Anisman and Marc Ekker has been accepted for publication at the Journal of Neurochemistry (JNC-2015-0237). Chapter 3 entitled, “Cellular and molecular changes following ablation of dopaminergic neurons in the larval zebrafish brain” consists of preliminary work that is currently being replicated and expanded on for publication. Chapter 4 entitled, “Regeneration of dopaminergic neurons following chemogenetic ablation in the adult zebrafish brain” is currently in preparation for submission.

AKNOWLEDMENTS

I would like to dedicate this work in memory of my grandparents who have always supported and believed in my scientific career. In addition, I would like to thank my mother and uncle, whom despite the vast physical distance that separated us during my studies, have always been by my side providing support and motivation throughout my career in Canada.

I am very lucky to have met and worked with Dr. Marc Ekker during these last few years. The opportunity to work with one of the world's leading scientist in the zebrafish field is a great honour and I will be forever grateful for his guidance and mentorship. I also would like to thank Dr. Ekker for the many opportunities he has provided to me as a student in his lab including the chance to participate in many international meetings, to speak at prestigious gatherings and the freedom to collaborate on different projects in addition to my thesis research.

I would like to thank my thesis advisory committee: Dr. Michael Schlossmacher, Dr. Paul Albert and Dr. Tom Moon, for their guidance and critical review of my work during my Ph.D. studies. Furthermore, I would like to thank Dr. Marie-Andrée Akimenko, Dr. Luc Poitras, Dr. Fabien Avaron, Dr. Mélanie Debiais-Thibaud and Dr. John Basso for discussions.

I would like to thank the many Ph.D. and post-doctoral fellows with whom I had the opportunity to collaborate with, whose work is not part of my Ph.D thesis. Namely I thank Dr. Yanwei Xi and Dr. Sandra Noble (from Dr. Ekker's lab), Dr. Shahram Eisa-

Beygi (from Dr. Moon's lab), Dr. Susie Huang (from Dr. Laurie Chan's lab) and Mrs. Stephanie McMillan (from Dr. Akimenko's lab).

I also would like to thank the great technicians in our department, Mr. Gary Hatch, Mr. Phillip Pelletier, Mrs. Jing Zang, Mr. Yves Genest, Ms. Lucille Joly, Ms. Lise Belanger and Mr. Andrew Ochalski for technical support. Furthermore, I thank Dr. Vera Tang, from the flow cytometry core facility at the faculty of medicine for help with FACS and Dr. Hymie Anisman from Carleton University for his help with HPLC. I also would like to thank Mr. Vishal Saxena, Mr. William Fletcher and Ms. Christine Archer for their work at the zebrafish facility.

During my journey in the Ekker lab, I had the amazing chance to train and learn from enthusiastic and dedicated undergraduate trainees with whom I worked and share found memories. In chronological order, I thank Mr. Yang Xu, Mr. Peter Goddard, Ms. Victoria Cusson, Ms. Camille Girard-Bock, Mr. Kevin Yoon, Mr. Ryan Gotfrit, Mr. Wilsom Lam, Mr. Jonathan Nhan and Mr. Matthew Guo.

Overall, there are many whom I have to thank during my journey and whose names were not listed here. Finally, I would like to thank the University of Ottawa academic staff for their support and the University of Ottawa and Faculty of Graduate Studies for research funding as well as the Parkinson's Research Consortium for funding my studies and offering an excellent learning environment. This research was made possible by funding from NSERC and CIHR.

STATEMENT OF CONTRIBUTIONS

Dr. Marc Ekker and I planed all experiments presented here. I conducted all experiments shown in this thesis in a collaborative effort with other researchers. I wrote my thesis and papers with revisions by Dr. Ekker and Dr. Noble.

In chapter 2, Mr. Peter Goddard, Ms. Victoria Cusson, Ms. Camille Girard-Bock and Dr. Sandra Noble helped with screening for a transgenic line. Dr. Sandra Noble helped with larval zebrafish live imaging, manual cell counts, fish dechorination and drug treatment. Mr. Kevin Yoon helped with fish dechorination, drug treatments and locomotor behaviour testing. Mr. Ryan Gotfrit helped with tail bend scores and Dr. Hymie Anisman helped with HPLC analysis.

In chapter 3, Mr. Wilsom Lam helped by performing parabiosis experiments and in optimizing CSF transfusions. Mr. Matthew Guo helped with qPCR analysis on larval zebrafish tissue.

In chapter 4, Dr. Sandra Noble helped with westerns, Dr. Hymie Anisman helped with HPLC analysis and Mr. Jonathan Nhan preformed cell counting on adult sections.

In Appendix 1, Mr. Kevin Yoon helped with locomotor behaviour assays and rescue experiments. In Appendix 2, Dr. Sandra Noble and Mr. Yang Xu helped with generation of *parkin* reporter constructs and transfections; this project was a collaborative effort with Dr. Schlossmacher.

ABSTRACT

Dopamine exerts an important role in the regulation of motor activity in humans. During the progression of Parkinson's disease, patients are faced with the progressive neurodegeneration of nigro-striatal dopamine neurons resulting in an array of pathological symptoms characteristic of the disease. Current treatment relies on targeting symptomatic aspects of the disease but currently Parkinson's disease is incurable. Targeting the regeneration of DA neurons in PD patients could offer an alternative therapeutic approach that could stall and perhaps even revert the progression of the disease and improve the quality of life for patients.

Here, I describe the generation of a transgenic zebrafish line for the non-invasive, conditional and specific ablation of dopaminergic neurons in both larval and adult zebrafish. Understanding the endogenous regenerative ability of the zebrafish may in the future contribute to the development of novel therapeutic approaches targeting DA neuron regeneration in humans.

The Tg(*dat:CFP-NTR*) line efficiently labels and ablates most clusters of DA neurons in both the larval and the adult zebrafish brain. Neuronal ablation is followed by a locomotor and tail bend phenotype as well as by an increase in exploratory behavior. Using double transgenic larvae, we showed through live imaging that loss of DA neurons induces an increase in *nestin* expression; in addition we show an increase in the number of proliferating cells and an up regulation of genes involved in neurogenesis and tissue repair. Adult zebrafish were able to fully recover their DA neuronal population in the olfactory bulb within 45 days post ablation.

Overall the Tg(*dat:CFP-NTR*) zebrafish offers a novel tool for the study of the molecular and cellular mechanisms driving the regeneration of DA neurons in the zebrafish brain and will be a useful tool for the field of regenerative medicine.

RÉSUMÉ

La dopamine joue un rôle important dans le contrôle de l'activité motrice chez l'homme. Lors de la progression de la maladie de Parkinson (PD), les patients subissent une dégénération progressive des neurones dopaminergiques (DA) dans la région négro-striatale et ceci cause une série de symptômes caractéristiques de la maladie. Les thérapies actuelles visent à améliorer les aspects symptomatiques de la maladie mais la maladie de Parkinson reste incurable. Une thérapie visant la régénération des neurones DA chez les patients atteint de PD peut constituer une alternative qui pourrait ralentir sinon renverser sa progression et améliorer ainsi la qualité de vie des patients.

Je décris dans cette thèse la production de poissons-zèbres transgéniques permettant l'ablation non-invasive, conditionnelle et spécifique des neurones dopaminergiques chez les juvéniles et les adultes. La connaissance des capacités régénératives du poisson-zèbre pourra contribuer au développement de thérapies nouvelles permettant la régénération des neurones DA chez l'humain.

La lignée transgénique Tg(*dat:CFP-NTR*) permet le marquage et l'ablation efficace des neurones DA dans le cerveau des poissons-zèbres juvéniles et adultes. L'ablation des neurones dans notre modèle résulte en un phénotype dans lequel la locomotion et les fléchissements de la queue sont affectés. Une augmentation du comportement exploratoire a été observée. Les larves transparentes sont un outil utile pour suivre, *in vivo*, les changements et pour les cribles à grande échelle. En utilisant des animaux doublement transgéniques, nous montrons, en utilisant l'imagerie en temps réel, que la perte des neurones DA cause une augmentation de l'expression de *nestin*. De plus,

nous montronsune augmentation du nombre de cellules en cours de prolifération ainsi qu'une augmentation de l'expression de gènes impliqués dans la neurogénèse et la réparation tissulaire. Les poissons-zèbres adultes ont pu complètement récupérer leur population de neurones DA dans le bulbe olfactif a l'intérieur de 45 jours suivant leur ablation.

Globalement, les poissons-zèbres Tg(*dat:CFP-NTR*) constituent un nouvel outil pour l'étude cellulaire et moléculaire des mécanismes menant à la régénération des neurones DA dans le cerveau et apporteront une contribution utile au domaine de la médecine régénérative.

TABLE OF CONTENTS

LIST OF FIGURES

LIST OF TABLES

LIST OF ABREVIATIONS

5-FU	5-fluorouracil
6-OHDA	6-hydroxydopamine
AADC	aromatic amino acid decarboxylase
Ac	anterior commissure
B. Arches	branchial arches
bp	base pairs
BrdU	5-bromo-2-deoxyuridine
CA	catecholamine
CFP	cyan fluorescent protein
CNS	central nervous system
CSF	cerebral spinal fluid
COMT	catechol-O-methyltransferase
DA	dopamine
DAT	dopamine transporter
DC	diencephalic cluster
dpl	days post-lesion
dpf	days post-fertilization
dpt	days post-treatment
EGFP	enhanced green fluorescent protein
FACS	fluorescence-activated cell sorting
fps	frames per second
GFAP	glial fibrillary acidic protein
hpf	hours post-fertilization
Hc	caudal hypothalamus
HPLC	high performance liquid chromatography
i.p.	intraperitoneal
i.m.	intramuscular
kb	kilobases (for DNA)
KD	knockdown
kDa	kilodaltons
KI	knockin
KO	knockout
LC	locus coeruleus
L-DOPA	L-3,4-dihydroxyphenylalanine
MAO	monoamine oxidase
MHB	midbrain hindbrain boundary
MPP^+	1-methyl-4-phenylpyridinium
MPTP	1-methyl-4-phenyl-1,2,3,6-tetrahydropyridine
Mtz	metronidazole
MO	morpholino oligonucleotide
NTR	nitroreductase
OB	olfactory bulb
O/N	overnight
OPC	oligodendrocyte precursor cells

PCNA	proliferating cell nuclear antigen
PD	Parkinson's disease
PNS	peripheral nervous system
PO	preoptic region
POa	anterior preoptic region
PPa	anterior part of parvocellular preoptic nucleus
PPp	posterior part of parvocellular preoptic nucleus
PPr	periventricular pretectal nucleus
Pr	pretectum
RAC	retinal amacrine cells
RGC	radial glial cells
SP	subpallium
Tg	transgenic
TH	tyrosine hydroxylase
TPp	periventricular nucleus of posterior tuberculum
Vc	central nucleus of ventral telencephalon
Vd	dorsal nucleus of ventral telencephalon
VMAT2	vesicular monoamine transporter 2
Vv	vental nucleus of vental telencephalon
WT	wild type

CHAPTER 1

INTRODUCTION: ZEBRAFISH (*DANIO RERIO*) AS A MODEL FOR NEURON ABLATION AND THE STUDY OF DOPAMINERGIC NEURON REGENERATION

Dopamine or 4-(2-aminoethyl) benzene-1, 2 diol is a neurohormone and neurotransmitter that plays a crucial role in regulating animal life by acting in both the central and peripheral nervous systems. Routinely referred to as DA, dopamine originating from the CNS can act as a neurohormone and be released to the hypophyseal portal system where it reaches the pituitary glands and sends an inhibitory signal for the secretion of prolactin (Ugrumov *et al.* 2012). DA in the peripheral nervous system (PNS) has been reported in the kidney, carotid bodies, peripheral arteries and parts of the gastrointestinal, genitourinary and endocrine systems (Eisenhofer *et al.* 1997; Iturriaga and Alcayaga 2004; Carey 2001; Pivonello *et al.* 2007; Hyun *et al.* 2002). It's known roles, include vasodilation, sodium excretion and myocardial contractions (Snider and Kuchel 1983).

Despite its importance in the PNS, for the purpose of our study, we will focus on the role played by DA in the CNS. Since its proposed role in the brain as more than merely a precursor to noradrenaline and adrenaline in the late 1950's (Carlsson *et al.* 1958), much research has shed light on the importance of dopamine in the maintenance of proper retinal adjustments and the regulation of sensory and motor programming, feeding, emotion, sleep, reward, attention, learning, motivation and memory (Smeets and González 2000; Björklund and Dunnett 2007; Yamamoto *et al.* 2013). As a member of the catecholamine group of neurotransmitters, DA is the precursor for both epinephrine and norepinephrine, but here we choose to focus mainly on the neurons which use DA as a neurotransmitter.

1.1 Dopamine biosynthesis

In dopaminergic neurons, the enzyme tyrosine hydroxylase (TH) is able to convert the amino acid L-tyrosine into an intermediate product L-DOPA, which is consequently decarboxylated into DA by the aromatic amino acid decarboxylase (AADC) enzyme and later packaged into synaptic vesicles by the vesicular monoamine transporter 2 (VMAT2), an important step for the stabilization of the highly reactive dopamine molecule (Meiser *et al.* 2013) (Fig.1.1).

The dopamine released into the synaptic cleft is known to act on G-protein coupled receptors of either the D1- or D2-like receptor family which are well conserved among different vertebrate species such as teleosts and mammals (Callier *et al.* 2012). D1- and D2-like receptors can be present post-synaptic and act respectively via an excitatory or inhibitory signaling cascades, or be present pre-synaptic as is the case with D2 receptors, where it acts as an auto-receptor and is used to inhibit neurotransmitter release (Benoit-Marand *et al.* 2001) (Fig. 1.1). The released dopamine can be reuptaken from the synaptic cleft by the dopamine transporter (DAT) which allows dopamine to re-enter dopaminergic neurons and either be re-packaged into synaptic vesicle through VMAT2 or to be degraded in the cytosol via the monoamine oxidase (MAO); alternatively, extra-cellular dopamine can also be up taken by glial cells where it is degraded by either MAO or catechol-O methyl transferase (COMT) (Fig. 1.1) (Meiser *et al.* 2013).

The elements needed for the biosynthesis and processing of DA such as TH, AADC, VMAT2, DAT, MAO and COMT have been identified in different species

among chordates and show a conserved presence and function among vertebrates such as teleost fish (e.g. *Danio rerio*) amphibians and mammals (Yamamoto and Vernier 2011).

Figure 1.1. Dopamine biosynthesis in the vertebrate brain. Dopaminergic neurons convert tyrosine into L-DOPA and consequently into dopamine (DA) via the action of tyrosine hydroxylase (TH) and the aromatic amino acid decarboxylase (AADC). Cytosolic dopamine is packaged into vesicles through the vesicular monoamine transporter 2 (Vmat2) and in response to an action potential, vesicles in the synaptic button release DA into the synaptic cleft where DA can act on a post-synaptic neuron either by acting on a D2-like or D1-like receptor which can be respectively inhibitory or excitatory. Extracellular DA can act on auto-receptors to control dopaminergic output, become degraded by catechol-O methyl transferase (COMT) or be re-uptaken into the dopaminergic neuron via the dopamine transporter (DAT). Following re-uptake, DA can either be repackaged into vesicles or be degraded by monoamine oxidase (MAO).

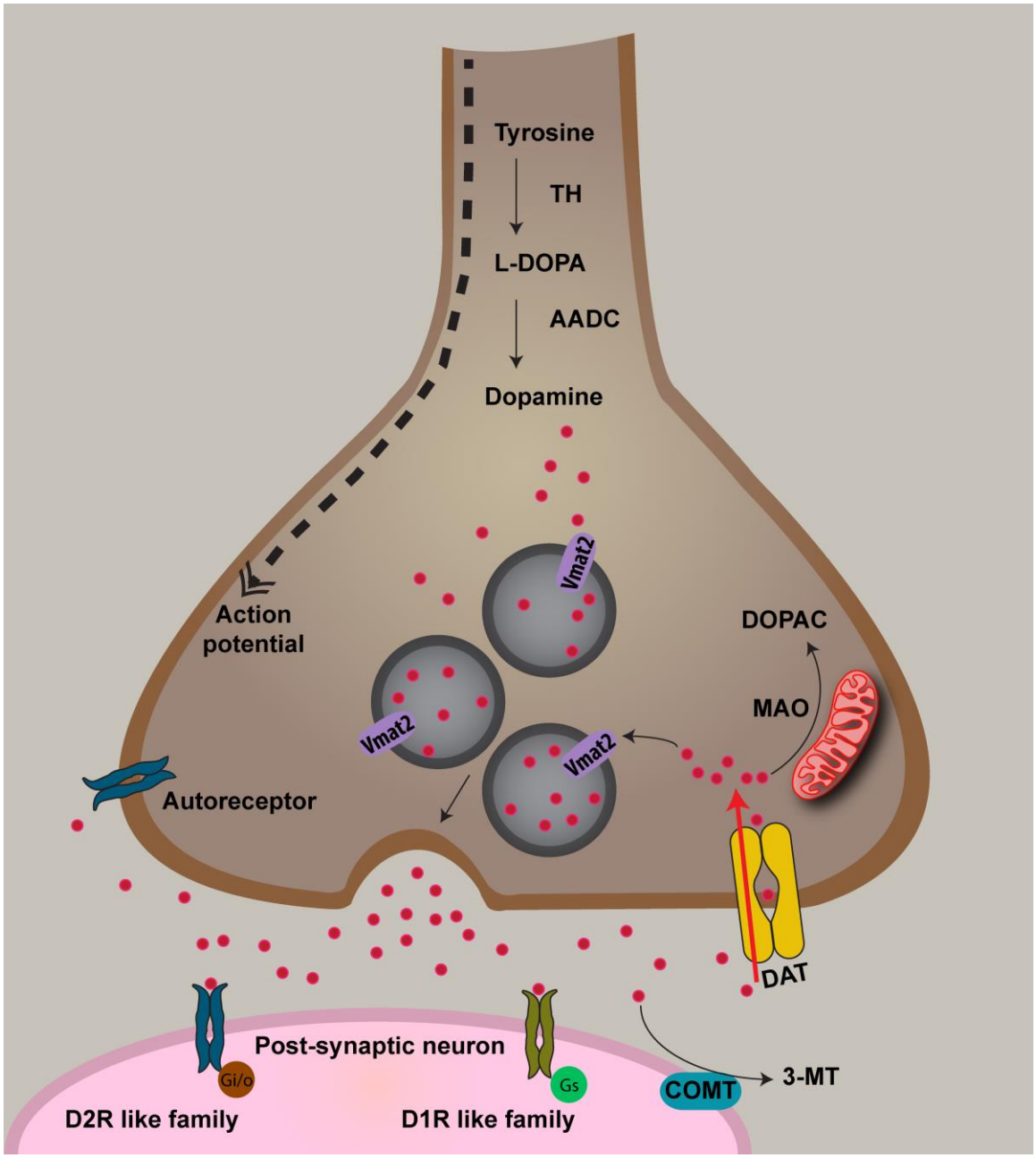
Tyrosine
TH
L-DOPA
AADC
Dopamine
Vmat2
Vmat2
Vmat2
Action potential
DOPAC
MAO
Autoreceptor
DAT
Post-synaptic neuron
Gi/o
Gs
COMT
3-MT
D2R like family
D1R like family

1.2 Dopaminergic neurons: anatomical distribution and projections

Although the different DA neuron populations in the brain share the common enzymes needed for the biosynthesis of dopamine, the anatomical localization of distinct DA neuron populations and the various regions with which their axons connect form networks responsible for various cognitive, behavioral and physiological functions.

The distribution and characterization of the catecholaminergic neuron clusters and their axonal projections are well described in the rodent brain and are classically categorized as clusters A1 to A17 and C1 to C3 (Kandel 2012). While clusters C1, C2 and C3 are adrenergic cells, and clusters A1 to A7 are noradrenergic neurons, the dopaminergic groups can be divided into: 1) a mesencephalic group which contains clusters A8 (retrorubral), A9 (substantia nigra) and A10 (ventral tagmental area), 2) a diencephalic group comprised of clusters A11 (caudal diencephalon), A12 (tuberal), A13 (zona incerta), and A14/A15 (periventricular), 3) an olfactory bulb group A16 and 4) a retinal group A17 (Smeets and González 2000) (Fig 1.2A).

Dopaminergic neurons form four major projections in the mammalian brain, three of which originate in the midbrain area. These include the nigrostriatal pathway which comprises of DA neurons in the substantia nigra projecting to the striatum which are important in the control of movement; the mesocortical & mesolimbic pathway which play a role in emotion, reward, memory, attention and motivation; and the tuberoinfundibular pathway which originates in the hypothalamus and projects to the pituitary where it plays an important role in the regulation of hormonal secretion (Kandel 2012).

Despite the differences in brain size and anatomy, many of these previously described dopaminergic clusters and neuronal projections described in the mammalian brain, are present and have been characterised in the zebrafish brain,

Larval zebrafish start to express DA neuron markers such as *dat* or *th* as early as 18 hpf (Holzschuh *et al.* 2001). By 5 dpf, larvae have established most DA neurons that are identified in the adult zebrafish brain (Fig 1.2B), including cells in the olfactory bulb, pretectum, telencephalon, preoptic area and diencephalon, in addition to retinal amacrine cells (Rink and Wullimann 2002b).

The categorization of catecholaminergic clusters in the zebrafish brain does not follow the classical mammalian A1-A17 nomenclature, and have been first described by Rink and Wullimann (2002). Although a newer nomenclature has been proposed (Sallinen *et al.* 2009), we will used the original labeling described by Rink and Wullimann (2002) throughout our work.

Dopaminergic olfactory bulb and retinal amacrine cells, which are found in all major vertebrate groups (Yamamoto and Vernier 2011), are named in the zebrafish based on their anatomical location (Fig 1.2B) and represent the mammalian groups A16 and A17, respectively. A group of dopaminergic neurons are found in the pretectum of zebrafish while no DA cells are found in the mature mammalian pretectum (Yamamoto and Vernier 2011; Filippi *et al.* 2007).

Other dopaminergic neurons present in the zebrafish brain include DC 0/1 (suggested to be equivalent to A13); DC 3 and DC 7 (suggested to be equivalent to A14 and A12); preoptic DA neurons (suggested to be equivalent to A15) and DC2, 4, 5 and 6

(suggested to be equivalent to group A11 and further discussed below) (Filippi *et al.* 2012; Schweitzer *et al.* 2012).

No DA neurons have been described in the midbrain of the zebrafish as opposed to the mammalian brain where clusters A8, A9 and A10 are found (Yamamoto and Vernier 2011). Despite the lack of mesencephalic DA neurons and projections, the zebrafish's diencephalic (DC) clusters 1, 2 and 4 have been reported to have ascending projections to the teleost's area equivalent to the striatum, which has been identified to be housed within the subpallium region of the telencephalon (Rink and Wullimann 2001), and thus these clusters have been proposed to represent the mammalian clusters A9/A10 (Rink and Wullimann 2001; Rink and Wullimann 2002b) and to form projections equivalent to those of the mammalian meso-strial pathway (Rink and Wullimann 2002a).

A more recent projectome analysis of the catecholaminergic neurons of the larval zebrafish (Tay *et al.* 2011) has suggested that DC clusters 2 and 4 are the only sources of scarcely occurring ascending projections into the larvae's subpallium. Furthermore, recent findings based on the analysis of DA neuron transcription factors has shown that DC 2 and 4 express the orthopedia (*otp*) transcription factor, which makes these neurons more similar to mammalian A11 cluster (Ryu *et al.* 2007) instead of the previously proposed A9/A10 clusters.

Furthermore, evidence from the larval catecholaminergic neuron projectome analysis indicates that most dendritic arborization and neuronal connections found in the subpallium are derived from local projections (Tay *et al.* 2011).

The constantly growing body of information available on the organization of dopaminergic neurons within the zebrafish brain, along with the projectome description

of these neurons, molecular and cellular characterization, and the understanding of their physiological roles when compared to their mammalian counterparts, has allowed the zebrafish to emerge as a model for conditions involving dopamine impairment and as a tool to study human disease, which will be discussed next.

Figure 1.2. Dopaminergic neuron distribution in the rodent and teleost brain and retina. A) Dopamine neurons in the rodent brain are arranged from A8-A17. Red circles indicate areas where neuron cell bodies reside, while dashed lines indicate their axonal projections. Blue arrows show landmark regions of the rodent brain. The retina is indicated below and contains dopaminergic neurons (A17), information adapted from (Prakash and Wurst 2006; Björklund and Dunnett 2007; Kandel 2012) . B) The zebrafish brain dopaminergic arrangement does not follow the classical A8-A17 nomenclature referred to in many mammalian models; instead it has a nomenclature system that varies from larval to adult. DA neuron nomenclature for larvae is shown in green, while adult nomenclature is shown in purple. Red circles indicate where DA cell bodies can be found and brain anatomical landmarks are written in black. Light blue dashed lines indicate equivalents in the rodent brain and brown dashed lines indicate projections proposed to be equivalent to the mammalian nigro-striatal connections, information adapted from (Parker *et al.* 2013; Tay *et al.* 2011; Schweitzer *et al.* 2012; Panula *et al.* 2010; Rink and Wullimann 2002b; Yamamoto *et al.* 2010).

A)

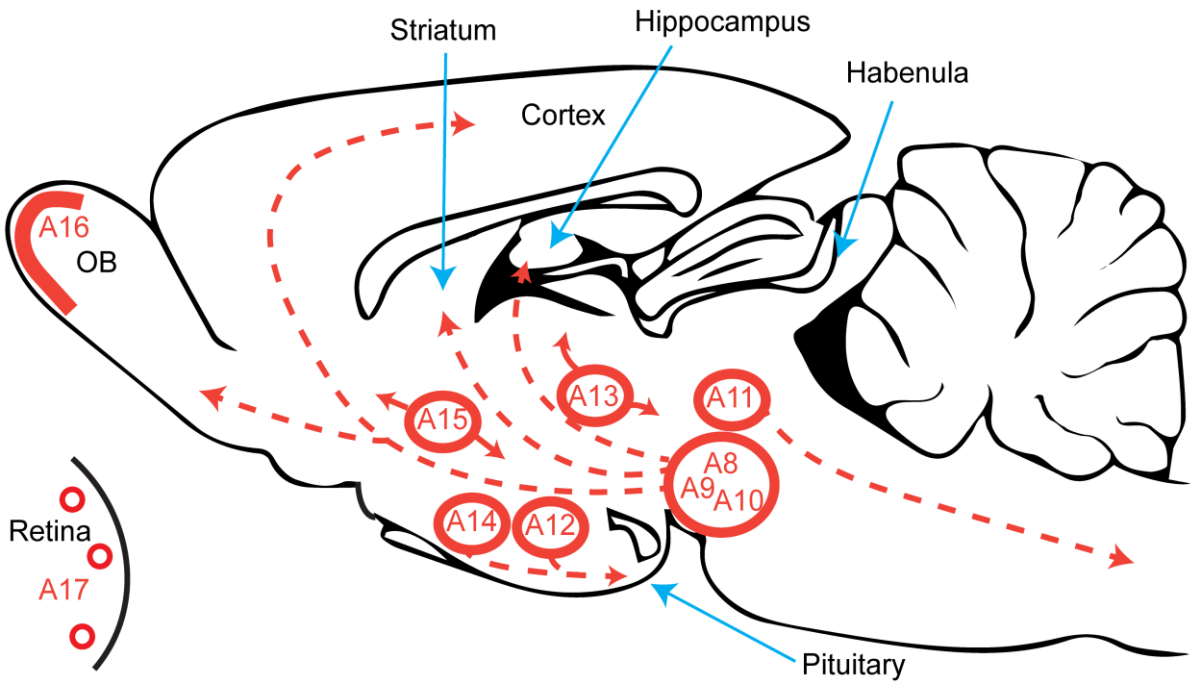
Striatum
Hippocampus
Habenula
Cortex
A16
OB
A15
A13
A11
A8
A9
A10
A14
A12
Retina
A17
Pituitary

B)

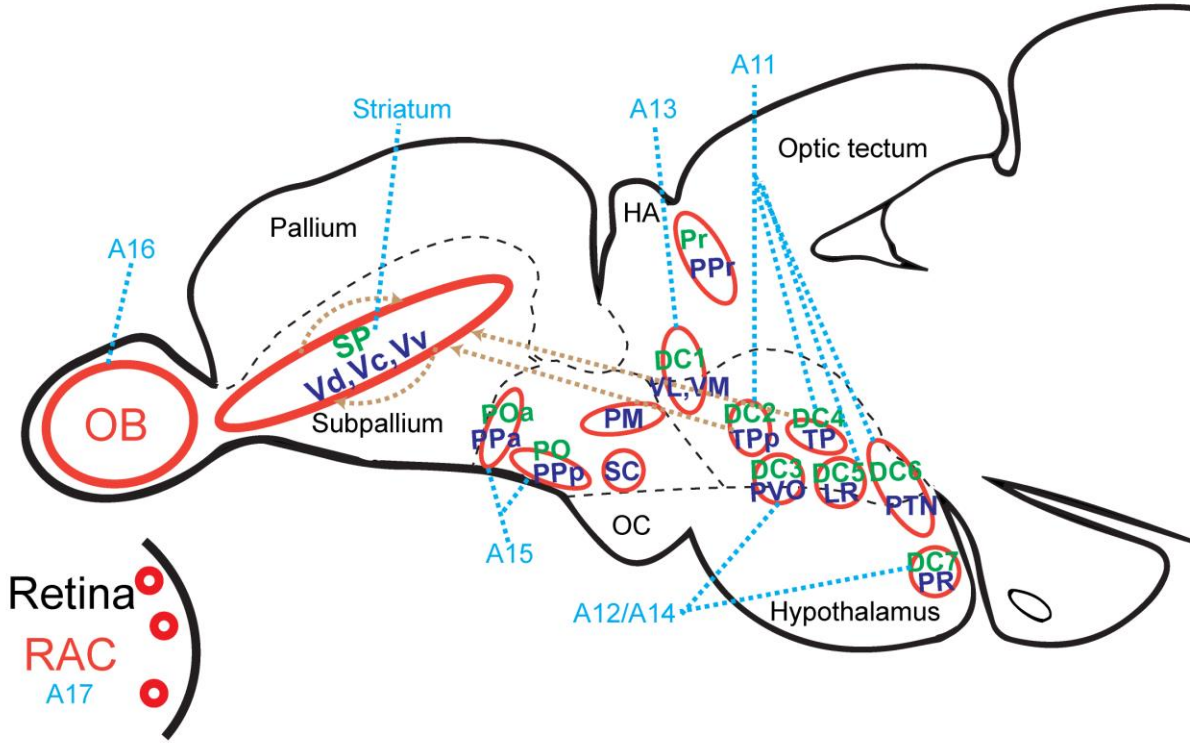
A11
Striatum
A13
Optic tectum
HA
Pallium
A16
Pr
PPr
SP
Vd,Vc,Vv
DC1
VL,VM
OB
Subpallium
POa
PPa
PM
DC2
TPp
DC4
TP
PO
PPp
SC
DC3
RVO
DC5
LR
DC6
PTN
OC
A15
DC7
PR
Retina
RAC
A17
A12/A14
Hypothalamus

1.3 Zebrafish as a model for human disease

With roughly 26,206 protein-coding genes and a 71.4% human to zebrafish gene orthology (Howe *et al.* 2013), the zebrafish has emerged as a model for the study of gene function, development and human disease. This highly prolific vertebrate species with an external development, is optically clear during the early stages of development and within the first week of life has developed the major organs and systems found in mammals such as the cardiovascular, the digestive and the nervous system (Rubinstein 2006).

The zebrafish toolbox, which includes the meganuclease (Soroldoni *et al.* 2009), Tol2 (Fisher *et al.* 2006) and PhiC31 (Roberts *et al.* 2014) technologies used for the optimization of transgene insertion into the *Danio rerio*'s genome, has allowed for the generation of different zebrafish transgenic lines that are used to facilitate the understanding of a vast array of biological processes.

Transgenic zebrafish lines include, in many cases, the use of gene specific regulatory elements to drive the expression of reporter genes (such as eGFP) which combined with the optical clarity of zebrafish larvae, makes this an useful model for tracking biological changes *in vivo*. Additionally, other technologies such as the nitroreductase mediated cell ablation (discussed in more detail in section 1.4) as well as the CRE-LoxP recombinase systems, further prompt the use of zebrafish in studies where both cell specific and time specific events can be regulated, and thus have allowed for the expansion of studies in the field of regeneration, neurogenesis and cell specific lineage tracing (Kroehne *et al.* 2011).

In addition to the applications of generating transgenic lines, mutagenesis studies done primarily through the ENU approach, and to some extent using retroviral mediated mutagenesis, have allowed the generation of zebrafish mutants for many human orthologous genes, which in many cases have shown to result in similar phenotypes related to those of human diseases (Lieschke and Currie 2007; Patton and Zon 2001). A reverse genetic approach has also been possible through the use of TILLING (Lieschke and Currie 2007) and more recently CRISPR mediated genome editing (Kimura *et al.* 2014) which is a promising tool for the manipulation of the zebrafish genome and for the modeling of human disease.

The ability of larval zebrafish to absorb compounds through water exposures, further validates the use of zebrafish as a model for toxicity screens (de Esch *et al.* 2012; Guo 2009). Indeed, their small size and optical clarity when combined with their amenability for *in vivo* cell labeling and *in vivo* phenotype tracking such as via locomotor activity make the larval zebrafish an ideal model for high throughput chemical screens (Rennekamp and Peterson 2015). These discovery-based drug screens, which aim to detect compounds capable of affecting the larval zebrafish at the cellular and phenotypic levels, have the final objective of identifying potential targets for novel human disease therapeutic approaches.

1.3.1 Zebrafish as a model for dopamine impairments

Impairments in DA neurotransmission have implications in the progression of different human conditions, which are attributed to the diferent roles played by dopamine in the CNS.

In humans, dopamine down regulation in the tuberoinfundibular pathway has been proposed to partly contribute to a condition known as hyperprolactinaemia, a common reason for female infertility as previously reviewed by Prakash and Wurst (2006). Dopamine in the mesocortico/limbic systems plays a critical roles in the development of drug addiction and addictive behaviors such as gambling (Adinoff 2004; Volkow *et al.* 2006), and to the development of depression and the psychotic symptoms of schizophrenia (Prakash and Wurst 2006).

The zebrafish has been used as model to study aspects of many of these previously mentioned dopamine impairment related conditions. For examples, it has been shown that in zebrafish, tyrosine hydroxylase immunoreactive fibers innervate luteinizing hormone cells where they act through D2Rs to inhibit reproduction in the female fish (Fontaine *et al.* 2013). Furthermore, exposure of the zebrafish to addictive drugs has been shown to alter the expression of elements linked to the dopamine synthesis pathway, and these elements play a role in addiction (Klee *et al.* 2011). Ethanol exposure, for example, has been shown to up-regulate levels of *th1* and *th2* in larval zebrafish (Puttonen *et al.* 2013), as well as to increase levels of dopamine neurotransmiter in adult fish (Chatterjee and Gerlai 2009). Cocaine administration in larvae has been shown to alter the expression levels of transcription factors involved in the formation of DA neurons such as *Lmx1b,*

Otp and *Nurr1* (Barreto-Valer *et al.* 2013) and nicotine exposure has been shown to increase the levels of DOPAC in adult zebrafish (Eddins *et al.* 2008).

Neuropsychiatric research has also used the zebrafish as a model for the role of dopamine in schizophrenia and ADHD (Norton 2013; Souza and Tropepe 2011). In larval zebrafish, loss of function of the ADHD-linked gene *lphn3.1* has been shown to result in the reduction and mis-patterning of ventral diencephalic DA neurons (Lange *et al.* 2012), while D2R activation in larval zebrafish has shown to suppress Akt activity, a signaling element which is down-regulated in schizophrenic patients (Souza *et al.* 2011).

Taken together, the zebrafish has been used as a model to understand different aspects of human disease and dopamine related disorders. Here, we aim to use the zebrafish to model the dopaminergic neuron loss observed in patients diagnosed with Parkinson's disease for the study of the regenerative potential of these cells.

1.3.2 Parkinson's disease and zebrafish PD models

Parkinson's disease (PD) is the most prevalent neurodegenerative movement disorder and the second most prevalent neurodegenerative conditions (second only to Alzheimer's disease) and can affect 1.5 percent of the global population over the age of 65 and up to 4 percent of the elderly populations over 80 years of age (Davie 2008; Meissner *et al.* 2011).

Although PD patients suffer from non-motor symptoms such as gastrointestinal dysfunction (e.g. constipation), sleep disorders (e.g. insomnia), neuropsychiatric disorders (e.g. depression, anxiety, panic attacks and dementia), autonomic symptom

(e.g. sexual dysfunction), and sensory symptoms (e.g. pain, olfactory and visual dysfunctions) (Chaudhuri and Schapira 2009); the hallmark symptoms of PD are characterized by the motor impairment described in PD patients.

The motor symptms of PD are often described by the acronym TRAP, which encompass (T) tremor at rest, (R) rigidity, (A) akinesia or bradykinesia and (P) postural instability (Jankovic 2008). These symptoms are said to arise due to a reduction in striatal dopamine neurotransmitter as a result of the progressive neurodegeneration of dopaminergic neurons which project from the substantia nigra into the striatum (Dauer and Przedborski 2003).

The progression of sporadic PD may start long before the appearance of motor symptoms. One of the pathological characteristics of PD, the formation of proteinatious inclusions termed Lewy bodies, has been said to commence in neurons of the lower brain stem in the dorsal motor nucleus of the vagus nerve and to expand into the pons, midbrain, basal forebrain and cerebral cortex, in addition to the olfactory system (Del Tredici *et al.* 2002). As previously reviewed, α-synuclein, the component of Lewy bodies, may mediate the transmission of the disease pathology across the different brain regions in a prion-like fashion (Visanji *et al.* 2013). Additionally, Braak and colleagues have proposed a "dual-hit" hypothesis, where a neurotropic pathogen (e.g. virus) could contribute to PD pathology by entering the brain either via the nasal or gastric route (Hawkes *et al.* 2007) and further progress into six different stages of the disease described as the Braak stages of PD (Hawkes *et al.* 2010).

Although the etiology of PD is not fully understood, both genetic and environmental/sporadic factors are involved in the onset of PD (Olanow and Tatton

1999), furthermore a "multiple-hit" hypothesis has been proposed where both genetic and environmental conditions in combination are said to contribute to the disease development (Sulzer 2007).

The current treatments available for PD patients rely heavily on the pharmacological management of their symptomatic effects, especially the motor phenotypes. These treatments involve the use of medications that target the dopaminergic system with the goal of compensating for loss of striatal DA. Levodopa, which is the precursor to DA, first introduced in 1968, still remains a commonly prescribed medication by physicians (Hickey and Stacy 2011). Inhibitors of COMT and MAO-β as well as surgical procedures such as deep-brain stimulation and non-pharmacological approaches such as exercise and physical therapy are other options for the management of disease symptoms (Connolly and Lang 2014; Pedrosa and Timmermann 2013).

To date, Parkinson's disease remains an incurable condition. Despite the ability to treat its symptoms, the progression of the neurodegeneration observed in the disease is inevitable and progressively debilitates patients.

Researchers working in the field of regenerative medicine with an interest in the understanding of neuron regeneration, hope to offer an alternative to the current PD treatments by attempting to restore the lost dopaminergic population in PD patients.

In addition to serving as a model for other dopaminergic impairments (see section 1.3.1), the zebrafish has been a well-studied model for PD. Many of the genes identified to be associated with Parkinson's disease such as *DJ1*, *Parkin*, *PINK1* and *LRRK2* have been detected in the zebrafish (Xi *et al.* 2011a; Bandmann and Burton 2010; Sager *et al.* 2010; Blandini and Armentero 2012; Flinn *et al.* 2008). Although, the zebrafish does not

express α-synuclein; knockdown (KD) of β- and γ-synucleins show a hypokinetic and decreased dopamine level phenotype (Milanese *et al.* 2012) in fish. Furthermore, KD of another gene, *PARL*, with an identified mutations in PD-patients (Shi *et al.* 2011), results in DA neuron mis-patterning and neuron degeneration (Noble *et al.* 2012) in larval zebrafish.

Most of the studies done on the zebrafish genetic models of PD involve the use of morpholino (MO) mediated gene KD, which included the KD of zebrafish *parkin* (Flinn *et al.* 2009), *dj1* (Bretaud *et al.* 2007), *pink1* (Xi *et al.* 2010; Sallinen *et al.* 2010; Anichtchik *et al.* 2008) and *lrrk2* (Sheng *et al.* 2010; Ren *et al.* 2011). Although MO mediated gene knockdown has been heavily employed in zebrafish research and believed to efficiently lead to gene KD (Nasevicius and Ekker 2000), more recent research suggests a poor correlation between the phenotypes obtained from MOs when compared to another reverse genetic approach, such as CRISPRs, showing an estimated discrepancy in 80 percent of morphant phenotypes (Kok *et al.* 2015). With this in mind, it will be interesting to study the phenotypes of knockout (KO) PD genes in the zebrafish, or even, the knock-in (KI) of human disease-like mutated forms of the various PD genetic mutations.

Alternatively, researchers have used toxins to model PD in the zebrafish. These include the use of pesticides/herbicides such as paraquat and rotenone (Bortolotto *et al.* 2014; Bretaud *et al.* 2004; Feng *et al.* 2014), as well as the neurotoxins like 6-hydroxydopamine (6-OHDA) and 1-methyl-4-phenyl-1,2,3,6-tetrahydropyridine (MPTP) (Anichtchik *et al.* 2004; Sallinen *et al.* 2009). These will be discussed in more detail in the next section.

1.3.3 Models of dopamine neuron ablation in the zebrafish

The ideal PD animal model would include the pathological characteristics of PD such as Lewy-body formation and DA neurodegeneration accompanied by a motor phenotype as well as non-motor symptom previously discussed (see section 1.3.2). Here for the purposes of modeling DA neuron loss, with the intent of investigating its regenerative ability, we will discuss commonly used models of DA neuron ablation with locomotor phenotypes in the zebrafish, which are summarized in Table 1.1.

MPTP was first identified in the 80's when a batch of synthetic opioids was found contaminated with MPTP as a drug synthesis byproduct which following consumption as a recreational drug had resulted in PD-like symptoms in several drug users (Bové and Perier 2012). Ever since, MPTP has been used as a neurotoxin to model PD in research animals such as sheep, dogs, guinea pigs, cats, mice, rats and non-human primates (Tieu 2011). MPTP is a lipophilic compound that after crossing the blood-brain barrier is taken up by astrocytes and converted into MPP^+ that is consequently released from astrocytes and taken up by dopaminergic neurons via the dopamine transporter. Once in DA neurons, MPP+ inhibits the complex I of the electron transport chain (Blesa *et al.* 2012). While rats have been shown to be less sensitive to MPTP than mice, MPTP has been shown to result in nigrostriatal DA damage in both monkeys and mouse, and to lead to the formation of inclusion bodies in monkeys and chronically MPTP treated mice, as previously reviewed (Tieu 2011).

The results from MPTP treatment in the zebrafish can vary, and result in differences in the degrees of neuronal damage and locomotor phenotypes among the work of different authors (summarized in Table 1.1). Many of these differences observed could be attributed to the lack of a standardized drug treatment and differences in the way scientists conduct and address locomotor changes. Although not formally addressed, the sensitivity of different strains of *Danio rerio* to MPTP could also vary, as has been shown to be the case between mouse strains (Blesa *et al.* 2012).

Both adult and larval zebrafish have been treated with MPTP. Larval treatment consists of water exposure at concentrations that usually vary from 0.1 to 1000 μM. The starting time for treatments varies from 1 to 3 dpf and ends usually when fish are 5 days old. These time preferences are usually representative of when the zebrafish are optically clear, making it amenable to visualize neuronal changes with either *in vivo* imaging or whole mount *in situ* hybridization or immunohistochemistry.

Overall, MPTP treatment has been linked to a decrease in *th* and *dat* transcript levels as addressed by *in situ* hybridization studies, as well as a decrease in TH immunoreactivity (Table 1.1). These changes are usually found in cells of the larval ventral diencephalon, but have also been detected in the pretectal, preoptic, hypothalamic, locus coerulius, olfactory bulb areas and in some of the serotonergic neurons of the paraventricular organ, across different studies (Table 1.1). MPTP has also shown to result in a decreased level in DA, NA and 5-HT neurotransmitter levels and to affect the development of GABAergic neurons (Souza *et al.* 2011; Sallinen *et al.* 2009). These phenotypes have been rescued in many cases with the administration of deprenyl or with the knockdown of the dopamine transporter (Table 1.1).

Despite reported efforts, no study has shown that MPTP induced cell death in the zebrafish via caspase co-locolization or with markers of DNA fragmentation such as with the TUNEL assay (Sallinen *et al.* 2009). Furthermore, it has been shown that despite a detectable neuronal and locomotor defect at 5 dpf, fish allowed to recover for 48 hours, free of MPTP, no longer show an affected phenotype at 7 dpf, further suggesting a transient effect on the neuronal population (Sallinen *et al.* 2009).

The locomotor phenotypes addressed in larvae treated with MPTP range from larval speed, total distance moved, response to touch and initiation of movement (Table 1.1) and are addressed using an array of different software such as the Noldus EthoVision and LSRtrack/analyse software as well as with manual data tracking and analysis.

The larval acclimatization periods prior to video recording vary anywhere from no acclimatization to 30 minutes, and video recordings last from 5 to 70 minutes which can be obtained under bright light or in dark with the use of an infrared camera, or with a combination of both light/dark cycles. Fish can be housed singly or in groups, and imaged in a watchglass, petri dishes, or multiwall plates of different sizes and shapes.

In summary, MPTP treated larvae show a hypokinetic phenotype, with a decrease in swimming speed, overall swimming distance, response to touch and initiation of movement episodes (Table 1.1), and some of these phenotypes have been rescued by the use of deprenyl and DA co-administration (Lam *et al.* 2005; McKinley *et al.* 2005; Souza *et al.* 2011).

Adult zebrafish have received MPTP either intraperitoneally (i.p.) or intramuscularly (i.m.) (Anichtchik *et al.* 2004; Bretaud *et al.* 2004). This administration regiment was sufficient to induce locomotor changes such as a decreased total swimming

distance and mean swimming velocity, in addition to a decrease in the neurotransmitters DA and NA. Despite such an effect, adult zebrafish showed no changes in the number or the arrangement of brain TH neuron populations or neuronal fibers following MPTP treatment, as has been shown by TH immunohistochemistry and western blotting. Combined with the lack of evidence for cell death, such as caspase-3 or TUNEL labeling, these evidences further suggest that MPTP is unable to induce DA neuron loss in adult zebrafish despite its ability to induce a locomotor phenotype (Table 1.1) and changes in neurotransmitter levels.

MPP^+ is the by-product of MPTP oxidation via the MAO-B. Unlike MPTP, MPP^+ does not cross the blood brain barrier (BBB) (Schmidt *et al.* 1997) and because of its polar characteristics, it depends on DAT to enter DAergic neurons (Dauer and Przedborski 2003). Larval administration of MPP^+ has been reported via water exposure of concentrations varying from 100 to 1000 μM starting when larvae were either 1 or 2 dpf and lasting until they were 4 days old (Table 1.1). Although MPP^+ does not cross the BBB, the zebrafish BBB is first detected when larvae are 3 dpf (Fleming *et al.* 2013). Overall, MPP^+ has been shown to decrease total swimming distance of larvae (Sallinen *et al.* 2009), mean velocity and percent of time spent moving with no effect on larval active velocity, which further suggests an effect on the initiation of movement but not on movement execution (Farrell *et al.* 2011). Similarly to MPTP, MPP^+ has been linked to a transient decrease in DA and NA neurotransmitter levels as well as a decreased TH immunohistochemistry of diencephalic DA neurons at 5 days but no longer at 7 dpf (Sallinen *et al.* 2009).

Adult zebrafish have received i.p. doses of MPP^+, but this resulted in no effect on fish locomotion with no recorded effects on brain dopaminergic neurons (Table 1.1). This could possibly be explained by the inability of MPP^+ to access the adult zebrafish brain, as these studies failed to look for the presence of this compound in the brain of tested animals such as by measuring levels of MPP^+ via high performance liquid chromatography (HPLC) (Bretaud *et al.* 2004).

6-OHDA closely resembles the structure of catecholamines and thus has a close affinity with catecholaminergic transporters such as DAT and NET (Dauer and Przedborski 2003). Because 6-OHDA does not readily cross the BBB it is in most cases injected stereotaxically into the nigro-striatal region of rats, mice, cats, dogs and monkeys (Blesa *et al.* 2012). In some instances, 6-OHDA is co-administered with a selective noradrenaline reuptake inhibitor to restrict neurotoxicity to dopaminergic neurons (Bové and Perier 2012). Although work has been done on the effects of 6-OHDA in larval zebrafish (Feng *et al.* 2014), further evidence is needed in order to properly understand the effects of 6-OHDA on DA neurons of larval zebrafish (Table 1.1).

The use of 6-OHDA in adult zebrafish has been limited to i.m. injections (Anichtchik *et al.* 2004). Although 6-OHDA is able to induce a locomotor phenotype described by a decreased total swimming distance and decreased mean velocity up to 6 days post treatment, this phenotype was no longer observable by day 9 (summarized on Table 1.1). Furthermore, despite a lack of staining for markers linked to cell death (such as TUNEL and caspase-3), immunohistochemistry and western blotting showed no differences in levels of Th despite a decrease in the levels of DA and NA from 1 to 9 days post treatment (Anichtchik *et al.* 2004).

It is still to be determined whether the lack of neuronal cell loss could be attributed to a weak bioavailability of 6-OHDA in the brain of adult zebrafish, as studies failed to look for 6-OHDA brain homogenates, for example, via HPLC analysis.

In our laboratory, we have attempted the direct injection of 6-OHDA into the adult zebrafish brain using either a cerebroventricular microinjection technique (Kizil and Brand 2011) or via stereotaxic injection into the zebrafish's posterior tuberculum (TPp). Although we were able to induce an observable locomotor phenotype (data not shown), both techniques are extremely invasive to the fish with high chances for non-specific tissue damage. During the procedure there is the need to generate a cranial incision which can lead to an open wound. This procedure is time-consumming and demands skill which makes it less amenable for neuronal ablation in multiple fish simultaneously when compared to other techniques which will be discussed later. Furthermore, due to the lack of a specialized zebrafish stereotaxic apparatus, the accuracy in reaching the desired site of injection can be highly variable from fish to fish.

The herbicide **paraquat** and the pesticide **rotenone** have also been used as environmental toxin models of PD. Because rotenone is a highly lipophilic compound it can cross the BBB and enter cells without the need of a specific transporter (Tieu 2011), while paraquat, whose structure resembles that of MPP^+ does not readily cross the BBB (Dauer and Przedborski 2003). Although rotenone and paraquat successfully induce PD-like pathology in rodent models such as the accumulation α-synuclein inclusions, as previously reviewed (Dauer and Przedborski 2003), exposure of larval zebrafish to these compounds resulted in neither a locomotor phenotype, nor in alterations in larval *th* cell populations (summarized in Table 1.1). Similar results were obtained with adult zebrafish

exposed to either chemical in their swimming water for up to 4 weeks (Bretaud *et al.* 2004). In addition, a 10 μg/L dose of rotenone has been shown to be lethal to the zebrafish, thus further reinforcing the role that rotenone has as a piscicide agent and highlighting its high toxicity to fish (Bretaud *et al.* 2004).

More recently, researchers have shown that chronic paraquat administration to adult zebrafish via i.p. injections is able to induce a locomotor phenotype such as a decrease in the total distance moved and mean velocity, despite showing no changes in Th protein levels (Bortolotto *et al.* 2014).

In addition to using neurotoxic models, **genetic models** of PD can also result in loss of dopaminergic neurons and locomotor phenotypes. These models include the knockdown of *parkin*, *PINK1*, *LRRK2*, *FBXO7* and β- and γ1-synucleins (Table 1.1). These models rely on the use of morpholino mediated gene knockdown, which are usually injected at the one-cell stage embryo. Unfortunately the effect of MOs is restricted to the early larval stages and last at the most up to 5 dpf, after which MO levels become too dilute and gene KD efficiency starts to decline. Thus, this approach shows little promise to be used in our study to address the regenerative ability of DA cells, as it is transiently effective.

Laser ablation is a useful approach to ablate specific cell types. Combined with the use of transgenic zebrafish lines, which label different cell populations with fluorescent markers, laser ablation can be employed to address the effects of single cell ablation and could be a means to study neuron regeneration. Indeed, in a recent article, dopaminergic neurons of diencephalic clusters 2, 4 and 5 have been laser ablated to study the role of these cell populations on larval locomotor behavior (summarized in Table 1.1)

(Jay *et al.* 2015). Current technology limits the use of this approach to larval zebrafish at stages when they are still optically clear (around 5 dpf). Furthermore, if a pigment free zebrafish line such as the casper fish (White *et al.* 2008) are not used, there may be a need to treat larvae with compounds to inhibit pigment formation such as 1-phenyl 2-thiourea (PTU) (Karlsson *et al.* 2001) which have been reported to cause side effects such as eye size reduction (Li *et al.* 2012b), suppression of thyroid hormone (Elsalini and Rohr 2003), alterations in retinoic acid and IGF levels (Bohnsack *et al.* 2011) and enhanced DA induced cell death (Higashi *et al.* 2000). Additionally, this procedure requires the immobilization and proper positioning of larvae, for example, by placing larvae into a drop of agarose and using an anesthetic such as MS-222 (Matthews and Varga 2012), which make this approach less amenable to mass processing.

An alternative approach that could fill the gaps in existing models for the ablation of DA neurons in both larval and adult zebrafish would be the use of a genetic conditional and specific cell ablation approach. These approaches could include the use of diphtheria toxin A (DTA), tamoxifen induced c-Myc^{ER} overexpression, caspase overexpression, HSV thymidine kinase/ganciclovir expression, M2 (H37A) toxic ion channel expression or via the nitroreductase enzyme expression (Curado *et al.* 2008; White and Mumm 2013).

Here, we opted to use the **nitroreductase cell ablation** approach, which has been shown to successfully ablate DA neurons of larval zebrafish diencephalic clusters 2 and 4 for the study of the role of these neurons on larval locomotor behavior (Table 1.1) (Lambert *et al.* 2012). This approach which allows for the permanent ablation of cells via an apoptotic process, confirmed in different studies by TUNEL staining and caspase

activation (Curado *et al.* 2007), is an ideal approach to address whether newly formed dopaminergic cell can be generated following neuronal loss and avoids possible misinterpretations caused by invasive cell damage methods.

Table 1.1. Summary of motor phenotypes following DA neuron damage in various zebrafish ablation models.

Model	Treatment Regiment	Type and Time of Motor Test	Results	Comments	References
Neurotoxins: **MPTP**	• Larvae • Exposed to 9 or 45 mg/L • From 1 to 5 dpf • Solutions changed daily	• Larval speed • 5 min recording following a 5 min acclimatization • Analysis conducted with DIAS 3.1 software • Analysis on 7 dpf larvae	• Decreased speed with both doses	• *th in situ* hybridization showed a decrease in diencephalic DA neurons with 45 mg/L but not with 9 mg/L dose analyzed at 5 dpf • No changes in th^{+} neurons in telencephalon or locus coeruleus	(Bretaud *et al.* 2004)
	• Larvae • Exposed to 100 or 1000 μM • From 1 to 4 dpf • Solutions changed daily	• Larval total distance swam • 10 min recording • Analysis conducted using EthoVision 3.1 • Analysis on 5, 6 and 7 dpf larvae in 48 well plate	• Decreased total distance moved only with 1000 μM dose at 5 and 6 dpf but no longer at 7-8 dpf	• TH immunohistochemistry showed a decrease in pretectal, diencephalic, preoptic and hypothalamic cell populations at 5 dpf but no longer at 7 dpf • There was a decrease in 5-HT neurons in the paraventricular organ and DA, NA and 5-HT neurotransmeter levels were decreased following 1000 μM dose at 5 dpf • Phenotype at 5 dpf was rescued by 100 μM deprenyl administration but not at 6 dpf	(Sallinen *et al.* 2009)
	• Larvae • Exposed to 800 μM • From 1 to 3 dpf	• Larval response to tactile stimulation • 30 min acclimatization • Test conducted at 3 dpf	• Weaker and shorter lasting trunk movement following touch stimulus	• *dat* and *th in situ* hybridization showed a decrease in diencephalic neurons at 2 and 3 dpf. • Neuronal population was rescued by 100 μM deprenyl administration	(Lam *et al.* 2005)
	• Larvae • Exposed to 5 and 10 μg/mL • From 1 to 4 dpf.	• Larval response to tactile stimulation (data not shown)	• At 5 μg/mL larvae moved slowly in response to touch while at 10 μg/mL larvae were immobile and non-responsive to touch.	• *dat* and *th in situ* hybridization showed a reduction in dopaminergic neurons in the pretectum and ventral diencephalon at 4 dpf. Olfactory bulb was also reduced and locus coeruleus neurons were marginally affected. • 100 μM deprenyl administration protected neurons from MPTP • DAT morpholino knowckdown prevented MPTP damage and allowed larvae to move in response to touch although still unable to swim away	(McKinley *et al.* 2005)
	• Larvae • Exposed to 0.1 and 1 μM • From 3 dpf to 5 dpf • Solution changed daily	• Larval initiation of movement regardless of distance and duration of movement • 30 min recording • Test conducted at 5 dpf in 24 well plate	• Both doses decreased the number of movements initiated by larvae	• TH immunohistochemistry showed an affect at pretectal DA cluster at 5 dpf whereas changes in diencephalon were not detectable • MPTP treatment resulted in a defective GABAergic neuron development • DA co-administration with MPTP rescued the number of movement episodes	(Souza *et al.* 2011)

Model	Treatment Regiment	Type and Time of Motor Test	Results	Comments	References
	• Adult • One dose of 150 or 225 or three doses of 75 mg/kg intraperitoneal (5 µL/g body weight) over one day • Dissolved in 0.9% NaCl	• Number of lines crossed in a 2-L tank filled with 1-L system water • Videos were recorded for 5 min from 0 to 6 days post injection	• Decreased line crossing at 225 mg/kg dose at days 2, 3, 5 and 6. No locomotor changes with other concentrations.	• TH immunohistochemistry showed no difference in dopaminergic neuron populations. • The 225 and 75 mg/kg drug treatments also resulted in increased opercular ventilation and darkened skin pigmentation	(Bretaud *et al.* 2004)
	• Adult • One 20 mg/kg dose injected intramuscularly 4-7 µL (0.5-0.7 g body weight) • Dissolved in 0.9% NaCl	• Distance moved, mean velocity and turning angle and zone preference • 10 min video recording following a 1 min acclimatization • Data was analyzed using EthoVision Pro 2.1 software at 1, 3, 6, and 9 days post injection	• Decreased in both total distances moved and mean velocity at days 1, 3 and 6 but no longer a statistically significant effect at 9 days post injection • Turning angle had a statistically significant increase only at 1 day post treatment • No statistically significant zone preference	• TH immunohistochemistry showed no difference in distribution, shape or number of TH^+ cells and axonal fibers • No differences were detected in TH levels using western blotting • There was no evidence of TUNEL nor caspase-3 labeling upon treatment • DA and NA levels were decreased from 1 through 12 days post injection • Histamine levels were increased at 1 day post treatment	(Anichtchik *et al.* 2004)
MPP^+	• Larvae • Exposed to 100, 500 and 1000 µM • From 1 to 4 dpf • Solution changed daily	• Larval total distance swam • 10 min video acquisition • Analysis conducted using EthoVision 3.1 at 5, 6 and 7 dpf in a 48 well plate	• Decrease in total distance moved with 500 µM at 5 and 6 dpf but no longer at 7 dpf. • 1000 µM only had an effect at 6 dpf.	• TH immunohistochemistry showed a decrease only in DA neurons of diencephalic cluster 1^b at 5 dpf with no longer an effect at 7 dpf • 1000 µM decreased DA and NA levels but not 5-HT • No effect on 5-HT immunohistochemistry	(Sallinen *et al.* 2009)

Model	Treatment Regiment	Type and Time of Motor Test	Results	Comments	References
	• Larvae • Exposed to 1mM • From 2 to 4 dpf.	• Larval mean velocity, active velocity and percent time moving • 10 min video recording • Analyzed using LSRtrack and LSRanalyse softwares. • 7 dpf larvae were imaged in 96 well plates.	• Decrease in both mean velocity and percent time moving but no effect on active velocity at 7 dpf	• Suggests that MPP^+ has an effect on the initiation of movement but not in their execution	(Farrell *et al.* 2011)
	• Adult • One dose of 75 mg/kg intraperitoneal (5 µL/g body weight) over one day • Dissolved in 0.9% NaCl	• Number of lines crossed in a 2-L tank filled with 1-L system water • Videos were recorded for 5 min from 0 to 6 days post injection	• No effect on locomotion	• Drug treatment resulted in increased opercular ventilation and darkened skin pigmentation	(Bretaud *et al.* 2004)
6-OHDA	• Larvae • Exposed to 0, 10, 50, 100 and 250 µM • From 2 to 4 dpf	• Swimming pattern, swimming distance and time spent at bottom of cuvette • 10 min video recording following a 2 min acclimatization • 5, 6 and 7 dpf larvae were imaged in 4.5x1x1 cm quartz cuvette	• Decreased swimming distance at 5, 6 and 7 dpf with 250 µM dose. The 100 µM dose had an effect only at 7 dpf • Increased time spent at bottom of cuvette at 5, 6 and 7 dpf with 250 µM dose	• TH immunohistochemistry was suggested by author to show a decrease in labeling following 250 µM dose, yet such labeling did not resemble previously published data on zebrafish TH labeling pattern • 100 µM vitamin E was suggested to rescue neuronal damage by immunohistochemistry and western blot at 5 dpf and shown to reverse total distance swam and time spent at bottom of 250 µM treated larvae to control levels at 5, 6 and 7 dpf (further analysis is needed to confirm findings) • 10 µM minocycline (microglia inhibitor) was shown to rescue 6-OHDA effect on swimming pattern, distance and time spent at bottom. Minocycline was also suggested to decrease expression of inflammatory genes (TNFα and *cd11b*) when co-administered with 6-OHDA • 2.5 and 25 µg/mL Sanemet was able to recover total distance moved at 5 and 6 dpf larvae but not at 7 dpf, and rescued the time larvae spent at bottom of cuvette at 5 dpf but not at 6 and 7 dpf	(Feng *et al.* 2014)

Model	Treatment Regiment	Type and Time of Motor Test	Results	Comments	References
	• Adult • One dose of 25 mg/kg injected intramuscularly 4-7 µL (0.5-0.7 g body weight) • Dissolved in 0.9% NaCl	• Distance moved, mean velocity, turning angle and zone preference • 10 min video recording following a 1 min acclimatization • Data was analyzed using EthoVision Pro 2.1 software at 1, 3, 6, and 9 days post injection	• Decreased velocity and total distance moved and increased turning angle at days 1, 3 and 6 post injection but no longer observable locomotor effects at 9 days post treatment • No statistically significant zone preference	• TH immunohistochemistry and western blotting did not show any differences in protein levels • No TUNEL nor caspase-3 evidence upon treatment • Decreased levels of DA and NA were maintained from 1 through 9 days post injection	(Anichtchik *et al.* 2004)
Paraquat	• Larvae • Exposed to 5 or 10 mg/L • From 1 to 5 dpf • Solutions changed daily	• Larval speed • 5 min recording following a 5 min acclimatization • Analysis conducted with DIAS 3.1 software • Analysis on 7 dpf larvae	• No effect on larval speed	• *th in situ* hybridization showed no difference in DA neuron population analyzed at 5 dpf but showed a non-statistically significant reduction in diencephalic DA neurons	(Bretaud *et al.* 2004)
	• Adult • Six intraperitoneal injections of either 10 or 20 mg/kg administered one injection every 3 days • 10 µL injection volume	• Number of line crossing, distance travelled, mean speed and time spent at different areas of tank were analyzed using ANY-maze software on 10 min videos recorded following a 30 s acclimatization period • Absolute turning angle was calculated based on 10 min videos from single fish swimming in a 20 cm round tank • Locomotor data were obtained 24 after each i.p. injection at days 1, 4, 7, 10, 13 and 16	• At 20 mg/kg there was a decrease in the number of lines crossed, total distance traveled and mean velocity of fish at all time points, while at 10 mg//kg a decrease was only observed at days 10, 13 and 16 • No difference in time spent on the upper portion of tank • 20 mg/kg paraquat resulted in a decrease in turning angle at all days except for day 10 and 16. While at 10 mg/kg larvae showed an increase in turning angle only at day 10	• Western blotting showed no change in levels of TH protein • Both treatments resulted in an increase in DA levels and a decrease in DOPAC • qRT-PCR showed a decrease in DAT gene expression at 10 mg/kg but not at 20 mg/kg • Y-maze test showed impaired acquisition and consolidation of spatial memory • No effect on social interaction	(Bortolotto *et al.* 2014)

Model	Treatment Regiment	Type and Time of Motor Test	Results	Comments	References
	• Adult • Exposure to 5 mg/L • For 4 weeks	• Number of lines crossed in a 2-L tank filled with 1-L system water • Videos were recorded for 5 min from 0 to 6 days post injection	• No effect on locomotion	• TH immunohistochemistry showed no difference in DA neurons • No effects on respiration nor skin pigmentation	(Bretaud *et al.* 2004)
Rotenone	• Larvae • Exposed to 5 or 10 µg/L • From 1 to 5 dpf • Solutions changed daily	• Larval speed • 5 min recording following a 5 min acclimatization • Analysis conducted with DIAS 3.1 software • Analysis on 7 dpf larvae	• No effect on larval speed	• *th in situ* hybridization showed no difference in DA neuron population analyzed at 5 dpf but showed a non-statistically significant reduction in diencephalic DA neurons	(Bretaud *et al.* 2004)
	• Adult • Exposure to 2 µg/L • For 4 week	• Number of lines crossed in a 2-L tank filled with 1-L system water • Videos were recorded for 5 min from 0 to 6 days post injection	• No effect on locomotion	• TH immunohistochemistry showed no difference in DA neurons • No effects on respiration nor skin pigmentation • 10 µg/L dose was lethal	(Bretaud *et al.* 2004)
Genetic: **PARK2 (*parkin*)**	• Larvae • MO[e] mediated KD[f]	• Total distance moved by spontaneously swimming larvae • 5 min recording following a 5 min acclimatization • Videos were analyzed using EthoVision Pro software • 5 dpf larvae were placed one per well in a 12 well plate for analysis	• No effect of total distance moved	• *th in situ* hybridization on 3 dpf larvae showed an approximate 20% decrease in diencephalic dopaminergic neurons • Decreased mitochondrial complex I activity • *aadc in situ* hybridization suggests no effect on serotonergic neurons of the Raphe nuclei • HuC and Islet1 immunostatining suggest no effect on other brain neuronal types nor spinal motor neurons	(Flinn *et al.* 2009)
	• Larvae • MO mediated KD	• Touch response and swimming behavior (data not shown)	• No effect on motor parameters	• *th in situ* hybridization and immunohistochemistry as well as quantitative PCR showed no differences in *th* levels at 3 dpf	(Fett *et al.* 2010)

Model	Treatment Regiment	Type and Time of Motor Test	Results	Comments	References
PARK6 (*PINK1*)	• Larvae • MO mediated KD	• Touch response at 3dpf (data not shown)	• Larvae did not swim away following tail touch	• General developmental delay was observed • TH immunohistochemistry showed a reduction in diencephalic neurons at 2 dpf • 5-HT immunohistochemistry showed not effect on this neuronal subgroup • Decreased immunostaining for Islet1 and acetylated tubulin suggest an effect on peripheral neurons	(Anichtchik *et al.* 2008)
	• Larvae • MO mediated KD	• Average speed and swimming pattern • 10 min recording • Analysis conducted using EthoVision 3.1 software • Analysis on 5 dpf larvae in 48 well plate	• No effect on locomotor parameters	• *th in situ* hybridization and immunohistochemistry showed a decrease in diencephalic neuronal populations at 5 dpf • *dat in situ* hybridization showed no difference in *dat* expressing cells • Immunohistochemistry showed no effect on serotonergic nor cholinergic systems • qPCR showed a decrease in *th1* and *th2* levels but not in *dat* nor *hdc*	(Sallinen *et al.* 2010)
	• Larvae • MO mediated KD	• Larval response to tactile stimulus at 3 dpf analyzed with ImageJ software • Larval swimming distance at 5 dpf analyzed with manual tracking of 90 second videos obtained following a 10 min acclimatization period	• Reduced response to tactile stimuli at 3 dpf • Reduced swimming distance at 5 dpf	• 10 μM SKF-38393 administration rescued larvae's response to touch • *th in situ* hybridization showed no difference in the number of DA neurons in the ventral diencephalon at 3 and 5 dpf but a reduction in DA neurons in diencephalic group 1 • Ventral diencephalic neurons were disorganized and asymmetrical	(Xi *et al.* 2010)
PARK8 (*LRRK2*)	• Larvae • MO mediated KD	• Larval distance moved • 30 second videos of 6 dpf larvae were analyzed using ImagJ software	• Decreased distance moved	• 1mM L-DOPA administration rescued locomotor defect • *th* and *dat in situ* hybridization showed a decrease in diencephalic DA neurons at 3 dpf • Western blot and qPCR analysis showed decreased TH expression	(Sheng *et al.* 2010)

Model	Treatment Regiment	Type and Time of Motor Test	Results	Comments	References
	• Larvae • MO mediated KD	• Response to tactile stimulus at 3 dpf analyzed with ImageJ software • Number of line crossings of 6 dpf larvae based on 5 min video recordings taken 10 min following aclimatization	• No locomotor phenotype was observed	• *th* and *dat in situ* hybridization showed no difference in neuronal cells	(Ren *et al.* 2011)
PARK15 (*FBXO7*)	• Larvae • MO mediated KD	• Larval swimming velocity at 4 dpf • Larvae were placed one per well in a 96 well plate and allowed to acclimatize for 15 min • Ethovision XT software was used to analyze data of videos taken of larvae during 3 alternating cycles of 10 min under white light and 10 min under darkness	• Severely effected larvae rarely showed motor activity • Moderately effected larvae showed decreased swimming velocity at 4 dpf	• Apomorphine co-administered with domperidone (3μM each) allowed for the improvement in swimming speed of morphant larvae • *th* and *dat in situ* hybridization showed a decrease in dopaminergic neurons in the diencephalic area	(Zhao *et al.* 2012)
β- and γ1-synucleins	• Larvae • MO mediated KD	• Displacement of spontaneously moving larvae • 15 larvae were place per well of a 12 well plate and analyzed for 8 hours daily from 2 to 7 dpf • Data was analyzed using Zebralab software	• β KD, γ1 KD and β and γ1 combined KD resulted in a decrease in swimming activity at 2 and 4 dpf but not at 3 dpf • A statistically significant reduction in swimming activity was only observed when both β and γ1 were KD at 5 and 6 dpf • Swimming activity was no longer effected at 7dpf	• *dat in situ* hybridization showed that β and γ1 combined KD resulted in a significant decrease in dopaminergic neurons at 2 dpf but no longer at 3 dpf • DA levels were reduced on larvae with the combined β and γ1 KD at 7 dpf with no changes in 5-HT levels	(Milanese *et al.* 2012)

Model	Treatment Regiment	Type and Time of Motor Test	Results	Comments	References
Chemogenetic ablation: **Nitroreductase**	• Larvae • Conditional cell ablation by Metronidazole administration starting with 5mM at 24 hpf and 10mM from 2 to 3 dpf • Ablation of orthopedia b^{+} DAnergic neurons located in DC clusters 4 and 6	• Total distance travelled and episode duration of free swimming 5 day old larvae • 10 larvae were placed in a 50 mm glass watch and allowed to rest for 5 min prior to a 10 min video acquisition • Data was analyzed using Ctrax software	• Ablation of DC 4 and 6 significantly reduced the total distance moved by larvae and increased the time of episode duration	• Immunohistochemistry for TH and GFP (endogenously expressed in DC clusters 4 and 6 by transgenic animals used Tg(*otpb.A:nfsb-EGFP*)) showed a decrease in both markers at 5dpf • *dat in situ* hybridization showed absence of staining at 3dpf • Increased TUNEL labeling and co-locolization with GFP expression	(Lambert *et al.* 2012)
Physical ablation: **Laser**	• Larvae • 20 to 30 seconds irradiation with 405nm laser at 50mW • Ablation of DC2 at 20-24 hpf and of DC 2,4 and 5 at 30-32 hpf on *ETvmat2: GFP* transgenic zebrafish	• Total distance swam, percent of time spent swimming, duration and mean velocity of bouts of beat-glide episodes at 4 dpf • Recordings were conducted in a dark chamber with infrared illumination • Fish were recorded individually for 10 min following a 15 min acclimatization period • Data analysis was done using Ctrax and JAABA software	• DC2 ablation resulted in decreased total distance swam, with a decreased time spent swimming • DC2 ablation had no effect on mean peak velocity nor movement duration during beat and glide episodes • Similar results were obtained with DC 2, 4 and 5 ablation	• Endogenous GFP expression and TH immunohistochemistry showed reduction in labeling of DC2, 4 and 5 cells	(Jay *et al.* 2015)

1.4 Nitroreductase mediated cell ablation

The use of nitroreductase (NTR) mediated cell ablation dates back to the mid 1990's when scientists started to use this approach to kill mammalian tumor cells (Bridgewater *et al.* 1995) for cancer gene therapy (Searle *et al.* 2004). The nitroreductase enzyme is encoded by the *nfsB* gene found in *Escherichia coli* and is a dimeric flavoenzyme that is reduced by either NADH or NADPH (Christofferson and Wilkie 2009). When in its reduced state, NTR can reduce nitroaromatic or quinone substances and is thus capable of converting non-toxic compounds such as CB1954 and metronidazole (Mtz) into a DNA cross-linking compound resulting in cell death through an apoptotic pathway (Wong and Zohar 2015; Searle *et al.* 2004; Pisharath and Parsons 2009).

In 2007, two laboratories pioneered the use of this ablation approach as a tool for cell specific ablation and regenerative studies in the zebrafish (Curado *et al.* 2007; Pisharath *et al.* 2007). Since then, this NTR based approach has been employed for the ablation of zebrafish cells such as pancreatic β cells (Pisharath *et al.* 2007; Moss *et al.* 2013), podocytes (Huang *et al.* 2013; Zhou and Hildebrandt 2012), skin cells (Chen *et al.* 2011), oocytes (White *et al.* 2011), germ cells (Dranow *et al.* 2013), cardiac cells (Curado *et al.* 2007; Zhang *et al.* 2013), osteoblasts (Singh *et al.* 2012b) and oligodendrocytes (Chung *et al.* 2013) in both larval and adult zebrafish.

The nitroreductase ablation method offers many advantages that make it ideal for regenerative studies. The fact that NTR can be expressed in specific cell populations by using cell specific gene regulatory elements makes this a tissue specific ablation method

whose ablation can be temporally controlled by the addition of a pro-drug such as metronidazole (Mtz) (Fig 1.3). Although the previously used pro-drug CB1954 has been shown to damage neighboring cells to intended targeted NTR expressing cells, the toxicity of Mtz is restricted to NTR expressing cells and thus shows no bystander effect (Curado *et al.* 2008).

The ability to create NTR-fluorescent protein fusions is also an advantage that allows for the *in vivo* tracking of cell ablation and regenerative processes. This, combined with the easy administration of the pro-drug Mtz which can be done via water exposure, allows for the ablation of zebrafih cells in large numbers of fish, which is a useful tool in studies such as large library drug screens which require high-throughput processing.

Unlike other methods such as thymidine kinase/ganciclovir, which require cellular division in order to kill cells, the NTR method is cell cycle independent. This is an ideal approach to kill non-dividing cells such as neurons. The use of NTR in the ablation of neurons has been reviewed to kill rods, cones and bipolar cells (Gemberling *et al.* 2013). Due to the ability of Mtz to cross the blood brain barrier (Nau *et al.* 2010) and access the brain, a number of brain cells have been successfully ablated by NTR/Mtz in the zebrafish including cells of the habenula, pineal gland, serotonergic and dopaminergic neurons, as is summarized in Table 1.2.

Here we opted to use the nitroreductase-metronidazole mediated cell ablation method to kill dopaminergic neurons in both larval and adult zebrafish in order to characterize the phenotype of fish lacking these cells and to address the regenerative potential for DA neurons at both larval and adult stages.

Figure 1.3. Nitroreductase mediate cell specific ablation. Nitroreductase expression can be targeted to specific cell populations using tissue specific gene regulatory elements. Here, the zebrafish's *dat cis*-regulatory elements, which endogenously lead to the production of DAT in DA neurons (purple), are used to drive the CFP (cyan) and NTR (orange) fusion protein. Upon administration of Mtz (pink), which is readily available to all cells, NTR reduces Mtz into a cytotoxic DNA crosslinking compound leading to DA neuron loss. Although Mtz is available to all cells, cells that do not use the *dat cis*-regulatory elements and consequently do not produce the CFP-NTR fusion will remain unaffected (cell depicted on the right).

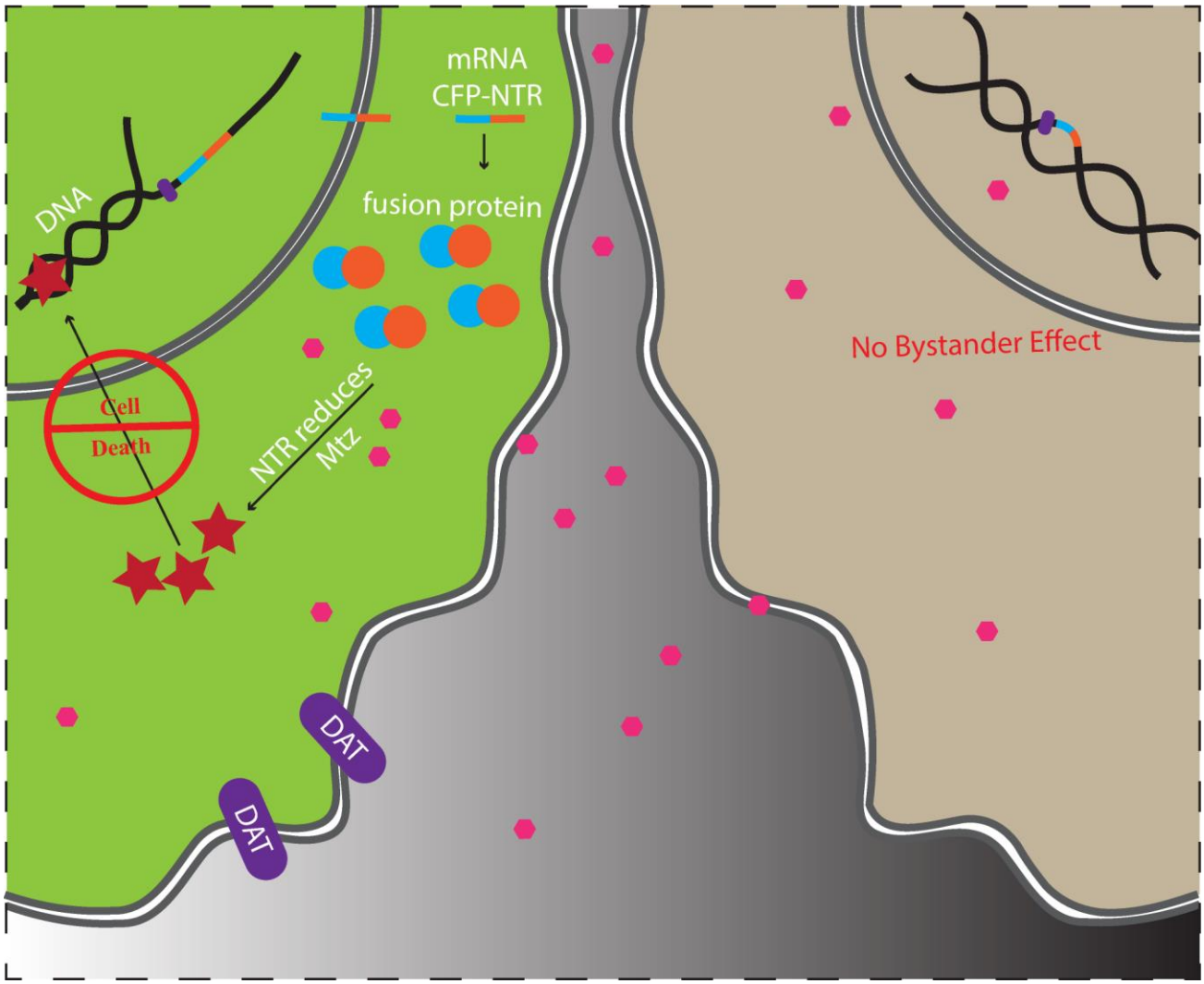
mRNA
CFP-NTR
fusion protein
DNA
Cell
Death
NTR reduces
Mtz
DAT
DAT
No Bystander Effect

Table 1.2. Larval and adult zebrafish brain cell ablation using the nitroreductase enzyme.

Targeted Cells	Transgenic Fish Used	Treatment	Comments	References
Habenular cells	Tg(*narp:GAL4VP16*;*UAS:nfsβ-mCherry*)	Larvae: 5 day old larvae were exposed to 10mM Mtz for 24 hours Adult: fish were exposed to 10mM Mtz in 0.2% DMSO for 24 hours	Cell death confirmed through TUNEL assay	(Agatsuma *et al.*, 2010)
Hypocretin neurons	Tg(*hctr:nfsβ-EGFP*)	Larvae: at 1 dpf larvae were exposed to 15mM Mtz for 48 hours	Loss of EGFP signal and hctr staining via in situ hybridization	(Elbaz *et al*., 2012)
Serotonergic neurons of the Dorsal Raphe	Tg(*tph2:nfsβ-mCherry*)y226	Larvae: at 3 dpf larvae were exposed to 10mM Mtz for 48 hours	Cell death was confirmed through TUNEL assay and live marker for caspase-3 like activity	(Yokogawa *et al*., 2012)
Brain neuronal cells	Double transgenic animals for NeuroG4-mCherry (a Gal4 enhancer trap line MU4465 labeling central nervous system and UAS-NTR-mCherry line)	Larvae: 5 dpf treated with 2mM Mtz (in DMSO) for 16 hours	Cell death confirmed through TUNEL assay	(van Ham *et al*., 2014)
Pineal and DA neurons	Pineal ablation was done using Tg(*tph2:nfsβ-mCherry*)y227; Ablation of preoptic, posterior tuberculum and hypothalamic Otp^{+} neurons were ablated using Tg(*otpb.A:Gal4*)zc67; DA cell ablation of DC 2 and 4 as well as DA groups 3,5,6,7 and a subset of LC neurons were ablated using double transgenics between Tg(*BAC th:Gal4VP16*)m1233 and Tg(*UAS-E1b:nfsβ-mCherry*)	Larvae: for pineal ablation, 1 day old larvae were exposed to 10mM Mtz for 48 hours All other ablations were conducted by exposing 3 day old larvae to 7.5mM Mtz for 24-36 hours	Changes in endogenous fluorescent protein expression and immunohistochemistry were used to show cell loss	(Fernandes *et al.*, 2012)
DA neurons of DC 2 and 4	Tg(*otpb.A:nfsβ-egfp*)	Larvae: at 24 hpf larvae were incubated in 5mM Mtz for 24 hours followed by an incubation in 10mM Mtz from 48 to 96 hpf	Cell death was confirmed with TUNEL staining	(Lambert *et al*., 2012)

1.5 Expression of NTR in DA neurons of the zebrafish brain

Different regulatory elements have been used to drive the expression of reporter genes in DA neurons of the zebrafish brain. An enhancer trap transgenic line *ETvmat2:EGFP* where EGFP has been inserted into the second intron of the *vesicular monoamine transporter2* (*vmat2*) gene (Wen *et al.* 2008), fluorescently labels arch associated neurons, sympathetic neurons, and cells of the locus coeruleus, ventral midbrain, posterior tuberculum, telecephalon, paraventricular organ of the posterior tuberculum, hypothalamus, pretectum, retina and epiphysis. In addition to the fact that not all of the labeled cells of the *ETvmat2:EGFP* line are DAergic, this is an enhancer trap line, which makes it difficult to generate new lines with the non-characterized regulatory elements of the *vmat2* gene.

A screen to identify enhancers which could be used to label dopaminergic neurons of the zebrafish has looked at 21 genes with putative roles in either the specification of DA neurons (such as the transcription factors *lmx1a.2*, *neurogenin*, *nr4a2a* (also known as *nurr1* in mammals), *otpa, otpb* and *pitx3*) or with genes involved in the regulation and function of DA neurons (such as *dat, aadc*, *th*, and *vmat2*)(Fujimoto *et al.* 2011). Although many of these putative regions failed to label and did not express a fluorescent reporter within the majority of zebrafish *th* expressing DA neurons in the brain simultaneously, this analysis led to the characterization of the *otpb.A* enhancer as a way to label Th positive neurons of the diencephalon (Fujimoto *et al.* 2011), and lines using these regulatory elements have been used in studies looking at DA neurons of DC 2 and 4 (Fernandes *et al.* 2012; Lambert *et al.* 2012).

Another transgenic line introducing a Ras membrane-anchored EGFP has been generated by placing the fluorescent reporter into a BAC containing 154kb including the upstream region and most of the sequence for the zebrafish *th* gene. This has been shown to label all positive cells for Th immunoreactive catecholaminergic clusters in the larval zebrafish (Tay *et al.* 2011). Neither the *th:rasGFP* nor the Tg(*BAC th:Gal4VP16)m1233* fish (Tay *et al.* 2011; Fernandes *et al.* 2012) which use these regulatory elements existed at the time when our experiments were first designed and were therefore not used here.

Previous work done using different *slc6a3* genomic fragments failed to induce the expression of a reporter gene in all of the DA clusters of the zebrafish brain simultaneously in either the Tg(*slc6a3[7kb]:egfp*) or Tg(*slc6a3[11kb]:egfp*), where the 11kb fragment led to expression of GFP in the pretectum and the 7kb led to GFP expression mainly in the habenula, hypothalamus and medulla of adult fish (Bai and Burton 2009). We have generated in our laboratory the Tg(*dat:EGFP*) line which uses a 13kb upstream genomic region and most of the zebrafish *dat* sequence to drive the expression of GFP in most of the DA neuron clusters of the zebrafish brain (Xi *et al.* 2011b) (Fig. 1.4). These *dat cis*-regulatory elements, which have also been used to drive the expression of mitochondrial-targeted mCherry in DA neurons of the zebrafish in the Tg(*dat:tom20 MLS-mCherry*) (unpublished data) (Fig. 1.4) were our choice to drive the expression of NTR in both larval and adult zebrafish brain DA neurons.

Figure 1.4. Transgenic fish using *dat cis*-regulatory elements. We have generated 3 lines using the dopamine transporter *cis*-regulatory elements of zebrafish to drive expression of different reporters in DA neurons of the zebrafish, including the expression of GFP (left), CFP-NTR fusion (middle) and mCherry targeted to the mitochondria (right).

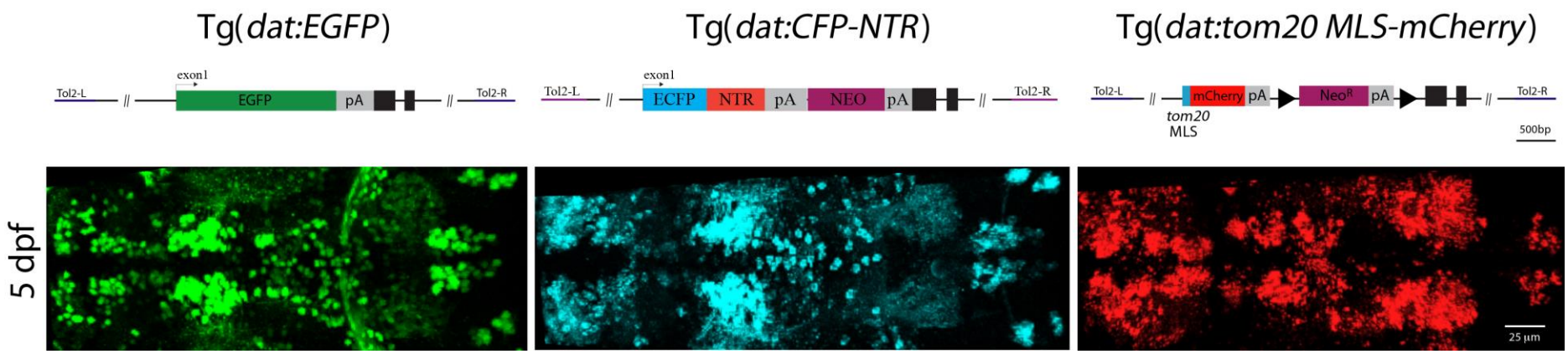
Tg(dat:EGFP)
Tg(dat:CFP-NTR)
Tg(dat:tom20 MLS-mCherry)
exon1
Tol2-L
EGFP
pA
Tol2-R
ECFP
NTR
NEO
mCherry
NeoR
tom20
MLS
500bp
5 dpf
25 µm

1.6 Animal models of brain DA neuron regeneration

The regeneration of DA neurons has been addressed in different animal models including the planaria, salamander and mouse (see Table 1.3).

DA neuron regeneration in the planaria has been addressed following neuronal damage using the neurotoxin 6-OHDA and was dependent on neoblast recruitment shown migrate from the trunk and repopulate DA cells in the dorsal region of the brain near the location where cells were lost, starting at 4 days-post-lesion (dpl) and fully recovering by 14 dpl (Nishimura *et al.* 2011). This recovery process which was also observed with DA levels and locomotor phenotype, was inhibited by X-ray irradiation (Nishimura *et al.* 2011), a process known to disturb neurogenesis and cell proliferation (Monje *et al.* 2002; Isono *et al.* 2012). In addition, a 5-FU study conducted by the same group suggests that proliferating stem cells pass through their S-phase 5 to 10 days prior to differentiating into DA neurons in the planarian brain. Indeed, Nishimura and colleagues suggest that some cells which enter S-phase in the trunk migrate to the head in the G2-phase where they respond to environmental clues to acquire a dopaminergic fate (Nishimura and Agata 2012).

Similar to the planaria, regeneration studies conducted on the dopaminergic system of the salamander rely on data obtained from the ablation of DA neurons using 6-OHDA (Parish *et al.* 2007). Parish and colleagues demonstrate that the salamander is able to fully regenerate mesencephalic and diencephalic DA neurons, which are neurons proposed to be homologous to those in the ventral tegmentum and substantia nigra areas of mammals, by 30 days post lesion and to also recover their locomotor phenotype (Table

1.3). This regenerative ability is dependent on $GFAP^{+}/Sox2^{+}$ quiescent ependymo-glial cells that migrate from the third ventricle into the area of neuron loss and give rise to DA neurons, a process that is inhibited by the administration of the anti-mitotic drug β-D-arabinofuroside (Parish *et al.* 2007). Furthermore, the involvement of Nurr1, engrailed1, Th and Msx1/2 in the process of the newt DA neuron regeneration is similarly observed in DA neuron development and neurogenesis in mammals (Parish *et al.* 2007).

More evidence from the laboratory of Dr. Andras Simon further suggests that the neurotransmitter dopamine negatively regulates the proliferative ability of ependymo-glia lining the newt's ventricle by acting on the D2 receptor expressed on ependymo-glia cells, thus inhibiting DA neuron regeneration (Berg *et al.* 2011). This leads to a model where quiescence of ependymal cells are kept under the control of DA, and when DA neurons are lost and DA is decreased there is a stimulus to induce proliferation and to form new DA neurons, which in turn form a loop that terminates the regenerative process and again, regulates the quiescence of ependymal cells (Berg *et al.* 2011; Berg *et al.* 2013).

DA neuron regeneration has also been proposed to take place in the substantia nigra of MPTP treated mice, 3 weeks following DA neuron damage (Zhao *et al.* 2003) (Table 1.3). Currently, these findings remain controversial as another group was unable to observe newly formed DA neurons in the adult mammalian SN following a 6-OHDA neuron ablation protocol (Frielingsdorf *et al.* 2004). Additional research shows the incorporation of BrdU in the SN of rodents as reviewed by Mochizuki (2011), although none of these cells have been shown to acquire a dopaminergic fate and the majority became microglia (Mochizuki 2011). Overall, more research is needed to determine if

mammals posses the endogenous ability to regenerate their DA population following damage to the SN.

More recently, scientists have demonstrated the regeneration of DA cells in the rodent olfactory bulb (Table 1.3) (Lazarini *et al.* 2014). Lazarini and colleagues show that following stereotaxic injection of 6-OHDA into the dorsal area of the OB, mice are able to recover their Th positive neuronal population within 56 dpl and are able to recover olfactory related behavior phenotypes within 2 months. This process is shown to increase microglial activation and proliferation, and in addition regeneration is said to be dependent on the recruitment of immature neurons to the glomerular layer with a significant number of new OB neurons originating from the SVZ (Lazarini *et al.* 2014).

Althought the zebrafish has been used to study the recovery process following brain injury (summarized in section 1.7), to our knowledge, there is no information regarding the regenerative ability of DA neurons following the specific loss of DA cells in the zebrafish brain. Understanding the regenerative ability of DA cells in the zebrafish brain will complement the knowledge obtained based on other models such as the salamander and the planaria and potentially lead to the identification of novel processes which have not been yet addressed. Here we opt to study DA neuron regeneration in the zebrafish due to the strength of the zebrafish as a model for regeneration and the molecular toolbox available to the zebrafish community which counts with the availability of transgeneic zebrfish lines such as the Tg(*dat:EGFP*) which allows for the labeling of DA neurons and the Tg(*nestin:GFP*) which allows for the labeling of neuron progenitor/stem cells. Using these tools scientists can track the regenerative process in the zebrafish brain *in vivo*.

Table 1.3. Different models of brain DA neuron regeneration.

Organism	DA neuron ablation approach	Regeneration	Comments	References
Planaria	6-OHDA	New TH cells were seen 4 days following ablation in the dorsal region of the brain and cell numbers were completely back to wild-type levels by 14 dpl[a]	• Regeneration dependent on neoblasts (pluripotent stem cells) • X-ray irradiation inhibited regenerative ability • Majority of newly formed DA neurons were BrdU negative • DA levels and locomotor phenotype recovered by 5 dpl	(Nishimura et al. 2011)
Salamander	Stereotaxic injection into 3rd ventricle of 6-OHDA	TH cell population was fully recovered in diencephalon and mesencephalon by 30 dpl	• Locomotor phenotype recovery at 30 dpl • BrdU shows an increased proliferative response 7 and 10 dpl • Regeneration is dependent of $GFAP^+$/ $Sox2^+$ ependymoglial cells which migrate from 3rd ventricle, by 13 dpl are found in deep layers and further mature into DA neurons • Nurr1, engrailed1, TH and Msx1/2 expression profile follow mammalian DA neuron development and DA neurogenesis pattern • Regeneration inhibited by the use of β-D-arabinofuroside	(Parish et al. 2007)
Mouse	Subcutaneous injection of MPTP	Increase in $BrdU^+$ and TH^+ cells in the substantia nigra 3 weeks following MPTP administration	• Two fold increase in BrdU labeling in TH^+ cells • New neurons formed 3 weeks following lesion • No changes in BrdU labeling in the subgranular zone of the DG	(Zhao et al. 2003)
Mouse	Injections into the dorsal glomerular layer (in the OB) 6-OHDA	TH^+ cells in the OB were fully recovered 56 days after 6-OHDA treatment	• Olfactory behavioral response recovered within 2 months • Microglia activated neuro-inflammatory response at the site of injury 7 dpl. Microglia proliferation was increased at 7 dpl with no changes in neuronal precursors nor oligodendrocyte progenitor proliferation • Regeneration dependent on recruitment of immature neurons to the GL • Significant number of new OB neurons originate from SVZ	(Lazarini et al. 2014)

1.7 Zebrafish as a model for the study of neurogenesis and brain regeneration

The adult zebrafish brain has a tremendous capacity for neurogenesis and its brain is filled with areas of resident mitotic cells, known as proliferation zones. These proliferation zones span the rostral-caudal axis of the zebrafish brain in areas of the olfactory bulb, telencephalon, preoptic area, hypothalamus, optic tectum, medulla oblongata and cerebellum (Zupanc *et al.* 2005).

When compared to the mammalian brain, which has two major proliferation zones, the subventricular and the subgranular zone (Ming and Song 2011), the 16 different proliferation zones of the zebrafish brain (Grandel *et al.* 2006) contribute to the highly prolific nature of the zebrafish brain with approximately 6000 new cells being born within 30 minutes corresponding to on average about 0.06% of the total cells in the teleost brain (Hinsch and Zupanc 2007), rates which are about two fold higher than those calculated in the rodent brain, as previously reviewed (Zupanc 2008).

The cells in these proliferation zones hold stem cell-like properties and are highly heterogeneous in nature especially across different brain regions. Unlike mammals, the proliferation zones of the zebrafish lack a continuous ependymal layer (as reviewed by (Schmidt *et al.* 2013; Ferretti and Prasongchean 2015)). The cells residing in these zones can be quiescent or slowly dividing, they can have cilia or be aciliated, some of these cells may be oligodendrocyte precursors (OPCs) others may or may not express glial cell markers such as GFAP; whereas these GFAP positive radial glial cells (RGCs) are said to be major players in adult brain neurogenesis with the ability of self-renewal and to form new neurons (for more in depth review and original articles please refer to (Grandel *et al.*

2006; Adolf *et al.* 2006; Chapouton *et al.* 2007; Kaslin *et al.* 2008; Lindsey *et al.* 2012; Schmidt *et al.* 2013; Kizil *et al.* 2012c; Ferretti and Prasongchean 2015; Pellegrini *et al.* 2007; März *et al.* 2010; Lam *et al.* 2009; Ito *et al.* 2010; Kaslin *et al.* 2013; Kaslin *et al.* 2009; Rothenaigner *et al.* 2011; Grandel and Brand 2012)).

The regenerative ability of animals was described by the presence of two main types of regeneration: epimorphic and morphallaxis, which are defined by the presence or absence of a blastema (Agata *et al.* 2007). Epimorphic regeneration relies on cell proliferation and on the formation of a blastema to give rise to a new tissue and differs from morphallaxis regeneration which relies minimally on cell proliferation and gives rise to new tissue based on the remodeling of already existing tissue (Bely and Nyberg 2010). Currently, due to the advances in the understanding of CNS regeneration, a new type of regeneration has been proposed and named interstitial regeneration where new neurons arising from stem and progenitor cells replace lost neurons in an already existing tissue (Becker and Becker 2015).

In the zebrafish, regeneration of brain tissue relies on the activation and migration of stem/progenitor cells to the site of injury and re-integration of newly formed neurons into an already existing tissue. Brain lesion studies in the adult zebrafish using techniques such as stab wound (Kroehne *et al.* 2011) or the injection of excitotoxic compounds such as quinolinic acid (Skaggs *et al.* 2014) have suggested that radial glial progenitors are the major contributors to the formation of new neurons following injury. These stab lesion studies contribute vastly to the knowledge of brain regeneration as we know it today. Findings based on this approach suggest that following injury there is a transient activation of microglia and OPCs locally as a means of removal of cellular debris

(Schmidt *et al.* 2013). In addition, reactive gliosis and inflammation are transient effects without the formation of scar tissues unlike in mammals (Ferretti and Prasongchean 2015; Baumgart *et al.* 2011; März *et al.* 2011; Kroehne *et al.* 2011) an attribute that grants the zebrafish its great regenerative ability (Godwin *et al.* 2014; Kizil *et al.* 2012b).

The inflammatory response following the stab lesion is suggested to be required and sufficient for inducing proliferation and neurogenesis in the injured zebrafish brain, which is contrary to the negative impact that inflammation has on neurogenesis in the mammalian brain (Kyritsis *et al.* 2012).

Further studies trying to uncover the molecular mechanisms of brain regeneration have also relied on data obtained from stab wound studies. This has allowed scientists to identify the activation of genes and elements, such as the transcription factor *gata3* which is essential but not sufficient to drive neurogenesis (Kizil *et al.* 2012c). *gata3* expression starts at 1 dpl in non-proliferating radial glial cells, peaking at 3 dpl and lasting until 7 dpl and is implied to play a role in the proliferation of RGCs (Kizil *et al.* 2012c). Another gene identified, *cxcr5*, which encodes a chemokine receptor, has been found in RGCs and is shown to also play a role in the proliferation of these cells and to be required for the differentiation of RGCs into neurons (Kizil *et al.* 2012a). Expression of *id1* (*inhibitor of DNA binding 1)* gene is involved in the maintenance of the stem cell pool in the injured zebrafish brain independent of an inflammatory response (Viales *et al.* 2015), while the *cysltr1 (cysteinyl leukotriene receptor 1)* gene is induced following brain lesion as part of an inflammatory response and a way through which leukotriene can increase the proliferation of RGCs (Kyritsis *et al.* 2012).

In addition to these regeneration specific changes, there are signals known to play a role during development, such as fibroblast growth factor (Fgf) and Notch, which also modulate regerative neurogenesis (as reviewed by (Becker and Becker 2015)). Thus recent findings suggest that in addition to regeneration specific genes and responses, elements that recapitulate aspects of development can be reactivated during the process of regeneration.

Overall, these brain injury experiments suggest that in the zebrafish, brain injury leads to an initial increase in necrotic and apoptotic markers within the first day post lesion, followed by a microglial and oligodendrocyte activation from 1 to 3 dpl, an increase in cell proliferation (mainly RGCs) within days 2-5 post lesion, resulting in the integration of new neurons at the site of injury within 21-35 dpl (Kishimoto *et al.* 2012; März *et al.* 2011; Kroehne *et al.* 2011; Skaggs *et al.* 2014; Baumgart *et al.* 2011).

Although much can be learned about the regenerative process from these lesion experiments, it is important to consider the possibility that secondary effects following this invasive procedure could influence the regeneration of brain neurons in the zebrafish (Goessling and North 2014). Stab lesions are invasive procedure that non-specifically affects neurons, glia, stem and progenitor cells, blood vessels and overall the global arrangement of the zebrafish brain. This process could differ greatly from the regenerative process observed based on less invasive and more cell specific techniques such as chemogenetic ablation methods which would more closely model the environment observed in the brain of patients suffering from neurodegenerative conditions such as Parkinson's disease. Thus, we aim to study the regenerative ability of the zebrafish from the perspective of a neuron specific ablation approach.

1.8 Objectives and hypothesis

Given the achieved and ongoing advancements made in the field of brain neuron regeneration gathered from zebrafish brain lesion experiments, along with the advantages of using zebrafish in neurogenesis and regeneration studies as a model for human disease (discussed previously on sections 1.3 and 1.7), the aims of this thesis are to: 1) generate a conditional and specific ablation method to kill dopaminergic neurons in both the larval and adult fish brain and 2) to address the endogenous regenerative ability of the zebrafish to recover lost DA neurons. Here, I hypothesize that following DA neuron loss there will be an increase in cell proliferation and recruitment of precursor cells that will acquire a dopaminergic characteristic to replace lost cells in the brains of both adult and larval zebrafish.

The primary goal of my work is to generate a transgenic zebrafish line expressing the cyan fluorescent protein–nitroreductase fusion protein in dopaminergic neurons by using the zebrafish dopamine transporter *cis*-regulatory elements. Using this transgenic line, I will optimize an ablation protocol with the pro-drug metronidazole, which will be used to address the locomotor/behavior phenotype of both larval and adult zebrafish following DA neuron loss.

Once a successful ablation protocol is achieved and cells are confirmed to be ablated, by showing changes in CFP as well as in other markers of DA neurons such as *dat* and Th, in combination with markers for apoptosis (active caspase-3), I will determine if these neurons can regenerate by tracking changes in CFP cell population as well as by labeling proliferating cells with BrdU for pulse-chase experiments.

To our knowledge, there is no study addressing the regenerative ability of DA neurons in the zebrafish following a tissue specific ablation protocol. This study will allow for the elucidation of the cellular and molecular mechanisms driving DA neuron regeneration, including changes in cell proliferation and gene regulation.

Furthermore, this model will allow for the understanding of the potential differences in regenerative processes governing regeneration in a cell specific manner versus in the context of more invasive and global tissue damage approaches such as stab wound.

This zebrafish model will be useful in the screening of genes, pharmaceuticals or elements that may regulate DA neuron regeneration. It is hoped that in the future, these molecules identified in the zebrafish may lead to potential therapeutic approaches for human conditions requiring DA neuron repair, as is the case in Parkinson's disease patients.

CHAPTER 2

CHEMOGENETIC ABLATION OF DOPAMINERGIC NEURONS LEADS TO TRANSIENT LOCOMOTOR IMPAIRMENTS IN LARVAL ZEBRAFISH

2.1 Abstract

To determine the impact of a controlled loss of dopaminergic neurons on locomotor function, we generated transgenic zebrafish, Tg(*dat*:*CFP-NTR*), expressing a cyan fluorescent protein-nitroreductase fusion protein (CFP-NTR) under the control of *dopamine transporter* (*dat*) *cis*-regulatory elements. Embryonic and larval zebrafish express the transgene in several groups of dopaminergic neurons, notably in the olfactory bulb, telencephalon, diencephalon and caudal hypothalamus. Administration of the pro-drug metronidazole (Mtz) resulted in activation of caspase 3 in CFP-positive neurons and in a reduction of *dat*-positive cells by 5 days post-fertilization (dpf). Loss of neurons coincided with impairments in global locomotor parameters such as swimming distance, percent time spent moving, as well as changes in tail bend parameters such as time to maximal bend and angular velocity. Dopamine levels were transiently decreased following Mtz administration. Recovery of some of the locomotor parameters was observed by 7 dpf. However, the total numbers of *dat*-expressing neurons were still decreased at 7, 12 or 14 dpf, even though there was evidence for production of new *dat*-expressing cells. Tg(*dat*:*CFP-NTR*) zebrafish provide a model to correlate altered dopaminergic neuron numbers with locomotor function and to investigate factors influencing regeneration of dopaminergic neurons.

2.2 Introduction

Dopaminergic neurons play essential regulatory functions in the central nervous system (CNS). In zebrafish, dopamine (DA) is thought to be involved in the regulation of social interaction (Scerbina *et al.* 2012), visual sensitivity (Li and Dowling 2000), learning (Eddins *et al.* 2008), addiction (Chatterjee and Gerlai 2009) and motor activity (Irons *et al.* 2013; Souza *et al.* 2011; Thirumalai and Cline 2008; Tran *et al.* 2015).

Behavioural changes and neurochemical deficiencies have been previously described in the zebrafish following administration of neurotoxins such as 6-hydroxydopamine (6-OHDA) and 1-methyl-4-phenyl-1,2,3,6-tetrahydropyridine (MPTP) which target the catecholaminergic neuron populations. Although dopaminergic neurons have been shown to regenerate in both the planarian (Nishimura *et al.* 2011) and salamander (Parish *et al.* 2007) neurotoxin based models, this has not been demonstrated in the zebrafish brain. This lack of information may be attributed, in part, to the fact that although 6-OHDA and MPTP induce both neurochemical and behavioural changes, no dopaminergic neuron loss and cell death are detected in zebrafish (Anichtchik *et al.* 2004). Indeed, in larval zebrafish, MPTP treatments results in a short-lived reduction in tyrosine hydroxylase (TH) immunoreactivity at 5 and 6 dpf which is recovered by 7 dpf and does not lead to signs of apoptosis or cell death.

To address the events that take place following dopamine neuron loss and to determine whether the ablated neuronal population can be re-established in the brain of larval zebrafish, we have used a nitroreductase-mediated genetic ablation approach. This method has been successfully implemented to ablate different cell types in the zebrafish brain such as hypocretin neurons, tryptophan hydroxylase-2-positive cells in the pineal

gland and in the raphe nuclei, orthopedia-positive dopamine neurons in diencephalic clusters 2 and 4, and cells of the habenula (Elbaz *et al.* 2012; Li *et al.* 2012a; Fernandes *et al.* 2012; Yokogawa *et al.* 2012; Lambert *et al.* 2012; Agetsuma *et al.* 2010).

Here, we have used the *dopamine transporter* (*dat*) *cis*-regulatory elements, previously reported to label dopaminergic cells of the zebrafish brain (Xi *et al.* 2011b), to drive the expression of the nitroreductase enzyme in Tg(*dat:CFP-NTR*) zebrafish. Metronidazole treatments of Tg(*dat:CFP-NTR*) zebrafish resulted in ablation of cells positive for both CFP and *dat* with no observable bystander effects. The initial ablation of CFP-positive neurons coincided with locomotor and tail-bend phenotypes. The CFP cell population remained lower after a recovery period even though zebrafish had recovered some of their locomotion parameters. The sustained decrease in CFP-positive neurons occurred despite generation of new CFP-positive cells.

2.3 Materials & Methods

2.3.1 Animal Care

All experiments were conducted using protocols approved by the University of Ottawa Animal Care Committee following guidelines of the Canadian Council on Animal Care. Wild-type (WT) adult zebrafish and larvae were maintained as previously described (Westerfield 2000). Embryos used in different drug exposures were obtained from multiple clutches, pooled and separated into their respective treatment groups.

2.3.2 Transgenesis

The CFP-NTR cassette (Curado et al., 2007) was placed in an intermediate vector containing two homologous sequences targeting the flanking regions of the EGFP sequence in the construct used to generate the Tg*(dat:EGFP)* zebrafish line (Xi et al., 2011). The linearized targeting vector was electroporated into DY 380 competent cells following heat activation of RecE/T genes for homologous recombination as previously described (Liu *et al.* 2003). Colonies were screened using Neomycin selection and DNA prepared from selected clones was sequenced. A successful recombination where the start codon of CFP-NTR had been properly inserted in frame with the ATG of exon 1 of *dat* was used to generate the Tg(*dat:CFP-NTR)* construct. The transgene was injected at 54 ng/μL along with *tol2* transposase mRNA (35 ng/μL) into one-cell stage WT zebrafish embryos for Tol2 mediated transgenesis (Fisher *et al.* 2006).

Injected embryos were raised to adulthood and screened for transmission of the transgene by mating primary injected individuals with WT fish and using a combination of PCR and fluorescent microscopy for progeny screening. Transgenic offspring were raised and the line was maintained successfully for several generations. Hemizygous transgenic individuals were mated with each other to generate homozygous animals. Only homozygous larvae were used throughout the experiments in this manuscript unless otherwise mentioned.

2.3.3 Quantitative real time PCR

Absolute quantification of the number of *cfp-ntr* transcripts was performed on a BioRad CFX96 instrument using SsoFast EvaGreen (BioRad) fluorescent dye supermix and the following *cfp* specific primers: Forward-GAACCGCATCGAGCTGAA and Reverse-TGCTTGTCGGCCATGATATAG. RNA was extracted from pools of 30 embryos either homozygous or hemizygous for the transgene using the RNeasy Midi kit (Qiagen) and reverse transcribed using the Quantitect reverse transcription kit (Qiagen). Quantification was done at least 3 independent times. No signal corresponding to the transgene was detected in wild type embryos (data not shown).

2.3.4 Ablation of DA neurons

Homozygous Tg(*dat:CFP-NTR*) embryos were dechorinated manually. Embryos were treated with 5mM metronidazole (Mtz) (Sigma-Aldrich) dissolved in 0.1% DMSO

in E3 embryo medium (Westerfield 2000) from 1 day post fertilization (dpf) to 2 dpf, and at 2 dpf the concentration of Mtz was increased to 7.5 mM. The larvae were left in this solution until 4 dpf with a fresh solution change every 24 hours. Embryos were kept in 10-cm dishes with 1 fish per mL of solution and at 28.5° C in complete darkness. At 4 dpf, fish were rinsed in E3 media at least 3 times and transferred to a clean dish with fresh embryo media for an additional day after which they were transferred to 1-L tanks with system water and were kept under a standard 14-hour light cycle and fed daily. Vehicle-treated larvae received 0.1% DMSO with the same schedule.

2.3.5 BrdU pulse-chase

A 10 mM 5-Bromo-2'-deoxyuridine (BrdU) (Sigma-Aldrich) solution was prepared in E3 embryo media and adjusted to pH 7.5. Larvae were exposed to BrdU in 10 mm glass petri dishes (Pyrex) and protected from light for 48 hours starting at 4 dpf.

2.3.6 Tracking and analysis of locomotor phenotype

To address the effects of neuron ablation on the spontaneous motor activity of larval zebrafish, 5, 6 or 7 dpf embryos were placed one-per-well into 24-well plates with clear bottoms and black sides as previously described (Farrell *et al.* 2011). Larvae were acclimatized for 25-30 min under an LED illumination source used to provide an even distribution of light across the multiwell plate prior to video recording. A Nikon D3100 DSLR camera with a 50 mm lens (Nikon) was mounted on a tripod and used to record 10

min videos of the larvae's spontaneous movements at 30 fps. All experiments were conducted in a temperature controlled room separate from the main zebrafish facility and the presence of the experimenter in the recording room was limited to the initial minute of recording in order to minimize extraneous stimuli. All videos were recorded between the 10:00 am and 4:00 pm.

Videos were tracked using the open-source *LSRtrack* software and the data was analyzed using the *LSRanalyze* function as previously described (Cario *et al.* 2011). Each well of the multiwell-plate was selected for accurate tracking using both an automated threshold and manual screening. A mean velocity threshold of 0.001 mm sec^{-1} was set, such that only motile fish were included in the analysis. Data was obtained from at least 3 independent video acquisitions.

2.3.7 Tail bend analysis

To address tail-bend changes in the initiation of larval swimming at 5 or 12 dpf, larvae were placed into 50 mm watch glasses (Thermo Fisher Scientific) in system water. Larvae were transferred to the aforementioned separate room, positioned over a LED trans-illumination light source and allowed to rest for 10 min to acclimatize to their new environment. Videos were recorded at 120 fps using a Grasshopper IEE-1394b (Point Grey) digital camera attached to a 40 mm lens (Nikon). Videos were acquired using the Fly Capture software (Point Grey) and the data was analyzed manually as previously described (Budick and O'Malley 2000). In brief, frames in which any of the 5 larvae present within the field of view were at rest and spontaneously initiated movement such

as a swimming or a turning episode were selected for analysis. The frame at which the fish had the smallest head to tail angle, prior to the change in tail direction, was defined as the time to maximal bend. The frames with the maximal bend for each event were printed and the maximal bend angle was calculated manually. A total of 30 random events obtained from 3 separate video acquisitions were used following either vehicle or Mtz treatment.

2.3.8 High performance liquid chromatography (HPLC)

Following neuron ablation, twenty vehicle or Mtz-treated larvae were collected in 1.5 mL Eppendorf tubes and stored in 500 μ L of homogenization solution (1mM Na_2EDTA, 0.3M chloroacetic acid (ClCHCOOH) and 10% methanol in HPLC grade water) with DHBA as an internal standard.

Tissue was homogenized by sonication using a Fisher Scientific Model 100 Sonic Dismembrator and protein levels were measured using Pierce BCA Protein Assay Kit (Thermo Scientific) in a FLUOstar Glalaxy (BMG LabTech) system. Homogenized samples were centrifuged for 20 minutes at 12000 g and transferred to HPLC vials. The supernatant (20 μl) was injected into a high performance liquid chromatography system (Aligent) consisting of an Iso-pump (G 1310A), auto sampler ALS (G 1329A), coolant system ALS-Term (G-1329), a stainless steel Eclipse XDB-C8 (5 μ m) 4.6 x 150 mm column situated in a thermostatic chamber (40 °C) and an electrochemical detector DECADE SDC (Antec Leyden) with an electrochemical flow cell VT-03 with a working electrode maintained at the potential of 0.60V relative to the reference electrode.

Determination of the area and height of the peaks was carried out with the aid of a Hewlett-Packard integrator.

The mobile phase consisted of 90 mM sodium phosphate monobasic, 1.7 mM 1-octane sulfuric acid sodium salt, 50 mM EDTA, 10% acetonitrile, 50 mM citric acid monohydrate and 5mM KCl in 200 mL of acetonitrile and was passed through a GS (0.22 μ m) filter.

Data were obtained from a minimum of seven independent runs for each treatment and time point.

2.3.9 Immunohistochemistry and *in situ* hybridization

Zebrafish larvae at different stages were anaesthetized with tricaine (Sigma) and fixed in 4% PFA overnight at 4°C. Larvae were washed in 1X PBS 3 times 10 minutes and dehydrated in a MeOH series for storage in 100% MeOH at -20°C until further use. *In situ* hybridization and immunohistochemistry were conducted as previously described (Xi *et al.* 2011b; Inoue and Wittbrodt 2011). Larvae used for cryosectioning were rehydrated in PBS and equilibrated in 30% sucrose prior to being embedded in OCT (Leica) for sectioning at 14-µm. Sections were stored at -20°C until further use. For BrdU immunohistochemistry, samples were treated with 2N HCl for 30 min at 37°C and rinsed in 0.1M sodium borate buffer pH 8.5 for 5 min.

The following primary antibodies were used: mouse anti-CFP (Clontech), rabbit anti-TH (Millipore), rat anti-BrdU (AbCam) and rabbit anti-Active Caspase3 (BD

Pharmingen). Secondary fluorescent antibodies were: goat anti-mouse Alexa-488, goat anti-rat Alexa-594 and goat anti-rabbit Alexa-647 (Molecular Probes).

2.3.10 Imaging and fluorescence quantification

For live imaging, fish were anaesthetized with tricaine and placed dorsal side up in a drop of 1% low melting point agarose (Life Technologies). Embryos were submerged in system water and imaged using a 25X water-dipping objective of a Nikon A1R MP multiphoton confocal microscope.

At 3 and 5 dpf, fluorescently stained samples were imaged using a 25X objective of a Nikon A1 confocal microscope or a 20X objective of an inverted Zeiss LSM 510 confocal microscope respectively.

Images used for fluorescent pixel quantification were taken under the same exposure conditions and were analyzed using Fiji software (Schindelin *et al.* 2012). In brief, z-stacks were combined to document the different catecholaminergic clusters along the zebrafish dorsal-ventral axis and analyzed as maximum intensity projections. The same size drawing selection tool was used to crop equivalent regions in different treatment groups. The average pixel intensity in each region was plotted.

Cell counts were done manually by researchers blinded to the experimental design.

2.3.11 Statistical analysis

Statistical comparison of multiple groups was conducted using a multiple t-test analysis with Holm-Sidak correction. Analysis of two groups with parametric distribution was conducted using an unpaired t-test where an alpha-value of 0.05 was defined as statistically significant. The D'Agostino and Pearson's test was used to confirm that the spontaneous locomotor activity data followed a non-parametric distribution, and statistical analysis was conducted using the Mann-Whitney test. For * $p \leq 0.05$, ** $p \leq 0.01$, *** $p \leq 0.001$, **** $p \leq 0.0001$ and n.s. = not significant $p > 0.05$. Error bars represent standard error of mean (SEM).

2.4 Results

2.4.1 Tg(*dat:CFP-NTR*) expresses fluorescent protein specifically in *dat*-positive cells

We have previously used the *cis*-regulatory elements of the zebrafish *dopamine transporter* (*dat*) gene to drive the expression of enhanced green fluorescent protein (EGFP) in most clusters of dopaminergic neurons in the zebrafish brain (Xi *et al.* 2011b). Here, we used these same regulatory elements to drive the expression of the cyan fluorescent protein-nitroreductase (CFP-NTR) fusion protein (Fig. 2.1A) for the conditional and specific ablation of *dat*-positive cells in the zebrafish brain.

The absolute copy numbers of *cfp-ntr* transcripts were compared in hemizygous and homozygous whole larvae of the same Tg(*dat*:*CFP-NTR*) line. Hemizygous larvae expressed approximately half the number of *cfp-ntr* transcripts when compared to homozygous larvae (p= 0.0242) (Fig. 2.1H) and consistently showed weaker fluorescence (Fig. 2.1B,E).

The temporal expression of the cyan fluorescent protein was similar to the EGFP expression in the Tg(*dat*:*EGFP*) fish (Xi *et al.* 2011b). Thus, at 3 dpf, expression was detected in cell clusters of the olfactory bulb (OB), telencephalon (Tel), pretectum (Pr), diencephalon (DC), caudal hypothalamus (Hc), locus coeruleus (LC), jaw and branchial arches (B. Arches) (Fig. 2.1C,F).

Double labeling with anti-CFP and anti-TH antibodies (see Figure A.1.1 in Appendix 1) was carried out to further verify transgene expression in the different clusters of dopaminergic neurons. Clusters were labeled according to the nomenclature

previously established (Rink and Wullimann 2002b), a schematic representation of which is shown in Fig. 2.1D,G. Unlike the Tg(*dat*:*EGFP*) zebrafish, we did not detect fluorescent protein expression in DC clusters 4, 5 and 6 of Tg(*dat*:*CFP-NTR*) animals. This lack of expression has also been observed when generating other transgenic zebrafish with the same regulatory elements (S. Noble, R. Godoy and M. Ekker, unpublished observations).

At 5 days post fertilization, clusters expressing CFP in the larval brain also expressed *dat* mRNA (Supp. Fig. 2.1). Independent z-projections obtained from a whole-mount immunolocalization and *in situ* hybridization showed co-localization of CFP and *dat* in the pretectum (Supp. Fig. 2.1A-A’’’), olfactory bulb (Supp. Fig. 2.1B-B’’’, C-C’’’), locus coeruleus (Supp. Fig. 2.1B-B’’, C-C’’), subpallium (Supp. Fig. 2.1C-C’’’), anterior preoptic region (Supp. Fig. 2.1D-D’’’), preoptic region (Supp. Fig. 2.1E-E’’’), diencephalic clusters 2 and 3 (Supp. Fig. 2.1D-D’’’), caudal hypothalamus (Supp. Fig. 2.1E-E’’’) and retinal amacrine cells (Supp. Fig. 2.1C-C’’, D-D’’, E-E’’). Furthermore, CFP was detected in axonal tracks of the anterior commissure (Ac) (Supp. Fig. 2.1C-C’’’) and ventral diencephalon (Supp. Fig. 2.1D, D’’).

Figure 2.1 Transgenic zebrafish expressing nitroreductase in *dat*-positive cells. (A) Transgene construct design. The *cis*-regulatory elements of the *dat* gene flanked by Tol2 arms from a previously described (Xi *et al.* 2011b) *dat*:*EGFP* construct (top panel), were used to generate the *dat*:*CFP-NTR* construct. The *dat* genomic sequences include all exons except for the last one and are approximately 30 kb in length. Two homologous arms (arm A and arm B, yellow and orange) were placed in a targeting vector (middle panel) that allowed the substitution of EGFP with a CFP/nitroreductase (NTR) fusion protein (bottom panel). (B-G) Expression patterns of CFP-NTR in Tg(*dat*:*CFP-NTR*) zebrafish. (B), CFP fluorescence signal intensity in live dorsal views of wild-type (CFP -/-), hemizygous (CFP+/-) and homozygous (CFP+/+) fish at 3 dpf. (C, E) CFP expression in the following DA neuron groups: OB (olfactory bulb), Tel (telencephalon), Pr (pretectum), DC (diencephalon), Hc (caudal hypothalamus) and LC (locus coeruleus) from a (C) dorsal and (F) lateral view. (D,G) Line drawings depicting the labeled DA neuron clusters as seen from a (D) dorsal or (G) lateral view. (H) Homozygous (Homo) zebrafish show an approximately two-fold higher level of CFP transcripts compared to hemizygous (Hemi) fish (n=30 fish, with 3 experimental replicates). Scale bars represent 100 µm.

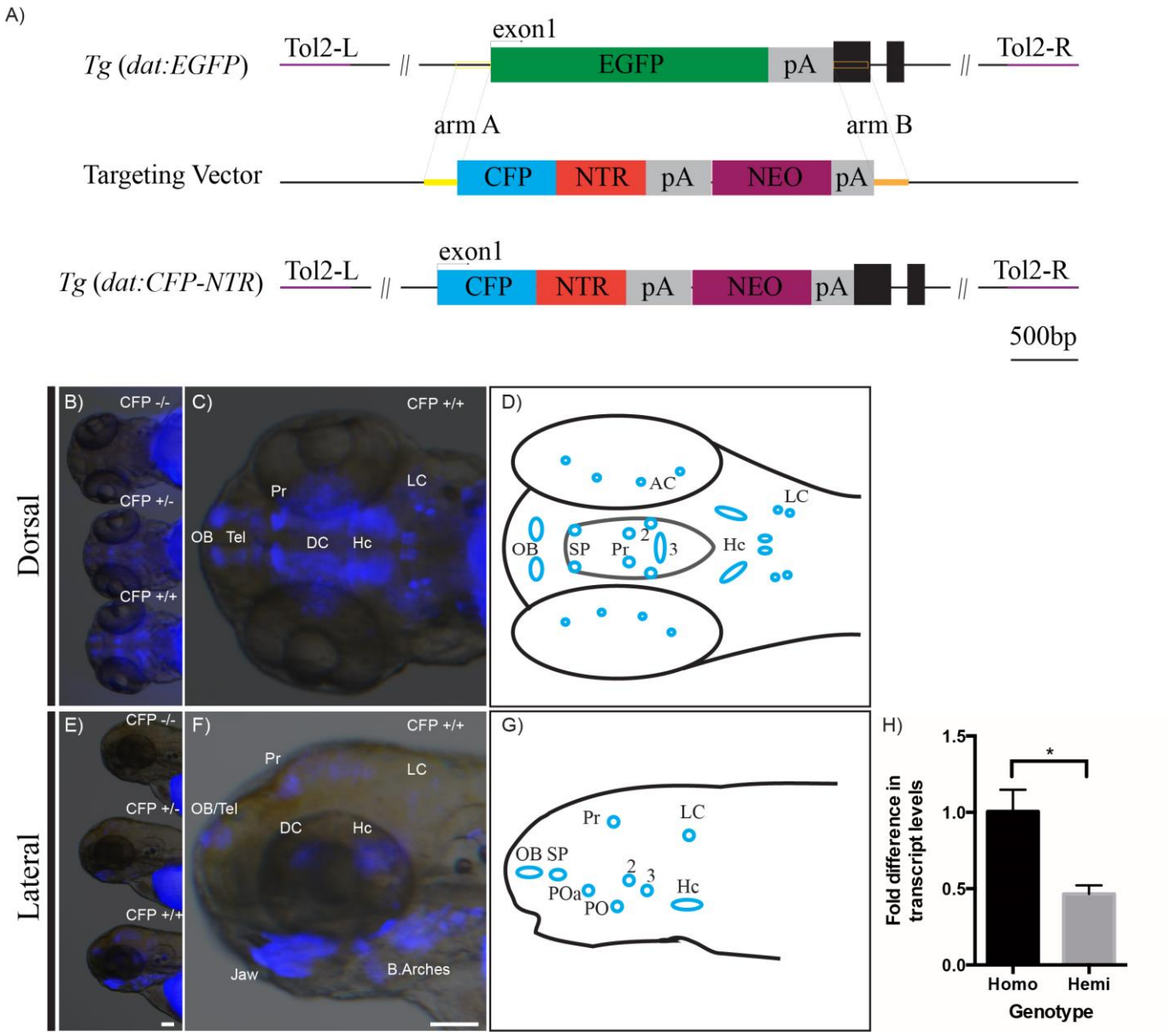
A)
Tg (dat:EGFP)
Tol2-L
exon1
EGFP
pA
Tol2-R
arm A
arm B
Targeting Vector
CFP
NTR
pA
NEO
pA
Tg (dat:CFP-NTR)
Tol2-L
exon1
CFP
NTR
pA
NEO
pA
Tol2-R
500bp
Dorsal
Lateral
B) CFP -/-
CFP +/-
CFP +/+
C) CFP +/+
Pr
LC
OB Tel
DC Hc
D)
AC
LC
OB
SP
Pr
2
3
Hc
E) CFP -/-
CFP +/-
CFP +/+
F) CFP +/+
Pr
LC
OB/Tel
DC Hc
Jaw
B.Arches
G)
Pr
LC
OB SP
2
3
POa
PO
Hc
H)
Fold difference in transcript levels
1.5
1.0
0.5
0.0
*
Homo
Hemi
Genotype

Supp Fig. 2.1. Co-localization of CFP-NTR transgene and *dopamine transporter* (*dat*) expression. Co-localization of CFP immunostaining and *dopamine transporter* (*dat*) *in situ* hybridization at 5 dpf. CFP- (blue) and *dat*- (magenta) positive cells are labeled in individual 6.4 µm thick optical sections (A through E). Retinal amacrine cells (RAC); anterior commissure (Ac); diencephalic clusters 2 and 3 (2 and 3); subpallium (SP); anterior preoptic area (POa) and preoptic area (PO). Enlarged insets of merged images are shown in the last column. Images are shown dorsal facing up and anterior facing left. Scale bars represent 50 µm.

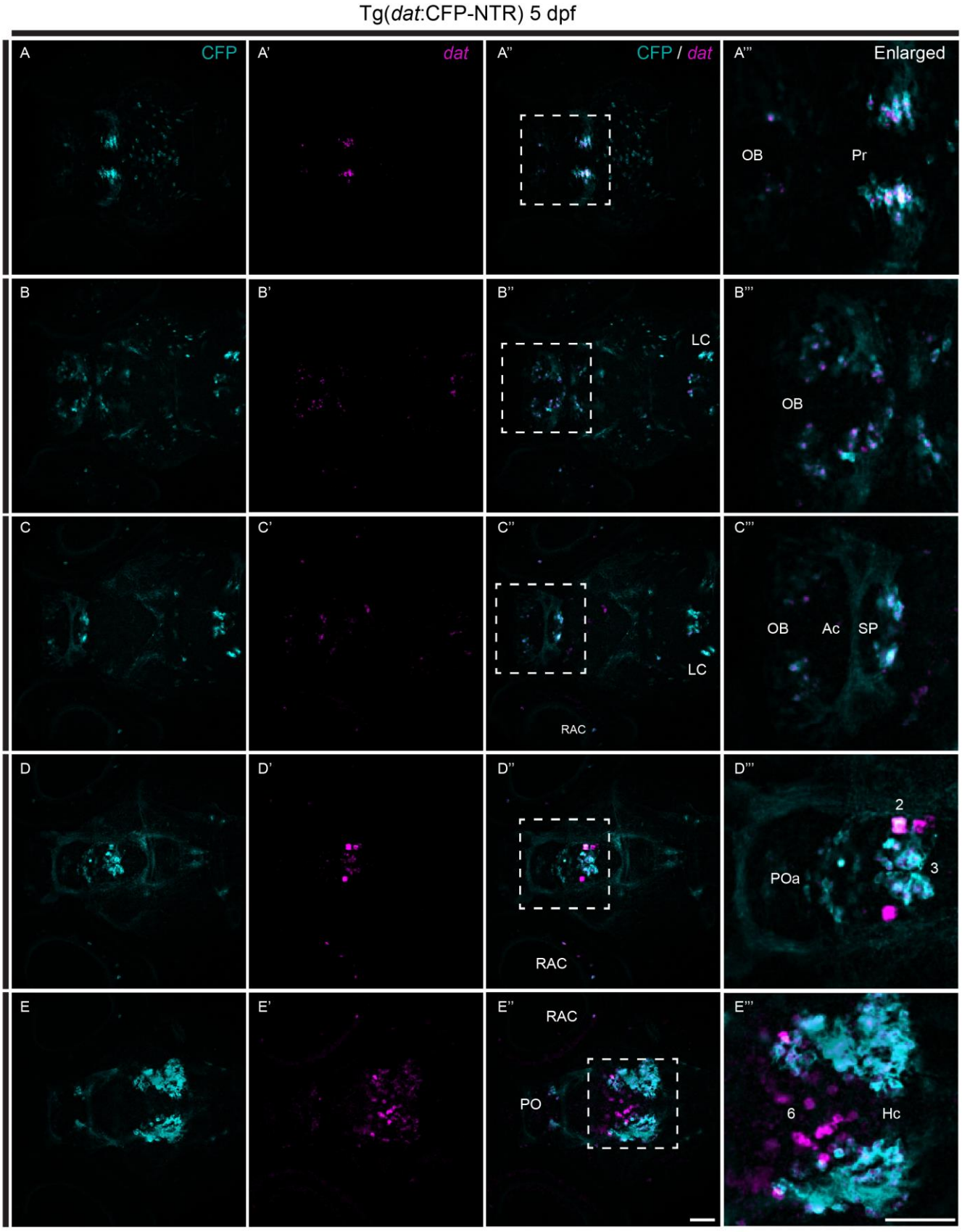
Tg(*dat*:CFP-NTR) 5 dpf
A
CFP
A'
dat
A''
CFP / *dat*
A'''
Enlarged
OB
Pr
B
B'
B''
LC
B'''
OB
C
C'
C''
LC
RAC
C'''
OB
Ac
SP
D
D'
D''
RAC
D'''
2
3
POa
E
E'
E''
RAC
PO
E'''
6
Hc

2.4.2 Metronidazole treatment specifically ablates CFP-NTR expressing neurons

The nitroreductase-metronidazole ablation system has been used to specifically ablate different cell types in larval zebrafish (Curado *et al.* 2007) including cells in the CNS, such as hypocretin neurons (Elbaz *et al.* 2012), tryptophan hydroxylase 2-positive cells in the dorsal raphe (Yokogawa *et al.* 2012) and dopaminergic cells of diencephalic clusters 4 and 5 (Lambert *et al.* 2012).

To address the efficiency of DA neuron ablation in Tg(*dat*:*CFP-NTR*) zebrafish, a Mtz dose response (5-25 mM) experiment was conducted at different stages of embryonic/larval development (see Table A.1 in Appendix 1). Hemizygous larvae required both a longer exposure time and higher concentrations of Mtz in order to elicit cell ablation, compared to homozygous larvae. Since higher and prolonged Mtz doses led to an abnormal motor phenotype in WT zebrafish (data not shown), we only used homozygous larvae throughout this study. This allowed us to adopt a Mtz administration regimen that had no observable effects on the motor phenotype of wild type zebrafish. Thus, embryos were exposed to 5 mM Mtz starting at 24-hour post fertilization (hpf) and to 7.5 mM Mtz from 48 hpf to 96 hpf (Fig. 2.2A). At 3 dpf, a clear reduction in fluorescent CFP protein expression was already observable in Tg(*dat*:*CFP-NTR*) larvae treated with Mtz, compared to controls (Fig. 2.2B’’). Metronidazole-treated fish showed a higher number of cells expressing the activated form of caspase 3 (Fig. 2.2B’’’), all of which co-localized with CFP-positive neurons. A representative image of this process in a telencephalic cluster is shown in Fig. 2.2B’’’’. Similar observations were made for the other clusters of CFP-labeled cells along the rostral-caudal and dorsal-ventral axes of the

zebrafish brain. These observations indicate specific apoptosis of cells expressing Tg(*dat*:*CFP-NTR*) following Mtz treatment.

At 5 dpf, most of the dopaminergic neurons and axonal arrangements present in adult zebrafish are well established (Schweitzer *et al.* 2012). At this time-point, we observed a major decrease in CFP expression in cells of the OB, SP, Pr, DC2/3, Hc, LC, RAC (Fig. 2.2C, see arrow heads) and axonal tracks of the ventral diencephalon (vDC) (Fig. 2.2C, see asterisk) of Mtz treated Tg(*dat*:*CFP-NTR*) fish. Contrary to the Tg(*dat*:*CFP-NTR*) animals, exposure of Tg(*dat*:*EGFP*) larvae to the same Mtz treatment resulted in no discernible changes in fluorescent protein expression, cell counts or cellular arrangement (Fig. 2.2C). This further indicates that the Mtz administration only has an effect on *dat*-positive cells that express NTR.

The observed decreases in CFP expression were accompanied by a decrease in the number of *dat* expressing cells, but had no effect on *dat* expression in cells that did not show CFP expression, such as cells of vDC 4,5,6 (Fig. 2.2C). Further quantification of fluorescence following Mtz administration, using different z-stacks obtained from live 2-photon imaging (Fig. 2.2D), showed that decreases in fluorescence were statistically significant in all major DA neuron clusters analyzed (Fig. 2.2E). When compared to vehicle-treated larvae, Mtz treatment led to a 67.2 ± 7.1% fluorescence decrease in the Pr (t-test, n= 3, $p< 0.001$), 66.3 ± 9.9% in the OB ($p= 0.0026$), 45.7 ± 11% in the SP ($p= 0.0142$), 56.2 ± 12.3% in DC2 and 3 ($p= 0.0103$) and 53.8 ± 17.9% in Hc ($p= 0.0399$) (Fig. 2.2E).

Figure 2.2 Ablation of *dat*-expressing cells in zebrafish larvae. (A) Time course of metronidazole (Mtz) administration. (B) The reductions in CFP-positive DA neurons (B'') in the forebrain are accompanied by an increase in caspase 3-positive neurons (B'''). Co-localization between CFP and caspase 3 immunostaining is shown in merged orthogonal views. DAPI was used as a nuclear stain (B'). (C) Maximum intensity projections of DA neuron clusters labeled with anti-CFP and a dat cRNA anti-sense probe at 5 dpf. Arrow heads (white) indicate areas of ablation in the Tg(*dat:CFP-NTR*) Mtz treated fish with comparable intact regions depicted in the vehicle treated Tg(*dat:CFP-NTR*) fish. Tg(*dat:EGFP*) fish (right panels) were used as a control demonstrating that Mtz administration does not result in cell ablation in the absence of NTR expression. (D) Live two-photon confocal imaging of the main DA neuron clusters in vehicle and Mtz treated fish at 5 dpf. (E) Quantification of the relative CFP fluorescence intensity in live fish at 5 dpf (n=3). Larvae are shown with the dorsal side facing up in panel (B) and with dorsal facing up and anterior facing left in panels (C) and (D). Scale bars represent 25 μm.

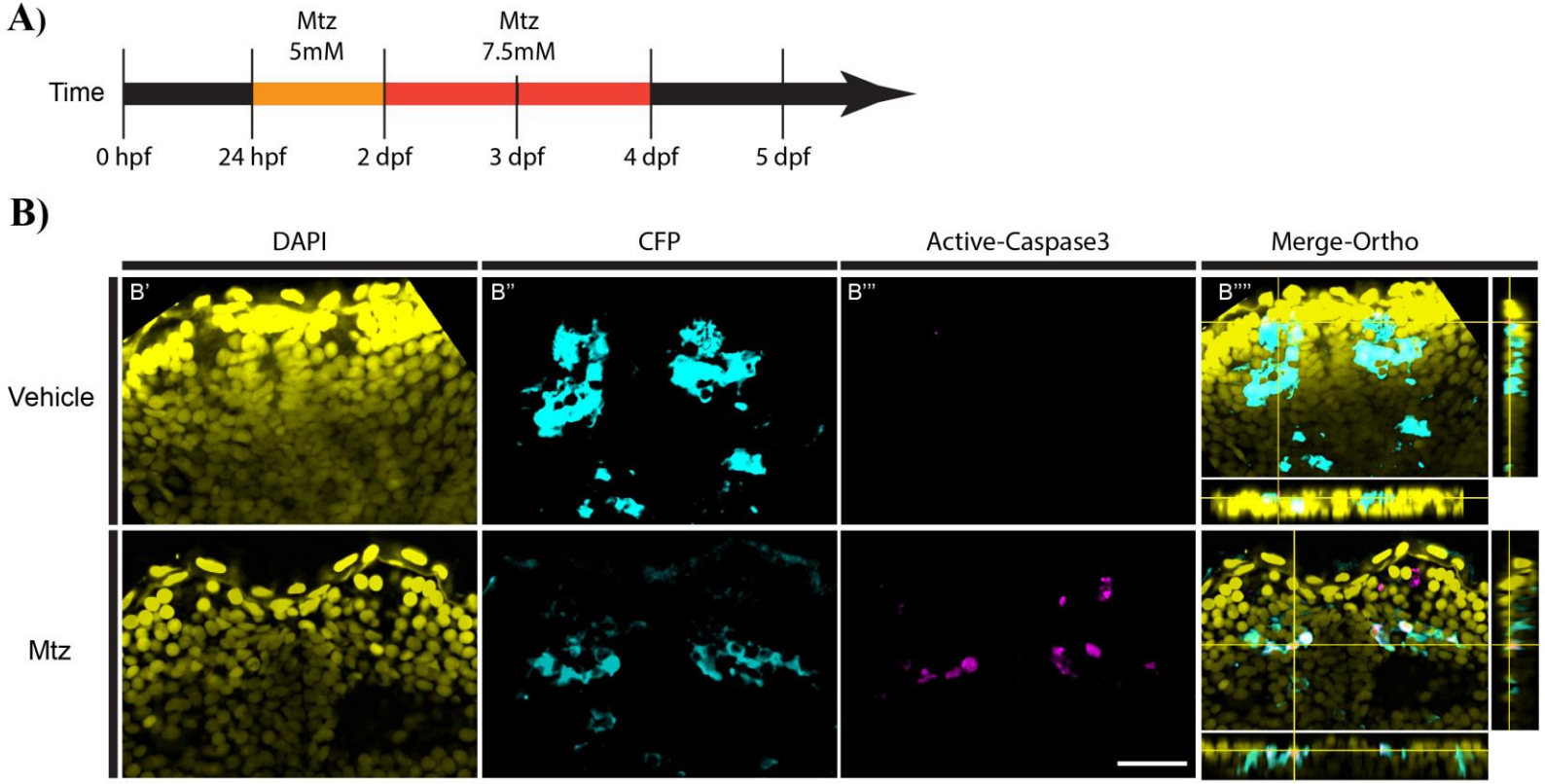
A)
Mtz
5mM
Mtz
7.5mM
Time
0 hpf
24 hpf
2 dpf
3 dpf
4 dpf
5 dpf
B)
DAPI
CFP
Active-Caspase3
Merge-Ortho
B'
B''
B'''
B''''
Vehicle
Mtz

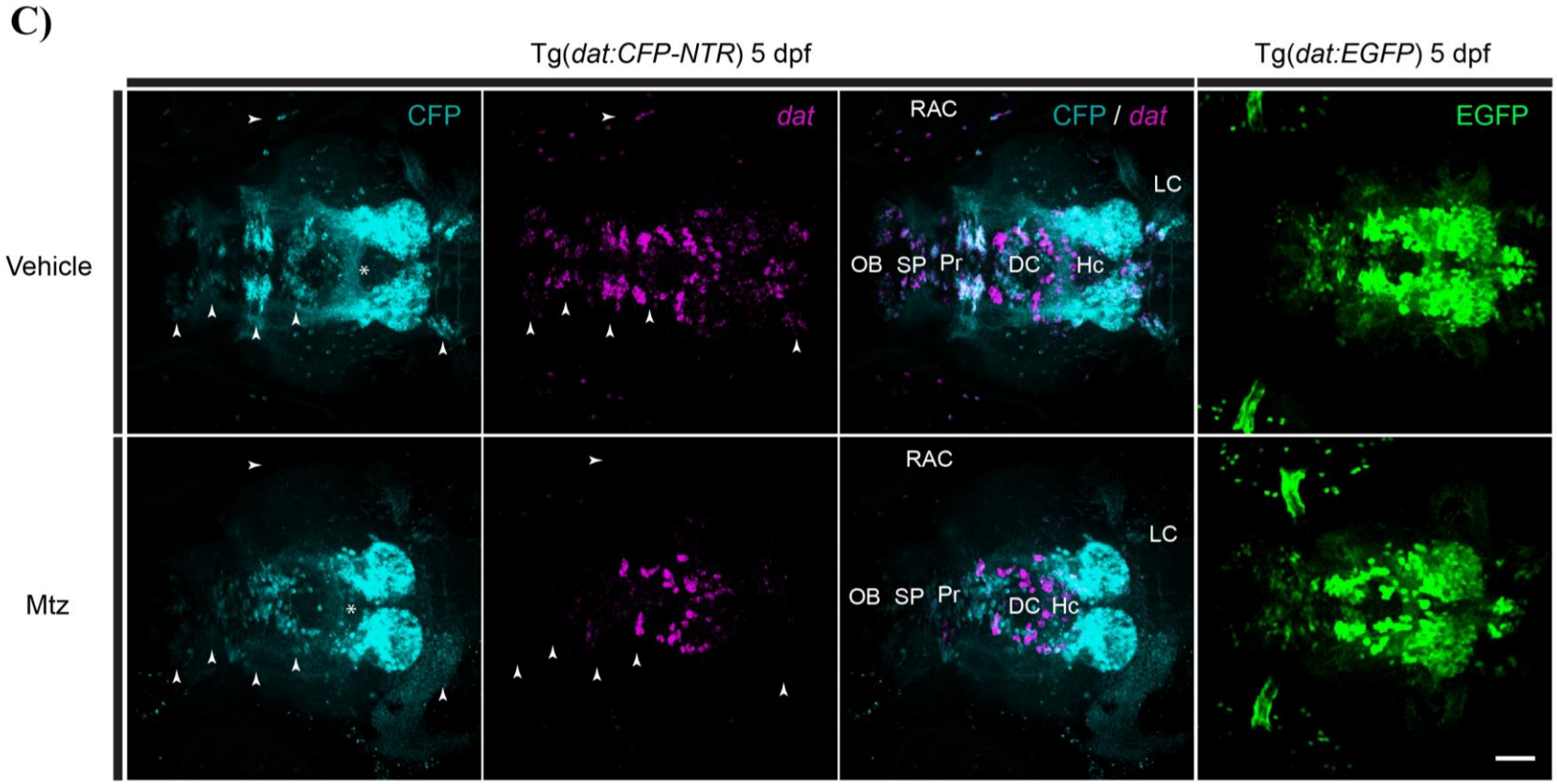
C)
Tg(dat:CFP-NTR) 5 dpf
Tg(dat:EGFP) 5 dpf
Vehicle
Mtz
CFP
dat
RAC
CFP / dat
LC
OB
SP
Pr
DC
Hc
EGFP

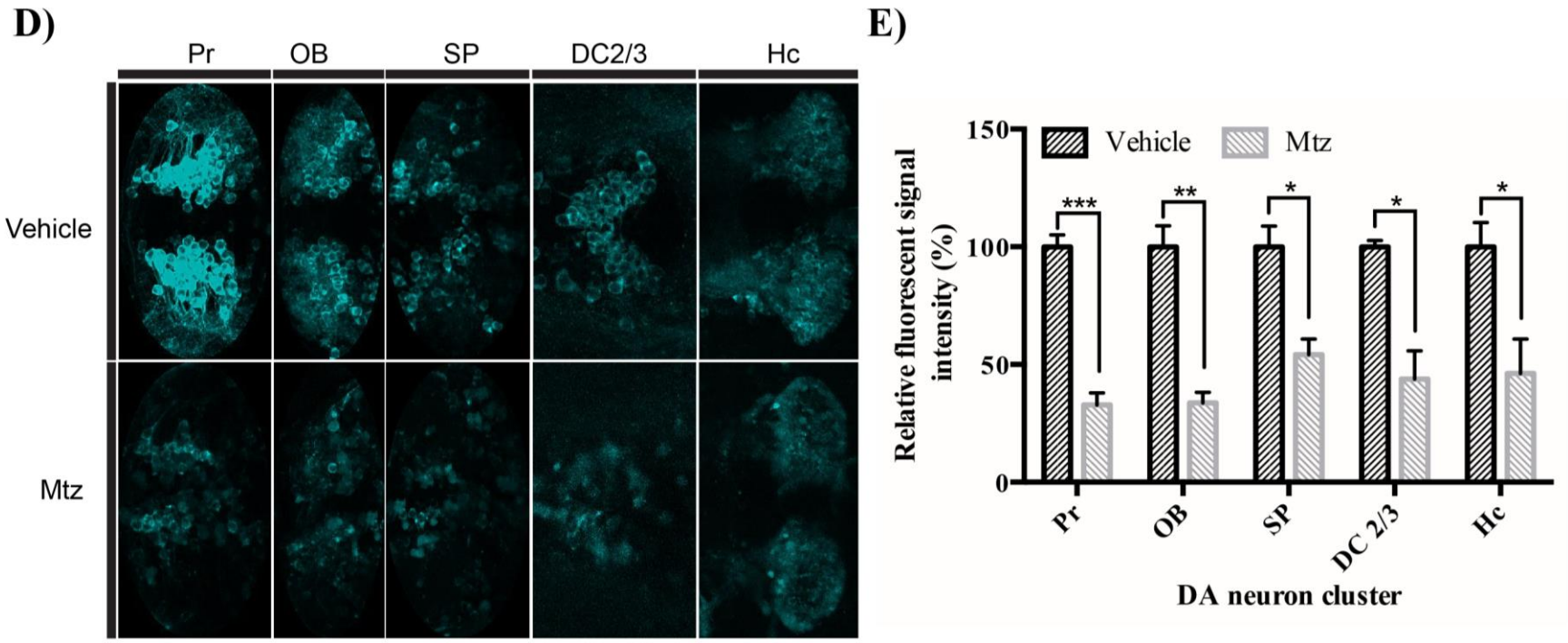
D)
Pr
OB
SP
DC2/3
Hc
Vehicle
Mtz
E)
Vehicle
Mtz
Relative fluorescent signal intensity (%)
150
100
50
0
***
**
*
*
*
Pr
OB
SP
DC 2/3
Hc
DA neuron cluster

2.4.3 Neuronal loss in Tg(*dat:CFP-NTR*) is accompanied by altered larval locomotion and tail bend parameters

Dopamine is a well-described neurotransmitter known for its role in mediating motor activity in the central nervous system of vertebrates (Yamamoto *et al.* 2013). Previous studies in zebrafish have shown that alterations in the dopaminergic network via neuron ablation, neurotoxicity or genetic manipulation can result in an observable motor phenotype in larvae (Lambert *et al.* 2012; Xi *et al.* 2010; Bretaud *et al.* 2004).

To address the effects of neuron ablation in Tg(*dat*:*CFP-NTR*) zebrafish on motor activity, we looked at five different swimming parameters of spontaneously moving 5, 6 and 7 day-old larvae including: total displacement, active velocity, percent time moving, active time duration and rest time duration (Fig. 2.3).

Metronidazole administration resulted in a 49% reduction in total larval displacement when compared to vehicle at 5dpf (n=34, p=0.0001) and in a 63.5% decrease at 6 dpf (n=17, p=0.0342) (Fig. 2.3A). On average, 5 and 6 dpf larvae respectively spent 40.4% (p=0.0017) and 38% (p=0.0211) less time moving in the arena (Fig. 2.3B) and 7.2 (p=0.0123) and 2.5 (p=0.0408) times longer at rest during their immotile intervals (Fig. 2.3E). The loss of CFP-positive cells was also associated with a 22.5% decrease in the length of active time (p=0.0003) (Fig. 2.3C) and a 15.6% reduction in the velocity of 5-day old larvae during activity (p=0.0021) (Fig. 2.3D). However, by 7 dpf, the above parameters were undistinguishable between Mtz-treated and control larvae (Fig. 2.3A-E).

Figure 2.3 Locomotor parameters following Mtz-medidated cell ablation.

Individual larvae were placed in a 24-well plate. (A) Total distance moved within 10 min; (B) Percentage of time moving during a period of 10 min; (C) Active time duration refers to the mean length of each episode of movement during a total period of 10 min; (D) Active velocity refers to the mean speed of movement during a period of 10 min; (E) Rest-time duration refers to the mean length of each inactive episode of movement during a period of 10 min. Each data point represents one fish. n=34 for 5dpf and =17 for 6 and 7 dpf.

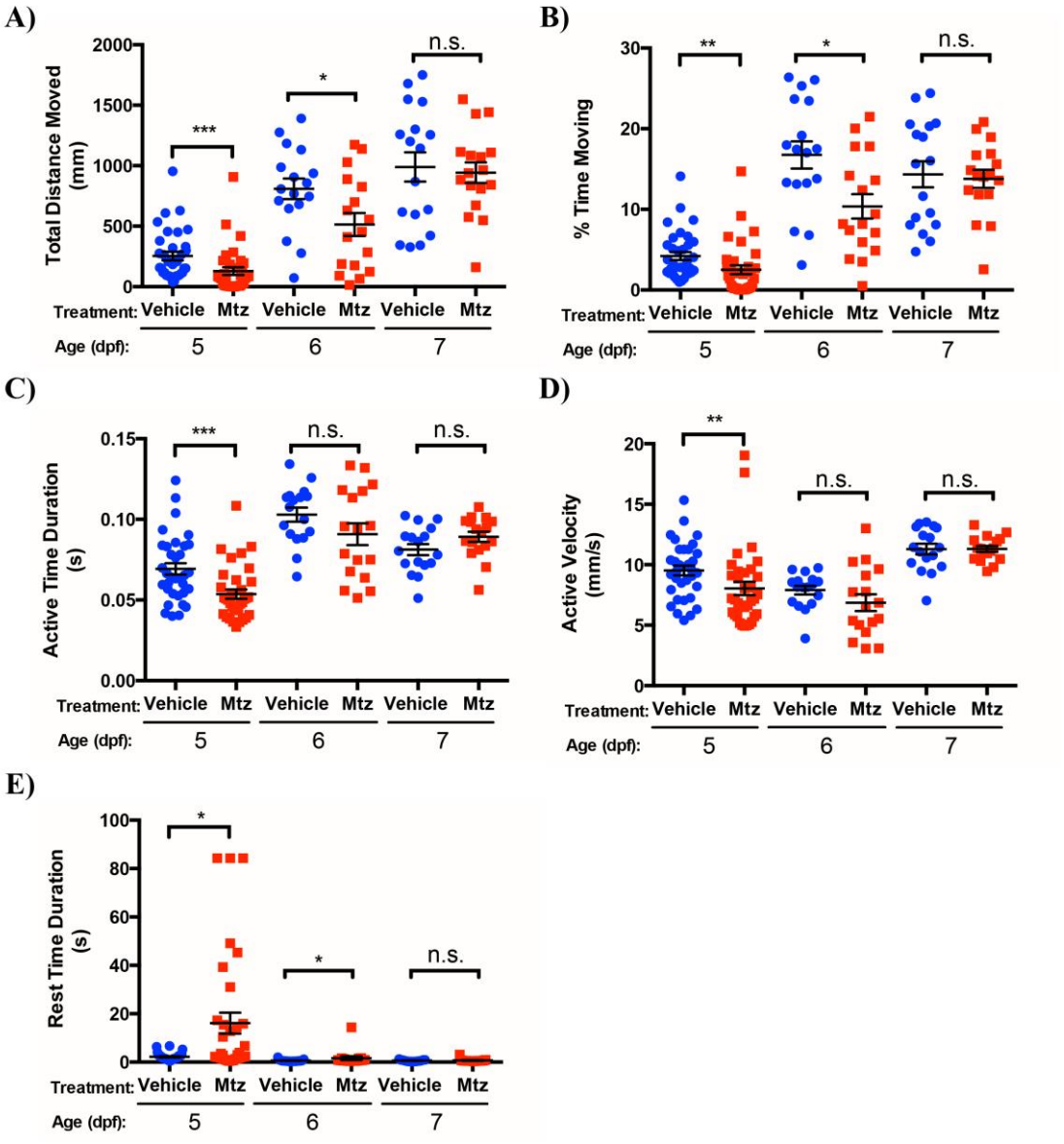
A)
Total Distance Moved (mm)
2000
1500
1000
500
0
***
*
n.s.
Treatment: Vehicle Mtz Vehicle Mtz Vehicle Mtz
Age (dpf): 5 6 7
B)
% Time Moving
30
20
10
0
**
*
n.s.
Treatment: Vehicle Mtz Vehicle Mtz Vehicle Mtz
Age (dpf): 5 6 7
C)
Active Time Duration (s)
0.15
0.10
0.05
0.00
***
n.s.
n.s.
Treatment: Vehicle Mtz Vehicle Mtz Vehicle Mtz
Age (dpf): 5 6 7
D)
Active Velocity (mm/s)
20
15
10
5
0
**
n.s.
n.s.
Treatment: Vehicle Mtz Vehicle Mtz Vehicle Mtz
Age (dpf): 5 6 7
E)
Rest Time Duration (s)
100
80
60
40
20
0
*
*
n.s.
Treatment: Vehicle Mtz Vehicle Mtz Vehicle Mtz
Age (dpf): 5 6 7

We used a high-speed camera to capture the angle at which larvae would bend during the initiation of swim behaviour and the time taken to reach such an angle in order to determine if loss of CFP-positive cells also resulted in additional motor differences. In addition to the above locomotor parameters of spontaneously swimming larvae, Mtz treatment also affected the tail bend parameters of 5 dpf fish (Fig. 2.4) during the initiation of movement in free-swimming larvae. Mtz treatment increased the time it took larvae to reach their maximal angular bend by 14.4% (n=30, p=0.0313) (Fig. 2.4B), increased their head to tail angle by 50.8% (p=0.0007) (Fig. 2.4C) which resulted in a decrease of 21.6% (p=0.0007) in bend amplitude (Fig. 2.4D) and an overall decrease of 28.5% in angular velocity (p=0.0012) (Fig. 2.4E). Unlike with the overall swimming behaviour (Fig. 2.3), which had returned to normal by 7 dpf in Mtz-treated animals, 12 day-old larvae still displayed an 11.2% (n=30, p=0.0409) increase in the time to maximal bend (Fig. 2.4B) and a 13.1% (n=30, p=0.0072) decrease in angular velocity (Fig. 2.4E).

Figure 2.4 Tail-bend measurements. (A) Schematic representation of tail bend measurements. (B) Average time to maximum bend; (C) Average head-to-tail angle; (D) Average bend amplitude; and (E) Average angular velocity. n=30 for each time point.

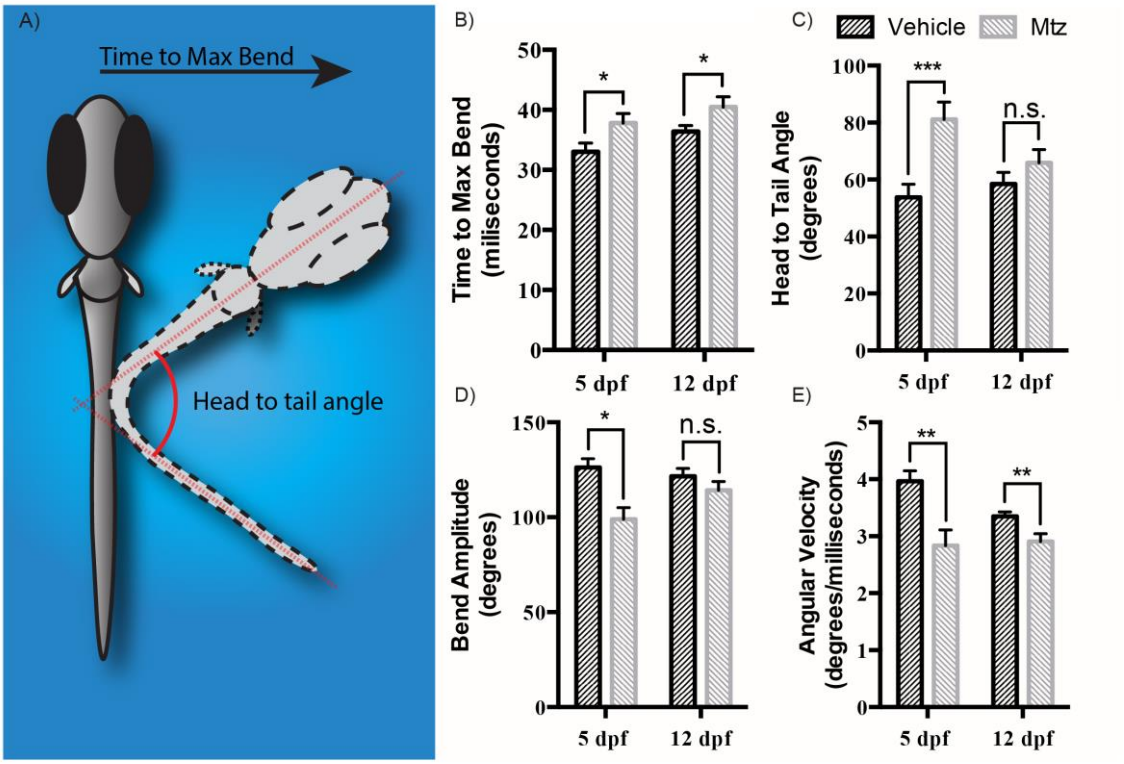
A)
Time to Max Bend
Head to tail angle
B)
Time to Max Bend (miliseconds)
50
40
30
20
10
0
*
*
5 dpf
12 dpf
C)
Vehicle
Mtz
Head to Tail Angle (degrees)
100
80
60
40
20
0
***
n.s.
5 dpf
12 dpf
D)
Bend Amplitude (degrees)
150
100
50
0
*
n.s.
5 dpf
12 dpf
E)
Angular Velocity (degrees/milliseconds)
5
4
3
2
1
0
**
**
5 dpf
12 dpf

2.4.4 Transient decrease in dopamine levels following neuronal ablation

We investigated the effects of CFP-positive neuron loss on the levels of dopamine, norepinephrine and serotonin in whole zebrafish larvae at 5, 6 and 7 days post fertilization (Fig. 2.5).

The levels of dopamine were reduced on average by 57% (n=8, p=0.0125) (Fig. 2.5A) in Mtz-treated larvae when compared to vehicle treatment 24 hours following the termination of drug administration, that is, when larvae were 5 days old. The decrease in dopamine levels was transient and levels had returned to those of controls by 6 days (n=9, p=0.4312) and 7 days (n=7, p=0.9286) (Fig. 2.5A). We observed no statistically significant changes in global levels of norepinephrine (Fig. 2.5B) or serotonin (Fig. 2.5C) in 5, 6 or 7 dpf larvae.

The strong locomotor phenotype observed in 5 dpf larvae but not in 7 dpf larvae (Fig. 2.3) is consistent with the transient reduction in DA levels. In order to address whether the recovery of DA neurotransmitter levels and locomotion parameters were due to a recovery in CFP-positive neurons or by an up-regulation of dopamine synthesis by the remaining neurons, we examined the CFP-positive neuronal populations at times of locomotor recovery.

Figure 2.5 Neurotransmitter levels following Mtz –mediated cell ablation in Tg(*dat*:*CFP-NTR*) fish. Twenty larvae belonging to each treatment group were collected at 5, 6 or 7 dpf and neurotransmitter levels were measured using HPLC. (A) Dopamine. (B) Norepinephrine. (C) Serotonin. Data shown as percent change compared to vehicle-treated larvae. At 5 dpf, n= 8; at 6 dpf, n=9; at 7 dpf, n=7.

A)

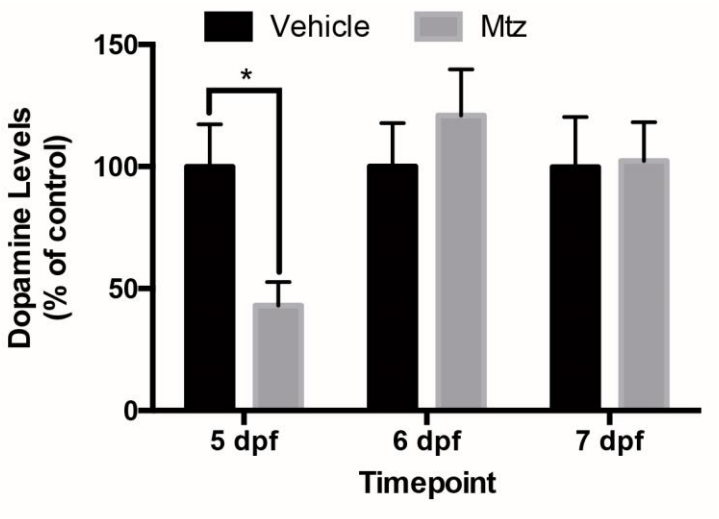
Vehicle
Mtz
*
150
100
50
0
Dopamine Levels
(% of control)
5 dpf
6 dpf
7 dpf
Timepoint

B)

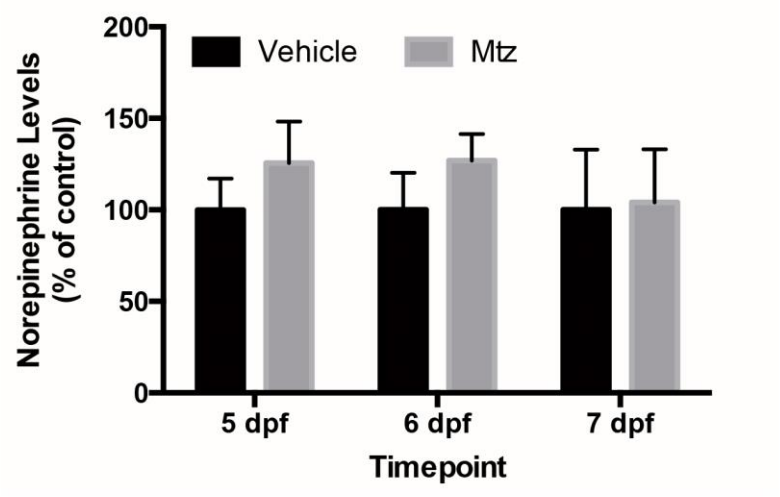
Vehicle
Mtz
200
150
100
50
0
Norepinephrine Levels
(% of control)
5 dpf
6 dpf
7 dpf
Timepoint

C)

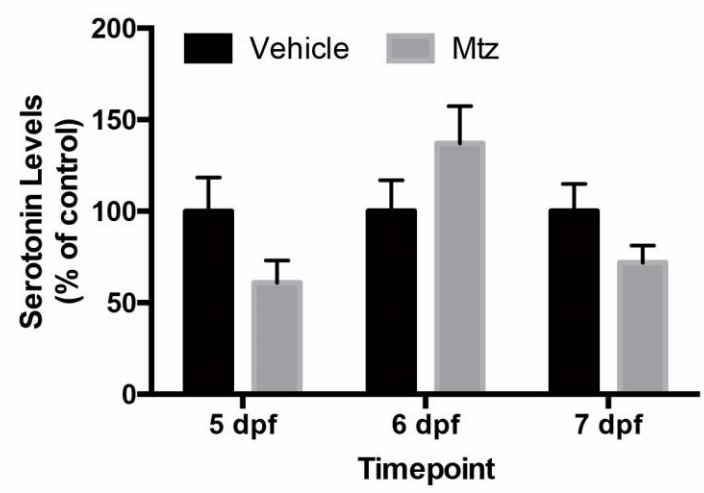
Vehicle
Mtz
200
150
100
50
0
Serotonin Levels
(% of control)
5 dpf
6 dpf
7 dpf
Timepoint

2.4.5 Mtz-induced neuronal loss is sustained despite formation of new neurons

To understand what happens to DA neurons of Tg(*dat*:*CFP-NTR*) zebrafish at time points past the recovery of some of their locomotor parameters, we assayed changes in CFP cell clusters using live imaging (Fig. 2.6). At 7 dpf, despite a recovery of several locomotor parameters, CFP fluorescence was still significantly decreased in Mtz-treated larvae when compared to controls. In the three clusters most amenable to live imaging due to their superficial localization, the OB, SP and Pr (Fig. 2.6A), we observed reductions in fluorescence intensity in 43.8% (n=3, p=0.01638), 28.1% (n=3, p=0.0449) and 47.2% (n=3, p=0.0168) of larvae, respectively (Fig. 2.6B). Similarly, *in vivo* analysis of 12-day-old larvae showed a persistent loss of CFP fluorescence (Fig. 2.6C), despite a recovery in most locomotor parameters.

Figure 2.6 Cell ablation experiments during the recovery period in Tg(*dat*:*CFP-NTR*) larvae. (A) Live two-photon confocal imaging of DA neuron clusters in the pretectum (Pr), olfactory bulb (OB) and subpallium (SP) of vehicle and Mtz-treated fish at 7 dpf. (B) Quantification of the relative CFP fluorescence intensity in live 7 dpf larvae A (n=3). (C) Live two-photon confocal imaging of DA neuron clusters in the pretectum (Pr), olfactory bulb (OB) and subpallium (SP) (arrowheads) of vehicle- and Mtz-treated fish at 12 dpf. A sustained loss of DA neurons is observed. Asterisks label non-specific auto-fluorescence in the skin. Images are shown dorsal facing up and anterior facing left. Scale bars represent 25 µm.

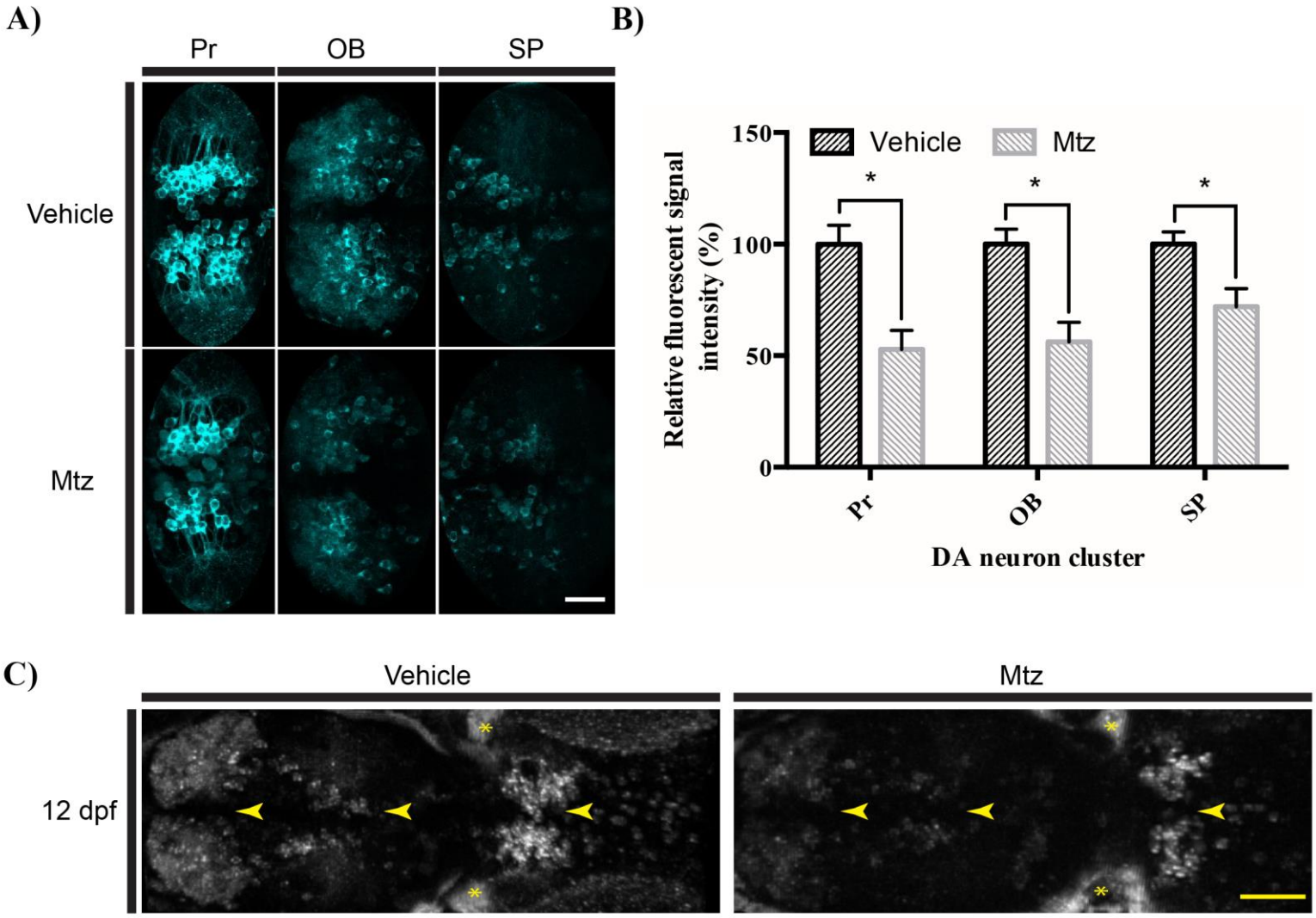
A)
Pr
OB
SP
Vehicle
Mtz
B)
Relative fluorescent signal intensity (%)
150
100
50
0
Vehicle
Mtz
*
*
*
Pr
OB
SP
DA neuron cluster
C)
Vehicle
Mtz
12 dpf

To address whether new CFP-positive neurons could still be formed post-ablation, we conducted a BrdU pulse-chase experiment immediately following the ablation protocol (Fig. 2.7A). Larvae received 10 mM BrdU starting at 4 dpf for a continuous 48 hours and then allowed to recover for 10 days in Mtz-free water (Fig. 2.7A). We focused on the olfactory bulb area, as 1) it is a major zone for neurogenesis in the vertebrate brain (Brann and Firestein 2014), and 2) it has been shown to recover from injury in the adult zebrafish brain (White *et al.* 2015). Thus, it would be a likely area to observe any recovery of cells post-injury.

Pulse-chase experiments with BrdU revealed new CFP neurons formed in the olfactory bulb (Fig. 2.7B) following neuronal injury. These cells may be a result of on-going larval brain development and/or a response to the ablation. CFP immunohistochemistry of 14-day-old larvae showed a 45% lower count in CFP-positive cells in the olfactory bulb (unpaired t-test, n=3, p=0.0158) (Fig. 2.7C) of Mtz treated animals compared to controls. Thus, Tg(*dat*:*CFP-NTR*) zebrafish were unable to repopulate the lost *dat*-positive cells back to levels comparable to those observed in wild-type larvae. Moreover, there was no statistical difference in the average number of cells positive for both BrdU and CFP in the olfactory bulb of Mtz-treated or control larvae (t-test, n=3, p=0.2879) (Fig. 2.7D). This suggests that the formation of new *dat*-expressing cells occurs after nitroreductase-metronidazole mediated ablation albeit not to a greater extent than in a normally developing larva.

Figure 2.7 New dopaminergic neurons form after Mtz treatment. (A) Pulse-chase experiment using 10 mM BrdU from 4 dpf to 6 dpf, that is, 2 and fr 4 days after the end of Mtz treatment, respectively. (B) Confocal z-stacks depicting co-localization of CFP and BrdU at 14 dpf (arrowheads). CFP- (blue) and BrdU- (purple) positive cells are labeled in individual 14 µm thick sections. (C) Quantification of the number of CFP-positive cells in 14 dpf fish (n=3). (D) Quantification of the number of cells positive for both CFP and BrdU at 14 dpf (n=3).

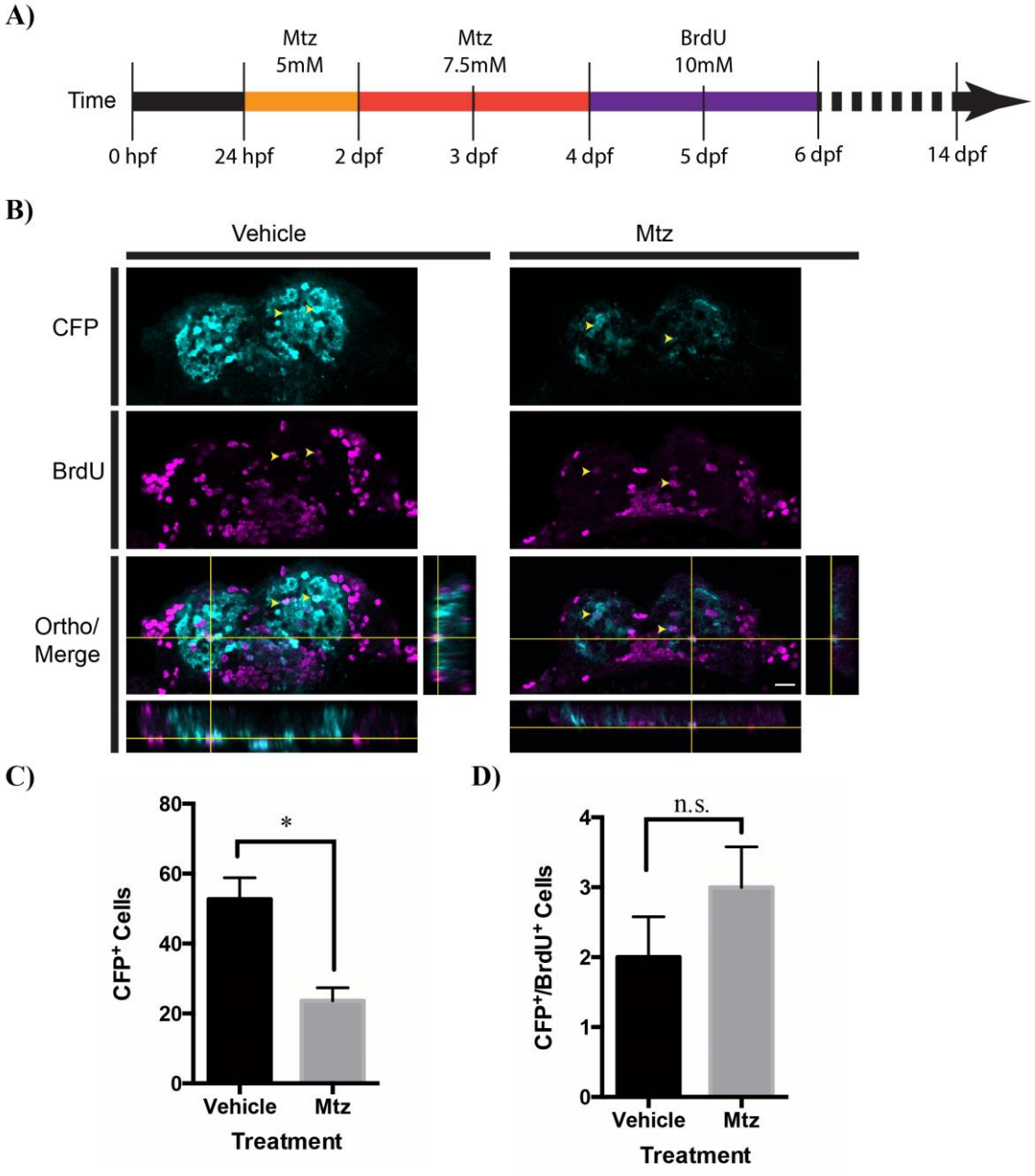
A)
Mtz
5mM
Mtz
7.5mM
BrdU
10mM
Time
0 hpf
24 hpf
2 dpf
3 dpf
4 dpf
5 dpf
6 dpf
14 dpf
B)
Vehicle
Mtz
CFP
BrdU
Ortho/
Merge
C)
CFP+ Cells
80
60
40
20
0
*
Vehicle
Mtz
Treatment
D)
CFP+/BrdU+ Cells
n.s.
4
3
2
1
0
Vehicle
Mtz
Treatment

2.5 Discussion

In this study, we used a genetic ablation approach in order to investigate how the brain of zebrafish larvae adapts to DA neuron loss. We have shown that despite sustaining lower numbers of CFP cells and a lasting tail bend phenotype, our line was able to recover several of its locomotor parameters and formed new DA neurons, albeit not at an increased rate, following cell ablation. Neurotoxins such as MPTP and MPP^+ have been previously reported to lead to a decrease in TH immunoreactivity and a locomotor phenotype in both 5- and 6-day-old larvae, but these drugs no longer have an observable effect by 7 dpf (Sallinen *et al.* 2009). Furthermore, no evidence for death of DA neurons was observed in those experiments. In contrast, we successfully observed death of *dat*-expressing cells following nitroreductase-metronidazole mediated ablation.

Larval zebrafish start to exhibit motor activity as early as 17 hours-post fertilization in the form of spontaneous tail contractions and within 48 hpf, they are able to respond to a touch stimulus and elicit an escape response (Saint-Amant and Drapeau 1998; Naganawa and Hirata 2011). Although the touch response test has been employed to study behavioural changes following the knockdown of PD-associated genes such as *pink1* (Xi *et al.* 2010; Anichtchik *et al.* 2008), *lrrk2* (Ren *et al.* 2011) and MPTP neurotoxin models (McKinley *et al.* 2005; Lam *et al.* 2005), here we opted to conduct locomotor assays starting at 5 dpf on free-swimming larvae. At this time, larvae were still optically clear and amenable to live imaging and most of the DA neuron clusters found in the adult brain are already visible (Schweitzer *et al.* 2012).

Chemical ablation with MPP^+ has been shown to lead to a reduction in the average movement velocity of 5 dpf larvae (Farrell *et al.* 2011). MPTP treatments

resulted in a decrease in the overall distance travelled (Bretaud *et al.* 2004; Sallinen *et al.* 2009). In our study, chemogenetic ablation of *dat*-positive neurons also resulted in a decrease in overall movement and swimming distance (Fig. 3). Interestingly, this phenotype was transient as fish recovered by 7 dpf (Fig. 3). This was also observed in the MPTP-treated larvae; however, in contrast to MPTP experiments where TH immunoreactivity was recovered by 7 dpf (Sallinen *et al.* 2009), Mtz treated Tg(*dat*:*CFP-NTR*) larvae showed a persistent decrease in CFP-positive cell numbers (Fig. 6).

In the Tg(*dat*:*CFP-NTR*) zebrafish, the patterns of CFP-NTR expression essentially mimicked those previously reported in the Tg(*dat:EGFP*) zebrafish except for diencephalic clusters 4 to 6, for reasons that are, at present, unclear. Targeting of the NTR gene to several groups of *dat*-expressing neurons led to their efficient ablation and to locomotor abnormalities, some of which were transient. The detection of active caspase 3 in CFP-positive cells following Mtz treatment in larvae (Fig. 2.2B) suggests that cell death occurred through the activation of the apoptotic pathway. This process has also been documented in the NTR-mediated ablation of cardiomyocytes (Curado *et al.* 2007) and orthopedia (*otp*)-positive neurons (Lambert *et al.* 2012) where the cytotoxic product derived from the reduction of the pro-drug Mtz has been shown to result in the activation of caspase 3, DNA fragmentation (as frequently demonstrated by TUNEL staining) and consequent cell loss.

Ablation of DA cells in the subpallium (SP), which has been previously identified to house the structure analogous to the mammalian striatum in teleosts (Rink and Wullimann 2001), is of particular importance to the motor phenotypes in Tg(*dat*:*CFP-NTR*) zebrafish. Recent work on the catecholaminergic projectome of larval zebrafish

has suggested that most subpallial projections originate from within the SP itself (Tay *et al.* 2011). Cells of the SP also send descending projections to the ventral diencephalic area which was previously suggested to display homologous functions to those of the human substantia nigra (Rink and Wullimann 2002b). Additionally, diencephalic cluster 2 which contributes only a few ascending DA neurons projecting to the subpallium (Tay *et al.* 2011) and which has been suggested to carry similar functions to the human meso-striatal dopaminergic neurons (Rink and Wullimann 2002b), is ablated in Tg(*dat*:*CFP-NTR*) fish.

Neurodegeneration of nigro-striatal DA neurons in human is implicated in the onset of motor phenotypes associated with Parkinson's disease (Jankovic 2008). Furthermore, during the progression of the disease, cell loss is also observed in other anatomical areas such as the olfactory bulb (OB) and the locus coeruleus (LC) (Del Tredici *et al.* 2002; Meissner *et al.* 2011). The locus coeruleus contains norepinephrine-producing neurons said to play an essential role in the locomotor phenotype of a knockout mouse model of PD lacking dopamine β–hydroxylase function (Rommelfanger *et al.* 2007). The ability of the Tg(*dat*:*CFP-NTR*) line to maintain a lasting ablation of *dat*-positive neurons in areas such as the OB, SP and LC provides an opportunity for the *in toto* analysis of live changes to the CFP cell population in the larval brain following ablation and recovery.

The schedule of NTR-mediated neuron ablation used in this study enabled larvae to recover from the injury at times when *in vivo* tracking of CFP fluorescent cells by two-photon microscopy is still possible for a period of at least 8 days. Despite recovery of several locomotor parameters by 7 dpf, larvae did not show complete recovery of the lost

CFP cell populations, at neither 7 nor 12 dpf. This suggests that the recovery of global locomotor changes in Mtz treated larvae may not require complete recovery of *dat*-expressing cell populations. These observations are consistent with the recovery of normal dopamine levels at 6 and 7 dpf, presumably through an increased production by the remaining dopaminergic neurons (Fig. 5A).

The olfactory bulb of vertebrates is an area rich in newly formed cells in the adult brain (Carleton *et al.* 2003). For this reason, we chose to examine the olfactory bulb in search of newly formed cells. Although we did see the appearance of new cells, this did not seem to occur at an increased magnitude compared to vehicle treated larvae. We cannot rule out that a more complete recovery of *dat*-expressing cells could be observed at time points later than 14 dpf. However, transgenic larvae treated with Mtz showed poor survival past this time point.

Overall, we have developed a model for the ablation of *dat*-positive cells in the larval zebrafish brain, which allows for the long lasting specific and conditional ablation of these cells. These fish will be a valuable tool for the understanding of molecular and cellular processes triggered by the loss of these cells. Combined with the amenability of larval zebrafish to live imaging and high-throughput studies, these fish will be a valuable tool for exploring novel avenues of regenerative approaches that could have implications in neurodegenerative conditions.

CHAPTER 3

CELLULAR AND MOLECULAR CHANGES FOLLOWING ABLATION OF DOPAMINERGIC NEURONS IN THE LARVAL ZEBRAFISH BRAIN

3.1 Introduction

The zebrafish has the ability to regenerate damaged tissue in their central nervous system to a degree that is higher than that described in other animal models of research such as mammals. Among this ability to regain structural and functional properties following CNS injury, lays the capacity of the zebrafish to regenerate brain tissue.

Intracellular and extracellular changes orchestrate the brain environment post injury to allow for tissue remodeling and regeneration to occur. Most of our knowledge concerning the ability of the zebrafish to regenerate brain tissue relies on experiments modeling a traumatic brain injury such as the stab lesion (März *et al.* 2011; Kishimoto *et al.* 2012). These studies show that stem and progenitor cells in the zebrafish proliferation zones increase proliferation and are recruited to sites of injury in a regenerative response (Kizil *et al.* 2012). In many cases ependymo-radial glia cells, many of which express the astrocyte marker (GFAP), are suggested to be the main contributors for CNS neuron regeneration in the zebrafish (Becker and Becker 2015).

This remodeling is dependent on the molecular reprograming of cells and many of these processes are important for the initiation of cell proliferation, precursor cell migration and fate determination, thus justifying the importance of gene expression studies in the understanding of processes driving regeneration.

Although factors such as Notch, Fgf, Bmp, Wnt, Shh, and Retinoic acid have been implicated in the regulation of stem-progenitor cell population and in the regenerative process, little is know about their regulation during zebrafish brain regeneration (Kizil *et al.* 2012). Here, we use a tissue specific chemogenetic ablation approach to ablate

dopaminergic neurons in the larval zebrafish brain and to follow the cellular and molecular changes that take place immediately post injury.

We used quantitative real time PCR to analyze the expression profile of a number of genes known to be involved in tissue regeneration or neurogenesis. We included the genes *PCNA*, *nestin* and *GFAP* as markers of early cell proliferation and cell cycling; the *gata3* gene which is involved in zebrafish brain regeneration; the gene *olig2* as a marker for oligodendrocyte precursors; the genes *pitx3* and *neurogenin1* as makers of fate determination of precursors into neuronal and dopaminergic cells; the neurotrophic gene *BDNF* (brain-derived neurotrophic factor)*;* and genes *axin2* and *shha* which are part of the Wnt and hedgehog signaling pathways.

Furthermore, we examined changes in the stem and progenitor cell population in larval zebrafish by conducting *in vivo* analyses of changes in *nestin*-driven GFP expression to address how and where cell proliferation was most affected in larvae following neuronal ablation at 5, 6 and 7 dpf. We further confirmed an increase in cell proliferation by showing that the numbers of PCNA positive cells were two-fold higher in Mtz treated animals.

The role of extracellular and blood-derived factors in the neurogenic process has previously been suggested in a parabiosis mouse model (Villeda *et al.* 2014; Villeda *et al.* 2011). Although the ability to generate two headed zebrafish parabionts has been previously described (Demy *et al.* 2013), we were unable to produce a two-headed zebrafish parabiont to study the possibility of blood-derived changes in the zebrafish. Instead, through a cerebral spinal fluid (CSF) transfusion protocol, we showed that following NTR/Mtz-mediated neuronal ablation, the larval zebrafish CSF induced a

decrease in fluorescent signal in recipient wild-type larvae. Although in its preliminary stages, we offer a model that, in the future, may allow for the identification of secreted elements that regulate the cellular environment following neuronal ablation.

Overall, we have found that the NTR/Mtz-mediated conditional and specific ablation of DA neurons in the larval zebrafish brain results in similar cellular and molecular mechanisms observed in the regenerative process in the adult zebrafish brain following stab lesion. These cellular and molecular mechanisms aid in remodeling and reorganization of the brain, which initiate a regenerative process.

3.2 Materials & Methods

3.2.1 Animal husbandry and fish lines

All experiments were conducted in agreement with the guidelines of the Canadian Council on Animal Care and approved by the University of Ottawa Animal Care Committee. Fish were maintained in a 14 hour light cycle at 28.5°C, as previously described (Westerfield 2000).

Homozygous Tg(*dat:CFP-NTR*) fish previously characterized (see Chapter 2) were bred with Tg(*-3.9nestin:GFP*) animals (Lam *et al.* 2009) to generate double transgenic animals (Tg(*dat:CFP-NTR;-3.9nestin:*GFP)) expressing CFP in DA neurons and GFP in proliferating cells.

Tg(*dat:tom20 MLS-mCherry*) zebrafish were previously characterized in our lab as expressing mCherry which is targeted to the mitochondria of dopaminergic neurons of

larval zebrafish (Noble S., Godoy R. and Ekker M., submitted), in the same populations of the Tg(*dat:CFP-NTR*).

3.2.2 Cell ablation

Double transgenic larvae were manually dechorionated at 24 hours post fertilization and exposed to 5mM metronidazole (Sigma) dissolved in 0.1 % DMSO until 2 days post fertilization and switched to a 7.5 mM Mtz solution until 4 dpf with fresh Mtz replaced daily. Exposed animals were protected from light. Control animals received 0.1% DMSO as vehicle treatment.

3.2.3 Histology and immunohistochemistry

Larvae were euthanized with an overdose of Tricaine MS-222 (Sigma) and fixed in 4% PFA overnight at 4°C. Fish were washed in 1X PBS and equilibrated in 30% sucrose. Larvae embedded in OCT (Leica) were cryosectioned 14-microns thick with a Leica CM-1850 cryostat and sections were stored at -20°C until further processing.

Immunohistochemistry was performed as previously described (Xi *et al.* 2011b). Mouse anti-PCNA (Dako) with a goat anti-mouse Alexa 488 (Life Technologies) secondary were used.

3.2.4 Imaging and cell counts

Live imaging was conducted using a Nikon A1R MP multiphoton microscope equipped with a 25X water-dipping objective, as previously described in Chapter 2.

Quantification of PCNA positive cells was done on a Nikon A1R confocal microscope with an Argon laser. Images were acquired as z-stacks of 1-micron thick optical sections and cell counts were done using NIS-Elements software. A scientist blinded to experimental conditions performed all cell counts.

3.2.5 RNA extraction, cDNA synthesis and qRT-PCR

Five-day-old larvae were killed with an overdose of Tricaine MS-222. Either whole larvae or isolated heads were immediately processed for RNA extraction. Larval heads were separated from bodies with N°5 fine forceps. Heads were placed in a 1.5mL Eppendorf tube with RLT buffer (Qiagen) containing 1% beta-mercaptoethanol (Sigma) and stored on ice until a total of 20 heads were collected.

RNA was extracted using an RNAeasy Mini Kit (Qiagen) according to manufacturer's instructions. Isolated RNA was eluted in 30 µL of nuclease-free water and stored at -80°C for further use. RNA concentrations were measured using a NanoDrop 2000 (Thermo Scientific) and a sample was run on a gel to verify RNA integrity.

For cDNA synthesis, 1µg of RNA was reverse transcribed using QuantiTect Reverse Transcription Kit (Qiagen) according to manufacturer's instructions using both oligo(dT) and random primers. cDNA was stored at -20°C until qRT-PCR was run.

The qRT-PCR reactions were prepared with SsoFast EveGreen Supermix (Bio-Rad) and run on a CFX-96 machine (Bio-Rad). Primers used are described on Table 3.1. A standard curve was prepared to determine the amplification efficiency of each primer pair and data was analyzed as described by the Pfaffl-method (Pfaffl 2001) where fold changes are relative to levels of vehicle treated animals and normalized to the housekeeping gene β-actin.

3.2.6 Parabiosis

The parabiosis protocol adopted here was modified based on previous work done by the Kissa lab (Demy *et al.* 2013). Briefly, parabiosis was performed on dechorinated embryos 2.5 to 4.3 hours post fertilization. Embryos were place in small pockets created by inserting the tip of a p1000 pipette tip into the surface of a petri dish filled with 2% UltraPure agarose (Invitrogen). Embryos were oriented using a blunt end glass pipette and a small layer of cells was removed from embryos using a glass micropipette with a 2-μm diameter. Following removal of cells from the blastula of each embryo, the two embryos were pushed into contact with one another at the site where cells had been removed. Blastula fusion took place for one hour in high calcium Ringer's solution containing antibiotics (3mM KCl, 10mM $CaCl_2$, 10mM HEPES, 100mM NaCl, 150μg/L methylene blue, 50 U/mL ampicillin and 0.5 μg/mL kanamycin). Fused embryos were than washed in antibiotic containing Ringers's solution (3mM KCl, 1mM $CaCl_2$, 10mM HEPES, 100mM NaCl, 150μg/L methylene blue, 50 U/mL ampicillin and 0.5 μg/mL kanamycin).

Parabiosis was performed between Tg(*dat:CFP-NTR*) and Tg(*dat:tom20 MLS-mCherry*) embryos.

3.2.7 CSF transfusion

Cerebral spinal fluid was collected from 5-day-old larvae. Larvae were placed into wells made in a petri dish filled with 1% UltraPure agarose (Invitrogen) and a glass micropipette mounted to microinjector setup (Narishige) was inserted into the embryo's brain ventricle as previously described (Gutzman and Sive 2009). A 3 second suction was applied to extract approximately 0.5 μL of CSF that was immediately injected into recipient larval zebrafish. Phenol red injections were used as controls in order to properly identify ventrical location and to confirm proper injection procedure (data not shown).

3.2.8 Statistical analysis

Multiple comparisons were performed with a 2-way ANOVA with Sidak post-hoc analysis. Pair wise comparisons were conducted using an unpaired t-test with statistical significance being defined by an alpha value of 0.05. For * $p \leq 0.05$, ** $p \leq 0.01$, *** $p \leq 0.001$, **** $p \leq 0.0001$ and n.s. = not significant $p > 0.05$. Error bars represent standard error of the mean (SEM).

3.3 Results

3.3.1 Neuronal ablation increases cell proliferation

To address the effects of dopamine neuron loss on the proliferating and stem cell populations of larval zebrafish, we generated a double transgenic line by crossing the Tg(*dat:CFP-NTR*) which expresses CFP-NTR in dopaminergic neurons of larval zebrafish (Fig. 3.1A) resulting in the ability to ablate these cells (see Chapter 2), with the Tg(*-3.9nestin:GFP*) line which labels the proliferating and stem cell population of the larval zebrafish in green (Fig. 3.1B)(Lam *et al.* 2009).

We adopted a cell ablation approach, as described in Chapter 2, where larvae were exposed to either 0.1% DMSO as vehicle treatment or to 5mM Mtz dissolved in DMSO for 24 hours starting at 1dpf followed by an exposure to 7.5mM Mtz until 4dpf (Fig. 3.2A). Live imaging using 2-photon microscopy was conducted to follow changes *in vivo* at 5, 6 and 7 days post fertilization to monitor proliferation changes soon after DA neuron ablation (Fig. 3.2B).

Dopaminergic neurons of the pretectum cluster (white arrows) are morphologically characterized by round shaped soma with fluorescent labels in the cytoplasm and axons with unlabeled nuclei. These cells are clearly detected at 5, 6 and 7 days post fertilization in vehicle treated animals, whereas, most of these cells disappear following Mtz treatment (Fig. 3.2B).

The fluorescent signals from *nestin* labeled cells were increased in Mtz treated animals when compared to those of vehicle treated animals, and we detected in a more

widespread pattern along the zebrafish ventricular area (pink arrows) (Fig. 3.2B) at 5, 6 and 7 dpf.

In addition to changes visualized following *in vivo* live imaging, an increase in the number of PCNA positive cells was also observed in sections of Mtz treated animals (Fig. 3.3) at 5 dpf. The numbers of PCNA positive cells counted in the area of the telencephalic ventricle (yellow box) (Fig. 3.3A) were 2-fold higher following metronidazole treatment (t-test, n=3, p= 0.023) (Fig. 3.3B).

Taken together both live imaging, and immunohistochemical analyses of larvae following neuronal ablation indicate that the resulting cell proliferation is most likely elicited as a stimulus for cellular regeneration.

Figure 3.1. **Tg(*dat:CFP-NTR;-3.9nestin:GFP*) ablates DA neurons and labels stem-progenitor cells.** A) Dorsal and lateral views of either a dissecting or a 2-photon microscopy image showing major neuron clusters in the larval zebrafish brain expressing the CFP-NTR fusion protein under the control of *dat cis*-regulatory elements. B) Double transgenic larvae were obtained by crossing Tg(*dat:CFP-NTR*) and Tg(-3.9*nestin:GFP*) for the characterization of changes in precursor/stem cells following DA neuron ablation. Scale bar = 200 microns. Olfactory bulb (OB), subpallium (SP), pretectum (Pr), preoptic area (PO), anterior preoptic area (POa), locus coeruleus (LC) and diencephalic clusters 2, 3 and 7 (2, 3, 7).

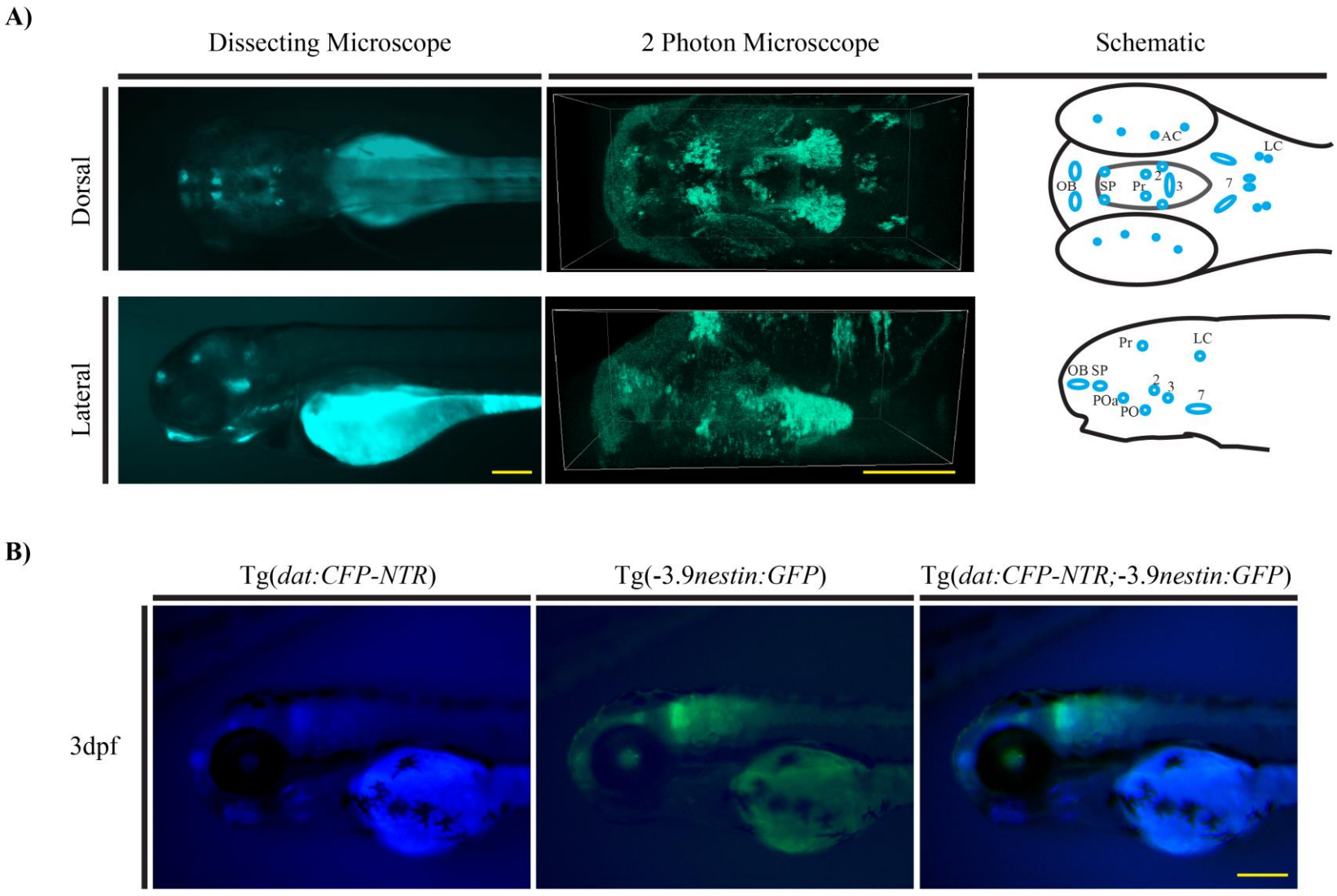
A)
Dissecting Microscope
2 Photon Microsccope
Schematic
Dorsal
Lateral
AC
LC
OB
SP
Pr
2
3
7
Pr
LC
OB SP
2
3
POa
PO
7
B)
Tg(*dat:CFP-NTR*)
Tg(-3.9*nestin:GFP*)
Tg(*dat:CFP-NTR;*-3.9*nestin:GFP*)
3dpf

Figure 3.2. **Ablation of CFP-positive cells increases *nestin* expression.** A) Timeline of metronidazole administration. B) Mtz treatment induces loss of dopaminergic neurons in the larval zebrafish pretectum from 5 to 7 days post fertilization (white arrows) and induces an increase in *nestin* expression (pink arrows). Scale bar = 50 microns.

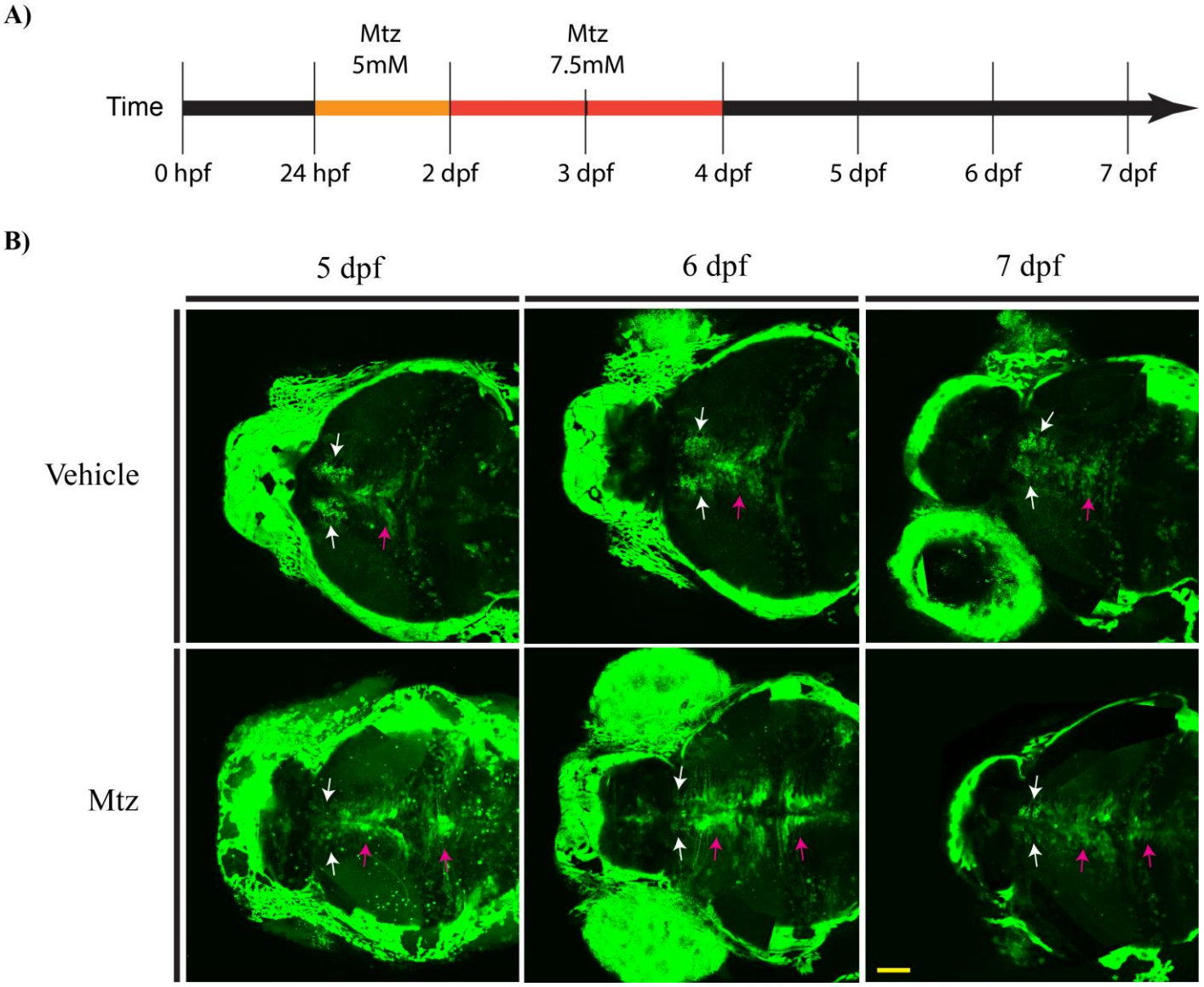
A)
Mtz
5mM
Mtz
7.5mM
Time
0 hpf
24 hpf
2 dpf
3 dpf
4 dpf
5 dpf
6 dpf
7 dpf
B)
5 dpf
6 dpf
7 dpf
Vehicle
Mtz

Figure 3.3. **Neuronal ablation increases cell proliferation.** A) PCNA immunohistochemistry on 5-day-old larvae indicates an increase in the number of proliferating cells in the telencephalon of larval zebrafish following Mtz treatment. B) Counts of PCNA positive cells within the yellow rectangle in panel A (n=3). Scale bar = 50 microns.

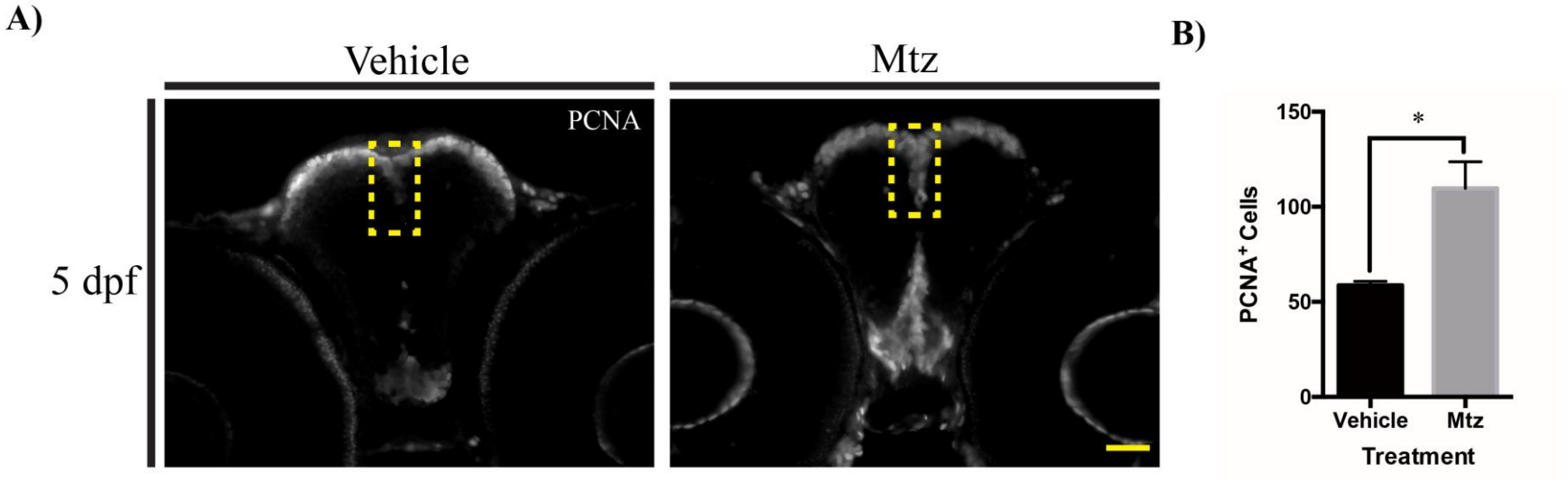
A)
Vehicle
Mtz
PCNA
5 dpf
B)
PCNA+ Cells
150
100
50
0
*
Vehicle
Mtz
Treatment

3.3.2 Gene expression changes following loss of dopaminergic neurons

We examined expression changes in genes with potential roles in cell proliferation, neurogenesis and dopamine neuron regeneration (Table 3.1). Among these genes, we looked at proliferating cell nuclear antigen (PCNA), nestin and glial fibrillary acidic protein (GFAP) as indicators of changes in cell proliferation, neuro-stem and radial glial cells. We further addressed changes in the transcription factor Olig2 (oligodendrocyte lineage tf2), Pitx3 (paired-like homeodomain 3) and Neurog1 (neurogenin 1), that have been associated with the differentiation of precursor cells into oligodendrocytes, neurons and dopaminergic cells, respectively. We also looked at changes in expression of the transcription factor Gata3 (GATA binding protein 3) that has been implicated in the regenerative process of the zebrafish brain since it is required for the proliferation of radial glial cells (Kizil *et al.* 2012a). We examined neurotrophic factor BDNF (brain-derived neurotrophic factor) with a known role in axonal regeneration (Wilhelm *et al.* 2012). Finally, we addressed changes in Wnt signaling pathway by looking at changes in Axin2 and in the hedgehog-signaling pathway by looking at changes in Shha (sonic hedgehog a).

Table 3.1. List of primers used for quantitative real-time PCR.

Gene of interest	Forward sequence	Reverse sequence	References
Actin	TGAATCCCAAAGCCAACAGAG	CCAGAGTCCATCACAATACCAG	unpublished
AXIN2	CCAGCAGCAAAGCCTTCAGT	GCGCGCACAAAGTAGACGTA	(Stulberg *et al.* 2012)
BDNF	ATAGTAACGAACAGGATGG	GCTCAGTCATGGGAGTCC	(Diekmann *et al.* 2009)
GATA3	AAATGCCATCTTTCCTGTGG	GAGGAGATGCGATCAAGAGG	(Kizil *et al.* 2012c)
GFAP	GGATGCAGCCAATCGTAAT	TTCCAGGTCACAGGTCAG	(Fan *et al.* 2010)
Nestin	ATGCTGGAGAAACATGCCATGCAG	AGGGTGTTTACTTGGGCCTGAAGA	(Fan *et al.* 2010)
Ngn1	TGCACAACCTTAACGACGCATTGG	TGCCCAGATGTAGTTGTGAGCGAA	(Fan *et al.* 2010)
OLIG2	GGAGGTCATGCCCTACGCT	GCAGCAGAGTGGCTATTTTAG	(Thummel *et al.* 2008)
PCNA	TACTCAGTGTCTGCTGTGGTTTCC	CATTTAATAAGTGCGCCCGC	unpublished
PITX3	GACAACAGTGACACAGAGAAGT	TGTCGGGATAACGGTTTCTC	(Barreto-Valer *et al.* 2012)
Shha	GCAAGATAACGCGCAATTCGGAGA	TGCATCTCTGTGTCATGAGCCTGT	(Fan *et al.* 2010)

We conducted a pilot experiment comparing the gene expression profiles of Mtz treated larvae relative to vehicle treated animals and normalized to actin in either whole larval samples or in brain samples alone (Fig. 3.4A). Although we observed similar trends in both whole larval samples and brain samples for some of the genes, others, such as Gata3, showed opposite changes in expression in the whole larvae and brain samples, and other genes such as Axin2 and Shha had a lower overall expression level when whole larvae were used for quantitative RT-PCR analysis (Fig. 3.4A). In order to examine tissue specific changes in gene expression that would reflect processes taking place in the brain, we decided to use only brain tissue for further analyses.

We detected an overall 8.9 fold increase in Axin2 expression (n=3, p=0.003), a 7.2 fold increase in Shha (n=3, p=0.007), a 5.7 fold increase in PCNA (n=3, p=0.046), a 3.4 fold increase in Olig2 (n=3, p=0.013), as well as increases of 5.9 fold in Gata3 (n=3, p=0.06) and of 4.3 fold in nestin expression (n=3, p=0.08) that did not reach statistical significance (Fig. 3.4B). Expression levels of neurogenin1, Pitx3, BDNF and GFAP did not appear to differ from those of vehicle treated animals (Fig. 3.4B).

Immunohistochemistry and live imaging experiments (Fig. 3.2 and 3.3) suggest an upregulation of nestin and PCNA, which is in agreement with qRT-PCR data from samples of 5dpf larval brains following DA neuron ablation. Overall, our data suggest an upregulation of genes involved in cell proliferation, as well as genes previously shown to influence neurogenesis and brain regeneration.

Figure 3.4. **Gene expression changes following Mtz treatment.** A) Heat map of fold changes in gene expression in Mtz treated larvae in relation to vehicle treated controls. Expression levels were normalized to actin. Samples were divided into tissue from either brain (n=3) or whole larvae (n=2). B) Fold change in gene expression levels in larval brain samples following Mtz treatment relative to vehicle treated larvae at 5 days post fertilization. Dashed line indicates vehicle levels set to 1 fold.

A)

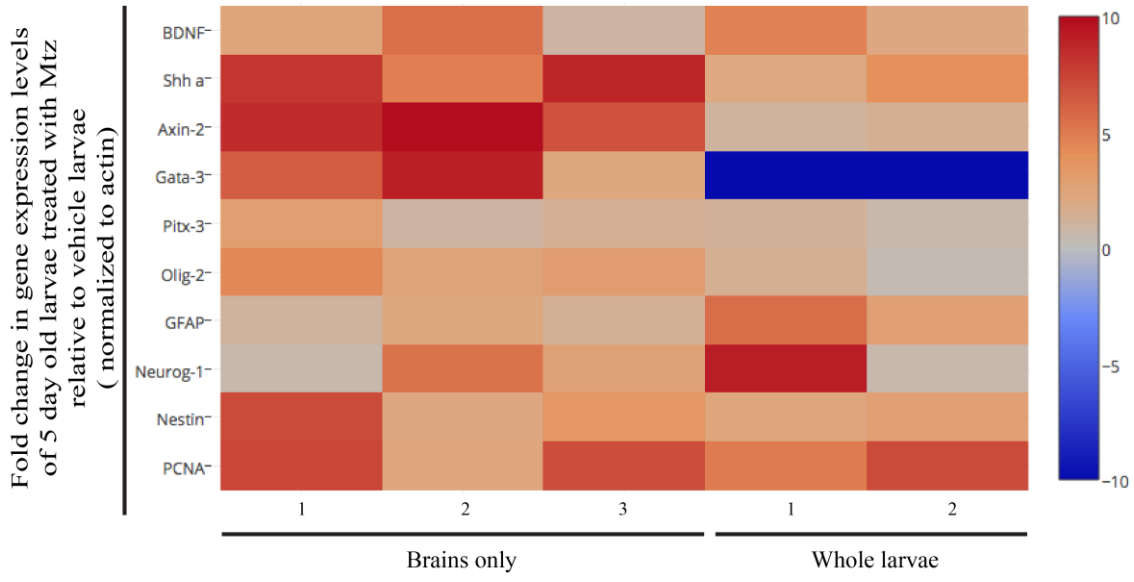
Fold change in gene expression levels of 5 day old larvae treated with Mtz relative to vehicle larvae (normalized to actin)
BDNF⁻
Shh a⁻
Axin-2⁻
Gata-3⁻
Pitx-3⁻
Olig-2⁻
GFAP⁻
Neurog-1⁻
Nestin⁻
PCNA⁻
1
2
3
1
2
Brains only
Whole larvae
10
5
0
−5
−10

B)

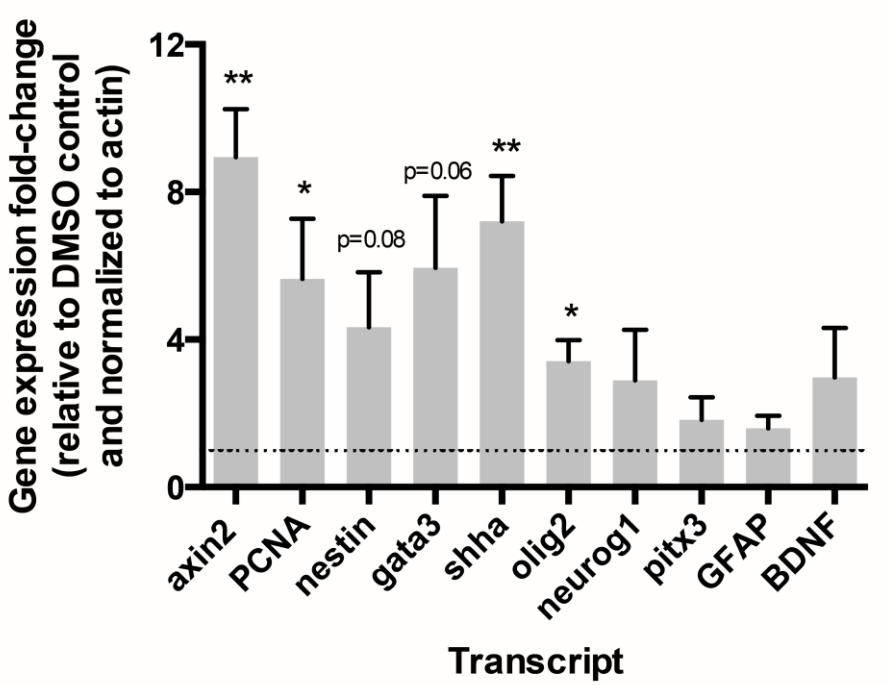
Gene expression fold-change (relative to DMSO control and normalized to actin)
12
8
4
0
**
*
p=0.08
p=0.06
**
*
axin2
PCNA
nestin
gata3
shha
olig2
neurog1
pitx3
GFAP
BDNF
Transcript

3.3.3 Extracellular signaling induces changes in the dopaminergic neuron population

The cellular milieu is an important regulator of processes such as neurogenesis and would thus be expected to play an essential role in the regenerative process of the zebrafish brain. Previous research conducted by the laboratory of Dr. Wyss-Coray, has elucidated the role of blood-borne factors in the regulation of adult neurogenesis. Through the use of heterochronic parabiosis experiments it has been shown that young mice paired with aged animals had an increase in CCL11 chemokine levels, a decrease in hippocampal neurogenesis and impaired learning and memory (Villeda *et al.* 2011). A more recent study by the same group, further suggested that exposure of older animals to blood from younger animals is able to improve age-linked cognitive decline, to increase the density of dendritic spines of mature neurons and to increase synaptic plasticity in the hippocampus (Villeda *et al.* 2014).

Here we attempted a parabiosis experiment between embryonic zebrafish with the objective of elucidating the effects of ablating dopaminergic neurons in one embryo on the neuronal population of an isochronic parabiont (Fig. 3.5A). Tg(*dat:CFP-NTR*) larvae were fused with Tg(*dat:tom20 MLS-mCherry*) embryos between the 256 and 512 cell stage and allowed to develop (Fig. 3.5B). Although this parabiosis procedure has been described to generate larvae with connected bodies and separate heads (Demy *et al.* 2013), which would be ideal for our *in vivo* analysis of changes in fluorescently labeled neuronal populations, we were unsuccessful in generating double headed parabionts (Fig. 3.5B).

In order to address whether extracellular signaling elements, present in the cerebral spinal fluid of larval zebrafish that underwent neuronal ablation, contained factors able to elicit changes in the neuronal population of age matched larvae, we employed a CSF transfusion protocol to transfer the CSF from Tg(*dat:CFP-NTR*) larvae following ablation into the brain ventricle of Tg(*dat:tom20 MLS-mCherry*) larvae (Fig. 3.6A). CSF from larvae treated with Mtz from 1 to 4 dpf were collected and immediately transferred into Tg(*dat:tom20 MLS-mCherry*) following a previously established ventricular microinjection protocol (Gutzman and Sive 2009).

Although preliminary, our data suggest that factors present in the CSF of Mtz treated animals are able to induce an overall decrease in fluorescent signal observed in Tg(*dat:tom20 MLS-mCherry*) larvae, whereas neither the ventricular injection alone nor the injection of CSF of un-ablated larvae were able to induce such changes (Fig. 3.6B).

Figure 3.5. **Larval zebrafish parabiosis experiments.** A) A schematic representation of the experimental approach using parabiosis experiment between a Tg(*dat:CFP-NTR*) (blue head) and a of Tg(*dat:tom20 MLS-mCherry*) larvae (red head) in order to address changes in mCherry expression following ablation of CFP positive cells. B) Embryos at 2.5 hpf were fused and allowed to grow as parabiont larvae. Despite a successful parabiosis, we were unable to generate double headed larvae.

A)

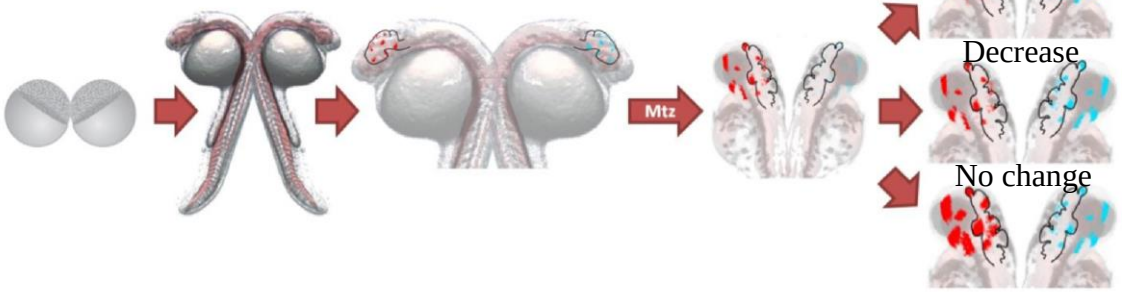
Mtz
Outcome:
Decrease
No change
Increase

B)

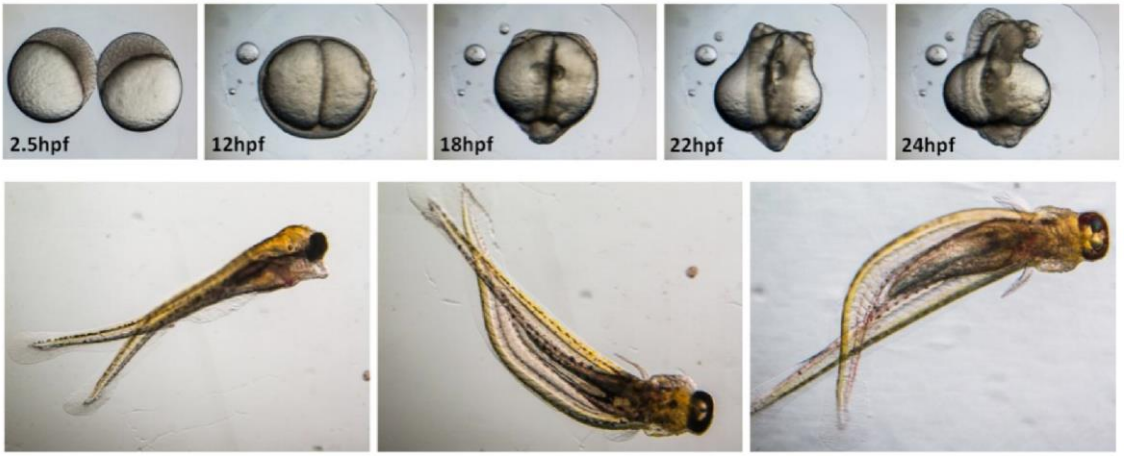
2.5hpf
12hpf
18hpf
22hpf
24hpf

Figure 3.6. **Cerebral spinal fluid transfusion experiment.** A) A schematic representation of the experimental approach using CSF transfusion from a Tg(*dat:CFP-NTR*) larvae (blue head) treated with Mtz, into a Tg(*dat:tom20 MLS-mCherry*) larvae (red head). CSF was collected when larvae were 5 dpf, 24 hours following the termination of Mtz exposure, and microinjected into age matched larvae. B) Contrary to injection only control larvae, or larvae receiving CSF from non-ablated animals, CSF from larvae following loss of DA neurons reduced the expression of mCherry fluorescence in recipient larvae. Scale bar = 50 microns.

A)

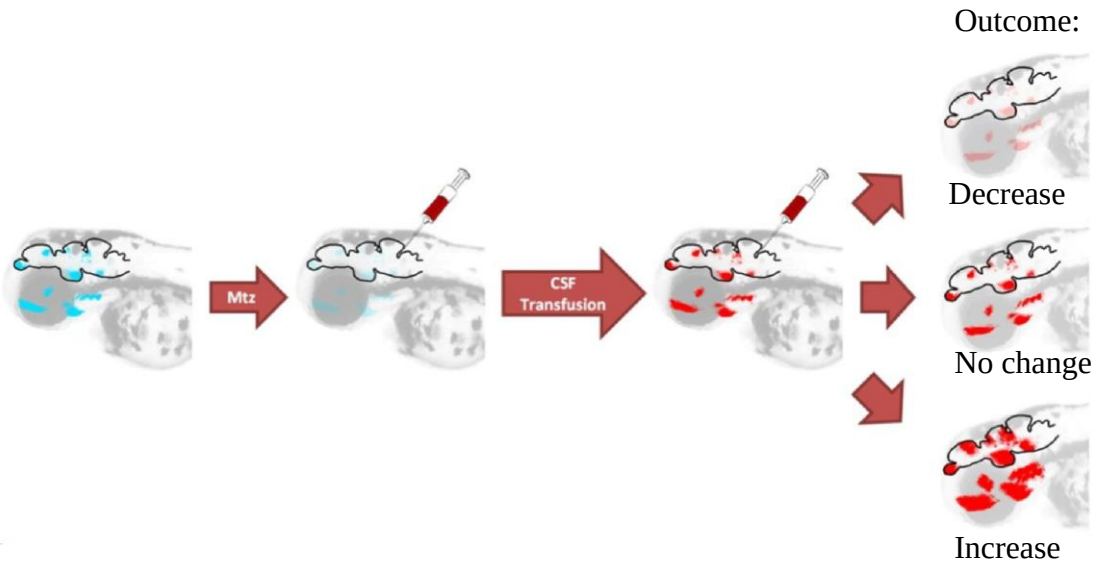
Outcome:
Mtz
CSF Transfusion
Decrease
No change
Increase

B)

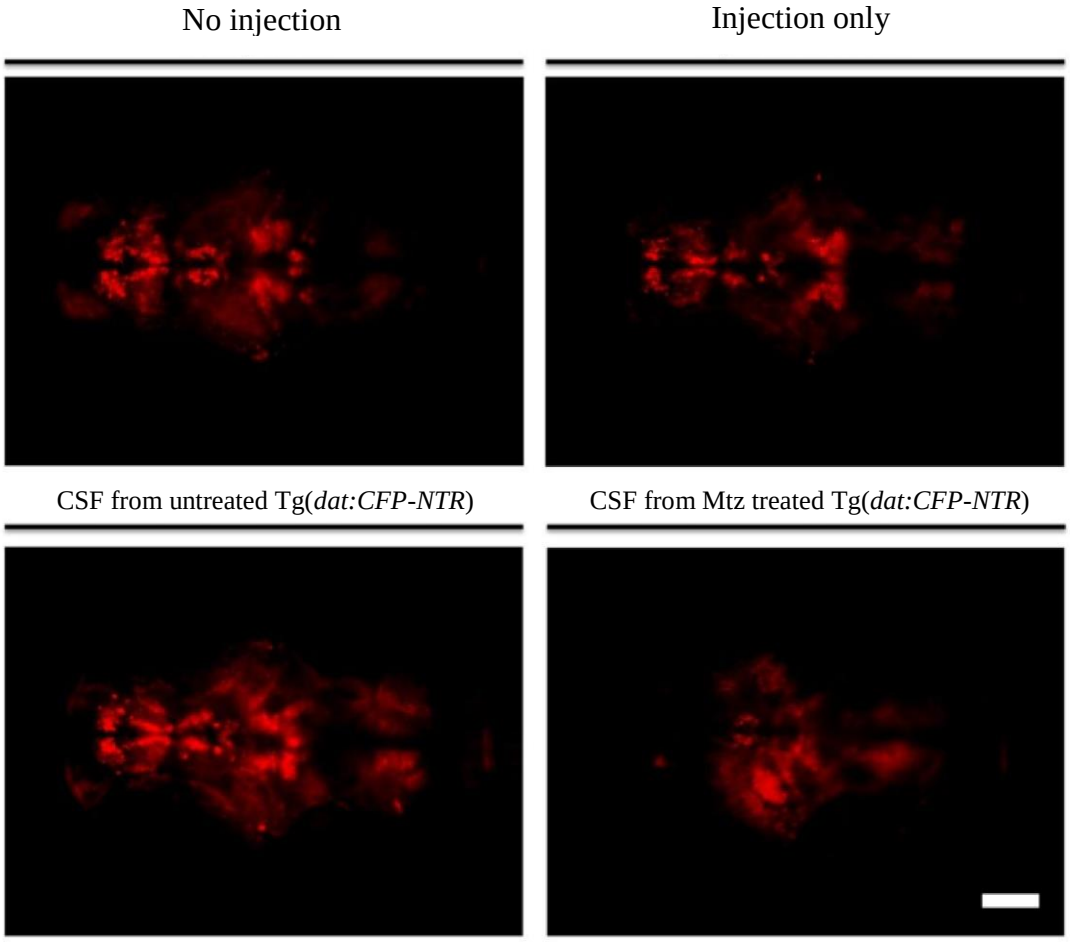
No injection
Injection only
CSF from untreated Tg(*dat:CFP-NTR*)
CSF from Mtz treated Tg(*dat:CFP-NTR*)

3.4 Discussion

We demonstrated that loss of dopaminergic neurons following MTZ-mediated ablation led to a regenerative response characterized by an increase in *nestin*-driven fluorescent reporter expression and an increase in the number of proliferating cells. Furthermore, the expression of potential genes involved in the regenerative process was up-regulated following neuronal ablation. We further demonstrate that our model is a useful tool for the tracking of cellular changes *in vivo* and for studying the effects of extracellular factors present in larval zebrafish neuronal populations following dopamine neuron ablation.

Nestin is an important marker for neural-stem and progenitor cells in the central nervous systems of mammals with similarly conserved function in the zebrafish. Recruitment of these precursor cells, which can give rise to both glia and neuronal cells, may be the most parsimonious way for the zebrafish brain to recover following injury. The expression of *nestin* in the early zebrafish embryo (24 hpf) is widespread throughout the central nervous system as development and neurogenesis is taking place and by 4 dpf its distribution is restricted to a faint area of expression located along the proliferation zones of the zebrafish brain which are close to the ventricle (Mahler and Driever 2007). Here, we show that following injury to DA neurons, *nestin* expression is more widespread and has a stronger expression in the damaged brain than in vehicle treated animals. Previous work has addressed the up-regulation of *nestin* during the regenerative process in the spinal cord of the zebrafish. Guo and colleagues have shown that *nestin* expression is up-regulated 1.58 fold at eleven days following spinal cord injury (Guo *et*

al. 2011), while others show that up-regulation of *nestin* takes place as early as 3 days post injury (Goldshmit *et al.* 2012). In addition, the up-regulation of *nestin* following spinal cord injury has also been reported in *Xenopus* tadpoles and in the newt (*Pleurodeles waltlii*) (Gaete *et al.* 2012; Zaky and Moftah 2014). *Nestin* has also been shown to be one of the earliest markers of proliferation in response to a mouse cortical impact brain trauma injury model and is required for brain remodeling following injury (Yu *et al.* 2008). This is similar to the rat traumatic brain injury model where an increase in the number of *nestin* expressing cells is observed as early as 1 day post-injury (Yi *et al.* 2013).

The initial increase in cell proliferation that we observed is in agreement with an increase in PCNA gene expression levels and the number of PCNA immunolabeled cells along the telencephalic ventricle. A number of studies have reported an increase in the number of PCNA positive cells in the zebrafish brain (Kishimoto *et al.* 2012; März *et al.* 2011) alongside an increase in the number of cells which uptake the thymidine analog, BrdU, (Kyritsis *et al.* 2012; Baumgart *et al.* 2011) following stab lesion experiments.

The number of olig2-expressing cells has also been shown to increase in response to spinal cord injury in the zebrafish suggesting that olig2 positive ependymal radial glial cells are the progenitors to spinal motor neurons (Reimer *et al.* 2008). Furthermore, the clustering of olig2-positive cells has been observed at the site of injury following brain stab wound experiments (März *et al.* 2011). This observation is in agreement with the up-regulation of olig2 we observed following neuronal loss.

Surprisingly, the levels of GFAP remained unchanged following MTZ-mediated ablation in Tg(*dat:CFP-NTR*) zebrafish. Most radial glial cells with ependymal features

found in the CNS of the zebrafish express the glial marker GFAP and are thought to be the main population of progenitor cells in the zebrafish CNS contributing to the zebrafish's regenerative ability (as reviewed by Becker and Becker, 2015). Although levels of GFAP remained unchanged in our animals, further analysis looking at other time points is needed to properly understand what is happening to GFAP expression. Indeed it has been suggested that upon activation, glial cells can lose the expression of GFAP and increase expression of *nestin* as they dedifferentiate (Goldshmit *et al.* 2012).

There was a strong trend for an increased expression of *gata3* following MTZ-mediated ablation, which was reminiscent of previous studies where the number of *gata3* expressing cells was increased following stab lesion to the zebrafish brain as early as 1 day post-injury (Kizil *et al.* 2012b). This transcription factor has been implicated in the proliferation of radial glial cells following injury.

Genes, such as *pitx3* and *neurogenin1* (Filippi *et al.* 2012; Filippi *et al.* 2007), involved in the determination of precursors into a neuronal and dopaminergic fate, were indistinguishable in ablated animals and vehicle treated controls, further indicating that shortly after ablation, there is no signal to direct progenitor cells into a dopaminergic fate.

Finally, we looked at both the Wnt and hedgehog signaling pathways whose roles in tissue regeneration has been previously described (Singh *et al.* 2012; Shin *et al.* 2011). Activation of the Wnt/β-catenin pathway has previously been involved in the planarian brain regeneration (Iglesias *et al.* 2011). Although little is known about the roles played by the Wnt pathway in the zebrafish brain regenerative process, Wnt is required for progenitor cell proliferation, migration and differentiation in mammals (as reviewed by (Kizil *et al.* 2012a)). Here, we show that *axin2* is up-regulated almost 9-fold in Mtz

treated animals when compared to vehicle controls. Axin2 is an important component of the Wnt signaling pathway. Wnt signaling has been shown to drive expression of *axin2* which acts as a negative regulator of the pathway by phosphorylating and promoting the degradation of β-catenin (Jho *et al.* 2002). *Axin2* has been found to be essential for the remyelination process in rodents (Fancy *et al.* 2011) and is up-regulated in the zebrafish during fin regeneration (Stoick-Cooper *et al.* 2006).

Similarly to Wnt, *shh* is associated with stem-progenitor cells proliferation in mammals but its function during brain regeneration in the zebrafish has yet to be described (as reviewed by (Kizil *et al.* 2012a)). In the zebrafish, *shh* has been implicated in the proliferation and differentiation of cells during bone regeneration following fin amputation (Quint *et al.* 2002) and an increase in *shha* has been described during motor neuron regeneration in adult zebrafish (Reimer *et al.* 2009). Here, we show that during dopamine neuron regeneration there is a 7.2-fold increase in *shha* expression.

It is important to consider that our analysis is restricted to a single time-point and that the temporal expression of these genes is likely to vary in order to drive remodeling of brain tissue following neuronal ablation. A more extensive analysis of these genes at different time points will be needed to better understand the regenerative process driving the regeneration of dopamine neurons in the zebrafish brain. These analyses should also be combined with *in situ* hybridization and immunohistochemistry as well as *in vivo* live imaging analysis in order to characterize the sites in the brain where changes are taking place.

Finally, we highlighted the importance of extracellular signaling during the regenerative process. Although preliminary, our data suggest that following neuron

ablation, factors in the CSF of affected larvae are able to reduce reporter gene expression in dopaminergic neurons of untreated samples.

In summary, the Tg(*dat:CFP-NTR*) transgenic zebrafish enable the study of the cellular and molecular processes that take place following brain dopaminergic neuron ablation. Combined with high-throughput methods such as RNAseq and large-scale drug screens, our model will allow for the unveiling of gene regulatory changes that take place during regeneration and the identification of potential targets that could in the future be used as therapeutic approaches to stimulate the regeneration of neurons in patients suffering from neurodegenerative conditions such as Parkinson's disease. Taken together, our data suggest that cell specific ablation in the zebrafish shares common characteristics with more invasive and non-specific approaches such as the adult brain stab lesion.

CHAPTER 4

REGENERATION OF DOPAMINERGIC NEURONS FOLLOWING CHEMOGENETIC ABLATION IN THE ADULT ZEBRAFISH BRAIN

4.1 Abstract

The zebrafish has been shown to carry the ability to regenerate brain tissue following traumatic brain injury. Here we employed a chemogenetic ablation approach to study the regeneration of dopaminergic neurons in adult fish. Tg(*dat:CFP-NTR*) animals treated with metronidazole showed a reduction in TH and CFP expression as well as in levels of dopamine. On the seventh week following treatment, levels of TH and CFP in the adult brain were recovered to vehicle treated levels. Here, we show that a recovery in both swimming phenotype and neuronal population correlated with an increase in production of new dopaminergic neurons in the brain of adult zebrafish following neuronal ablation. Overall, we have established a model for the study of dopaminergic neuron regeneration in the adult zebrafish.

4.2 Introduction

Over the last decade, the zebrafish has emerged as a strong model for the study of neurogenesis and brain regeneration as reviewed by (Schmidt *et al.* 2013; Becker and Becker 2015). Unlike mammals, which have two main proliferation zones – the subgranular and subventricular zones (Ming and Song 2011; Kempermann 2011), the zebrafish holds 16 different zones of proliferation in the brain (Grandel *et al.* 2006; Adolf *et al.* 2006).

This ability to hold numerous cells in a proliferating stage allows for the recruitment of stem-progenitor cells to multiply and migrate following damage to brain

tissue in order to allow cells to then remodel the brain environment in a regenerative fashion (März *et al.* 2011; Kroehne *et al.* 2011). Much of the knowledge available on the ability of the adult zebrafish to regenerate brain tissue comes from invasive tissue damage models such as stab lesion studies (Kishimoto *et al.* 2012). Here, we set to investigate the ability of the zebrafish to regenerate its dopaminergic neurons following a non-invasive, conditional and cell-specific ablation approach.

Although neurotoxins such as MPTP and 6-OHDA have been described to induce dopaminergic neurodegeneration with Parkinson's disease-like pathology and phenotype in research models such as rodents, non-human primates, the planarian and salamander (Parish *et al.* 2007; Nishimura *et al.* 2011; Dauer and Przedborski 2003), their use in the adult zebrafish has not led to a decrease in the numbers of brain dopaminergic cells, despite a transient locomotor phenotype (Bretaud *et al.* 2004; Anichtchik *et al.* 2004). To overcome this barrier we set to establish an adult model for the conditional and specific ablation of dopaminergic neurons by expressing the nitroreductase enzyme under the *cis*-regulatory elements of the zebrafish's dopamine transporter.

Parkinson's disease is the second most prevalent neurodegenerative condition affecting the elderly and understanding the regenerative potential for dopaminergic neurons in the zebrafish brain may provide insights in the cellular and molecular mechanism involved in this process that may lead to novel therapeutic approaches targeting endogenous regeneration of DA neurons in PD patients.

Here we showed that, similar to the zebrafish larvae (Godoy et al, 2015 JNC-2015-0237), Mtz treatment of adult Tg(*dat:CFP-NTR*) zebrafish led to the ablation of dopaminergic neurons along the adult brain. Neuronal ablation was consistent with a

decrease in both TH and CFP protein levels and with a reduction in dopamine levels. Despite the normal ability to start and maintain movement, neuronal loss induced an increase in the time that fish spent in the upper half of the tank and the number of times fish would cross the midline between the upper and lower halves of the tank. We observed a transient place preference phenotype that recovered by 45 days post ablation. Furthermore, these results correlated with a recovery in TH and CFP expression levels and in the number of CFP and TH positive cell counts. Finally, we observed an increase in the number of CFP positive cells that incorporated BrdU, indicating that such recovery was attributed to the formation of new dopaminergic neurons in the adult zebrafish brain.

Overall, our model offers new opportunities for the understanding of dopaminergic neuron regeneration from a non-invasive, conditional and cell-specific ablation approach in the adult zebrafish.

4.3 Materials & Methods

4.3.1 Animal care and transgenic animals

All experiments were conducted in agreement with the guidelines of the Canadian Council on Animal Care and approved by the University of Ottawa Animal Care Committee.

We have generated and characterized the Tg(*dat:CFP-NTR*) line (Godoy et al, 2015 Chapter 2), and experiments were conducted on homozygous animals at 8 to 10 months of age. All fish used were females, unless otherwise specified.

Fish were maintained as previously described (Westerfield 2000).

4.3.2 Histology and immunohistochemistry

Adult zebrafish were sacrificed by immobilization in ice-cold water followed by immediate decapitation. Heads were fixed in 4% PFA overnight at 4°C and skulls were then decalcified and equilibrated in 20% sucrose. Fourteen-micron thick sections were cut using a Leica CM-1850 cryostat and stored at -20°C for further immunohistochemical analysis.

Sections were defrosted at room temperature for 30 min, washed in 1X PBS and incubated overnight (ON) with primary antibody in PBSTx at 4°C. Following primary antibody incubation, sections were washed 3X in PBSTx at RT and incubated with secondary antibody for 2 hours at RT. Sections were mounted with DAPI-containing mounting media (Vector Labs). Antibodies used included mouse anti-CFP (Clontech), rabbit anti-TH (Millipore), rat anti-BrdU (AbCam), goat anti-mouse Alexa-488, goat anti-rabbit Alexa-594 and goat anti-rat Alexa-647 (Molecular Probes).

4.3.3 Imaging and cell counts

Global ablation patterns on 14-µm thick sections were analyzed using a Zeiss Axiophot epifluorescent microscope and images were processed using Fiji software (Schindelin *et al.* 2012).

Cell counts were conducted on images acquired by a Nikon A1 confocal microscope with 1-µm thick optical sections. Data was analyzed using the NIS-Elements

software and orthogonal views were used to assure correct cell co-localization. A researcher blinded to the experimental design conducted all cell counts.

4.3.4 Cell ablation

Adult zebrafish were exposed to either vehicle: 0.2% dimethyl sulfoxide (DMSO) (Sigma) or to 10 mM metronidazole (Mtz) (Sigma) dissolved in 0.2% DMSO. Both drug and vehicle solutions were prepared using fish facility system water.

Fish were place one fish per tank into a 1 L breeding tank (Aquatic Habitats) filled with 500 mL of either vehicle or Mtz solution and treated for 24 hours in a room acclimatized to 28°C with the tanks shielded from light exposure. Fish were not feed during the exposure.

Upon termination of exposure, 500 mL of fresh system water was added to the exposure solution and incubated for 30 minutes. Fish were then moved into another tank containing clean water and this process was repeated a total of 3 times with 1-hour intervals between switches. Fish were then placed into static 10 L glass tanks with an AquaClear 20 power filter and feeding resumed. Fish stayed in the static tank for 24 hours prior to being returned into tanks with circulating water.

Adult Tg(*dat:EGFP*) fish previously characterized in our laboratory (Xi *et al.* 2011b) also received the same treatment and were used as controls in both ablation experiments and behavior analysis.

4.3.5 BrdU labeling

The labeling of proliferating cells was done using 5-bromo-2'-deoxyuridine (BrdU) (Sigma) for immunohistochemical detection. A 2.5 mg/mL solution of BrdU was prepared in 110 mM NaCl pH 7 fresh during the week of BrdU administration. Small aliquots were made and stored at -80°C protected from light and defrosted immediately prior to use throughout the week.

Fish received 5 µL of solution per 0.1 grams of body weight immediately prior to Mtz or vehicle exposure and repeatedly every 48 hours for a total of 5 intraperitoneal (i.p.) injections. Adult fish were 3 cm in length and weighed on average 0.55 grams.

Regeneration of DA neurons was examined 45 days post-treatment by immunohistochemical analysis.

4.3.6 High performance liquid chromatography (HPLC)

Adult brain samples were processed for HPLC analysis either as single intact brains (referred to as whole brain), or single brains dissected into 3 main areas: one containing both the olfactory bulb and telencephalon (OB/Tel), one containing the diencephalon and midbrain (DC/Mid) and another containing the hindbrain region. Brains were dissected on ice cold homogenization solution (1mM Na_2EDTA, 0.3M chloroacetic acid (ClCHCOOH) and 10% methanol in HPLC grade water) and stored in 500 µL of the same, quickly frozen in dry ice and stored at -80°C until further processing. DHBA was used as an internal standard.

Brain tissue was homogenized via sonication using a Fisher Scientific Model 100 Sonic Dismembrator and protein levels were measured using Pierce BCA Protein Assay Kit (Thermo Scientific) in a FLUOstar Galaxy (BMG LabTech) system. Homogenized samples were centrifuged for 20 minutes at 12000xg and transferred to HPLC vials. The supernatant (20 µl) was injected into a high performance liquid chromatography system (Aligent) consisting of an Iso-pump (G 1310A), auto sampler ALS (G 1329A), coolant system ALS-Term (G-1329), a stainless steel Eclipse XDB-C8 (5 µm) 4.6 x 150 mm column situated in a thermostatic chamber (40°C) and an electrochemical detector DECADE SDC (Antec Leyden) with an electrochemical flow cell VT-03 with a working electrode maintained at the potential of 0.60V relative to the reference electrode. Determination of the area and height of the peaks was carried out with the aid of a Hewlett-Packard integrator.

The mobile phase consisted of 90 mM sodium phosphate monobasic, 1.7 mM 1-octane sulfuric acid sodium salt, 50 mM EDTA, 10% acetonitrile, 50 mM citric acid monohydrate and 5 mM KCl in 200 mL of acetonitrile and was passed through a GS (0.22 µm) filter.

4.3.7 Western blotting

Brains were removed from fish's skull and processed for homogenization on ice, with a pestle and mortar in buffer containing protease inhibitor, as previously described (Xi *et al.* 2010). Protein content was then quantified by bicinchoninic acid (BCA) assay and separated in a 4-20% SDS-PAGE gel. Immunoblotting with a mouse anti-CFP

(Clontech), rabbit anti-TH (Millipore), rabbit anti-actin (Sigma) with a donkey anti-rabbit-IgG-HRP (GE Healthcare) and a goat anti-mouse-IgG-HRP (Jackson Immuno Research) secondary was detected using a chemiluminescence detection kit (GE Healthcare).

Care was taken to avoid saturation of bands and at least 3 replicates were used for the relative quantification of band intensity using ImageJ software.

4.3.8 Locomotor phenotype

Initiation of movement and global swimming parameters

In order to address the effects of neuronal ablation on adult zebrafish swimming parameters, we addressed locomotor changes by following the movement of fish in a 2-D perspective and tracking fish from the top of their tanks either 1 or 7 days post treatment.

Prior to video recordings fish were place in a light-cycle and temperature controlled room, similar to, but separated from, the main zebrafish facility, and allowed to acclimatize for at least 4 days. The presence of personnel in this room was limited to the first minute of video recording to minimize extraneous stimuli to the fish.

Fish were placed one per tank into a 1L breeding tank (Aquatic Habitats) filled with system water. Tanks were positioned overtop a translucent-white light box with trans-illumination provided by an LED light source to minimize the generation of heat or light flickering during video recordings. Fish were allowed to acclimatize over the light box for 20 minutes prior to video recordings.

A Nikon 3100 DSLR camera equipped with a 50 mm Nikon lens was attached to a tripod and positioned on top of the light box to maintain the entire tank in the field of view of the videos. 10-minute videos were recorded at 30 fps.

Data analysis was performed using the Ctrax software with its included Matlab toolboxes (Branson *et al.* 2009), originally developed to track *Drosophila* but recently adapted to track larval zebrafish (Lambert *et al.* 2012; Decker *et al.* 2014) and used here to track and analyze the adult locomotor phenotype.

Top and bottom place preference

In addition to looking at global swimming parameters, we addressed the fish's preference for either the top half or the bottom half of their 1L tank and the number of times they would cross the mid-line of the tank. For this, the same Nikon camera and lens described above were placed in front of the 1L tank, focusing on the line dividing the height of the tank into 2, while maintaining the entire tank in the field of view. A 25-minute long acclimatization took place prior to capturing 5-minute long videos recorded at 30 fps.

Data analysis was conducted manually. Briefly, videos were viewed using QuickTime software and the number of times the fish crossed the midline of the tank was scored manually. A crossing event was defined by the crossing of the nose of a fish, here defined as the reference point. A second parameter, the percent of time spent on the top half of the tank was also measured manually with a stopwatch. An experimenter blinded to the experimental design obtained all measurements.

4.3.9 Statistical analysis

Statistical significance of pair-wise comparisons of normally distributed data was analysed using a standard t-test. Multiple comparisons were addressed with a 2-way ANOVA with Sidak post-hoc analysis. For * $p \leq 0.05$, ** $p \leq 0.01$, *** $p \leq 0.001$, **** $p \leq 0.0001$ and n.s. = not significant $p > 0.05$. Error bars represent standard error of the mean (SEM).

4.4 Results

4.4.1 Tg(*dat:CFP-NTR*) animals express cyan fluorescent protein in the brain of adult fish

The Tg(*dat:CFP-NTR*) fish express the CFP-NTR fusion protein in the same clusters as previously described in the larval zebrafish as represented in Figure 4.1A. The expression patterns and fluorescence intensity were consistent across different generations (data not shown). These CFP expressing cells include cells in the olfactory bulb (OB), dorsal, central, ventral areas of the ventral telencephalon (Vd,Vc,Vv), anterior and posterior part of parvocellular preoptic nucleus (PPa and PPp) periventricular pretectal nucleus (PPr), periventricular nucleus of posterior tuberculum (TPp), paraventricular organ (PVO) and nucleus of posterior recess (PR) (Fig. 4.1A).

Characterization of CFP expression in the adult Tg(*dat:CFP-NTR*) zebrafish was conducted in homozygous females 8 to 10 months of age, and the CFP signal was

amplified by detection with an anti-CFP antibody in 14 micron thick cryosections (Fig. 4.1B).

Initially an entire brain was sectioned and processed for immunohistochemistry with both an anti-CFP (Fig. 4.1B a'-i') and an anti-TH antibody (Fig. 4.1B a''-i'') to characterize which dopaminergic clusters were labeled along the rostral caudal axis of the adult brain (Fig. 4.1B a-i). Many of the CFP identified cells in the rostral and caudal areas of the OB (Fig. 4.1B a,b) co-localized with TH expression, pointing to the catecholaminergic nature of these cells, which was also observed in the ventral telencephalon (Fig. 4.1B c), the PPa/PPp (Fig 4.1B. d-f), the PVO (Fig. 4.1B e), the PPr and diencephalon (Fig. 4.1B g-i). Although some CFP positive cells did not co-label with tyrosine hydroxylase, this could be attributed to the fact that the TH antibody used in our experiments more readily recognizes the zebrafish Th1 epitope and does not recognize cells that would be positive for Th2 (Yamamoto *et al.* 2010), further analysis using other markers of dopaminergic cells such as Vmat2, Aadc, and Th2 via immunohistochemistry or *in-situ* hybridization is needed to further characterize the nature of these CFP^{+} cells.

Figure 4.1. Tg(*dat:CFP-NTR*) expresses CFP-NTR fusion protein in the brain of adult fish. A) Schematic representation of CFP positive cell populations in the adult zebrafish CNS. Cyan circles indicate where CFP^{+} cell bodies were identified. Green label represents larval nomenclature, while purple labels represent adult classification (based on Schweitzer *et al.* 2012). B) Adult zebrafish, 8 to 10 months old were sectioned 14-µm thick and stained with anti-CFP (a to i) and with anti-TH (a' to i') antibodies. Images are shown as merge (a'' to i'') and as zoomed version (a''' to i'''). Scale bars are 100 microns.

A)

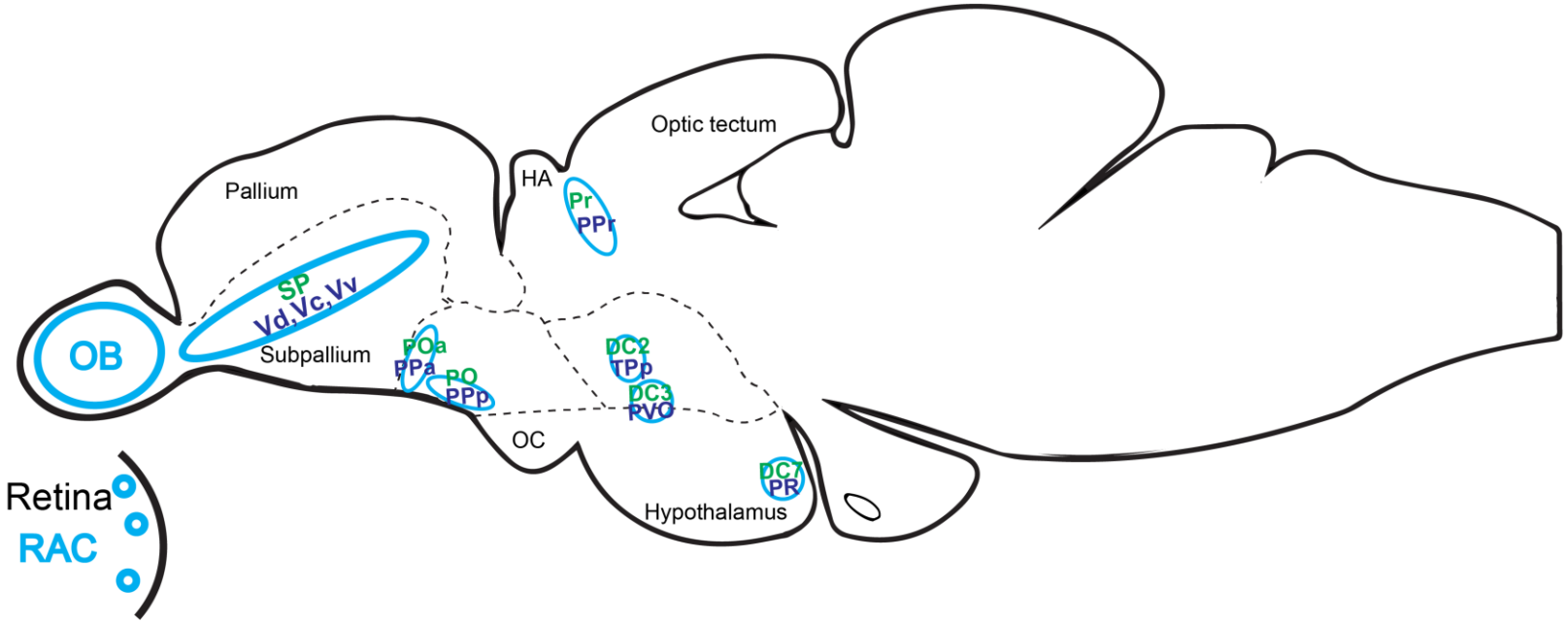
Optic tectum
HA
Pallium
Pr
PPr
SP
Vd,Vc,Vv
OB
Subpallium
POa
PPa
PO
PPp
DC2
TPp
DC3
RVO
OC
DC7
PR
Hypothalamus
Retina
RAC

B)

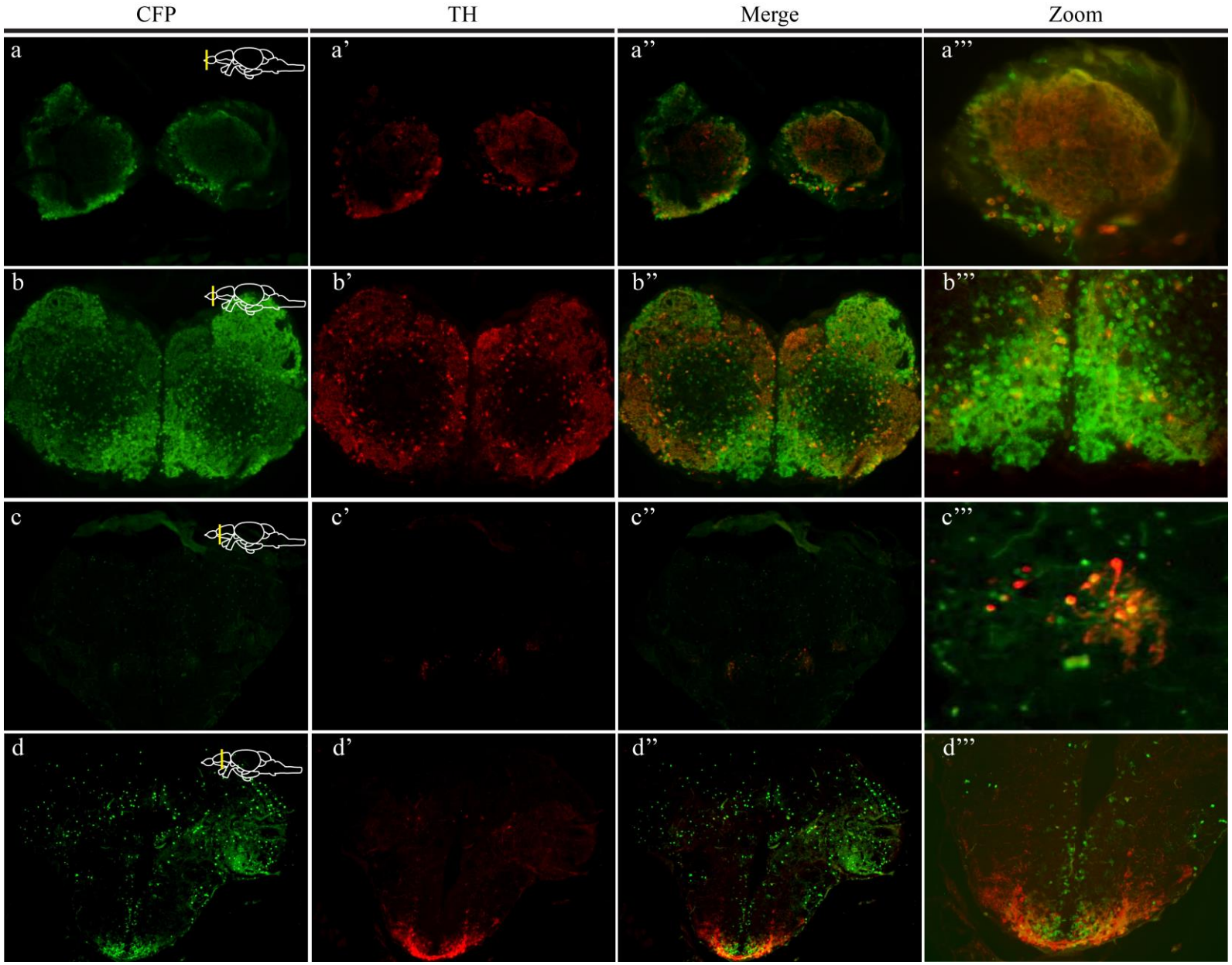

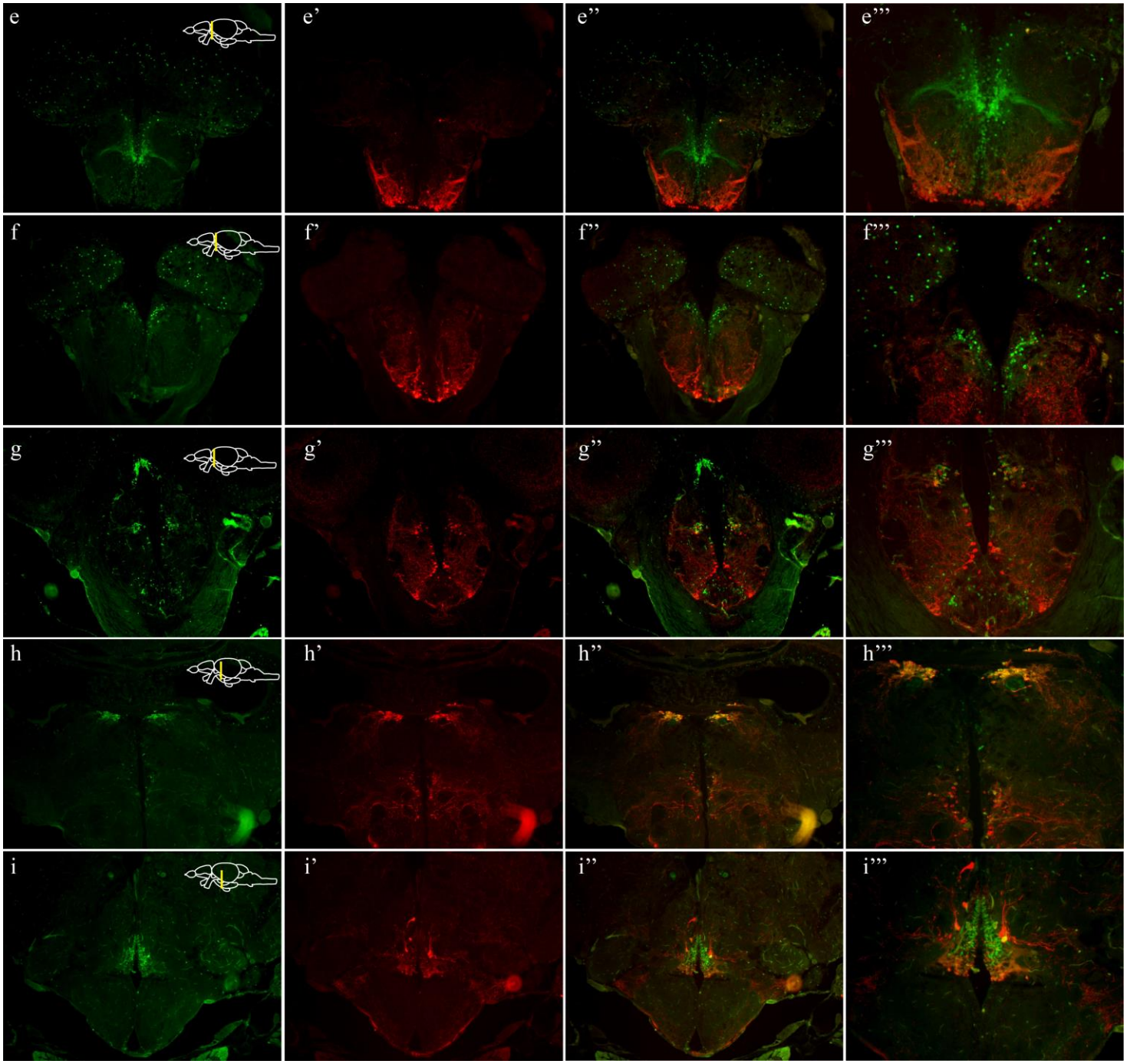
e
e'
e''
e'''
f
f'
f''
f'''
g
g'
g''
g'''
h
h'
h''
h'''
i
i'
i''
i'''

4.4.2 Metronidazole drug administration ablates CFP positive cells in the adult Tg(*dat:CFP-NTR*) zebrafish and results in decreased levels of dopamine neurotransmitter

The nitroreductase-mediated cell ablation approach has been employed to ablate different cell populations in the adult zebrafish including osteoblasts in the zebrafish fin (Singh *et al.* 2012b), germ cells (White *et al.* 2011; Dranow *et al.* 2013), pancreatic β-cells (Moss *et al.* 2009), oligodendrocytes (Chung *et al.* 2013) cardiomyocytes (Zhang *et al.* 2013) and cells of the zebrafish habenula (Agetsuma *et al.* 2010).

We carried out a pilot study to address an optimal delivery method, drug dose and treatment length for optimal ablation of CFP positive cells in the Tg(*dat:CFP-NTR*) fish brain, where maximal numbers of cells could be ablated without any observable deleterious and non-specific effects of the pro-drug administration. As previously suggested (Curado *et al.* 2008), we found that Mtz doses higher than 10 mM increased the mortality of adult Tg(*dat:CFP-NTR*) fish. We also found that although a 5 mM Mtz administration did not lead to mortality, it was much less efficient at ablating cells than with a 10 mM Mtz regiment (data not shown). Finally, although a multiple day administration of 10 mM Mtz also showed deleterious effects in adult fish, a single 24-hour Mtz dose administration resulted in optimal CFP^+ cell ablation with no observable deleterious effects (Fig. 4.2A).

Fish were exposed to 10 mM Mtz dissolved in 0.2% DMSO in fish facility water. Tg(*dat:EGFP*) adults exposed to the same regiment were not affected by the Mtz protocol as will be further discussed.

We observed that maximal cell loss was observed seven days following the termination of Mtz exposure (Fig. 4.2A). Both female and male animals showed a decrease in global levels of both TH and CFP protein levels as shown by western blots on whole brains normalized to the house keeping gene actin (Fig. 4.2B-E). When compared to vehicle treated animals, females showed, on average, a decrease of 15(± 4.8)% in global levels of TH (t-test, n=3, p= 0.058) (Fig. 4.2B) and an 80(± 1.5)% decrease in global levels of CFP (n=3, p=0.002) (Fig. 4.2C). Males had a decrease of 26(± 3.8)% in levels of TH (n=3, p=0.063) (Fig. 4.2D) and a 77(± 0.8)% reduction in CFP (n=3, p=0.08) (Fig. 4.2E) when compared to vehicle treated controls.

Figure 4.2. Ablation of CFP positive cells in the Tg(*dat:CFP-NTR*) fish. A) Timeline of the ablation protocol employed on adult fish. Fish were first transferred into a room dedicated for drug exposure and allowed to acclimatize for at least 4 days. Fish were treated in system water containing 10mM metronidazole dissolved in 0.2% DMSO. Treatment lasted 24-hours and was conducted in tanks protected from light. Neuronal ablation reached a maximum at 7 days post treatment. B) TH protein levels of female whole brains decreased at 7 days post treatment in Mtz treated animals when compared to vehicle treated Tg(*dat:CFP-NTR*) fish and following normalization to the housekeeping gene actin. C) CFP protein levels in female brain samples at 7 dpt. D) TH protein levels on male animals at 7 dpt. E) CFP protein levels in male brain samples at 7 dpt. (n=3)

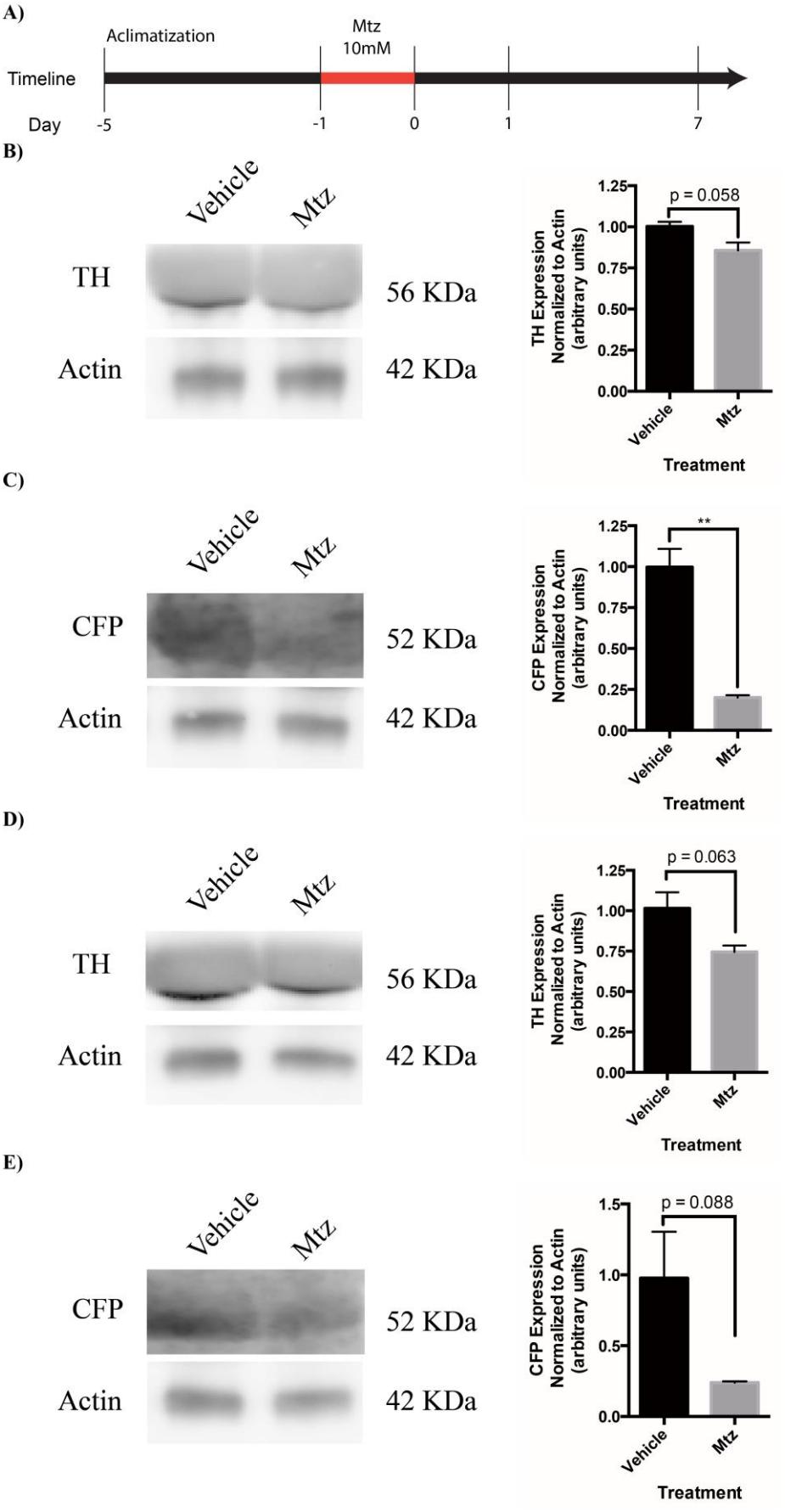
A)
Aclimatization
Mtz
10mM
Timeline
Day
-5
-1
0
1
7
B)
Vehicle
Mtz
TH
56 KDa
Actin
42 KDa
p = 0.058
TH Expression
Normalized to Actin
(arbitrary units)
1.25
1.00
0.75
0.50
0.25
0.00
Vehicle
Mtz
Treatment
C)
Vehicle
Mtz
CFP
52 KDa
Actin
42 KDa
**
CFP Expression
Normalized to Actin
(arbitrary units)
1.25
1.00
0.75
0.50
0.25
0.00
Vehicle
Mtz
Treatment
D)
Vehicle
Mtz
TH
56 KDa
Actin
42 KDa
p = 0.063
TH Expression
Normalized to Actin
(arbitrary units)
1.25
1.00
0.75
0.50
0.25
0.00
Vehicle
Mtz
Treatment
E)
Vehicle
Mtz
CFP
52 KDa
Actin
42 KDa
p = 0.088
CFP Expression
Normalized to Actin
(arbitrary units)
1.5
1.0
0.5
0.0
Vehicle
Mtz
Treatment

The loss of CFP^+ cells was accompanied by a decrease in levels of dopamine neurotransmitter at 7 days post-treatment (Fig. 4.3B), but not at 1 dpt (Fig. 4.3A) when examined by high performance liquid chromatography. At 7 dpt, HPLC analysis was conducted either on single intact whole brains of both males and females, or on dissected areas of single brains divided into 3 main areas: an area containing the olfactory bulb and telencephalon (OB/Tel), one containing the diencephalon and midbrain (DC/Mid) and another containing the hindbrain area (Hind) (Fig. 4.3).

Although the OB/Tel of both males and females had on average 50% less dopamine, this did not reach statistical significance, most likely due to our small sample size (n=3). The DC/Mid area of both females and males showed a decrease of 60% (2-way ANOVA, n=3, p=0.015) and 61% (n=3, p=0.009), respectively, in the levels of dopamine when compared to vehicle treated animals (Fig. 4.3B). The hindbrain and whole brain samples of females were also affected following Mtz treatment and showed 68% (n=3, p=0.07) and 65 % (n=3, p=0.09) decreases in dopamine, respectively. In males, levels were more robust with 86% (n=3, p=0.01) and 80% (n=3, p=0.02) decrease, respectively (Fig. 4.3B). There were no statistically significant changes in the levels of norepinephrine and serotonin in these same samples, suggesting a specific targeting of dopaminergic neurons.

Figure 4.3. Mtz treatment results in a decrease in dopamine levels. High performance liquid chromatography was employed to address the levels of DA in the OB/Tel area, the DC/Mid area and the Hind area or in whole brain samples at either 1 dpt (A) or at 7 dpt (B). Dopamine levels are shown as a percent change relative to levels detected in vehicle treated animals. Areas from individual fish were analyzed independently, n=3.

A)

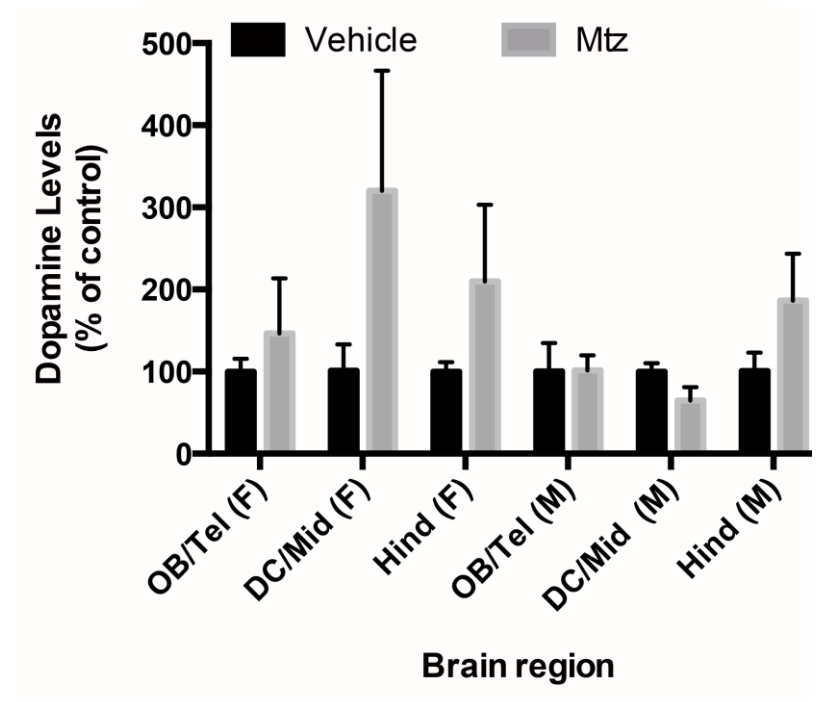
Vehicle
Mtz
Dopamine Levels (% of control)
500
400
300
200
100
0
OB/Tel (F)
DC/Mid (F)
Hind (F)
OB/Tel (M)
DC/Mid (M)
Hind (M)
Brain region

B)

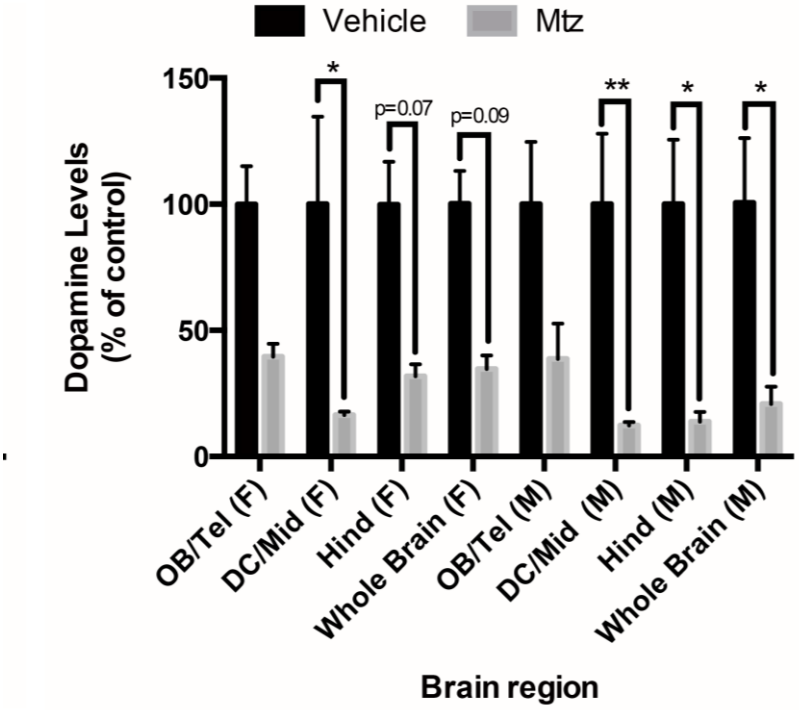
Vehicle
Mtz
Dopamine Levels (% of control)
150
100
50
0
*
p=0.07
p=0.09
**
*
*
OB/Tel (F)
DC/Mid (F)
Hind (F)
Whole Brain (F)
OB/Tel (M)
DC/Mid (M)
Hind (M)
Whole Brain (M)
Brain region

We further addressed the effects of Mtz treatment on the different neuronal populations expressing CFP previously described in Figure 4.1. Immunohistochemical analysis was performed on 14-micron thick sections for both CFP and TH (Fig. 4.4) and an overall decrease in both markers was observed in the major dopaminergic neuron populations labeled in the Tg(*dat:CFP-NTR*) zebrafish. We observed a decrease in CFP and TH in the olfactory bulb of Mtz treated animals (Fig. 4.4 b-b’’’) when compared to vehicle treated animals (Fig. 4.4 a-a’’’), as well as changes in the ventral telencephalic population (Fig. 4.4 d-d’’’ vs. c-c’’’), pretectal area (Fig. 4.4 f-f’’’ vs. e-e’’’ arrows) and cells of the diencephalon, including the pear shaped dopaminergic neurons of DC cluster 2 (arrows) and the neurons of DC cluster 3 (Fig. 4.4 h-h’’’ vs. i-i’’’), were also detected.

Figure 4.4. Immunohistochemical analysis of cell ablation in the adult Tg(*dat:CFP-NTR*) brain. At 8 to 10 months of age, adult zebrafish brains were sectioned 14-µm thick, from vehicle or Mtz treated fish collected 7 days post treatment. Sections were stained with anti-CFP (a to i) and with anti-TH (a' to i') antibodies. Images are shown as merge (a'' to i'') and as zoomed version (a''' to i'''). Rows a-a'' and b-b'' are shown at 20X magnification and enlarged versions at 40X. Scale bars are 100 microns.

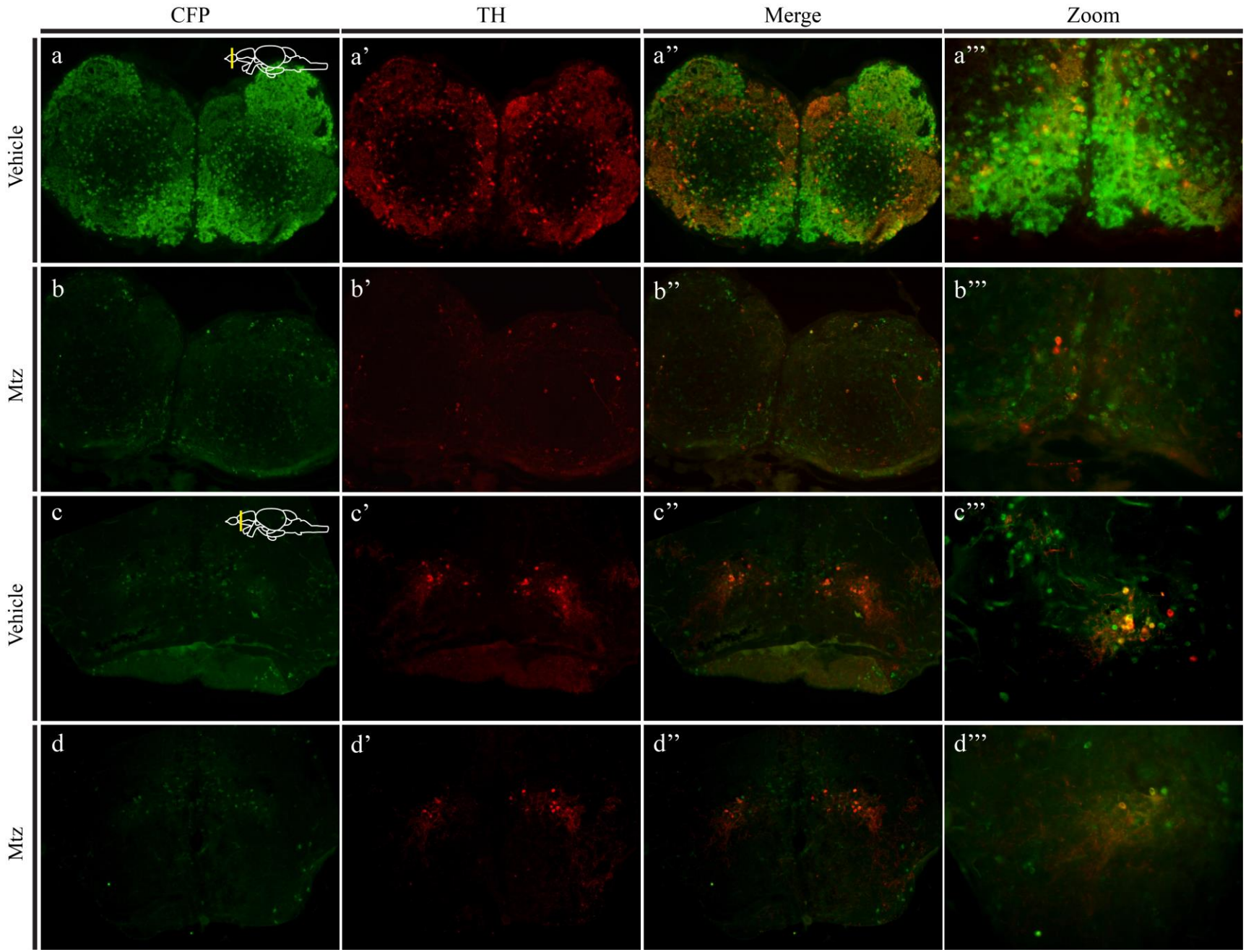
CFP
TH
Merge
Zoom
Vehicle
Mtz
Vehicle
Mtz
a
a'
a''
a'''
b
b'
b''
b'''
c
c'
c''
c'''
d
d'
d''
d'''

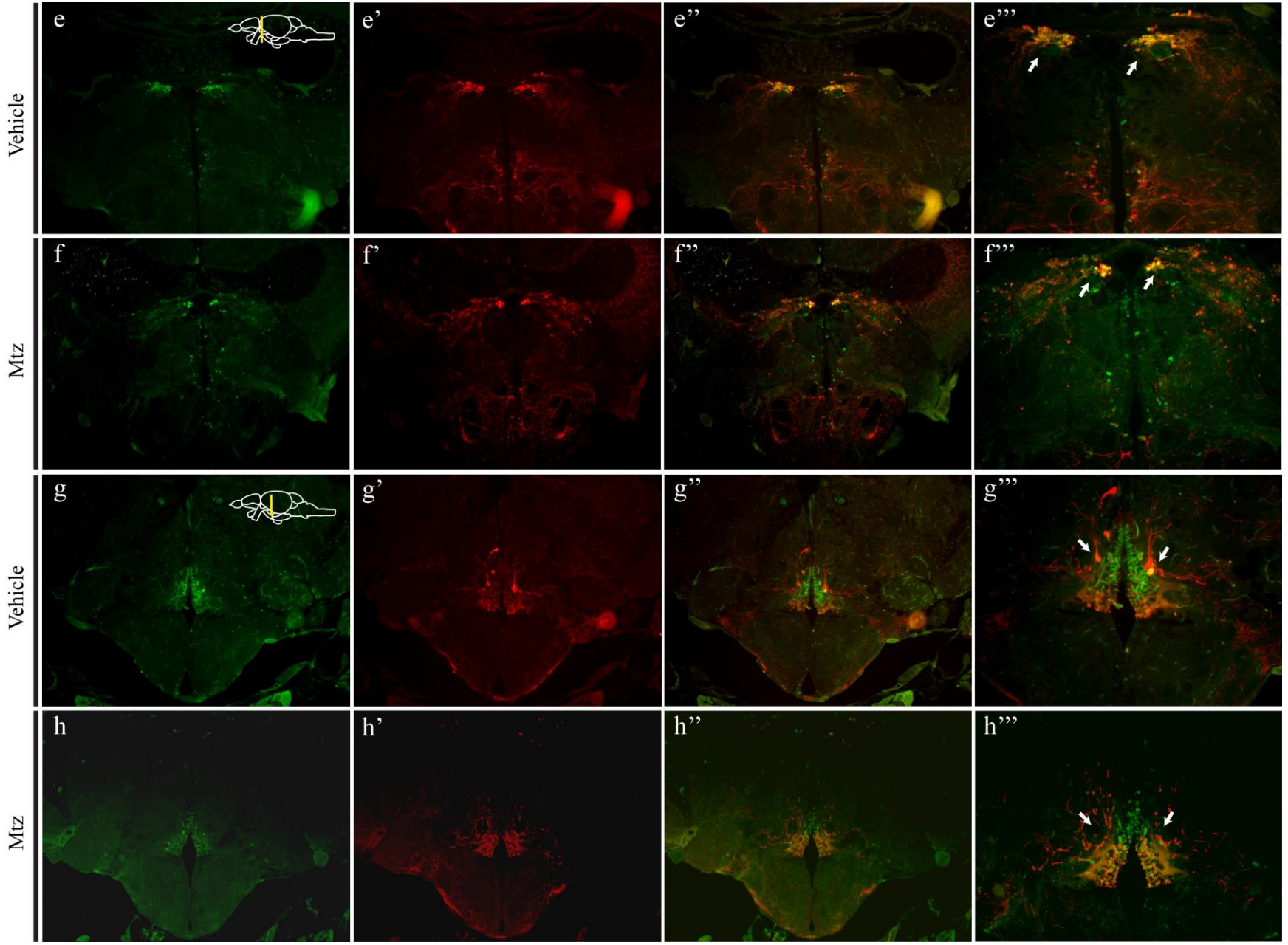
Vehicle
Mtz
Vehicle
Mtz
e
e'
e''
e'''
f
f'
f''
f'''
g
g'
g''
g'''
h
h'
h''
h'''

We initially addressed these changes in 3 subareas of the olfactory bulb classified as rostal (r), medial (m) and caudal (c) OB (Fig. 4.5B-D). To further quantify the degree of neuron ablation in the different CFP neuronal clusters, we used confocal microscope images taken of 1-micron thick optical sections to quantify the number of CFP single positive, TH single positive and CFP and TH double positive cells (Fig. 4.5A).

Metronidazole treatment resulted in 83% (2-way ANOVA, n=3, p=0.0003), 52.6% (n=3, p=0.011) and 59.6% (n=3, p=0.005) reduction in CFP^+ cells in the rostral, medial and caudal areas of the olfactory bulb, respectively (Fig. 4.5B), when compared to vehicle treated animals. The number of TH labeled cells was also reduced by 85% (n=3, p=0.0001), 66.6% (n=3, p=0.0004) and 72.6% (n=3, p=0.0002) in the OBr, OBm and OBc, respectively (Fig. 4.5 C). Furthermore, a similar trend was observed when looking for double labeled CFP and TH positive cells, where in the OBr there was a 76.7% (n=3, p=0.005), in the OBm there was a 66.1% (n=3, p=0.013) and in the OBc an observable 64.7% (n=3, p=0.015) reduction in the number of positive cells expressed as a percent of labeled cells relative to control animals (Fig. 4.5D).

Figure 4.5. Quantification of cell loss in the olfactory bulb of Tg(*dat:CFP-NTR*). A) Representative images of sections stained with CFP, TH and with the nuclear stain DAPI. Images were taken using a Nikon A1 confocal microscope with 1-micron thick optical sections and were used to count cells positive for CFP (B), positive for TH (C) and double positives for both CFP and TH (D). The olfactory bulb was subcategorized into a rostral (r), medial (m) and caudal (c) region. Data presented as percent changes relative to counts in vehicle control samples. For * $p \leq 0.05$, ** $p \leq 0.01$, *** $p \leq 0.001$, **** $p \leq 0.0001$ and n.s. = not significant $p > 0.05$. Scale bar = 50 microns.

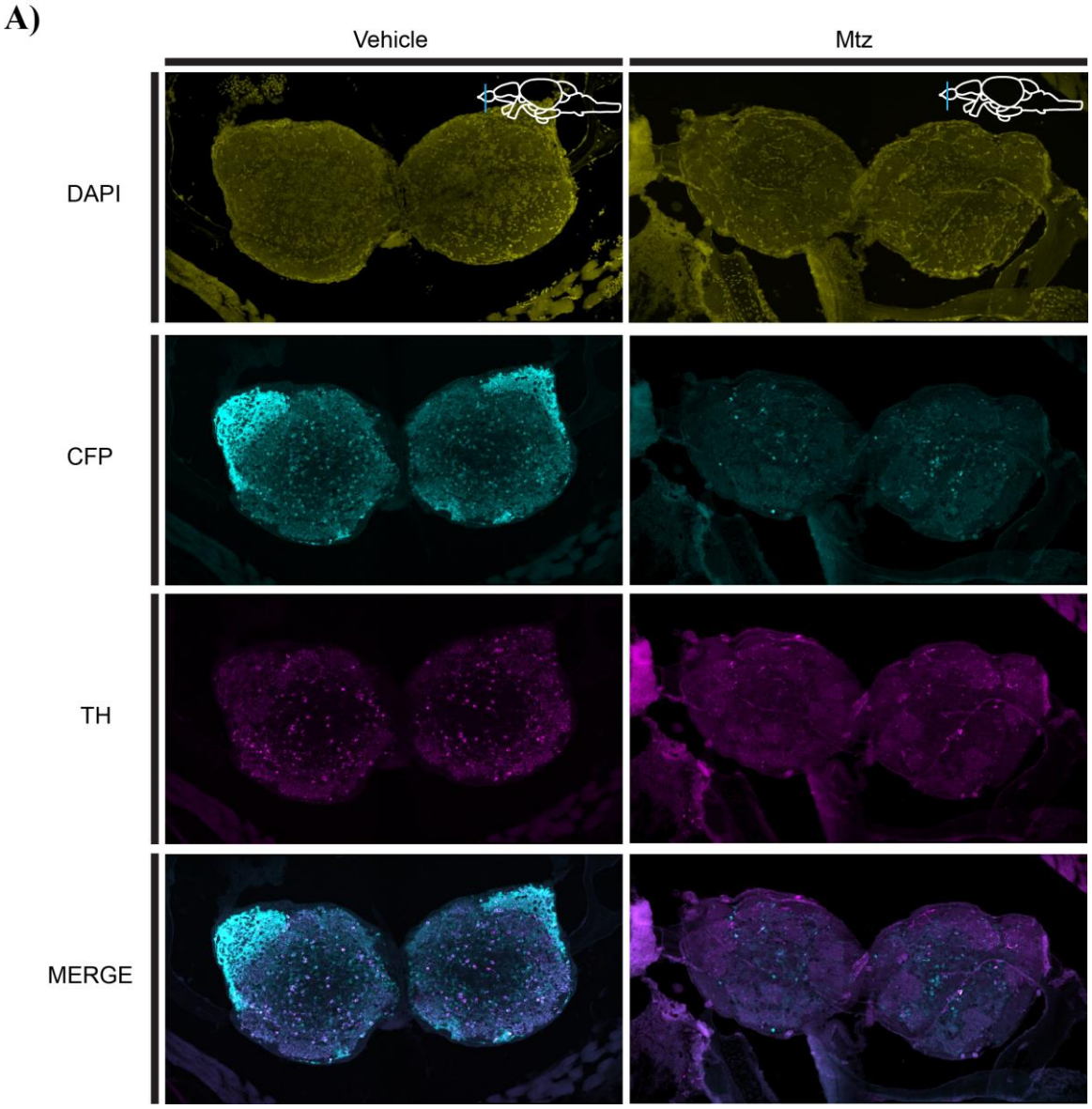
A)
Vehicle
Mtz
DAPI
CFP
TH
MERGE

B)

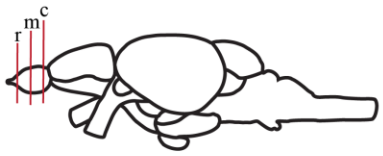
r
m
c

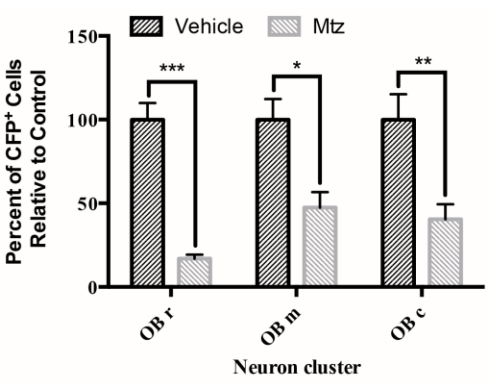
Vehicle
Mtz
Percent of CFP+ Cells Relative to Control
150
100
50
0
***
*
**
OB r
OB m
OB c
Neuron cluster

C)

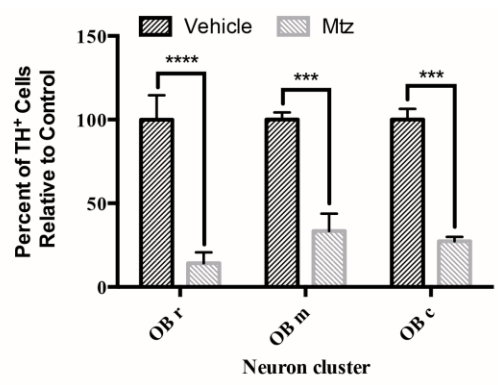
Vehicle
Mtz
Percent of TH+ Cells Relative to Control
150
100
50
0
****
***
***
OB r
OB m
OB c
Neuron cluster

D)

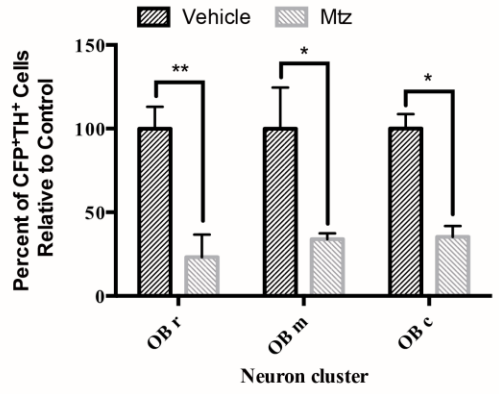
Vehicle
Mtz
Percent of CFP+TH+ Cells Relative to Control
150
100
50
0
**
*
*
OB r
OB m
OB c
Neuron cluster

4.4.3 Ablation of CFP positive cells does not change global locomotor parameters nor the initiation or maintenance of movement but results in an increase in midline crossings and a longer time spent in the upper half of the tank

Loss of dopaminergic neurons is associated with a locomotor phenotype often described in patients with Parkinson's disease. These locomotor changes have been modeled in both larval and adult zebrafish models of dopamine neuron damage (Xi *et al.* 2010; Anichtchik *et al.* 2008; Sallinen *et al.* 2009; Anichtchik *et al.* 2004) (for more in depth review see Table 1.1). Here, we tested whether the loss of CFP^{+} cells in the Tg(*dat:CFP-NTR*) fish was sufficient to induce a locomotor deficit in the adult fish.

We looked primarily at the free swimming ability of adult Tg(*dat:CFP-NTR*) prior to drug treatment and at 7 days post-treatment (Table 4.1). The swimming patterns of adult fish were individually tracked in a behavior tank following an acclimatization period. The data was analyzed using the Ctrax software (Branson *et al.* 2009), originally developed to track *Drosophila* but optimized by us to track adult fish in a similar way to previous work done using this software to track larval zebrafish (Lambert *et al.* 2012).

Table 4.1. Adult Free Swimming Parameters in Tg(*dat:CFP-NTR*) Zebrafish. Fish were acclimatized in the recording chamber for 20 minutes before video recordings either 1 day prior or 7 days following Mtz or vehicle exposure. Free-swimming parameters were measured during a 10 minutes video recording at 30 fps made using a 40 mm Nikon lens attached to a D3000 DSLR Nikon Camera. Data was analyzed using the open source tracking software Ctrax following optimization for zebrafish use.

Parameter	Description[#]	Mean Values* Pre-treatment Day 1			Mean Values* Post-treatment Day 7		
		Vehicle	Mtz	P-value	Vehicle	Mtz	P-value
dtot	Total distance moved (m)	31.9	10.1	0.48	21.3	22.5	0.62
dtheta	Angular velocity (rad/s)	0.03	0.02	0.73	-0.09	0.05	0.36
absdtheta	Angular speed (rad/s)	3.30	1.35	0.69	1.92	2.06	0.85
d2theta	Angular acceleration (rad/s^2)	0.27	0.08	0.56	0.32	-0.45	0.08
absd2theta	Absolute angular acceleration (d2theta)(rad/s^2)	19.8	7.66	0.63	14.90	15.62	0.94
velmag_ctr	Speed (mm/s)	47.4	15.0	0.47	32.1	33.2	0.91
du_ctr	Forward velocity of centerpoint (mm/s)	43.7	12.5	0.41	28.3	31.5	0.71
dv_ctr	Sideway velocity of the centerpoint (mm/s)	-0.84	-0.06	0.41	-0.67	-0.13	0.45
phi	Velocity direction (rad)	-0.01	0.11	0.16	0.06	-0.03	0.42
yaw	Difference between velocity direction and orientation (rad)	-0.01	-0.01	0.67	-0.02	0.03	0.37
absyaw	Absolute difference between velocity direction and orientation (rad)	0.90	1.83	0.17	0.72	0.30	0.13
velmag	Speed of the center of rotation (mm/s)	37.9	11.5	0.43	25.6	27.8	0.74
du_cor	Forward velocity of the center of rotation (mm/s)	36.7	10.4	0.40	24.2	27.1	0.66
Dv_cor	Sideway velocity of center of rotation (mm/s)	-0.32	0.01	0.22	-0.09	0.06	0.43
absdv_cor	Sideways speed of center of rotation (mm/s)	5.77	1.74	0.46	4.14	3.61	0.78
flipdv_cor	Sideways velocity of the center of rotation (mm/s)	0.69	0.08	0.43	0.075	-0.18	0.24
accmag	Acceleration of the center of rotation (mm/s^2)	333	123	0.67	247	154	0.57

#According to descriptions provided by Ctrax, *n=4

A total of 17 parameters were addressed and included aspects such as the total distance moved, speed, angular acceleration, angular velocity and others as described in Table 4.1. No differences were observed among 2 different groups of Tg(*dat:CFP-NTR*) analyzed prior to drug treatment nor at 7 dpt. A trend toward a reduction in the angular acceleration of Mtz treated animals at 7 dpt was observed but did not reach statistical significance when compared to vehicle treated controls (n=4, p=0.08) (Table 4.1). Tg(*dat:EGFP*) animals were not affected by Mtz treatment and did not differ from vehicle treated animals.

Following drug treatment, it was noticed that Mtz treated animals tended to explore the top half of their home tank more often than controls. Previous research suggests that when placed into a novel tank environment, adult wild type fish tend to seek protection by diving into the bottom of the tank (Cachat *et al.* 2010). This behavior activity, which has been shown to alter in the presence of anxiogenic and anxiolytic compounds (Cachat *et al.* 2011) is a commonly used measure for anxiety-related phenotype in adult zebrafish (Wong *et al.* 2010; Stewart *et al.* 2014) with more anxious fish tending to spend less time at the surface portion of the tank.

In order to address whether there was a difference in the length of time that fish spent near the surface of a tank, we used 1L-breeding tanks and drew a line across the middle of the tank (Fig. 4.6A) and measured the number of times a fish crossed the tank's midline and the percent of time they spent in the top half of the tank over a five minute video recording. No differences were observed in the time spent above the line or in the number of midline crossings prior to drug administration (Fig. 4.6B,C). Upon drug treatment the fish tended to spend an increased amount of time in the top half of the tank

first noticeable at 1dpt and reaching a maximum at 7 dpt. At 7 dpt, Mtz treated fish spent on average 24% of the time on the top half of the tank, whereas vehicle treated animals only spent 6.3% of the time above the line (2-way ANOVA, n=7, p=0.007) (Fig. 4.6B). Although a trend towards a higher percent of time spent above the line by Mtz treated animals was still observable at day 38, Mtz treated fish analyzed from days 40 to 45 post-treatment did not differ from those treated with vehicle only (Fig. 4.6B). A similar trend was observed for the number of midline crossings. Starting at 1 dpt, Mtz treated fish tended to cross the midline more often than controls. This increase, reached statistical significance at days 5, 7 and persisting until day 38 (Fig. 4.6C). On days 5, 7 and 38 Mtz treated fish moved 77 (2-way ANOVA, n=7, p=0.016), 89 (n=7, p=0.0021) and 65 (n=7, p=0.02) times across the midline when compared to 24, 26 and 13 times for vehicle treated control animals, respectively (Fig. 4.6C). Mtz fish started to recover at 40 dpt, and by day 45, were indistinguishable from vehicle controls (Fig. 4.6C). Tg(*dat:EGFP*) animals treated with Mtz did not behave differently than vehicle treated animals demonstrating a specific effect of the ablation on CFP^{+} cells in the Tg(*dat:CFP-NTR*).

Taken together our data suggests that loss of dopaminergic cells and a decrease in DA levels in the Tg(*dat:CFP-NTR*) zebrafish and was not sufficient to affect the global parameter of free swimming animals but resulted in an increased exploratory behavior with a greater percent of time spent on the top portion of the tank and an increased number of midline crossings. Furthermore, this phenotype was short -lived and returned to control levels by day 45-post treatment.

Figure 4.6. Mtz treatment of Tg(*dat:CFP-NTR*) fish resulted in an increase in exploratory behavior and a higher percent of time spent at the surface of the tank. A) Schematic representation of the side view of the behavior set up. Single fish were placed into 1L breeding traps with a midline drawn half way through the tank. Five minute-long videos were acquired with a minimum of seven biological replicates obtained from three different exposure experiments. B) Percent of time spent above midline. C) Number of times a fish crossed the midline.

A)

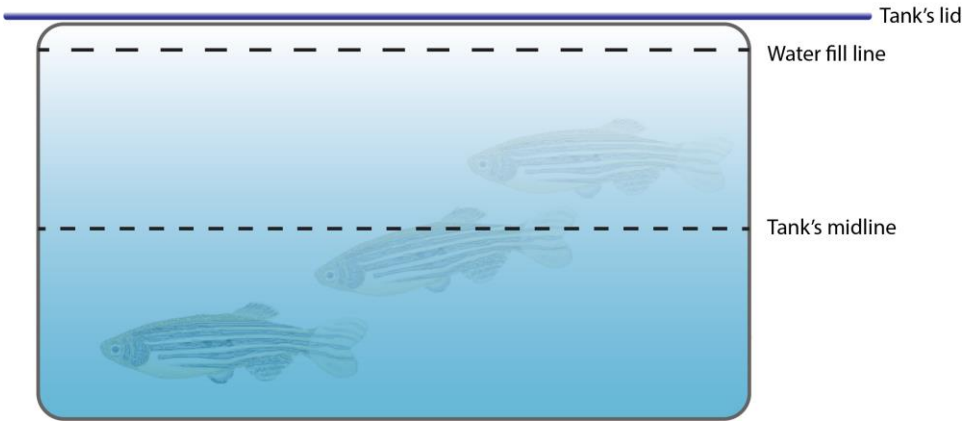
Tank's lid
Water fill line
Tank's midline

B)

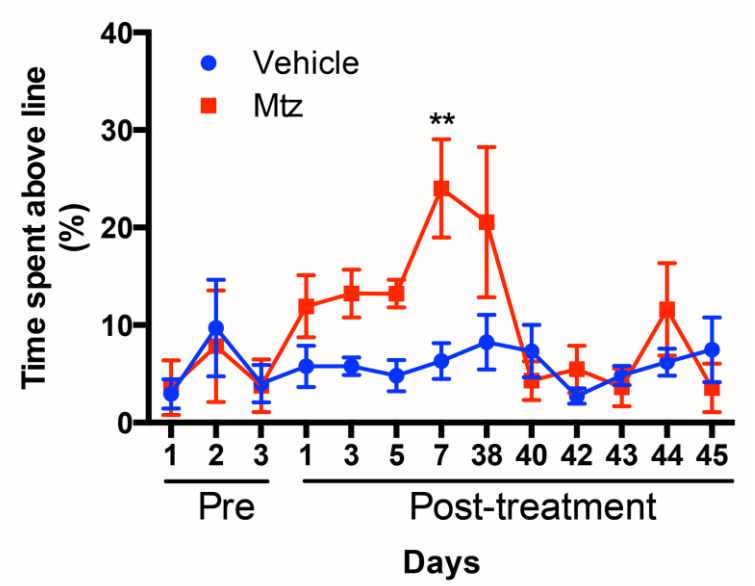
Time spent above line (%)
Vehicle
Mtz
**
40
30
20
10
0
1 2 3 1 3 5 7 38 40 42 43 44 45
Pre
Post-treatment
Days

C)

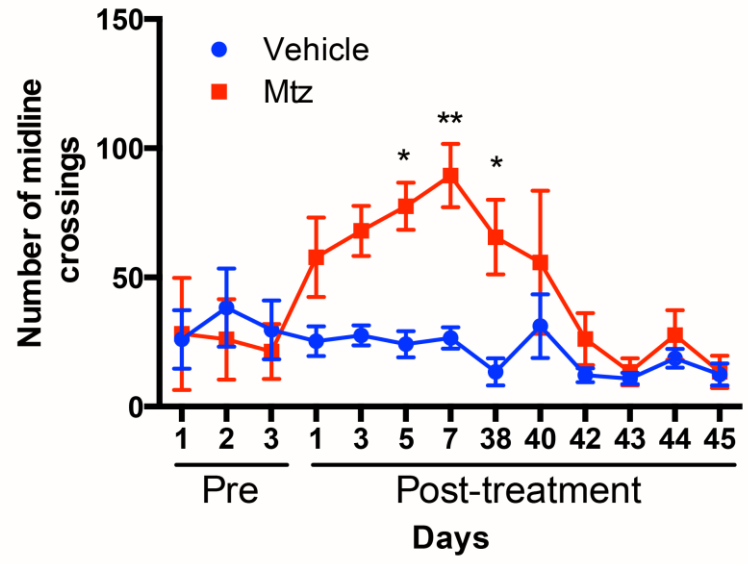
Number of midline crossings
Vehicle
Mtz
**
*
*
150
100
50
0
1 2 3 1 3 5 7 38 40 42 43 44 45
Pre
Post-treatment
Days

4.4.4 Regeneration of CFP positive cells

Since Mtz treated animals fully recovered their behavioral phenotype by 45 days post treatment, we set to test if this rescue in phenotype was correlated with a recovery in the number of CFP positive cells, previously shown to be ablated at 7 dpt.

Levels of both TH and CFP were undistinguishable in Mtz treated animals and vehicle treated female (Fig. 4.7 A, B) and males (Fig. 4.7 C, D) as shown by relative quantification of protein levels normalized to actin in our immunoblotting experiments.

Figure 4.7. Recovery of global CFP and TH levels in Tg(*dat:CFP-NTR*) at 45 days post-treatment. Immunoblotting experiment showing recovery in TH levels (A, C) in the female (A) and male (C) brains and CFP levels in females (B) and males (D).

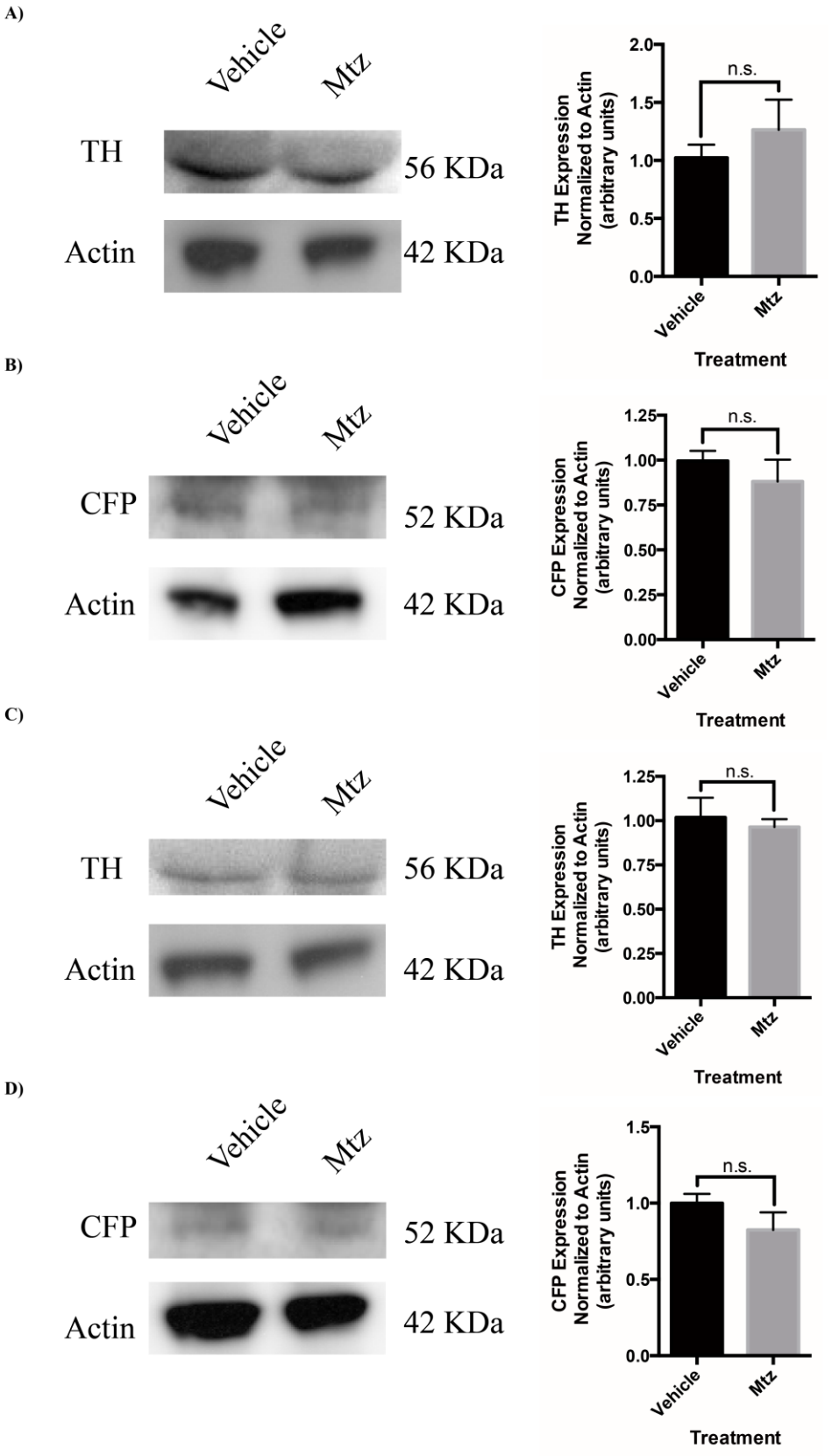
A)
Vehicle
Mtz
TH
56 KDa
Actin
42 KDa
TH Expression Normalized to Actin (arbitrary units)
2.0
1.5
1.0
0.5
0.0
n.s.
Vehicle
Mtz
Treatment
B)
Vehicle
Mtz
CFP
52 KDa
Actin
42 KDa
CFP Expression Normalized to Actin (arbitrary units)
1.25
1.00
0.75
0.50
0.25
0.00
n.s.
Vehicle
Mtz
Treatment
C)
Vehicle
Mtz
TH
56 KDa
Actin
42 KDa
TH Expression Normalized to Actin (arbitrary units)
1.25
1.00
0.75
0.50
0.25
0.00
n.s.
Vehicle
Mtz
Treatment
D)
Vehicle
Mtz
CFP
52 KDa
Actin
42 KDa
CFP Expression Normalized to Actin (arbitrary units)
1.5
1.0
0.5
0.0
n.s.
Vehicle
Mtz
Treatment

Furthermore we detected no differences in the numbers of CFP or TH, nor in cells positive for TH and CFP in the rostral, medial and caudal areas of the olfactory bulb of Mtz treated animals when compared to vehicle animals 45 dpt (Fig. 4.8B, C, D).

In order to demonstrate that the recovery in CFP and TH positive cell populations was the result of newly formed cells, which emerged due to a regenerative process following neuronal damage, we administered BrdU starting immediately prior to Mtz treatment, recurring every 48 hours, for a total of 5 i.p. injections (Fig. 4.8A). This pulse-chase experiment demonstrated that at 45 dpt, there was no significant difference in the numbers of BrdU positive cells in the OB of Mtz treated animals compared to vehicle treatment (Fig. 4.8E), yet Mtz treated animals had on average 3.6 (2-way ANOVA, n=3, p=0.05) and 5.2 (n=3, p=0.002) fold higher presence of cells positive for BrdU and CFP in the OBr and OBm, respectively when compared to vehicle treatment (Fig. 4.8F).

Overall, our data suggests, that, by 45 dpt, adult zebrafish are able to recover global levels of CFP and TH which were previously decreased at 7 dpt, and that neuronal cell counts in the OB of adult fish were indistinguishable from those of non-ablated animals. This recovery in CFP expressing cells was further shown to be newly formed cells that incorporated the thymidine analog BrdU.

Figure 4.8. Cell recovery in the olfactory bulb 45 days post-treatment. A) Fish received 5 intraperitoneal injections of BrdU (purple arrow heads) starting immediately prior to the neuronal ablation protocol and repeatedly every 48 hours until 7 days post-treatment. The number cells positive for CFP (B), TH (C) and CFP with TH (D) were indistinguishable from cell numbers in vehicle treated animals in the rostral, medial and caudal areas of the OB. The numbers of BrdU retaining cells at 45 dpt were identical to those of non-ablated animals (E), Yet Mtz treated animals showed a higher number of neurons positive for both BrdU and CFP (F).

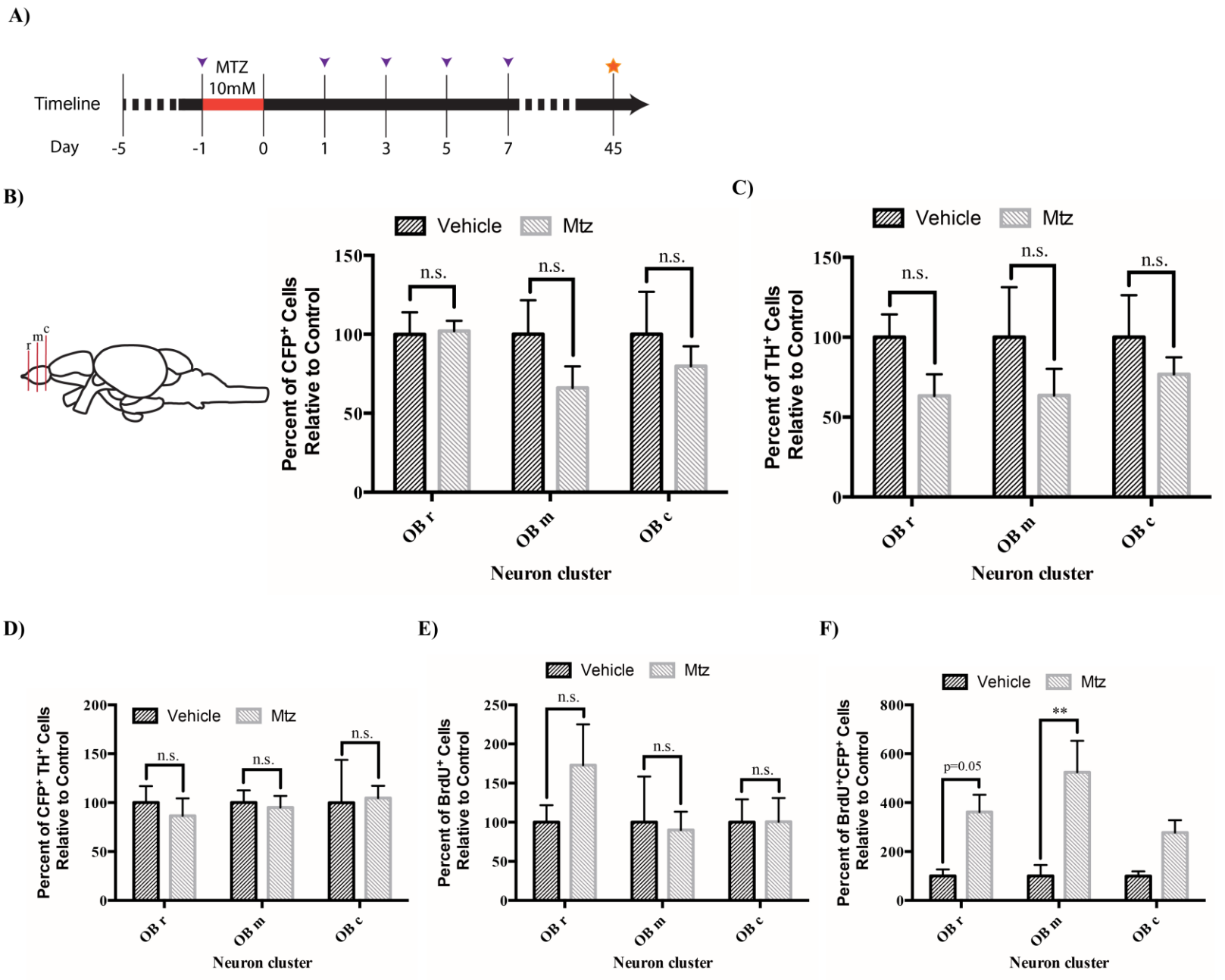
A)
MTZ
10mM
Timeline
Day
-5
-1
0
1
3
5
7
45
B)
r
m
c
Vehicle
Mtz
Percent of CFP+ Cells Relative to Control
n.s.
OB r
OB m
OB c
Neuron cluster
C)
Percent of TH+ Cells Relative to Control
D)
Percent of CFP+ TH+ Cells Relative to Control
E)
Percent of BrdU+ Cells Relative to Control
F)
Percent of BrdU+CFP+ Cells Relative to Control
p=0.05
**

4.5 Discussion

The zebrafish is an emerging experimental system for the understanding of brain cell regeneration. Much of the current knowledge of the ability of adult fish to regenerate brain tissue comes from studies which rely on non-specific ablation approaches, such as stab wound experiments were demonstrated to result in stem/progenitor cell proliferation and on the recruitment of these cells to the site of injury (Becker and Becker 2015; Baumgart *et al.* 2011; Kyritsis *et al.* 2012; März *et al.* 2011). Here, we developed a non-invasive, conditional and cell-specific ablation approach to study the regenerative potential of dopaminergic neurons in the brain of adult zebrafish.

Although neurotoxins such as MPTP and 6-OHDA have been employed to ablate DA neurons in adult animal models, such as in rodents and in the salamander (Gibrat *et al.* 2009; Parish *et al.* 2007), neuronal ablation has not been demonstrated in adult zebrafish treated with these neurochemicals (Bretaud *et al.* 2004; Anichtchik *et al.* 2004). Thus, we opted to use the nitroreductase mediated conditional and specific ablation approach previously shown to kill specific cell populations in the adult zebrafish (Curado *et al.* 2008).

Here, we describe that the Tg(*dat:CFP-NTR*) line, previously shown to have the ability to specifically ablate dopaminergic neurons of the larval zebrafish (Godoy et al, 2015 Chapter 2), continues to express the CFP-NTR fusion protein in the brain of adult zebrafish in places consistent with those labeled in larval zebrafish, in populations that represent the different dopaminergic clusters of the adult fish. Some transgenic zebrafish lines, such as those employing the Gal4/UAS approach, have been reported to experience

transcriptional gene silencing as adults, which in many cases can be attributed to the methylation of the transgene which can be also dependent on the site of transgene integration in the zebrafish genome (Akerberg *et al.* 2014; Goll *et al.* 2009; Akitake *et al.* 2011).

Although not all CFP cells co-labeled with the catecholaminergic neuron marker tyrosine hydroxylase, this may be attributed to the preferential binding of our TH antibody to the *th1* epitope, thus excluding *th2* positive cells (Yamamoto *et al.* 2010). Further analysis using immunohistochemistry and *in situ* hybridization with other markers of dopaminergic neurons and for other cell type markers will help to further characterize the full nature of all CFP positive cells across the adult zebrafish brain.

In our model, water exposure delivery of metronidazole for 24 hours was sufficient to reduce global levels of both CFP and TH proteins seven days post-treatment. Accompanying this process, we observed a decrease in global levels of dopamine, as well as a decrease in dopamine in three main areas of the brain tested individually including the olfactory bulb-telencephalon, diencephalon-midbrain and hindbrain area at seven days but not shortly after drug exposure at 1 dpt. No changes in serotonin nor in norepinephrine were detected, neither globally or within individual regions at 1 nor at 7 dpt. These results suggest that there is a lag where Mtz needs to first access the targeted tissue through the circulation in order to exert its effect in NTR positive cells, ultimately, leading to reduced CFP reporter production, apoptosis and clearing of the cells from the tissue, resulting in a maximal decrease in the DA specific cell markers seven days post-treatment. This time frame has been similarly observed for the ablation of cells of the adult zebrafish habenula (Agetsuma *et al.* 2010). Furthermore, the specific decreases in

dopamine levels (Fig. 4.3) but not in other neurotransmitters (data not shown) further reinforced the specific ablation of dopaminergic neurons in our model.

Changes in protein levels were accompanied by an absence of cell body, indicating a loss of neurons and not simply a down regulation of these proteins, as has been quantified by cell counts in three different areas of the olfactory bulb. Immunohistochemistry on sectioned tissue also indicates a similar trend in other areas where dopaminergic neurons are found in the adult zebrafish brain such as the ventral telencephalon, preoptic area, diencephalon and pretectal areas. However, more extensive quantification of cell counts of sectioned tissue is still needed.

Neuronal ablation in our model was insufficient to elicit changes in global locomotor parameters, such as total distance swam and speed of free-swimming adult animals. In our line, we target and ablated cells in the ventral telencephalon of the zebrafish, an area known to house the zebrafish's equivalent of the mammalian's striatum (Tay *et al.* 2011) and whose internal projections could carry similar function to those of the mammalian nigro-striatal dopaminergic pathway. Despite not observing a locomotor effect, ablation of the subpallial neurons and other neurons (i.e. DC2 cells) previously described to carry functions linked to the initiation and maintenance of movement in larval zebrafish (Lambert *et al.* 2012; Jay *et al.* 2015), suggest that a compensatory mechanism may be responsible for maintaining baseline levels of movement initiation and maintenance in our Tg(*dat:CFP-NTR*) fish. Indeed, neurons of DC4 which are not labeled nor ablated in our line, have been shown to carry similar roles to those of DC2 in the maintenance of movement in larval zebrafish (Jay *et al.* 2015). The fact that we do not ablate 100% of the DA neurons in our model, further suggests that the remaining cells

are still able to compensate and carry out cellular functions necessary for the maintenance of movement in these Tg(*dat:CFP-NTR*) animals.

Despite a lack of locomotor phenotype, adult zebrafish demonstrated a place preference and higher exploratory behavior leading to an increase in the number of midline crossings and a higher percent of time in the top half of their tanks. At this point, it is unclear whether this phenotype results from the direct ablation of dopaminergic neurons labeled with CFP or whether it is a secondary effect. Further pharmacological analyses with agonists, antagonists and receptor blockers are needed to identify the cause of such phenotype.

The place preference and higher exploratory phenomena observed were short lived and by 45 days post-treatment Mtz animals were indistinguishable from vehicle treated animals. This recovery in phenotype was also accompanied by a recovery in global levels of TH and CFP and in the number of cells counted in the three main areas of the olfactory bulb. The ratio of newly formed cells which incorporated BrdU during the S-phase were also higher in Mtz treated animals at 45 dpt, indicating that these were newly formed neurons.

Interestingly, counts of BrdU positive cells alone did not differ between those observed in vehicle and Mtz treated animals. Although loss of dopaminergic neurons in Mtz treated animals could have induced an increase in cell proliferation, and thus BrdU labeling as previously seen with the regenerative process reported in stab wound experiments (Kishimoto *et al.* 2012; März *et al.* 2011), many of these cells which did not give rise to CFP positive cells must have died along the way to day 45 post-recovery. In addition, it has been shown that many BrdU labeled cells in the mammalian dentate gyrus

die before reaching maturity (Kempermann 2011; Dayer *et al.* 2003); however, this still remains to be addressed in our model.

Taken together we have a model for dopamine neuron ablation in the adult brain that overcomes problems with previous ablation methods. Our model allows for the detection of newly formed cells together with a recovery in phenotype. Further studies using the Tg(*dat:CFP-NTR*) fish will allow for the understanding of cellular and molecular processes governing the regeneration of dopamine neurons in the adult zebrafish. Furthermore, our model will allow for the identification of a regenerative process following a tissue specific ablation approach, which more closely resembles the cellular milieu found in patients with neurodegenerative conditions such as PD, and allow for the comparison to the regenerative processes of more invasive ablation techniques, such as stab wound lesions.

CHAPTER 5

GENERAL DISCUSSION & PERSPECTIVES

5.1 Discussion and future directions

The objectives of my Ph.D. studies were to develop a model to address the regeneration potential of dopaminergic neurons in the brain. This would lead to the investigation of the molecular and cellular processes driving this phenomenon. We believe that our work will contribute greatly to the field of regenerative medicine with a clinical impact for the development and targeting of future therapeutic approaches aiming to restore the dopaminergic neuron population lost in patients diagnosed with Parkinson's disease.

Although the etiology of PD is currently idiopathic, with both genetic and environmental factors contributing to the development of the disease (Klein and Westenberger 2012), all patients diagnosed with this condition suffer from an unstoppable progressive neurodegeneration that becomes ever more debilitating (Connolly and Lang 2014). PD is the second most prevalent neurodegenerative disorder affecting the elderly today and despite the availability of treatments that manage the symptoms of the disease (see Chapter 1), it is still incurable (Klein and Schlossmacher 2006). Thus, it is imperative to seek alternative approaches to ameliorate or revert the progression of PD. One potential approach is through regenerative medicine.

There is no doubt that with the biotechnological advances that are being made with induced pluripotent stem (iPS) cells, hope lies in their application for the treatment of Parkinson's disease. Engraftment of embryonic stem cell (ESC) derived DA neurons has been shown to occur in an MPTP primate model and in a 6-OHDA rat model, as

previously reviewed (Nishimura and Takahashi 2013). Human iPSCs have been shown to be a source of neural progenitor cells and to engraft and survive as DA neurons for as long as six months in a monkey MPTP model (Kikuchi *et al.* 2011). The risk of tumorigenicity of human iPSCs has been a concern in the field (Lee *et al.* 2013) but, more recently, scientists were able to transplant autologous iPSC-derived DA neurons into a non-human primate PD model where cells survived for up to two years with an increase in motor activity, neuronal survival and outgrowth which have been observed without the need for immunosuppression (Hallett *et al.* 2015). Together with applications such as genome editing and combined gene therapy (Okano and Yamanaka 2014; Yasuhara *et al.* 2015), the use of iPSCs holds a promising future. Human clinical trials (Politis and Lindvall 2012) have yet to decide the fate of such therapy for Parkinson's disease.

It is well recognized that mammals hold a much more restricted ability to regenerate brain tissue than other animals such as the planaria, salamander and the zebrafish (Becker and Becker 2015; Iglesias *et al.* 2011; Agata and Umesono 2008; Kaslin *et al.* 2008). During my studies, I decided to investigate the endogenous capabilities of dopamine neuron to regenerate in the teleost fish, *Danio rerio*, as there is an increasing body of work describing the molecular and cellular processes involved in brain tissue repair in the adult fish specially following traumatic brain injury such as stab lesions (Kishimoto *et al.* 2012; Kizil *et al.* 2012b; Kroehne *et al.* 2011; Baumgart *et al.* 2011; Kizil *et al.* 2012c). To the best of my knowledge, no previous study has described the regenerative ability of DA neurons following tissue specific neuronal loss.

In addition to the molecular and cellular methods available for research in the zebrafish, among many the ease for transgenesis, we opted to use the zebrafish as a model for its high-throughput capabilities for screening and detecting fluorescent reporter activity in the brain of optically clear zebrafish larvae and for the ability to house a large number of adult animals which can be used for adult brain regeneration studies through the use of genomic, metabolomics, lipidomic, proteomic and epigenetic screens with a discovery-based intention to detect new features in the regenerative process.

Throughout this dissertation, I described the generation of a novel transgenic zebrafish model, Tg(*dat:CFP-NTR*), that enables the ablation of DA neurons in both larval and adult zebrafish in a non-invasive, conditional and specific manner. Here, we showed that the Tg(*dat:CFP-NTR*) zebrafish expressed CFP in cells where *dat* and TH were expressed and that upon metronidazole (MTZ) administration, CFP positive cells underwent apoptosis (as demonstrated by caspase-3 staining).Levels of TH, CFP and *dat* were reduced and cell bodies were no longer detected. Furthermore, we have shown that this effect was limited to NTR-expressing neurons and that Tg(*dat:EGFP*) larvae exposed to the same Mtz regiment were no different than control animals, thus excluding non-specific effects of the pro-drug. The establishment of this transgenic model overcomes the difficulties encountered with the currently available neurotoxin models previously describe in Chapter 1.

Loss of DA neurons led to a specific reduction of DA neurotransmitter in both larval and adult zebrafish with no differences in the levels of serotonin and norepinephrine. Changes in DA neuron population and neurotransmitter levels correlated with a locomotor phenotype in larval zebrafish described by a deficit in global swimming

parameters and an affected tail bend phenotype (Chapter 2). These responses are consistent with different larval zebrafish models of dopamine neuron ablation previously described in Chapter 1. The locomotor phenotype in our model was likely specific to brain DA cell ablation and not due to defects in spinal motor neurons, since no differences were observed in the zn1 and znp1 neuronal arrangement in the trunk of treated and control larvae (Chapter 2 and Figure A.1.2 in Appendix 1). Furthermore, 3-day-old larvae treated with Mtz showed no difference in their response to a touch stimulus applied to their trunk when compared to control larvae but instead tended to initiate spontaneous movement less frequently (Figure A.1.3 in Appendix 1). This further suggests a deficit in movement initiation and execution and not a sensory impairment.

Pharmacological treatment with the dopamine receptor (D2 and D3) agonist Quinpirole partially rescued the swimming phenotype of 5-day-old larvae but no effect was observed with the D1/D5 receptor agonist SKF-38393 or with the dopamine precursor L-DOPA (Appendix 1). The use of L-DOPA has been reported to rescue a locomotor phenotype in larval zebrafish (Giacomini *et al.* 2006). In addition, the effects of both Quinpirole and SKF-38393 have previously been examined in wild-type larval zebrafish (Irons *et al.* 2013) demonstrating that the larval zebrafish is sensitive to drugs targeting dopamine receptors and dopamine biosynthesis. In a detailed study of the effects of dopaminergic drugs on larval zebrafish locomotor phenotype, Irons and colleagues (2013) describe that some of these drugs preferentially elicit a phenotype depending on light or darkness conditions. Thus, in the future, analysis of larval behavior using a light-dark cycle may allow for a better understanding of what neuronal circuitries contribute to the larval locomotor phenotype in our transgenic animals. In addition to

pharmacological approaches, a more recent study used a detailed electrophysiological approach to describe the neuronal connections of dopaminergic neurons of DC2 (Jay *et al.* 2015). A similar approach could lead to further characterize the specific neuronal connections involved in the locomotor phenotype of our larvae.

Despite a sustained loss in CFP and TH expressing cells, we observed that larval zebrafish showed a transient global locomotor and tail bend phenotype that was recovered to control levels by 7 and 12 dpf, respectively (Chapter 2). This rescue in phenotype was also consistent with a recovery in global levels of dopamine in larval zebrafish, suggesting that non-ablated cells may have up-regulated their DA biosynthesis; however, further testing for this hypothesis is required.

Contrary to our expectations, the spontaneous swimming parameters of adult fish were not altered following neuronal ablation (Chapter 4), despite confirmed cell ablation and a decrease in DA levels. Since not all DA neurons of the adult zebrafish brain were ablated in Tg(*dat:CFP-NTR*) animals, perhaps were the remaining neuronal connections sufficient to maintain the ability of adult fish to initiate and sustain free-swimming behaviour, which was not the case in larval zebrafish. Ablation of CFP positive cells Tg(*dat:CFP-NTR*) fish resulted in an increased number of crossings of the tank's midline and in a higher percentage of time spent in the upper half of the recording tanks (Chapter 4), suggesting an increased exploratory behavior. Studies conducted on adult zebrafish indicate that when placed into a novel environment, wild-type fish tend to seek protection by diving into the bottom of the tank which is followed by a gradual increase in exploratory behavior (Cachat *et al.* 2010). This habituation response in the adult zebrafish, which is comparable to the rodent open field test (Cachat *et al.* 2010), can be

used as a measure of anxiety-related phenotype (Wong *et al.* 2010; Stewart *et al.* 2014). Indeed research has shown that anxiogenic compounds such as an alarm pheromone decrease the time wild-type fish spend in the upper half of a tank, while anxiolytic compounds, such as fluoxetine, ethanol and morphine, increase the time zebrafish spend at the top portion of a tank (Cachat *et al.* 2011). Similarly to transgenic zebrafish, the transient knockdown of *tyrosine hydroxylase* in larval zebrafish results in an impaired novel tank habituation behavior in adult fish that is described by an increase in the time fish spend in the upper portion of their tank (Formella *et al.* 2012). It is important to consider that the adult zebrafish has a range of complex behaviors, such as learning, memory, social interaction and cognition (Gerlai 2014; Stewart *et al.* 2011). Further testing will be needed to determine the origins of the altered midline crossing behavior in MTZ-treated Tg(*dat:CFP-NTR*) It will be interesting to test whether this exploratory is consistent with different anxiety related behavior tests, such as the light-dark box or following stressors such as an exposure to a predator and or following a netting stress (Stewart *et al.* 2014; Tran *et al.* 2014). It will also be interesting to determine if there are changes in cortisol levels of adult Tg(*dat:CFP-NTR*) fish treated with Mtz when compared to vehicle-treated animals and to find out if these changes are directly linked to a decrease in DA neuronal population and DA neurotransmitter levels or if this is a secondary response to our ablation protocol.

Finally, we demonstrate the usefulness of the Tg(*dat:CFP-NTR*) zebrafish in visualizing the regenerative process *in vivo* by tracking changes in *nestin* driven fluorescent reporter in Tg(*dat:CFP-NTR;-3.9nestin:GFP*) animals by using live two-photon imaging. We showed that following neuronal ablation, there is an increase in cell

proliferation, and an up-regulation of genes involved in neurogenesis and regeneration (Chapter 3). Furthermore, brain dopaminergic neuron counts in the olfactory bulb of adult animals were returned to vehicle levels 45 days following the ablation procedure. This, combined with BrdU labeling, reinforces that additional CFP expressing cells at 45 dpt were indeed newly formed neurons (Chapter 4).

Overall, our data demonstrates that the zebrafish is able to recover DA neurons following a non-invasive conditional and specific ablation procedure. Neuronal regeneration in Tg(*dat:CFP-NTR*) zebrafish appears to follow a similar path to that observed during regeneration following traumatic brain injury, in that neuronal precursor and stem cells proliferate and differentiate into cells the animal needs to replace. Although we only described the regeneration of olfactory bulb DA cells in this thesis, a similar regenerative ability was observed in the telencephalon of adult fish (data not shown) and further analysis is underway to describe the regenerative ability of the other DA neuron clusters labeled in Tg(*dat:CFP-NTR*) zebrafish.

The use of the Tg(*dat:CFP-NTR*) zebrafish will allow for the precise identification of cellular processes driving their neuro-regenerative ability such as the specific nature of precursor cells, as well as the anatomical origin and the genetic changes governing this process. I am currently undertaking a tissue dissociation and flow cytometry-based analysis for counting cells labeled with different markers to precisely quantify changes in cell proliferation, fluorescence intensity levels and changes in cell populations following neuronal ablation at various time points using micro dissected areas of the adult zebrafish brain. Flow cytometry has been described as a sensitive and efficient way to quantify immunolabeled cells with results comparable to those of

immunohistochemistry (Balu *et al.* 2009a) and has been used to quantify neurogenesis in the adult brain of rodents (Bilsland *et al.* 2006; Balu *et al.* 2009b). FACS will be further employed to isolate specific cell populations of Tg(*dat:CFP-NTR*) animals following Mtz treatment for further analysis using RNAseq technology. In addition, it will be particularly interesting to look at the epigenetic events governing changes of proliferating cells and stem cells during the regenerative process.

5.2 Conclusions

Overall, we have shown that the Tg(*dat:CFP-NTR*) is a useful tool to investigate DA neuron regeneration in both larval and adult zebrafish. We have shown that DA neuron ablation results in locomotor and behavior impairments in the zebrafish and that following ablation there are changes in cell proliferation and in the expression of genes involved in neurogenesis and brain regeneration. Finally, we have shown that cells of the olfactory bulb of adult zebrafish fully recover to control levels within 45 days from ablation. Future applications using our model will further the knowledge of the molecular and cellular mechanisms driving the regenerative process and will serve as a basis for new therapeutic targets for regenerative therapy for patients suffering with the progressive neurodegeneration of DA neurons, such as those with Parkinson's disease.

APPENDICES

Appendix 1: CFP expression pattern characterization, Mtz dose response and effects motor neurons, locomotor phenotype, touch response and pharmacological rescue experiments

This work is complementary to the research presented on chapter 2 "Chemogenetic ablation of dopaminergic neurons leads to transient locomotor impairments in larval zebrafish". Here we show the colocolization of CFP, TH and *dat* in whole mount 3 day-old larvae (Figure A.1.1) and the drug dose response of larvae to different Mtz treatments (Table A.1). Aditionally, we show that at 5 dpf despite an effect in ablating brain DA neurons, Mtz treatment had no effect on the arrengment of motor neurons (Figure A.1.2). Furthermore, at 3 dpf, Mtz treated larvae responded to touch stimulus similarly to vehicle treated animals but tended to initiate spontaneous movement less frequently. At 5 dpf, the impaired locomotor phenotype was partially improved by the D2/D3 receptor agonist quinpirole but not to full vehicle treated levels. The D1/D5 receptor agonist SKF-38393 and the DA precursor L-DOPA exerted no improvement on the locomotor phenotype of larvae following neuron ablation (Figure A.1.3).

Figure A.1.1 Characterization of CFP expressing cells in larval zebrafish. Whole mount immunohistochemistry for CFP (blue) and TH (green) and whole mount *in situ* hybridization using a *dat* cRNA probe (red) at 3 dpf. Z-stack maximal intensity pojections of 1 micron tick optical sections. Images are shown dorsal facing up and anterior facing left. Scale bars represent 50 µm.

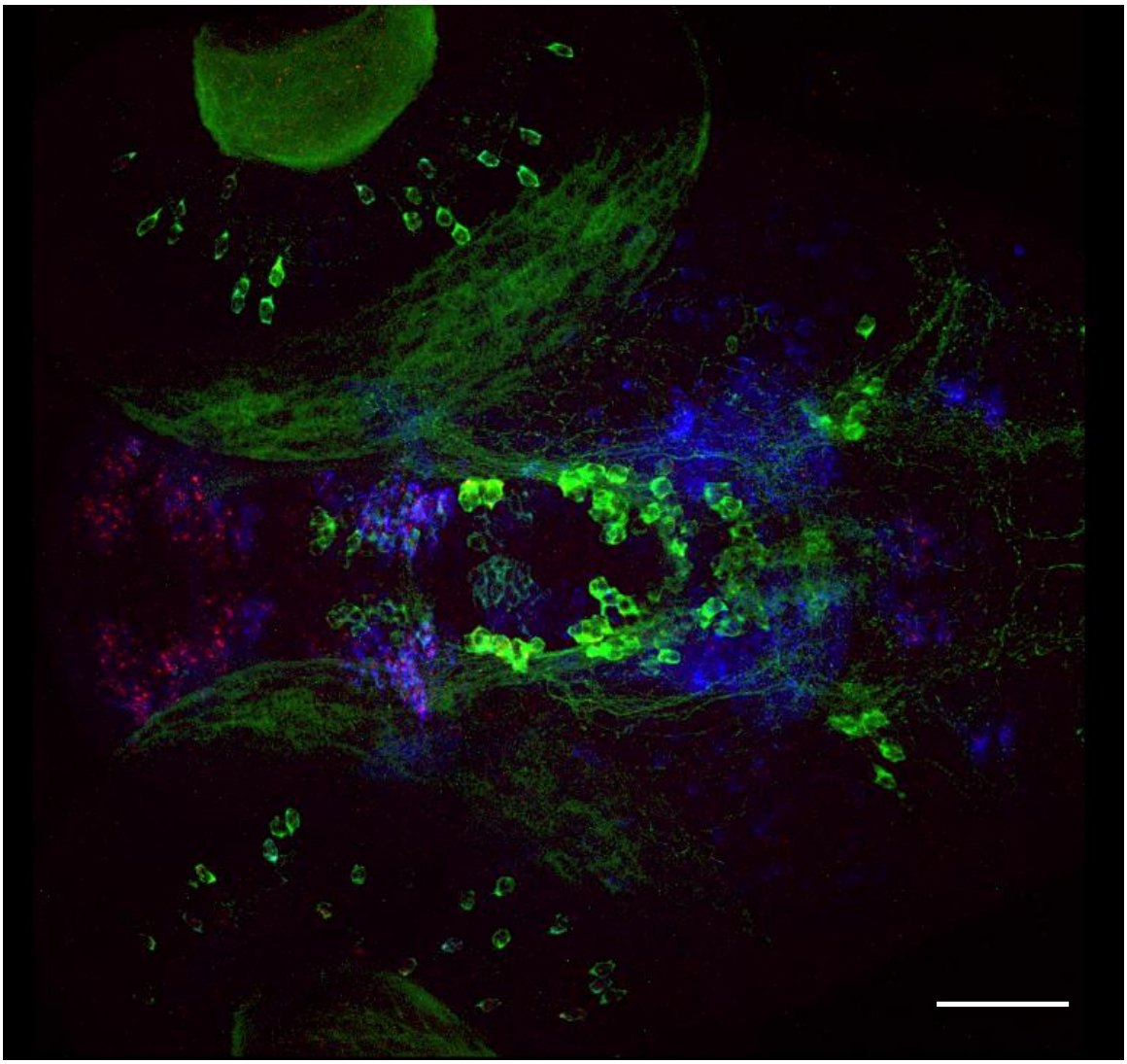

Table A.1. Mtz dose response in larval zebrafish

Mtz dose	Phenotype
25 & 20 mM	Induced mortality
15 mM	Induced mortality
10 mM	No mortality OE 1413 DMSO OE 1413 Mtz WT DMSO WT Mtz 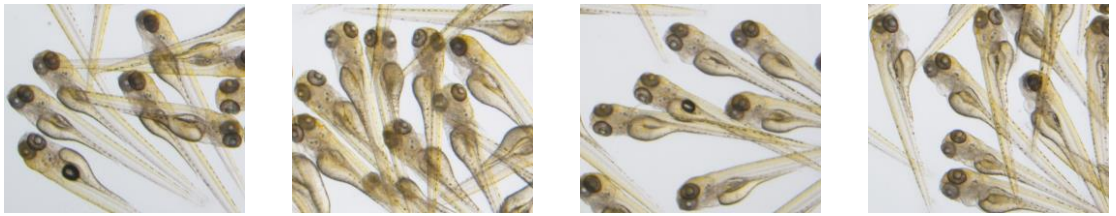
7.5 mM	No observable deleterious effect CFP cell ablation efficiency similar to 10 mM dose OE 1413 DMSO OE 1413 Mtz WT DMSO WT Mtz 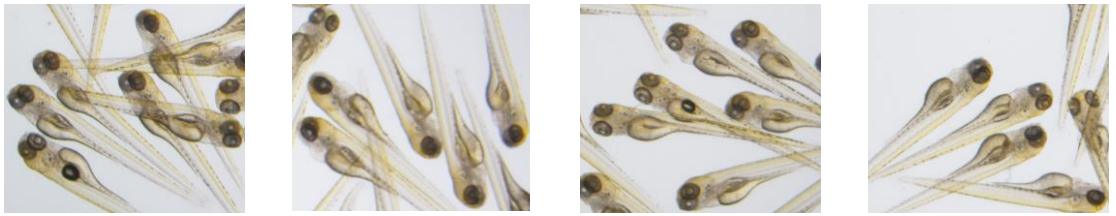
5 mM	Lower ablation efficiency than 7.5mM OE 1413 DMSO OE 1413 Mtz WT DMSO WT Mtz 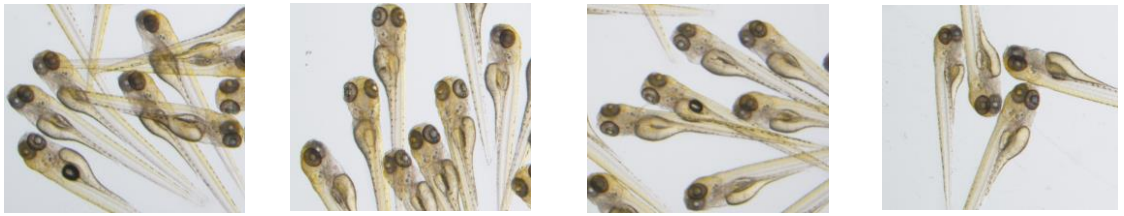

Figure A.1.2. Mtz treatment does not affect motor neuron arrangement. Vehicle and Mtz treated larvae had no difference in Zn1 and Znp1 antibody (obtained from the Developmental Studies Hybridoma Bank) staining in the somites of larval zebrafish at 5 dpf. Images show rostral facing left caudal facing right. Scale = 50 μm

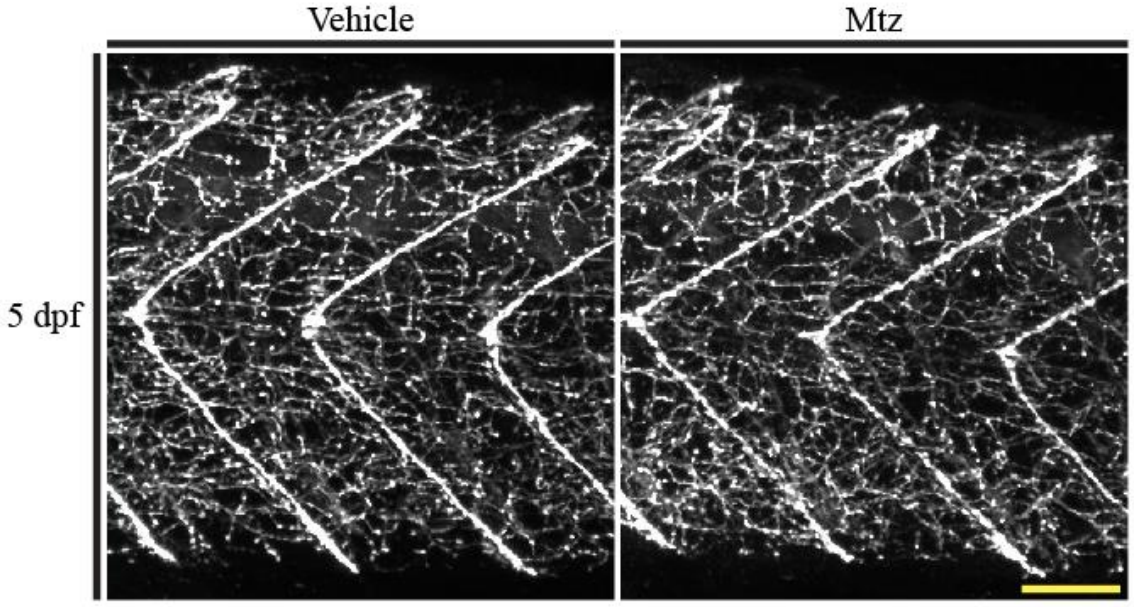
Vehicle
Mtz
5 dpf

Figure A.1.3 Larval locomotor phenotype. A) Touch response test. A touch stimulus was applied to the trunk of 3-day-old larvae and animals that did not respond to touch within 0.4 seconds were categorized as non-motile. B) No differences were observed in touch response between Mtz and vehicle treated larvae. Mtz larvae tended to initiate spontaneous movement less frequently than vehicle treated animals (X^2-test). C) Schematic representation of spontaneously swimming 5 day old larvae. D) Total distance moved by larvae over a 10 minute video recording (ANOVA).

A)

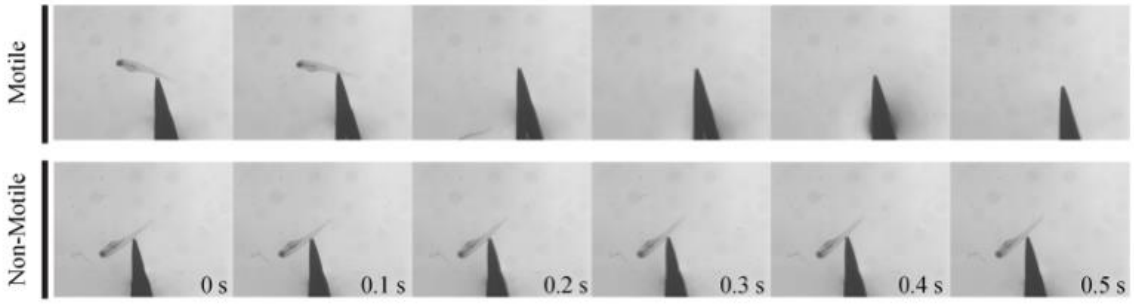
Motile
Non-Motile
0 s
0.1 s
0.2 s
0.3 s
0.4 s
0.5 s

B)

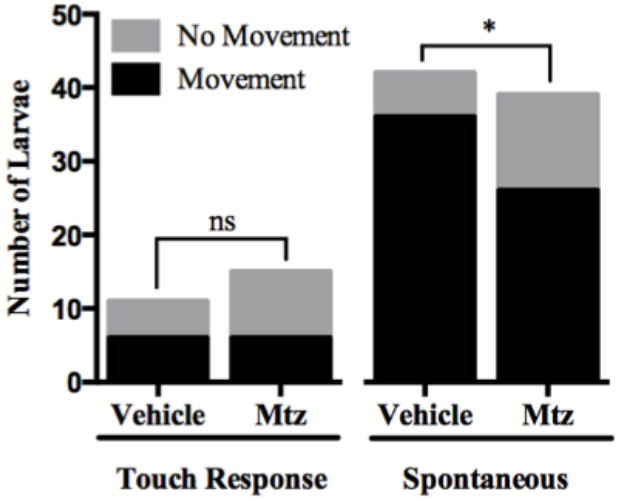
No Movement
Movement
Number of Larvae
50
40
30
20
10
0
ns
*
Vehicle
Mtz
Vehicle
Mtz
Touch Response
Spontaneous

C)


Vehicle
Mtz
SKF-38393
Quinpirole
L-DOPA

D)

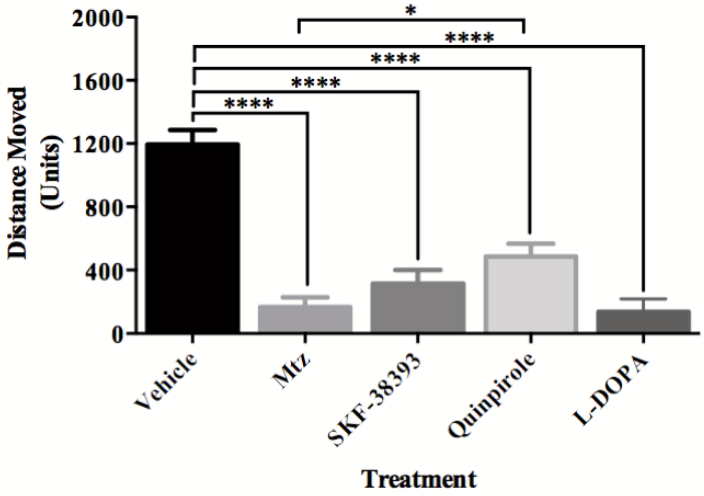
Distance Moved (Units)
2000
1600
1200
800
400
0
*
****
****
****
****
Vehicle
Mtz
SKF-38393
Quinpirole
L-DOPA
Treatment

Appendix 2: *parkin* driven GFP expression in transgenic zebrafish

Parkin gene regulation and mutations have important implications in the study of Parkinson's disease. In a collaborative effort with the laboratory of Dr. Michael Schlossmacher, we set to investigate potential *parkin cis*-regulatory elements that would allow for the expression of a fluorescent reporter (EGFP) to track *parkin* activation *in vivo* using the zebrafish.

Here we studied the ability of different segments of the Japanese pufferfish (*Takifugu rubripes*; fugu) *parkin* gene to induce fluorescent reporter expression in both mammalian cell culture and in primary injected zebrafish larvae. We choose to use the fugu *parkin* as it is 350-fold smaller than the human *parkin* locus. After preliminary work using different *fuparkin* fragments (Fig 2.1) we show that the 820 bp and 310 bp sequence flanking the upstream region to the transcription start site are able to drive EGFP expression in Chinese hamster ovary (CHO) cell line (Fig. 2.2). These reporter constructs, which contained the Tol2 elements, were injected into one-cell zebrafish embryos and we observed a stronger fluorescent expression with the 820 bp sequence 48 hours following injection (Fig. 2.3). We are currently screening progeny of injected animals to identify a transgenic line that will be used as a tool to track changes in *parkin* expression *in vivo*.

Figure A.2.1. Constructs containing different fragments tested to drive fluorescent reporter expression.

a) *fuparkin*+EGFP+pDrive

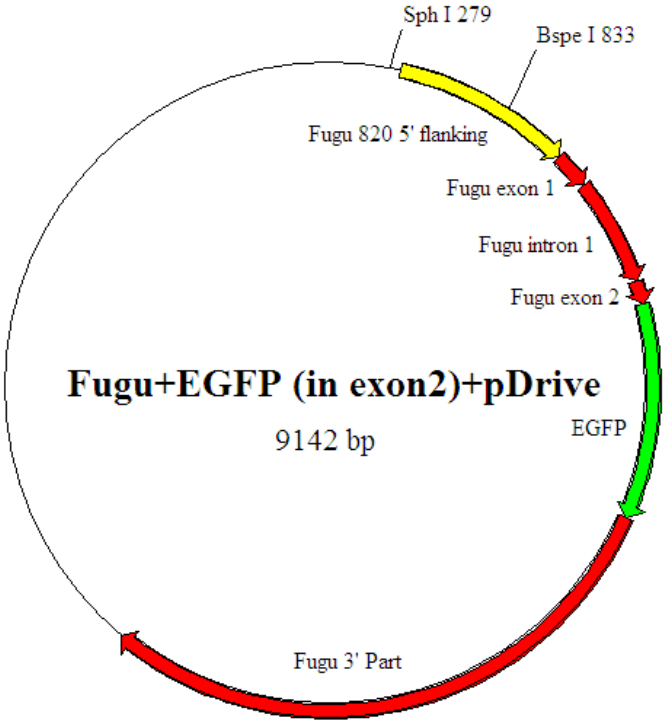

b) *fuparkin*-510+EGFP+pDrive

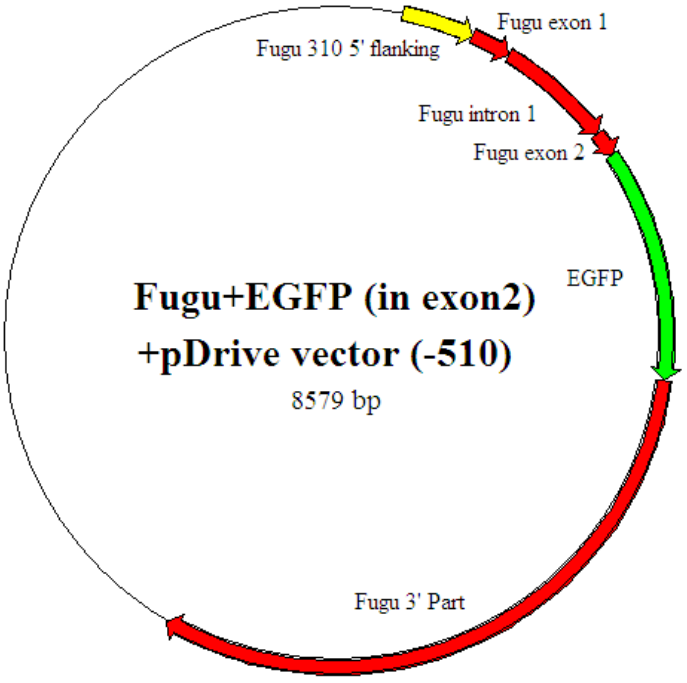

c) CMV+*fuparkin*+EGFP+pcDNA3.1

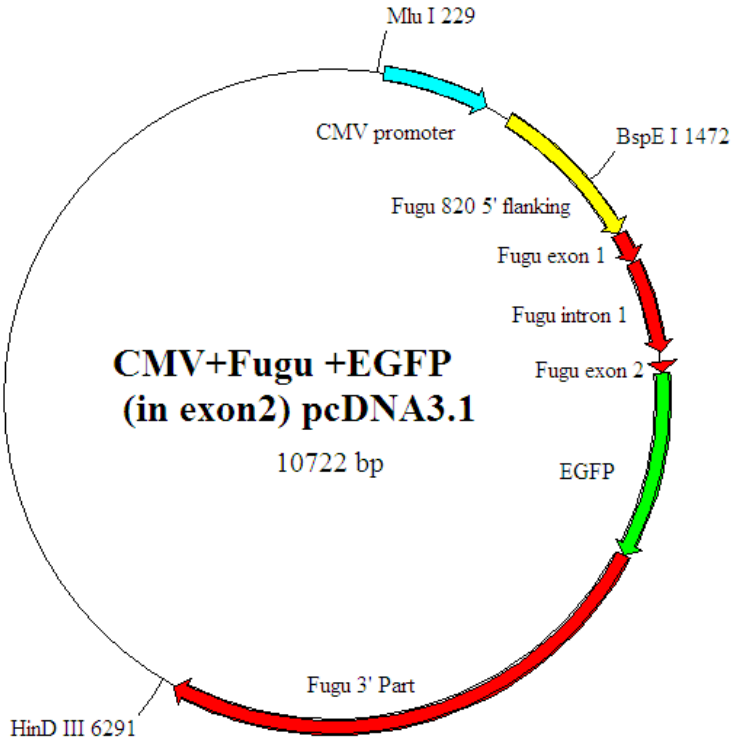

d) CMV+*fuparkin*-510+EGFP+pcDNA3.1

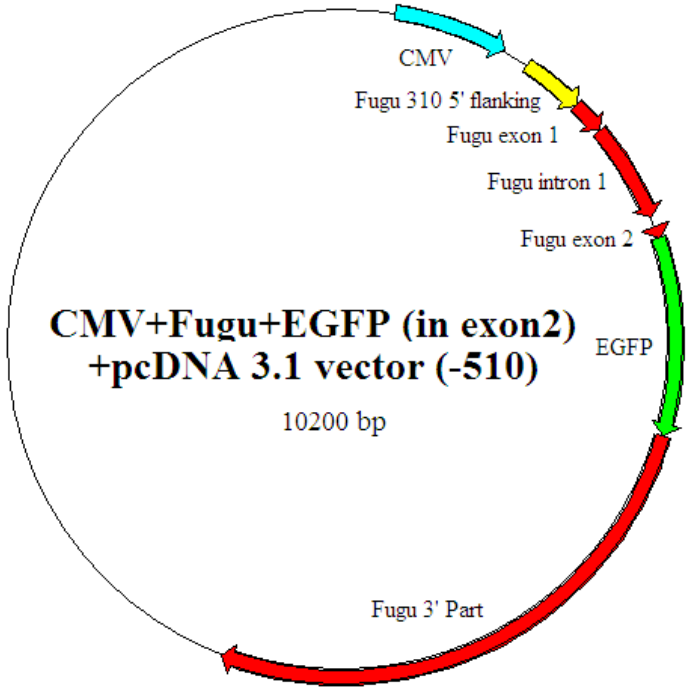

e) *fuparkin*-510+EGFP+pcDNA3.1

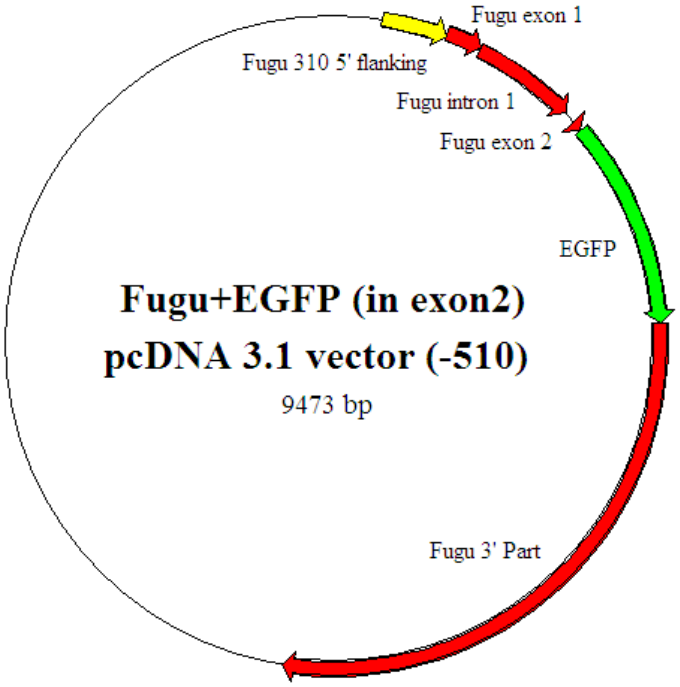

f) Tol2+820 bp flanking+EGFP

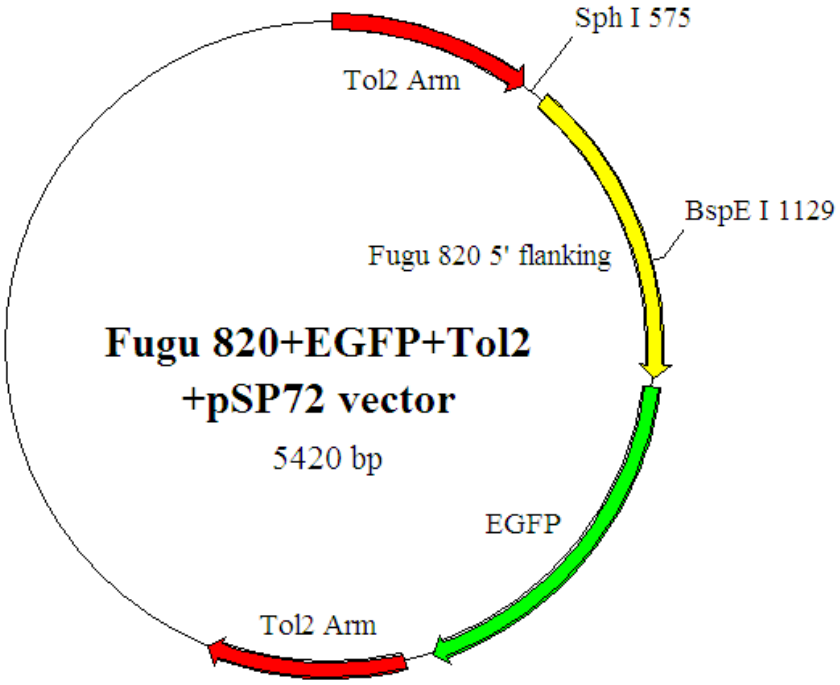

g) Tol2+310 bp flanking+EGFP

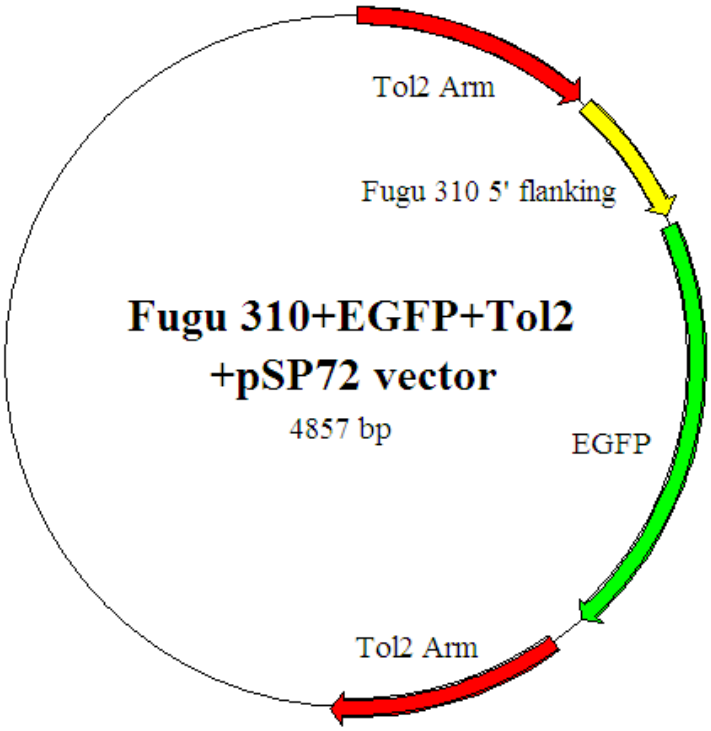

Figure A.2.2. Fluorescent reporter expression in CHO cells. Analysis of transfected cells at 24 hours (A) and at 48 hours (B) post transfection. RL (regular light).

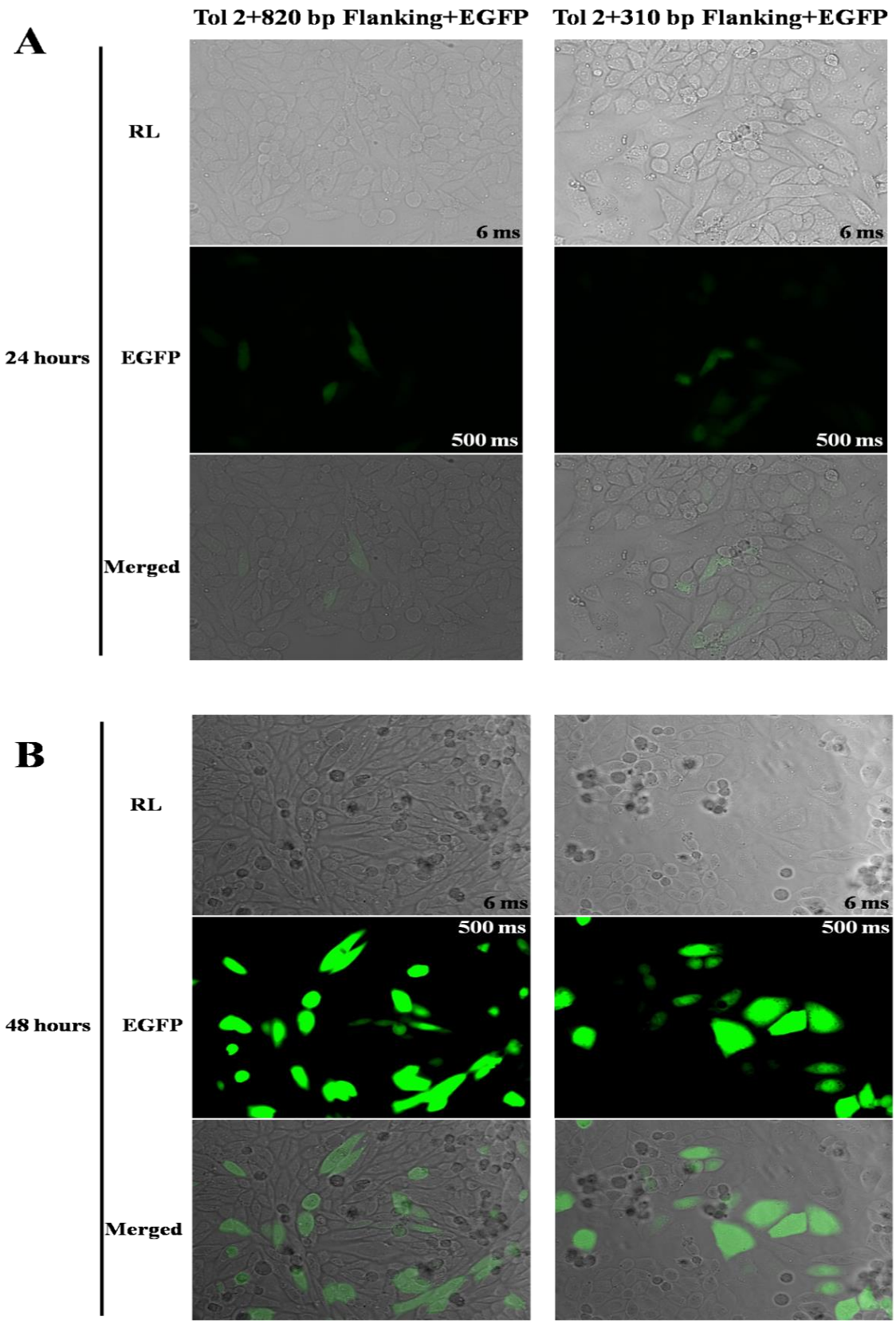
A
Tol 2+820 bp Flanking+EGFP
Tol 2+310 bp Flanking+EGFP
RL
EGFP
Merged
24 hours
6 ms
500 ms
B
48 hours

Figure A.2.3. Fluorescent reporter expression in primary injected zebrafish embryos. Analysis of transfected cells at 24 hours (A) and at 48 hours (B) post transfection. RL (regular light).

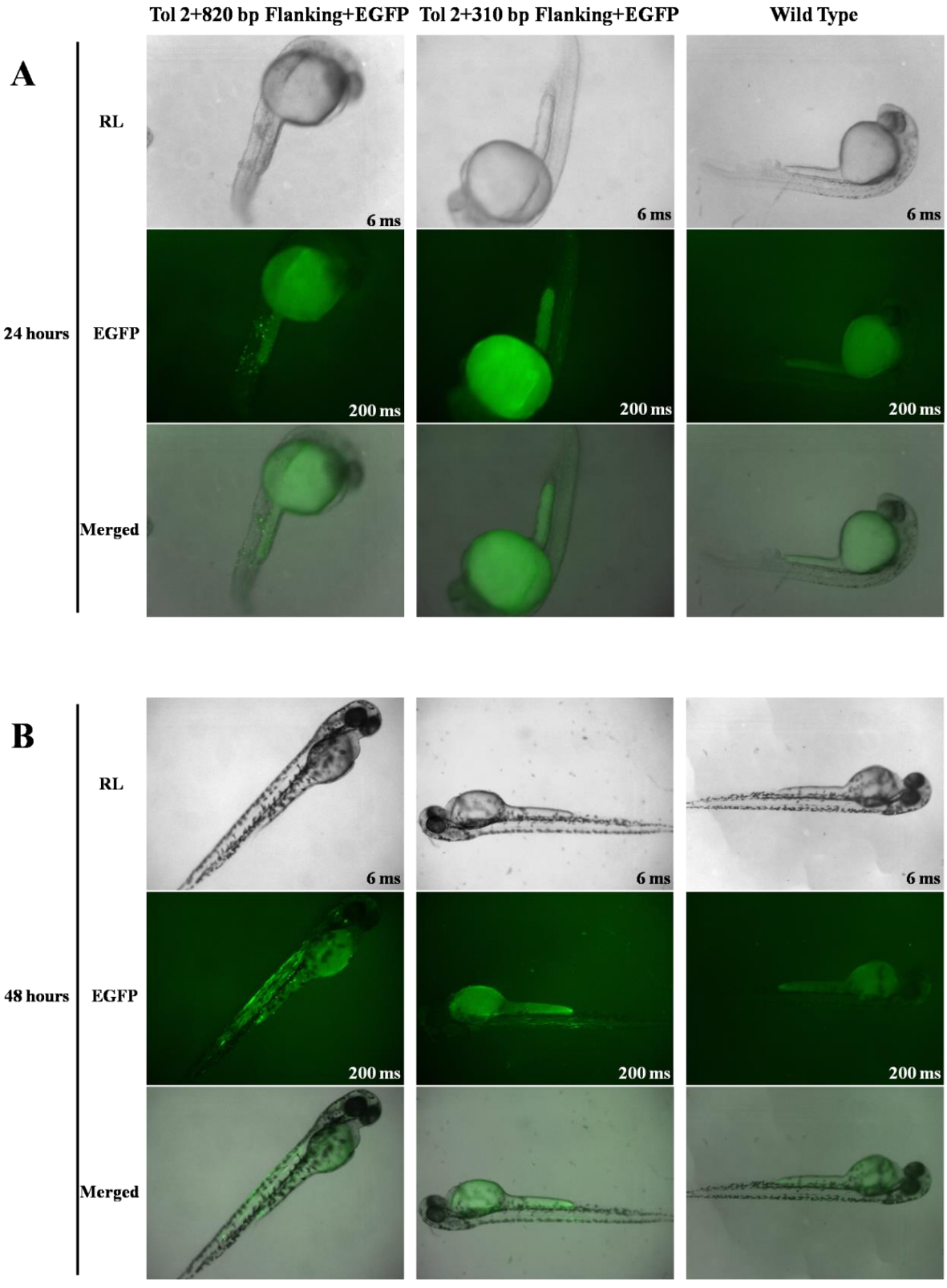
Tol 2+820 bp Flanking+EGFP
Tol 2+310 bp Flanking+EGFP
Wild Type
A
RL
24 hours
EGFP
Merged
6 ms
200 ms
B
RL
48 hours
EGFP
Merged
6 ms
200 ms

Appendix 3: List of my contributions to manuscripts not presented in this thesis

- Xi Y., Yu M., **Godoy R**., Hatch G., Poitras L., Ekker M. (2011) Transgenic zebrafish expressing green fluorescent protein in dopaminergic neurons of the ventral diencephalon. *Dev. Dyn.* **240**, 2539–2547.
- Noble S., Ismail A., **Godoy R**., Xi Y., Ekker M. (2012) Zebrafish Parla- and Parlb-deficiency affects dopaminergic neuron patterning and embryonic survival *J. Neurochem.* **122**, 196–207.
- Noble S., **Godoy R**., Ekker M. (2015) Transgenic zebrafish expressing mCherry in the mitochondria of dopaminergic neurons. *Zebrafish.* (Under review ZEB-2015-1085).
- Huang S.S.Y., **Godoy R**., Noble S., Ekker M., Chan H.M. (2015) Effects of methylmercury on Parkinson-like phenotypes in zebrafish (*Danio rerio*) larvae. (Manuscript under submission)
- Eisa-Beygi S., Kwong R.W.M., Noble S., **Godoy R**., Moon T., Ekker M. Molecular and pathophysiological processes underlying spontaneous intracerebral hemorrhage (ICH) in developing zebrafish (*Danio rerio*). (Manuscript prepared)

REFERENCES

Adinoff B. (2004) Neurobiologic processes in drug reward and addiction. *Harv. Rev. Psychiatry* **12**, 305–320.

Adolf B., Chapouton P., Lam C. S., Topp S., Tannhäuser B., Strähle U., Götz M., Bally-Cuif L. (2006) Conserved and acquired features of adult neurogenesis in the zebrafish telencephalon. *Dev. Biol.* **295**, 278–293.

Agata K., Saito Y., Nakajima E. (2007) Unifying principles of regeneration I: Epimorphosis versus morphallaxis. *Dev. Growth Differ*. **49**, 73–78.

Agata K., Umesono Y. (2008) Brain regeneration from pluripotent stem cells in planarian. *Philos. Trans. R. Soc. B. Biol. Sci.* **363**, 2071–2078.

Agetsuma M., Aizawa H., Aoki T., Nakayama R., Takahoko M., Goto M., Sassa T., et al. (2010) The habenula is crucial for experience-dependent modification of fear responses in zebrafish. *Nat. Neurosci.* **13**, 1354–1356.

Akerberg A. A., Stewart S., Stankunas K. (2014) Spatial and temporal control of transgene expression in zebrafish *PLoS One* **9**, e92217.

Akitake C. M., Macurak M., Halpern M. E., Goll M. G. (2011) Transgenerational analysis of transcriptional silencing in zebrafish. *Dev. Biol* **352**, 191–201.

Anichtchik O. V., Kaslin J., Peitsaro N., Scheinin M., Panula P. (2004) Neurochemical and behavioural changes in zebrafish Danio rerio after systemic administration of 6-hydroxydopamine and 1-methyl-4-phenyl-1,2,3,6-tetrahydropyridine *J. Neurochem.* **88**, 443–453.

Anichtchik O., Diekmann H., Fleming A., Roach A., Goldsmith P., Rubinsztein D. C. (2008) Loss of PINK1 function affects development and results in neurodegeneration in zebrafish *J. Neurosci.* **28**, 8199–8207.

Bai Q., Burton E. A. (2009) Cis-acting elements responsible for dopaminergic neuron-specific expression of zebrafish slc6a3 (dopamine transporter) in vivo are located remote from the transcriptional start site. *Neuroscience* **164**, 1138–1151.

Balu D. T., Hodes G. E., Anderson B. T., Lucki I. (2009a) Enhanced Sensitivity of the MRL/MpJ Mouse to the neuroplastic and behavioral effects of accute and chronic antidepressant treatments. *Exp. Clin. Psychopharmacol.* **34**, 1764–1773.

Balu D. T., Hodes G. E., Hill T. E., Ho N., Rahman Z., Bender C. N., Ring R. H., et al. (2009b) Flow cytometric analysis of BrdU incorporation as a high-throughput method for measuring adult neurogenesis in the mouse. *J. Pharmacol. Toxicol. Methods* **59**, 100–107.

Bandmann O., Burton E. A. (2010) Genetic zebrafish models of neurodegenerative diseases. *Neurobiol. Dis.* **40**, 58–65.

Barreto-Valer K., Lopez-Bellido R., Rodriguez R. E. (2013) Cocaine modulates the expression of transcription factors related to the dopaminergic system in zebrafish *Neuroscience* **231**, 258–271.

Barreto-Valer K., López-Bellido R., Macho Sánchez-Simón F., Rodríguez R. E. (2012) Modulation by cocaine of dopamine receptors through miRNA-133b in zebrafish embryos. *PLoS One* **7**, e52701.

Baumgart E. V., Barbosa J. S., Bally-Cuif L., Götz M., Ninkovic J. (2011) Stab wound injury of the zebrafish telencephalon: a model for comparative analysis of reactive gliosis. *Glia* **60**, 343–357.

Becker C. G., Becker T. (2015) Neuronal regeneration from ependymo-radial glial cells: cook, little pot, cook *Dev. Cell* **32**, 516–527.

Bely A. E., Nyberg K. G. (2010) Evolution of animal regeneration: re-emergence of a field. *Trends Ecol. Evol.* **25**, 161–170.

Benoit-Marand M., Borrelli E., Gonon F. (2001) Inhibition of dopamine release via presynaptic D2 receptors: time course and functional characteristics in vivo *J. Neurosci* **21**, 9134–9141.

Berg D. A., Belnoue L., Song H., Simon A. (2013) Neurotransmitter-mediated control of neurogenesis in the adult vertebrate brain. *Development* **140**, 2548–2561.

Berg D. A., Kirkham M., Wang H., Frisen J., Simon A. (2011) Dopamine controls neurogenesis in the adult salamander midbrain in homeostasis and during regeneration of dopamine neurons. *Cell Stem Cell* **8**, 426–433.

Bilsland J. G., Haldon C., Goddard J., Oliver K., Murray F., Wheeldon A., Cumberbatch J., McAllister G., Munoz-Sanjuan I. (2006) A rapid method for the quantification of mouse hippocampal neurogenesis in vivo by flow cytometry. *J. Neurosci. Methods* **157**, 54–63.

Björklund A., Dunnett S. B. (2007) Dopamine neuron systems in the brain: an update. *Trends Neurosci.* **30**, 194–202.

Blandini F., Armentero M.-T. (2012) Animal models of Parkinson's disease. *FEBS J.* **279**, 1156–1166.

Blesa J., Phani S., Jackson-Lewis V., Przedborski S. (2012) Classic and new animal models of Parkinson's disease. *J. Biomed. Biotechnol.* **2012**, 1–10.

Bohnsack B. L., Gallina D., Kahana A. (2011) Phenothiourea sensitizes zebrafish cranial neural crest and extraocular muscle development to changes in retinoic acid and IGF signaling. *PLoS One* **6**, e22991.

Bortolotto J. W., Cognato G. P., Christoff R. R., Roesler L. N., Leite C. E., Kist L. W., Bogo M. R., Vianna M. R., Bonan C. D. (2014) Long-term exposure to paraquat alters behavioral parameters and dopamine levels in adult zebrafish (Danio Rerio). *Zebrafish* **11**, 142–153.

Bové J., Perier C. (2012) Neurotoxin-based models of Parkinson's disease. *Neuroscience* **211**, 51–76.

Brann J. H., Firestein S. J. (2014) A lifetime of neurogenesis in the olfactory system *Front. Neurosci.* **8**, 182.

Branson K., Robie A. A., Bender J., Pietro Perona, Dickinson M. H. (2009) High-throughput ethomics in large groups of Drosophila. *Nat Meth* **6**, 451–457.

Bretaud S., Allen C., Ingham P. W., Bandmann O. (2007) p53-dependent neuronal cell death in a DJ-1-deficient zebrafish model of Parkinson's disease. *J. Neurochem.* **100**, 1626-35

Bretaud S., Lee S., Guo S. (2004) Sensitivity of zebrafish to environmental toxins implicated in Parkinson's disease. *Neurotoxicol. Teratol.* **26**, 857–864.

Bridgewater J. A., Springer C. J., Knox R. J., Minton N. P., Michael N. P., Collins M. K. (1995) Expression of the bacterial nitroreductase enzyme in mammalian cells renders them selectively sensitive to killing by the prodrug CB1954 *Eur. J. Cancer* **31A**, 2362–2370.

Budick S. A., O'Malley D. M. (2000) Locomotor repertoire of the larval zebrafish: swimming, turning and prey capture *J. Exp. Biol.* **203**, 2565–2579.

Cachat J., Stewart A., Grossman L., Gaikwad S., Kadri F., Chung K. M., Wu N., et al. (2010) Measuring behavioral and endocrine responses to novelty stress in adult zebrafish. *Nat. Protoc.* **5**, 1786–1799.

Cachat J., Stewart A., Utterback E., Hart P., Gaikwad S., Wong K., Kyzar E., Wu N., Kalueff A. V. (2011) Three-dimensional neurophenotyping of adult zebrafish behavior. *PLoS One* **6**, e17597.

Callier S., Snapyan M., Crom S., Prou D., Vincent J.-D., Vernier P. (2003) Evolution and cell biology of dopamine receptors in vertebrates. *Biol. Cell* **95**, 489–502.

Carey R. M. (2001) Theodore Cooper lecture: renal dopamine system: paracrine regulator of sodium homeostasis and blood pressure *Hypertension* **38**, 297–302.

Cario C. L., Farrell T. C., Milanese C., Burton E. A. (2011) Automated measurement of zebrafish larval movement. *J. Physiol.* **589**, 3703–3708.

Carleton A., Petreanu L. T., Lansford R., Alvarez-Buylla A., Lledo P.-M. (2003) Becoming a new neuron in the adult olfactory bulb *Nat. Neurosci.* **6**, 507–518.

Carlsson A., Lindqvist M., Magnusson T., Waldeck B. (1958) On the presence of 3-hydroxytyramine in brain *Science* **127**, 471.

Chapouton P., Jagasia R., Bally-Cuif L. (2007) Adult neurogenesis in non-mammalian vertebrates. *BioEssays* **29**, 745–757.

Chatterjee D., Gerlai R. (2009) High precision liquid chromatography analysis of dopaminergic and serotoninergic responses to acute alcohol exposure in zebrafish. *Behav. Brain Res.* **200**, 208–213.

Chaudhuri K. R., Schapira A. H. (2009) Non-motor symptoms of Parkinson's disease: dopaminergic pathophysiology and treatment. *Lancet Neurol.* **8**, 464–474.

Chen C.-F., Chu C.-Y., Chen T.-H., Lee S.-J., Shen C.-N., Hsiao C.-D. (2011) Establishment of a transgenic zebrafish line for superficial skin ablation and functional validation of apoptosis modulators in vivo. *PLoS One* **6**, e20654.

Christofferson A., Wilkie J. (2009) Mechanism of CB1954 reduction by Escherichia coli nitroreductase. *Biochem. Soc. Trans.* **37**, 413.

Chung A.-Y., Kim P.-S., Kim S., Kim E., Kim D., Jeong I., Kim H.-K., et al. (2013) Generation of demyelination models by targeted ablation of oligodendrocytes in the zebrafish CNS. *Mol. Cells* **36**, 82–87.

Connolly B. S., Lang A. E. (2014) Pharmacological treatment of Parkinson disease. *JAMA* **311**, 1670.

Curado S., Anderson R. M., Jungblut B., Mumm J., Schroeter E., Stainier D. Y. R. (2007) Conditional targeted cell ablation in zebrafish: A new tool for regeneration studies. *Dev. Dyn.* **236**, 1025–1035.

Curado S., Stainier D. Y. R., Anderson R. M. (2008) Nitroreductase-mediated cell/tissue ablation in zebrafish: a spatially and temporally controlled ablation method with applications in developmental and regeneration studies. *Nat. Protoc.* **3**, 948–954.

Dauer W., Przedborski S. (2003) Parkinson's disease: mechanisms and models *Neuron* **39**, 889–909.
Davie C. A. (2008) A review of Parkinson's disease. *Br. Med. Bull.* **86**, 109–127.
Dayer A. G., Ford A. A., Cleaver K. M., Yassaee M., Cameron H. A. (2003) Short-term and long-term survival of new neurons in the rat dentate gyrus. *J. Comp. Neurol.* **460**, 563–572.
de Esch C., Slieker R., Wolterbeek A., Woutersen R., de Groot D. (2012) Zebrafish as potential model for developmental neurotoxicity testing. *Neurotoxicol Teratol* **34**, 545–553.
Decker A. R., McNeill M. S., Lambert A. M., Overton J. D., Chen Y.-C., Lorca R. A., Johnson N. A., et al. (2014) Abnormal differentiation of dopaminergic neurons in zebrafish trpm7 mutant larvae impairs development of the motor pattern. *Dev. Biol.* **386**, 1–12.
Del Tredici K., Rüb U., De Vos R. A. I., Bohl J. R. E., Braak H. (2002) Where does parkinson disease pathology begin in the brain *J. Neuropathol. Exp. Neurol.* **61**, 413–426.
Demy D. L., Ranta Z., Giorgi J.-M., Gonzalez M., Herbomel P., Kissa K. (2013) Generating parabiotic zebrafish embryos for cell migration and homing studies. *Nat. Meth.* **10**, 256–258.
Diekmann H., Anichtchik O., Fleming A., Futter M., Goldsmith P., Roach A., Rubinsztein D. C. (2009) Decreased BDNF levels are a major contributor to the embryonic phenotype of Huntingtin knockdown zebrafish. *J. Neurosci* **29**, 1343–1349.
Dranow D. B., Tucker R. P., Draper B. W. (2013) Germ cells are required to maintain a stable sexual phenotype in adult zebrafish. *Dev. Biol.* **376**, 43–50.
Eddins D., Petro A., Williams P., Cerutti D. T., Levin E. D. (2008) Nicotine effects on learning in zebrafish: the role of dopaminergic systems. *Psychopharmacology* **202**, 103–109.
Eisenhofer G., Aneman A., Friberg P., Hooper D., Fåndriks L., Lonroth H., Hunyady B., Mezey E. (1997) Substantial production of dopamine in the human gastrointestinal tract *J. Clin. Endocrinol. Metab.* **82**, 3864–3871.
Elbaz I., Yelin-Bekerman L., Nicenboim J., Vatine G., Appelbaum L. (2012) Genetic ablation of hypocretin neurons alters behavioral state transitions in zebrafish *J. Neurosci.* **32**, 12961–12972.
Elsalini O. A., Rohr K. B. (2003) Phenylthiourea disrupts thyroid function in developing zebrafish *Dev. Genes Evol.* **212**, 593–598.
Fan C.-Y., Cowden J., Simmons S. O., Padilla S., Ramabhadran R. (2010) Gene expression changes in developing zebrafish as potential markers for rapid developmental neurotoxicity screening. *Neurotoxicol. Teratol.* **32**, 91–98.
Fancy S. P. J., Harrington E. P., Yuen T. J., Silbereis J. C., Zhao C., Baranzini S. E., Bruce C. C., et al. (2011) Axin2 as regulatory and therapeutic target in newborn brain injury and remyelination. *Nat. Neurosci* **14**, 1009–1016.
Farrell T. C., Cario C. L., Milanese C., Vogt A., Jeong J.-H., Burton E. A. (2011) Evaluation of spontaneous propulsive movement as a screening tool to detect rescue of Parkinsonism phenotypes in zebrafish models. *Neurobiol. Dis.* **44**, 9–18.

Feng C.-W., Wen Z.-H., Huang S.-Y., Hung H.-C., Chen C.-H., Yang S.-N., Chen N.-F., Wang H.-M., Hsiao C.-D., Chen W.-F. (2014) Effects of 6-Hydroxydopamine exposure on motor activity and biochemical expression in zebrafish (Danio Rerio) larvae. *Zebrafish* **11**, 227-39.

Fernandes A. M., Fero K., Arrenberg A. B., Bergeron S. A., Driever W., Burgess H. A. (2012) Deep brain photoreceptors control light-seeking behavior in zebrafish larvae *Curr. Biol.* **22**, 2042–2047.

Ferretti P., Prasongchean W. (2015) Adult neurogenesis and regeneration: focus on nonmammalian vertebrates, in *Stem Cell Biology and Regenerative Medicine* (Kuhn H. G., Eisch A. J., eds), pp. 1–21. Springer New York, New York, NY.

Fett M. E., Pilsl A., Paquet D., van Bebber F., Haass C., Tatzelt J., Schmid B., Winklhofer K. F. (2010) Parkin is protective against proteotoxic stress in a transgenic zebrafish model. *PLoS One* **5**, e11783.

Filippi A., Dürr K., Ryu S., Willaredt M., Holzschuh J., Driever W. (2007) Expression and function of nr4a2, lmx1b, and pitx3 in zebrafish dopaminergic and noradrenergic neuronal development. *BMC Dev. Biol.* **7**, 135.

Filippi A., Jainok C., Driever W. (2012) Analysis of transcriptional codes for zebrafish dopaminergic neurons reveals essential functions of Arx and Isl1 in prethalamic dopaminergic neuron development. *Dev. Biol.* **369**, 133–149.

Fisher S., Grice E. A., Vinton R. M., Bessling S. L., Urasaki A., Kawakami K., McCallion A. S. (2006) Evaluating the biological relevance of putative enhancers using Tol2 transposon-mediated transgenesis in zebrafish. *Nat. Protoc.* **1**, 1297–1305.

Fleming A., Diekmann H., Goldsmith P. (2013) Functional characterisation of the maturation of the blood-brain barrier in larval zebrafish. *PLoS One* **8**, e77548.

Flinn L., Bretaud S., Lo C., Ingham P. W., Bandmann O. (2008) Zebrafish as a new animal model for movement disorders. *J. Neurochem.* **106**, 1991–1997.

Flinn L., Mortiboys H., Volkmann K., Koster R. W., Ingham P. W., Bandmann O. (2009) Complex I deficiency and dopaminergic neuronal cell loss in parkin-deficient zebrafish (Danio rerio). *Brain* **132**, 1613–1623.

Fontaine R., Affaticati P., Yamamoto K., Jolly C., Bureau C., Baloche S., Gonnet F., Vernier P., Dufour S., Pasqualini C. (2013) Dopamine inhibits reproduction in female zebrafish (Danio rerio) via three pituitary D2 receptor subtypes. *Endocrinology* **154**, 807–818.

Formella I., Scott E. K., Burne T. H. J., Harms L. R., Liu P.-Y., Turner K. M., Cui X., Eyles D. W. (2012) Transient knockdown of tyrosine hydroxylase during development has persistent effects on behaviour in adult zebrafish (Danio rerio). *PLoS One* **7**, e42482.

Frielingsdorf H., Schwarz K., Brundin P., Mohapel P. (2004) No evidence for new dopaminergic neurons in the adult mammalian substantia nigra *Proc. Natl. Acad. Sci. U.S.A.* **101**, 10177–10182.

Fujimoto E., Stevenson T. J., Chien C.-B., Bonkowsky J. L. (2011) Identification of a dopaminergic enhancer indicates complexity in vertebrate dopamine neuron phenotype specification. *Dev. Biol.* **352**, 393–404.

Gaete M., Muñoz R., Sánchez N., Tampe R., Moreno M., Contreras E. G., Lee-Liu D., Larraín J. (2012) Spinal cord regeneration in Xenopus tadpoles proceeds through activation of Sox2-positive cells *Neural Dev.* **7**, 13.
Gemberling M., Bailey T. J., Hyde D. R., Poss K. D. (2013) The zebrafish as a model for complex tissue regeneration. *Trends in Genet.* **29**, 611–620.
Gerlai R. (2014) Fish in behavior research: Unique tools with a great promise *J. Neurosci. Methods* **234**, 54–58.
Giacomini N. J., Rose B., Kobayashi K., Guo S. (2006) Antipsychotics produce locomotor impairment in larval zebrafish. *Neurotoxicol. Teratol.* **28**, 245–250.
Gibrat C., Saint-Pierre M., Bousquet M., Lévesque D., Rouillard C., Cicchetti F. (2009) Differences between subacute and chronic MPTP mice models: investigation of dopaminergic neuronal degeneration and α-synuclein inclusions. *J. Neurochem.* **109**, 1469–1482.
Godwin J., Kuraitis D., Rosenthal N. (2014) Extracellular matrix considerations for scar-free repair and regeneration: Insights from regenerative diversity among vertebrates. *Int. J. Biochem. Cell Biol.* **56**, 47–55.
Goessling W., North T. E. (2014) Repairing quite swimmingly: advances in regenerative medicine using zebrafish. *Dis Models Mech.* **7**, 769–776.
Goldshmit Y., Sztal T. E., Jusuf P. R., Hall T. E., Nguyen-Chi M., Currie P. D. (2012) Fgf-dependent glial cell bridges facilitate spinal cord regeneration in zebrafish. *J. Neurosci.* **32**, 7477–7492.
Goll M. G., Anderson R., Stainier D. Y. R., Spradling A. C., Halpern M. E. (2009) Transcriptional silencing and reactivation in transgenic zebrafish. *Genetics* **182**, 747–755.
Grandel H., Brand M. (2012) Comparative aspects of adult neural stem cell activity in vertebrates. *Dev. Genes Evol.* **223**, 131–147.
Grandel H., Kaslin J., Ganz J., Wenzel I., Brand M. (2006) Neural stem cells and neurogenesis in the adult zebrafish brain: Origin, proliferation dynamics, migration and cell fate. *Dev. Biol.* **295**, 263–277.
Guo S. (2009) Using zebrafish to assess the impact of drugs on neural development and function. *Expert Opin. Drug Discov.* **4**, 715–726.
Guo Y., Ma L., Cristofanilli M., Hart R. P., Hao A., Schachner M. (2011) Transcription factor Sox11b is involved in spinal cord regeneration in adult zebrafish. *Neuroscience* **172**, 329–341.
Gutzman J. H., Sive H. (2009) Zebrafish Brain Ventricle Injection. *J. Vis. Exp.* 26.
Hallett P. J., Deleidi M., Astradsson A., Smith G. A., Cooper O., Osborn T. M., Sundberg M., et al. (2015) Successful function of autologous iPSC-derived dopamine neurons following transplantation in a non-human primate model of Parkinson's disease. *Cell Stem Cell* **16**, 269–274.
Hawkes C. H., Del Tredici K., Braak H. (2007) Parkinson's disease: a dual-hit hypothesis. *Neuropathol. Appl. Neurobiol.* **33**, 599–614.
Hawkes C. H., Del Tredici K., Braak H. (2010) A timeline for Parkinson's disease. *Parkinsonism Relat. Disord.* **16**, 79–84.
Hickey P., Stacy M. (2011) Available and emerging treatments for Parkinson's disease: a review *Drug Des. Devel. Ther.* **5**, 241–254.

Higashi Y., Asanuma M., Miyazaki I., Ogawa N. (2000) Inhibition of tyrosinase reduces cell viability in catecholaminergic neuronal cells *J. Neurochem.* **75**, 1771–1774.
Hinsch K., Zupanc G. K. H. (2007) Generation and long-term persistence of new neurons in the adult zebrafish brain: A quantitative analysis. *Neuroscience* **146**, 679–696.
Holzschuh J., Ryu S., Aberger F., Driever W. (2001) Dopamine transporter expression distinguishes dopaminergic neurons from other catecholaminergic neurons in the developing zebrafish embryo *Mech. Dev.* **101**, 237–243.
Howe K., Clark M. D., Torroja C. F., Torrance J., Berthelot C., Muffato M., Collins J. E., et al. (2013) The zebrafish reference genome sequence and its relationship to the human genome. *Nature*, 1–7.
Huang J., Mckee M., Huang H. D., Xiang A., Davidson A. J., Lu H. A. J. (2013) A zebrafish model of conditional targeted podocyte ablation and regeneration. *Kidney Int.* **83**, 1193–1200.
Hyun J.-S., Baig M. R., Yang D.-Y., Leungwattanakij S., Kim K.-D., Abdel-Mageed A. B., Bivalacqua T. J., Hellstrom W. J. G. (2002) Localization of peripheral dopamine D1 and D2 receptors in rat and human seminal vesicles *J. Androl.* **23**, 114–120.
Iglesias M., Almuedo-Castillo M., Aboobaker A. A., Saló E. (2011) Early planarian brain regeneration is independent of blastema polarity mediated by the Wnt/β-catenin pathway. *Dev. Biol.* **358**, 68–78.
Inoue D., Wittbrodt J. (2011) One for all--a highly efficient and versatile method for fluorescent immunostaining in fish embryos *PLoS One* **6**, e19713.
Irons T. D., Kelly P. E., Hunter D. L., MacPhail R. C., Padilla S. (2013) Acute administration of dopaminergic drugs has differential effects on locomotion in larval zebrafish. *Pharmacol. Biochem. Behav.* **103**, 792–813.
Isono M., Otsu M., Konishi T., Matsubara K., Tanabe T., Nakayama T., Inoue N. (2012) Proliferation and differentiation of neural stem cells irradiated with X-rays in logarithmic growth phase. *Neuroscience Res.* **73**, 263–268.
Ito Y., Tanaka H., Okamoto H., Ohshima T. (2010) Characterization of neural stem cells and their progeny in the adult zebrafish optic tectum. *Dev. Biol.* **342**, 26–38.
Iturriaga R., Alcayaga J. (2004) Neurotransmission in the carotid body: transmitters and modulators between glomus cells and petrosal ganglion nerve terminals. *Brain Res. Brain Res. Rev.* **47**, 46–53.
Jankovic J. (2008) Parkinson's disease: clinical features and diagnosis. *Journal of Neurology, Neurosurgery & Psychiatry* **79**, 368–376.
Jay M., De Faveri F., McDearmid J. R. (2015) Firing dynamics and modulatory actions of supraspinal dopaminergic neurons during zebrafish locomotor behavior. *Curr. Biol.* **25**, 435–444.
Jho E.-H., Zhang T., Domon C., Joo C.-K., Freund J.-N., Costantini F. (2002) Wnt/beta-catenin/Tcf signaling induces the transcription of Axin2, a negative regulator of the signaling pathway *Mol. Cell. Biol.* **22**, 1172–1183.
Kandel E. (2012) *Principles of Neural Science, Fifth Edition (Principles of Neural Science (Kandel))*, (Kandel E. R., Schwartz J. H., Jessell T. M., Siegelbaum S. A., Hudspeth A. J., eds). McGraw-Hill Professional.
Karlsson J., Hofsten von J., Olsson P.-E. (2001) Generating transparent zebrafish: a refined method to improve detection of gene expression during embryonic development. *Mar. Biotechnol.* **3**, 0522–0527.

Kaslin J., Ganz J., Brand M. (2008) Proliferation, neurogenesis and regeneration in the non-mammalian vertebrate brain. *Philos. Trans. R. Soc. B Biol. Sci.* **363**, 101–122.
Kaslin J., Ganz J., Geffarth M., Grandel H., Hans S., Brand M. (2009) Stem cells in the adult zebrafish cerebellum: initiation and maintenance of a novel stem cell niche *J. Neurosci.* **29**, 6142–6153.
Kaslin J., Kroehne V., Benato F., Argenton F., Brand M. (2013) Development and specification of cerebellar stem and progenitor cells in zebrafish: from embryo to adult. *Neural Dev.* **8**, 1–1.
Kempermann G. (2011) *Adult neurogenesis 2: stem cells and neuronal development in the adult brain*. Oxford Univeristy Press, New York.
Kikuchi T., Morizane A., Doi D., Onoe H., Hayashi T., Kawasaki T., Saiki H., Miyamoto S., Takahashi J. (2011) Survival of human induced pluripotent stem cell-derived midbrain dopaminergic neurons in the brain of a primate model of Parkinson's disease *J Parkinsons Dis* **1**, 395–412.
Kimura Y., Hisano Y., Kawahara A., Higashijima S.-I. (2014) Efficient generation of knock-in transgenic zebrafish carrying reporter/driver genes by CRISPR/Cas9-mediated genome engineering. *Sci. Rep.* **4**, 6545.
Kishimoto N., Shimizu K., Sawamoto K. (2012) Neuronal regeneration in a zebrafish model of adult brain injury. *Dis. Models Mech.* **5**, 200–209.
Kizil C., Brand M. (2011) Cerebroventricular microinjection (CVMI) into adult zebrafish brain is an efficient misexpression method for forebrain ventricular cells. *PLoS One* **6**, e27395.
Kizil C., Dudczig S., Kyritsis N., Machate A., Blaesche J., Kroehne V., Brand M. (2012a) The chemokine receptor cxcr5 regulates the regenerative neurogenesis response in the adult zebrafish brain. *Neural Dev.* **7**, 1–1.
Kizil C., Kaslin J., Kroehne V., Brand M. (2012b) Adult neurogenesis and brain regeneration in zebrafish. *Dev. Neurobio* **72**, 429–461.
Kizil C., Kyritsis N., Dudczig S., Kroehne V., Freudenreich D., Kaslin J., Brand M. (2012c) Regenerative Neurogenesis from Neural Progenitor Cells Requires Injury-Induced Expression of Gata3. *Dev. Cell* **23**, 1230–1237.
Klee E. W., Schneider H., Clark K. J., Cousin M. A., Ebbert J. O., Hooten W. M., Karpyak V. M., Warner D. O., Ekker S. C. (2011) Zebrafish: a model for the study of addiction genetics. *Hum Genet* **131**, 977–1008.
Klein C., Schlossmacher M. G. (2006) The genetics of Parkinson disease: implications for neurological care. *Nat. Clin. Pract. Neurol.* **2**, 136–146.
Klein C., Westenberger A. (2012) Genetics of Parkinson's disease. *Cold Spring Harbor Perspectives in Medicine* **2**.
Kok F. O., Shin M., Ni C.-W., Gupta A., Grosse A. S., van Impel A., Kirchmaier B. C., et al. (2015) Reverse genetic screening reveals poor correlation between morpholino-induced and mutant phenotypes in zebrafish. *Dev. Cell* **32**, 97–108.
Kroehne V., Freudenreich D., Hans S., Kaslin J., Brand M. (2011) Regeneration of the adult zebrafish brain from neurogenic radial glia-type progenitors. *Development* **138**, 4831–4841.
Kyritsis N., Kizil C., Zocher S., Kroehne V., Kaslin J., Freudenreich D., Iltzsche A., Brand M. (2012) Acute inflammation initiates the regenerative response in the adult zebrafish brain. *Science* **338**, 1353-6.

Lam C. S., Korzh V., Strähle U. (2005) Zebrafish embryos are susceptible to the dopaminergic neurotoxin MPTP. *Eur. J. Neurosci.* **21**, 1758–1762.
Lam C. S., März M., Strähle U. (2009) gfap and nestin reporter lines reveal characteristics of neural progenitors in the adult zebrafish brain. *Dev. Dyn.* **238**, 475–486.
Lambert A. M., Bonkowsky J. L., Masino M. A. (2012) The conserved dopaminergic diencephalospinal tract mediates vertebrate locomotor development in zebrafish larvae *J. Neurosci.* **32**, 13488–13500.
Lange M., Norton W., Coolen M., Chaminade M., Merker S., Proft F., Schmitt A., Vernier P., Lesch K.-P., Bally-Cuif L. (2012) The ADHD-susceptibility gene lphn3.1 modulates dopaminergic neuron formation and locomotor activity during zebrafish development. *Mol. Psychiatry* **17**, 946–954.
Lazarini F., Gabellec M. M., Moigneu C., de Chaumont F., Olivo-Marin J. C., Lledo P. M. (2014) Adult neurogenesis restores dopaminergic neuronal loss in the olfactory bulb. *J. Neurosci.* **34**, 14430–14442.
Lee A. S., Tang C., Rao M. S., Weissman I. L., Wu J. C. (2013) Tumorigenicity as a clinical hurdle for pluripotent stem cell therapies. *Nat. Med.* **19**, 998–1004.
Li L., Dowling J. E. (2000) Effects of dopamine depletion on visual sensitivity of zebrafish *J. Neurosci.* **20**, 1893–1903.
Li X., Montgomery J., Cheng W., Noh J. H., Hyde D. R., Li L. (2012a) Pineal photoreceptor cells are required for maintaining the circadian rhythms of behavioral visual sensitivity in zebrafish *PLoS One* **7**, e40508.
Li Z., Ptak D., Zhang L., Walls E. K., Zhong W., Leung Y. F. (2012b) Phenylthiourea specifically reduces zebrafish eye size *PLoS One* **7**, e40132.
Lieschke G. J., Currie P. D. (2007) Animal models of human disease: zebrafish swim into view. *Nat. Rev. Genet.* **8**, 353–367.
Lindsey B. W., Darabie A., Tropepe V. (2012) The cellular composition of neurogenic periventricular zones in the adult zebrafish forebrain. *J. Comp. Neurol.* **520**, 2275–2316.
Liu P., Jenkins N. A., Copeland N. G. (2003) A highly efficient recombineering-based method for generating conditional knockout mutations *Genome Res.* **13**, 476–484.
Mahler J., Driever W. (2007) Expression of the zebrafish intermediate neurofilament Nestin in the developing nervous system and in neural proliferation zones at postembryonic stages. *BMC Dev. Biol.* **7**, 89.
Matthews M., Varga Z. M. (2012) Anesthesia and euthanasia in zebrafish *ILAR J.* **53**, 192–204.
März M., Chapouton P., Diotel N., Vaillant C., Hesl B., Takamiya M., Lam C. S., Kah O., Bally-Cuif L., Strähle U. (2010) Heterogeneity in progenitor cell subtypes in the ventricular zone of the zebrafish adult telencephalon. *Glia* **58**, 870-88.
März M., Schmidt R., Rastegar S., Strähle U. (2011) Regenerative response following stab injury in the adult zebrafish telencephalon. *Dev. Dyn.* **240**, 2221–2231.
McKinley E. T., Baranowski T. C., Blavo D. O., Cato C., Doan T. N., Rubinstein A. L. (2005) Neuroprotection of MPTP-induced toxicity in zebrafish dopaminergic neurons. *Brain Res. Mol. Brain Res.* **141**, 128–137.
Meiser J., Weindl D., Hiller K. (2013) Complexity of dopamine metabolism *Cell Commun. Signal* **11**, 34.

Meissner W. G., Frasier M., Gasser T., Goetz C. G., Lozano A., Piccini P., Obeso J. A., et al. (2011) Priorities in Parkinson's disease research *Nat. Rev. Drug Discov.* **10**, 377–393.
Milanese C., Sager J. J., Bai Q., Farrell T. C., Cannon J. R., Greenamyre J. T., Burton E. A. (2012) Hypokinesia and reduced dopamine levels in zebrafish lacking β- and γ1-synucleins *J. Biol. Chem.* **287**, 2971–2983.
Ming G.-L., Song H. (2011) Adult neurogenesis in the mammalian brain: significant answers and significant questions. *Neuron* **70**, 687–702.
Mochizuki H. (2011) Adult neurogenesis in Parkinson's disease, in *Neurogenesis in the Adult Brain II*, (Seki T., Sawamoto K., Parent J. M., Alvarez-Buylla A. A.-B. A., eds), pp. 23–36. Springer Japan.
Monje M. L., Mizumatsu S., Fike J. R., Palmer T. D. (2002) Irradiation induces neural precursor-cell dysfunction. *Nat. Med.* **8**, 955–962.
Moss J. B., Koustubhan P., Greenman M., Parsons M. J., Walter I., Moss L. G. (2009) Regeneration of the pancreas in adult zebrafish. *Diabetes* **58**, 1844–1851.
Moss L. G., Caplan T. V., Moss J. B. (2013) Imaging beta cell regeneration and interactions with islet vasculature in transparent adult zebrafish. *Zebrafish* **10**, 249–257.
Naganawa Y., Hirata H. (2011) Developmental transition of touch response from slow muscle-mediated coilings to fast muscle-mediated burst swimming in zebrafish. *Dev. Biol.* **355**, 194–204.
Nasevicius A., Ekker S. C. (2000) Effective targeted gene "knockdown" in zebrafish *Nat. Genet.* **26**, 216–220.
Nau R., Sorgel F., Eiffert H. (2010) Penetration of drugs through the blood-cerebrospinal fluid/blood-brain barrier for treatment of central nervous system infections. *Clin. Microbiol. Rev.* **23**, 858–883.
Nishimura K., Kitamura Y., Agata K. (2012) *Regeneration of Brain and Dopaminergic Neurons Utilizing Pluripotent Stem Cells: Lessons from Planarians*. INTECH Open Access Publisher.
Nishimura K., Inoue T., Yoshimoto K., Taniguchi T., Kitamura Y., Agata K. (2011) Regeneration of dopaminergic neurons after 6-hydroxydopamine-induced lesion in planarian brain. *J. Neurochem.* **119**, 1217–1231.
Nishimura K., Takahashi J. (2013) Therapeutic application of stem cell technology toward the treatment of Parkinson's disease *Biol. Pharm. Bull.* **36**, 171–175.
Noble S., Ismail A., Godoy R., Xi Y., Ekker M. (2012) Zebrafish Parla- and Parlb-deficiency affects dopaminergic neuron patterning and embryonic survival *J. Neurochem.* **122**, 196–207.
Norton W. H. J. (2013) Toward developmental models of psychiatric disorders in zebrafish *Front. Neural Circuits* **7**, 79.
Okano H., Yamanaka S. (2014) iPS cell technologies: significance and applications to CNS regeneration and disease. *Mol. Brain* **7**, 22.
Olanow C. W., Tatton W. G. (1999) Etiology and pathogenesis of Parkinson's disease *Annu. Rev. Neurosci.* **22**, 123–144.
Panula P., Chen Y. C., Priyadarshini M., Kudo H., Semenova S., Sundvik M., Sallinen V. (2010) The comparative neuroanatomy and neurochemistry of zebrafish CNS systems of relevance to human neuropsychiatric diseases. *Neurobiol. Dis.* **40**, 46–57.

Parish C. L., Beljajeva A., Arenas E., Simon A. (2007) Midbrain dopaminergic neurogenesis and behavioural recovery in a salamander lesion-induced regeneration model. *Development* **134**, 2881–2887.
Parker M. O., Brock A. J., Walton R. T., Brennan C. H. (2013) The role of zebrafish (Danio rerio) in dissecting the genetics and neural circuits of executive function *Front. Neural Circuits* **7**, 63.
Patton E. E., Zon L. I. (2001) The art and design of genetic screens: zebrafish *Nat. Rev. Genet.* **2**, 956–966.
Pedrosa D. J., Timmermann L. (2013) Review: management of Parkinson's disease *Neuropsychiatr Dis Treat* **9**, 321–340.
Pellegrini E., Mouriec K., Anglade I., Menuet A., Le Page Y., Gueguen M.-M., Marmignon M.-H., Brion F., Pakdel F., Kah O. (2007) Identification of aromatase-positive radial glial cells as progenitor cells in the ventricular layer of the forebrain in zebrafish. *J. Comp. Neurol.* **501**, 150–167.
Pfaffl M. W. (2001) A new mathematical model for relative quantification in real-time RT-PCR *Nucleic Acids Res.* **29**, e45.
Pisharath H., Parsons M. J. (2009) Nitroreductase-mediated cell ablation in transgenic zebrafish embryos *Methods Mol. Biol.* **546**, 133–143.
Pisharath H., Rhee J. M., Swanson M. A., Leach S. D., Parsons M. J. (2007) Targeted ablation of beta cells in the embryonic zebrafish pancreas using E. coli nitroreductase. *Mech. Dev.* **124**, 218–229.
Pivonello R., Ferone D., Lombardi G., Colao A., Lamberts S. W. J., Hofland L. J. (2007) Novel insights in dopamine receptor physiology. *Eur. J. Endocrinol.* **156**, S13–S21.
Politis M., Lindvall O. (2012) Clinical application of stem cell therapy in Parkinson's disease. *BMC Med.* **10**, 1.
Prakash N., Wurst W. (2006) Development of dopaminergic neurons in the mammalian brain. *Cell. Mol. Life Sci.* **63**, 187–206.
Puttonen H. A. J., Sundvik M., Rozov S., Chen Y.-C., Panula P. (2013) Acute ethanol treatment upregulates Th1, Th2, and Hdc in larval zebrafish in stable networks *Front Neural Circuits* **7**, 102.
Quint E., Smith A., Avaron F., Laforest L., Miles J., Gaffield W., Akimenko M.-A. (2002) Bone patterning is altered in the regenerating zebrafish caudal fin after ectopic expression of sonic hedgehog and bmp2b or exposure to cyclopamine *Proc. Natl. Acad. Sci. U.S.A.* **99**, 8713–8718.
Reimer M. M., Kuscha V., Wyatt C., Sorensen I., Frank R. E., Knuwer M., Becker T., Becker C. G. (2009) Sonic hedgehog is a polarized signal for motor neuron regeneration in adult zebrafish. *J. Neurosci.* **29**, 15073–15082.
Reimer M. M., Sorensen I., Kuscha V., Frank R. E., Liu C., Becker C. G., Becker T. (2008) Motor neuron regeneration in adult zebrafish. *J. Neurosci.* **28**, 8510–8516.
Ren G., Xin S., Li S., Zhong H., Lin S. (2011) Disruption of LRRK2 does not cause specific loss of dopaminergic neurons in zebrafish *PLoS One* **6**, e20630.
Rennekamp A. J., Peterson R. T. (2015) 15 years of zebrafish chemical screening. *Curr. Opin. Chem. Biol.* **24**, 58–70.
Rink E., Wullimann M. F. (2001) The teleostean (zebrafish) dopaminergic system ascending to the subpallium (striatum) is located in the basal diencephalon (posterior tuberculum) *Brain Res.* **889**, 316–330.

Rink E., Wullimann M. F. (2002a) Connections of the ventral telencephalon and tyrosine hydroxylase distribution in the zebrafish brain (Danio rerio) lead to identification of an ascending dopaminergic system in a teleost *Brain Res. Bull.* **57**, 385–387.
Rink E., Wullimann M. F. (2002b) Development of the catecholaminergic system in the early zebrafish brain: an immunohistochemical study *Brain Res. Dev. Brain Res.* **137**, 89–100.
Roberts J. A., Miguel-Escalada I., Slovik K. J., Walsh K. T., Hadzhiev Y., Sanges R., Stupka E., et al. (2014) Targeted transgene integration overcomes variability of position effects in zebrafish. *Development* **141**, 715–724.
Rommelfanger K. S., Edwards G. L., Freeman K. G., Liles L. C., Miller G. W., Weinshenker D. (2007) Norepinephrine loss produces more profound motor deficits than MPTP treatment in mice *Proc. Natl. Acad. Sci. U.S.A.* **104**, 13804–13809.
Rothenaigner I., Krecsmarik M., Hayes J. A., Bahn B., Lepier A., Fortin G., Gotz M., Jagasia R., Bally-Cuif L. (2011) Clonal analysis by distinct viral vectors identifies bona fide neural stem cells in the adult zebrafish telencephalon and characterizes their division properties and fate. *Development* **138**, 1459–1469.
Rubinstein A. L. (2006) Zebrafish assays for drug toxicity screening. *Expert Opin. Drug Metab. Toxicol.* **2**, 231–240.
Ryu S., Mahler J., Acampora D., Holzschuh J., Erhardt S., Omodei D., Simeone A., Driever W. (2007) Orthopedia homeodomain protein is essential for diencephalic dopaminergic neuron development *Curr. Biol.* **17**, 873–880.
Sager J. J., Bai Q., Burton E. A. (2010) Transgenic zebrafish models of neurodegenerative diseases. *Brain Struct. Funct*. **214**, 285–302.
Saint-Amant L., Drapeau P. (1998) Time course of the development of motor behaviors in the zebrafish embryo. *J. Neurobiol.* **37**, 622.
Sallinen V., Kolehmainen J., Priyadarshini M., Toleikyte G., Chen Y.-C., Panula P. (2010) Dopaminergic cell damage and vulnerability to MPTP in Pink1 knockdown zebrafish. *Neurobiol. Dis.* **40**, 93–101.
Sallinen V., Torkko V., Sundvik M., Reenilä I., Khrustalyov D., Kaslin J., Panula P. (2009) MPTP and MPP+ target specific aminergic cell populations in larval zebrafish. *J. Neurochem.* **108**, 719–731.
Scerbina T., Chatterjee D., Gerlai R. (2012) Dopamine receptor antagonism disrupts social preference in zebrafish: a strain comparison study. *Amino Acids* **43**, 2059–2072.
Schindelin J., Arganda-Carreras I., Frise E., Kaynig V., Longair M., Pietzsch T., Preibisch S., et al. (2012) Fiji: an open-source platform for biological-image analysis *Nat. Meth.* **9**, 676–682.
Schmidt D. E., Ebert M. H., Lynn J. C., Whetsell W. O. (1997) Attenuation of 1-methyl-4-phenylpyridinium (MPP+) neurotoxicity by deprenyl in organotypic canine substantia nigra cultures *J. Neural Transm.* **104**, 875–885.
Schmidt R., Strähle U., Scholpp S. (2013) Neurogenesis in zebrafish - from embryo to adult *Neural Development* **8**, 3.
Schweitzer J., Löhr H., Filippi A., Driever W. (2012) Dopaminergic and noradrenergic circuit development in zebrafish. *Dev. Neurobiol* **72**, 256–268.
Searle P. F., Chen M.-J., Hu L., Race P. R., Lovering A. L., Grove J. I., Guise C., et al. (2004) Nitroreductase: a prodrug-activating enzyme for cancer gene therapy *Clin.*

Exp. Pharmacol. Physiol. **31**, 811–816.
Sheng D., Qu D., Kwok K. H. H., Ng S. S., Lim A. Y. M., Aw S. S., Lee C. W. H., et al. (2010) Deletion of the WD40 domain of LRRK2 in zebrafish causes Parkinsonism-like loss of neurons and locomotive defect. *PLoS Genet.* **6**, e1000914.
Shi G., Lee J. R., Grimes D. A., Racacho L., Ye D., Yang H., Ross O. A., Farrer M., McQuibban G. A., Bulman D. E. (2011) Functional alteration of PARL contributes to mitochondrial dysregulation in Parkinson's disease. *Hum. Mol. Genet.* **20**, 1966–1974.
Shin K., Lee J., Guo N., Kim J., Lim A., Qu L., Mysorekar I. U., Beachy P. A. (2011) Hedgehog/Wnt feedback supports regenerative proliferation of epithelial stem cells in bladder. *Nature* **472**, 110–114.
Singh B. N., Doyle M. J., Weaver C. V., Koyano-Nakagawa N., Garry D. J. (2012a) Hedgehog and Wnt coordinate signaling in myogenic progenitors and regulate limb regeneration. *Dev. Biol.* **371**, 23–34.
Singh S. P., Holdway J. E., Poss K. D. (2012b) Regeneration of amputated zebrafish fin rays from de novo osteoblasts. *Dev. Cell* **22**, 879–886.
Skaggs K., Goldman D., Parent J. M. (2014) Excitotoxic brain injury in adult zebrafish stimulates neurogenesis and long-distance neuronal integration. *Glia* **62**, 2061-79.
Smeets W. J., González A. (2000) Catecholamine systems in the brain of vertebrates: new perspectives through a comparative approach *Brain Res. Brain Res. Rev.* **33**, 308–379.
Snider S. R., Kuchel O. (1983) Dopamine: an important neurohormone of the sympathoadrenal system. Significance of increased peripheral dopamine release for the human stress response and hypertension *Endocr. Rev.* **4**, 291–309.
Soroldoni D., Hogan B. M., Oates A. C. (2009) Simple and efficient transgenesis with meganuclease constructs in zebrafish *Methods Mol. Biol.* **546**, 117–130.
Souza B. R., Romano-Silva M. A., Tropepe V. (2011) Dopamine D2 receptor activity modulates Akt signaling and alters GABAergic neuron development and motor behavior in zebrafish larvae *J. Neurosci.* **31**, 5512–5525.
Souza B. R., Tropepe V. (2011) The role of dopaminergic signalling during larval zebrafish brain development: a tool for investigating the developmental basis of neuropsychiatric disorders *Rev. Neurosci* **22**, 107–119.
Stewart A. M., Braubach O., Spitsbergen J., Gerlai R., Kalueff A. V. (2014) Zebrafish models for translational neuroscience research: from tank to bedside *Trends Neurosci.* **37**, 264–278.
Stewart A., Gaikwad S., Kyzar E., Green J., Roth A., Kalueff A. V. (2011) Modeling anxiety using adult zebrafish: A conceptual review. *Neuropharmacology* 62, 135-43.
Stoick-Cooper C. L., Weidinger G., Riehle K. J., Hubbert C., Major M. B., Fausto N., Moon R. T. (2006) Distinct Wnt signaling pathways have opposing roles in appendage regeneration. *Development* **134**, 479–489.
Stulberg M. J., Lin A., Zhao H., Holley S. A. (2012) Crosstalk between Fgf and Wnt signaling in the zebrafish tailbud. *Dev. Biol.* **369**, 298–307.
Sulzer D. (2007) Multiple hit hypotheses for dopamine neuron loss in Parkinson's disease. *Trends Neurosci.* **30**, 244–250.

Tay T. L., Ronneberger O., Ryu S., Nitschke R., Driever W. (2011) Comprehensive catecholaminergic projectome analysis reveals single-neuron integration of zebrafish ascending and descending dopaminergic systems. *Nat. Commun.* **2**, 171–12.

Thirumalai V., Cline H. T. (2008) Endogenous dopamine suppresses initiation of swimming in prefeeding zebrafish larvae *J. Neurophysiol.* **100**, 1635–1648.

Thummel R., Kassen S. C., Enright J. M., Nelson C. M., Montgomery J. E., Hyde D. R. (2008) Characterization of Müller glia and neuronal progenitors during adult zebrafish retinal regeneration. *Exp. Eye Res.* **87**, 433–444.

Tieu K. (2011) A Guide to Neurotoxic Animal Models of Parkinson's Disease. *Cold Spring Harbor Perspectives in Medicine* **1**, (1) a009316.

Tran S., Chatterjee D., Gerlai R. (2014) Acute net stressor increases whole-body cortisol levels without altering whole-brain monoamines in zebrafish *Behav. Neurosci.* **128**, 621–624.

Tran S., Nowicki M., Muraleetharan A., Gerlai R. (2015) Differential effects of dopamine D1 and D 2/3 receptor antagonism on motor responses *Psychopharmacology* **232**, 795–806.

Ugrumov M. V., Saifetyarova J. Y., Lavrentieva A. V., Sapronova A. Y. (2012) Developing brain as an endocrine organ: Secretion of dopamine. *Mol. Cell. Endocrinol.* **348**, 78–86.

Viales R. R., Diotel N., Ferg M., Armant O., Eich J., Alunni A., März M., Bally-Cuif L., Rastegar S., Strähle U. (2015) The helix-loop-helix protein Id1 controls stem cell proliferation during regenerative neurogenesis in the adult zebrafish telencephalon. *Stem Cells* **33**, 892–903.

Villeda S. A., Luo J., Mosher K. I., Zou B., Britschgi M., Bieri G., Stan T. M., et al. (2011) The ageing systemic milieu negatively regulates neurogenesis and cognitive function. *Nature* **477**, 90–94.

Villeda S. A., Plambeck K. E., Middeldorp J., Castellano J. M., Mosher K. I., Luo J., Smith L. K., et al. (2014) Young blood reverses age-related impairments in cognitive function and synaptic plasticity in mice *Nat. Med.* **20**, 659–663.

Visanji N. P., Brooks P. L., Hazrati L.-N., Lang A. E. (2013) The prion hypothesis in Parkinson's disease: Braak to the future *Acta Neuropathol. Commun.* **1**, 1–1.

Volkow N. D., Wang G. J., Telang F., Fowler J. S., Logan J., Childress A. R., Jayne M., Ma Y., Wong C. (2006) Cocaine cues and dopamine in dorsal striatum: mechanism of craving in cocaine addiction. *J. Neurosci.* **26**, 6583–6588.

Wen L., Wei W., Gu W., Huang P., Ren X., Zhang Z., Zhu Z., Lin S., Zhang B. (2008) Visualization of monoaminergic neurons and neurotoxicity of MPTP in live transgenic zebrafish. *Dev. Biol.* **314**, 84–92.

Westerfield M. (2000) *The zebrafish book. A guide for the laboratory use of zebrafish (Danio Rerio)*. Univ. of Oregon Press, Eugine.

White D. T., Mumm J. S. (2013) The nitroreductase system of inducible targeted ablation facilitates cell-specific regenerative studies in zebrafish. *Methods* **62**, 232–240.

White E. J., Kounelis S. K., Byrd-Jacobs C. A. (2015) Plasticity of glomeruli and olfactory-mediated behavior in zebrafish following detergent lesioning of the olfactory epithelium. *Neuroscience* **284**, 622–631.

White R. M., Sessa A., Burke C., Bowman T., LeBlanc J., Ceol C., Bourque C., et al. (2008) Transparent adult zebrafish as a tool for in vivo transplantation analysis. *Cell Stem Cell* **2**, 183–189.
White Y. A. R., Woods D. C., Wood A. W. (2011) A transgenic zebrafish model of targeted oocyte ablation and de novo oogenesis. *Dev. Dyn.* **240**, 1929–1937.
Wilhelm J. C., Xu M., Cucoranu D., Chmielewski S., Holmes T., Lau K., Bassell G. J., English A. W. (2012) Cooperative roles of BDNF expression in neurons and schwann cells are modulated by exercise to facilitate nerve regeneration. *J. Neurosci.* **32**, 5002–5009.
Wong K., Elegante M., Bartels B., Elkhayat S., Tien D., Roy S., Goodspeed J., et al. (2010) Analyzing habituation responses to novelty in zebrafish (Danio rerio). *Behav. Brain Res.* **208**, 450–457.
Wong T.-T., Zohar Y. (2015) Production of reproductively sterile fish: A mini-review of germ cell elimination technologies. *Gen. Comp. Endocrinol*.
Xi Y., Noble S., Ekker M. (2011a) Modeling Neurodegeneration in Zebrafish. *Curr. Neurol. Neurosci. Rep.* **11**, 274–282.
Xi Y., Ryan J., Noble S., Yu M., Yilbas A. E., Ekker M. (2010) Impaired dopaminergic neuron development and locomotor function in zebrafish with loss of pink1function. *Eur. J. Neurosci.* **31**, 623–633.
Xi Y., Yu M., Godoy R., Hatch G., Poitras L., Ekker M. (2011b) Transgenic zebrafish expressing green fluorescent protein in dopaminergic neurons of the ventral diencephalon. *Dev. Dyn.* **240**, 2539–2547.
Yamamoto K., Mirabeau O., Bureau C., Blin M., Michon-Coudouel S., Demarque M., Vernier P. (2013) Evolution of dopamine receptor genes of the D1 class in vertebrates. *Mol. Biol. Evol.* **30**, 833–843.
Yamamoto K., Ruuskanen J. O., Wullimann M. F., Vernier P. (2010) Differential expression of dopaminergic cell markers in the adult zebrafish forebrain. *J. Comp. Neurol.* **519**, 576–598.
Yamamoto K., Vernier P. (2011) The evolution of dopamine systems in chordates *Front Neuroanat* **5**, 21.
Yasuhara T., Kameda M., Agari T., Date I. (2015) Regenerative medicine for Parkinson's disease *Neurol. Med. Chir. (Tokyo)* **55**, 113–123.
Yi X., Jin G., Zhang X., Mao W., Li H., Qin J., Shi J., Dai K., Zhang F. (2013) Cortical endogenic neural regeneration of adult rat after traumatic brain injury. *PLoS One* **8**, e70306.
Yokogawa T., Hannan M. C., Burgess H. A. (2012) The dorsal raphe modulates sensory responsiveness during arousal in zebrafish. *J. Neurosci.* **32**, 15205–15215.
Yu T. S., Zhang G., Liebl D. J., Kernie S. G. (2008) Traumatic brain injury-induced hippocampal neurogenesis requires activation of early nestin-expressing progenitors. *J. Neurosci.* **28**, 12901–12912.
Zaky A. Z., Moftah M. Z. (2014) Neurogenesis and growth factors expression after complete spinal cord transection in Pleurodeles waltlii *Front. Cell Neurosci*. **8**, 458.
Zhang R., Han P., Yang H., Ouyang K., Lee D., Lin Y.-F., Ocorr K., et al. (2013) In vivo cardiac reprogramming contributes to zebrafish heart regeneration. *Nature* **498**, 497–501.

Zhao M., Momma S., Delfani K., Carlen M., Cassidy R. M., Johansson C. B., Brismar H., Shupliakov O., Frisen J., Janson A. M. (2003) Evidence for neurogenesis in the adult mammalian substantia nigra *Proc. Natl. Acad. Sci. U.S.A.* **100**, 7925–7930.

Zhao T., Zondervan-van der Linde H., Severijnen L.-A., Oostra B. A., Willemsen R., Bonifati V. (2012) Dopaminergic neuronal loss and dopamine-dependent locomotor defects in Fbxo7-deficient zebrafish. *PLoS One* **7**, e48911.

Zhou W., Hildebrandt F. (2012) Inducible podocyte injury and proteinuria in transgenic zebrafish. *J. Am. Soc. Nephrol.* **23**, 1039–1047.

Zupanc G. K. H. (2008) Adult Neurogenesis in Teleost Fish. In *Neurogenesis in the Adult Brain I* (pp. 137-167). Springer Japan.

Zupanc G. K. H., Hinsch K., Gage F. H. (2005) Proliferation, migration, neuronal differentiation, and long-term survival of new cells in the adult zebrafish brain. *J. Comp. Neurol.* **488**, 290–319.